Departament d'Arquitectura de Computadors

Doctoral Dissertation

VISIBLE, NEAR INFRARED AND THERMAL HAND-BASED IMAGE BIOMETRIC RECOGNITION

By

XAVIER FONT i ARAGONÈS at Universitat Politècnica de Catalunya in partial fulfilment for the PhD degree

Thesis Advisor: **Dr. MARCOS FAÚNDEZ ZANUY**

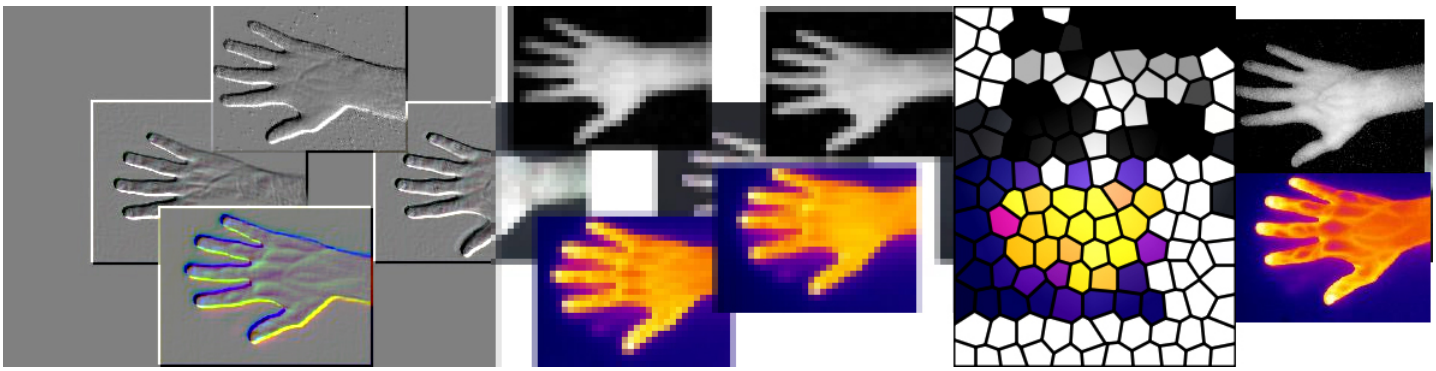

★ ★

For those who leave no one behind!

⋆

Als meus fills Marc i Ingrid
A la meva dona Chris i
Als meus pares Carme i Aleix

★ ★

Acknowledgements

Apart from my effort, the success of any project depends largely on the inspiration and guidelines of many others. No one walks alone on the journey of life. Much of what I have learned over the years came as the result of being helped for others. They inspired me and, subconsciously contributed in some way getting this project come true. Firstly, I would like to thank my wife Chris and children Marc and Ingrid, who show how easy is to get a smile anytime and anywhere. My brother Sergi for his unconditional support and Jordi for playing good music, as well. I would like to thank Toni, Anna, Julia, Conrad and Loli for its relentless energy and good moments.

My thanks and appreciations also go to Antonio F., Montserrat A., Ton S., Xavier M. and Pilar M. all of them talented professionals who taught me more than what was merely supposed to. I take this opportunity to express my gratitude to the people who have been instrumental in the successful completion of this project. I would like to show my greatest appreciation to Dr. Marcos Faundez for his huge support. My sincere thanks to those who have been absolutely open to push me forward, my greatest gratitude to Virginia Espinosa, also for my department mates Carles Paul, Albert Monté, Josep Roure and Joan Jou. My thanks and appreciations also go to my office mate Alfons Palacios always in a positive mindset. I do not forget my colleagues Montse Rabassa and Eduard de Bru who have been always giving me wings.

I do not forget help coming from Ruben Hernandez and Jiri Mekyska that in some way helped me going a step further.

An enormous support has always come up from Juan Garcia and Jeff Judge when English have been involved. My sincerely greatest thanks for them.

Abstract

Biometric Recognition refers to the automatic identification of a person based on his or her anatomical characteristic or modality (i.e., fingerprint, palmprint, face) or behavioural (i.e., signature) characteristic. It is a fundamental key issue in any process concerned with security, shared resources, network transactions among many others. Arises as a fundamental problem widely known as recognition, and becomes a must step before permission is granted. It is supposed that protects key resources by only allowing those resources to be used by users that have been granted authority to use or to have access to them. Biometric systems can operate in verification mode, where the question to be solved is *Am I who I claim I am?* or in identification mode where the question is *Who am I?*

Scientific community has increased its efforts in order to improve performance of biometric systems. Depending on the application many solutions go in the way of working with several modalities or combining different classification methods. Since increasing modalities require some user inconvenience many of these approaches will never reach the market. For example working with iris, face and fingerprints requires some user effort in order to help acquisition.

This thesis addresses hand-based biometric system in a thorough way. The main contributions are in the direction of a new multi-spectral hand-based image database and methods for performance improvement. The main contributions are:

i) The first multi-spectral hand-based image database from both hand faces: palmar and dorsal. Biometric database are a precious commodity for research, mainly when it offers something new like visual (VIS), near infrared (NIR) and thermography (TIR) images at a time. This database with a length of 100 users and 10 samples per user constitute a good starting point to check algorithms and hand suitability for recognition.

ii) In order to correctly deal with raw hand data, some image preprocessing steps are necessary. Three different segmentation phases are deployed to deal with VIS, NIR and TIR images specifically.

Here, it is highlighted some of the tough questions to address:

- VIS: overexposed images, ring fingers and the cuffs
- TIR: cold finger
- NIR: coloured Nails and noise image

Once image segmented, two different approaches are prepared to deal with the segmented data. These two approaches called: **Holistic** and **Geometric** define the main focus to extract the feature vector. These feature vectors can be used alone or can be combined in some way. Many questions can be stated: e.g. *which approach is better for recognition?*, *Can fingers alone obtain better performance than the whole hand?* and *Is thermography hand information suitable for recognition due to its thermoregulation properties?*

A complete set of data ready to analyse, coming from the holistic and geometric approach have been designed and saved to test. Some innovative geometric approach related to curvature will be demonstrated.

iii) Finally the Biometric Dispersion Matcher (BDM) is used in order to explore how it works under different fusion schemes, as well as with different classification methods. It is the intention of this research to contrast what happen when using other methods close to BDM like Linear Discriminant Analysis (LDA) or Fisher as well as if using entirely different methods like K nearest neighbor (KNN) or logistic regression. At this point, some interesting questions will be solved, e.g. by taking advantage of the finger segmentation (as five different modalities) to figure out if they can outperform what the whole hand data can teach us.

α β ς δ ε φ γ η ι ϑ κ λ μ ν ο π χ ρ ς τ υ ω ξ ψ ζ

Resum

El Reconeixement Biomètric fa referència a la identificació automàtica de persones fent us d'alguna característica o modalitat anatòmica (empremta digital) o d'alguna característica de comportament (signatura). És un aspecte fonamental en qualsevol procés relacionat amb la seguretat, la compartició de recursos o les transaccions electròniques entre d'altres. És converteix en un pas imprescindible abans de concedir l'autorització. Aquesta autorització, s'entén que protegeix recursos clau, permeten així, que aquests siguin utilitzats pels usuaris que han estat autoritzats a utilitzar-los o a tenir-hi accés. Els sistemes biomètrics poden funcionar en verificació, on es resol la pregunta: *Soc jo qui dic que soc?* O en identificació on es resol la qüestió: *Qui soc jo?*

La comunitat científica ha incrementat els seus esforços per millorar el rendiment dels sistemes biomètrics. En funció de l'aplicació, diverses solucions s'adrecen a treballar amb múltiples modalitats o combinant diferents mètodes de classificació. Donat que incrementar el número de modalitats, representa a la vegada problemes pels usuaris, moltes d'aquestes aproximacions no arriben mai al mercat.

La tesis contribueix principalment en tres grans àrees, totes elles amb el denominador comú següent: Reconeixement biometric a través de les mans.

i) La primera d'elles constitueix la base de qualsevol estudi, les dades. Per poder interpretar, i establir un sistema de reconeixement biomètric prou robust amb un clar enfocament a múltiples fonts d'informació, però amb el mínim esforç per part de l'usuari es construeix aquesta Base de Dades de mans multi espectral. Les bases de dades biomètriques constitueixen un recurs molt preuat per a la recerca; sobretot si ofereixen algun element nou com es el cas. Imatges de mans en diferents espectres electromagnètics: en **visible** (VIS), en **infraroig** (NIR) i en **tèrmic** (TIR). Amb un total de 100 usuaris, i 10 mostres per usuari, constitueix un bon punt de partida per estudiar i posar a prova sistemes multi biomètrics enfocats a les mans.

ii) El segon bloc s'adreça a les dues aproximacions existents en la literatura per a tractar les dades en brut. Aquestes dues aproximacions, anomenades **Holística** (tracta la imatge com un tot) i **Geomètrica** (utilitza càlculs geomètrics) defineixen el focus alhora d'extreure el vector de característiques. Abans de tractar alguna d'aquestes dues aproximacions, però, és necessària l'aplicació de diferents tècniques de preprocessat digital de la imatge per obtenir les regions d'interès desitjades. Diferents problemes presents a les imatges s'han hagut de solucionar de forma original per a cadascuna de les tipologies de les imatges presents: VIS, NIR i TIR.

- VIS: imatges sobre exposades, anells, mànigues, braçalets.
- NIR: Ungles pintades, distorsió en forma de soroll en les imatges
- TIR: Dits freds

La segona àrea presenta aspectes innovadors, ja que a part de segmentar la imatge de la ma, es segmenten tots i cadascun dels dits (feature-based approach). Així aconseguim contrastar la seva capacitat de reconeixement envers la ma de forma completa. Addicionalment es presenta un conjunt de procediments geomètrics amb la idea de comparar-los amb els provinents de l'extracció holística.

La tercera i última àrea contrasta el procediment de classificació anomenat Biometric Dispersion Matcher (BDM) amb diferents situacions. La primera relacionada amb l'efectivitat respecte d'altres mètode de reconeixement, com ara l'Anàlisi Lineal Discriminant (LDA) o bé mètodes com KNN o la regressió logística. Les altres situacions que s'analitzen tenen a veure amb múltiples fonts d'informació, quan s'apliquen tècniques de normalització i/o estratègies de combinació (fusió) per millorar els resultats.

Els resultats obtinguts no deixen lloc per a la confusió, i són certament prometedors en el sentit que posen a la llum la importància de combinar informació complementària per obtenir rendiments superiors.

Contents

List of Figures

List of Tables

Listings

Part I.

Thesis Motivation and Goals

Chapter 1.

Thesis Introduction

Albert Einstein

Any intelligent fool can make things bigger and more complex...
It takes a touch of genius - and a lot of courage to move in the opposite direction.

Overview

In this chapter, it is introduced the original problem to be resolved during the thesis. However, the thesis has gone a step further, covering the entire steps involved in a new biometric system. That is the design and acquisition of data, the segmentation process, the extraction steps to generate quality data and to carry out recognition, and finally review throughout different techniques and strategies. Some tough questions do not initially assumed but forced to face are presented.

Contents

1.1. Initial Motivation

This thesis was originally intended as an extension of a previously thesis called Biometric Dispersion Matcher (BDM) [49] developed within our research group at Tecnocampus

Mataró (TCM). The main issue not addressed on that previous work was fusion methods through BDM in the context of multi-modal data base. Several questions should have been resolved in order to light the strengths of BDM over other classification methods, commonly used in pattern recognition problems. Among these methods, we can find Linear Discriminant Analysis (LDA), Fisher Discriminant Analysis (FDA), Logistic regression, K Nearest Neighbor (KNN), Karhunen Loeve transform with Nearest Mean Classifier (KLNM) and Support Vector Machine (SVM). Another crucial issue involves fusion methods and normalization techniques. These issues are related with system performance when working with different sources of information. Some reasonable question came up in such environment: can we avoid normalization when only BDM is used no matter where the data came from? If so, does BDM outperform other methods with normalizing techniques? Published details of the thesis can be found in [51, 52, 53]. The main advantages of BDM may be summarized as follows:

- Solve a question linked with a two class problem: Do these two vectors belong to the same user?
- It is possible to manage an open set without the must to train the classifier again
- BDM does not train a model for each user but one universal model that decides whether or not two vectors are from the same user
- The method came up with a natural way of variable discrimination through discriminant variance
- Good bias variance trade-off for estimations linked with Gaussian models
- Deployed in three different situation with signatures, face images and hand geometry obtaining good performance

This initial extension of the BDM was the main objective of this thesis. Some of the questions concerning BDM were linked with multi-modal environments (involving different physiological and behavioral characteristics). Here, some of them are listed:

- *Is it necessary to normalize scores (proximity measure) when all modalities use the same method, say BDM?*
- *Is it better using different methods although normalization will be a must?*
- *Is it better working with similar or dissimilar methods in order to improve performance?*
- *Is it possible to improve system performance working with some additional information rather than match score?*

Nevertheless, currently there has been a lot of research in two major fields where our research group wants to be involved with. The first one is the construction of a new multi-spectral hand-based database image, ready to be tested. This database has some spectrum not quite generally used in recognition through hands: thermographic data. The other one, from multi biometric sources. To be precise, multi-modal is called when the biometric system has different biometric characteristics such as hand, palm print, signature and iris. Three different sensors were used, one for each spectrum. Thus, this thesis works for a multi-sensor data base that can be seen as a multi-modal database. In order to keep the originality and innovation of the thesis, two fundamental aspects have been added (new to our best knowledge). This means, first: build a **Visible** (VIS), **Near Infrared** (NIR) and **Thermographic** (TIR) Hand-Based Database Image. And second, within this data base, build at least two data sets, one coming from a **geometric** feature extraction approach and the other one coming from an **holistic** feature extraction approach.

For **holistic approach**, it is understood a method that deals with the whole **image**. It is recognised using global features information, such as spectrum or texture information. Sometimes other variants are used, like a variant called **feature-based approach**. Such alternative takes feature-based information from the hand, like the five fingers (thumb, index, middle, ring and pinky fingers), the wrist and the fist. Using these features it is possible to uniquely identify users. For **geometric approach** is understood any method that takes into account geometric computations like lengths or widths, usually taken from the five fingers or the hand envelope(contour). These constructions allow to test different approaches to figured out which combination gives the most in identification or verification problems, say for example: VIS+NIR, VIS+TIR, NIR+TIR, VIS+NIR+TIR both with holistic and geometric approach. The other way around is combining different spectrum bands and different feature extraction algorithms: H for Holistic and G for geometric:

Proposed Deploymend Combination With Bands and Extraction Approach

- $VIS_H + VIS_G$
- $NIR_H + NIR_G$
- $TIR_H + TIR_G$
- $VIS_H + VIS_G + NIR_H + NIR_G$
- $VIS_H + VIS_G + TIR_H + TIR_G$
- $NIR_H + NIR_G + TIR_H + TIR_G$
- $VIS_H + VIS_G + NIR_H + NIR_G + TIR_H + TIR_G$

These results will be compared through different data fusion schemes. All of them at score level, which means dealing with the normalization techniques in order to have coherent data fusion methods.

1.1.1. Database

The construction of a new database is something challenging. The reason remains clear because there are some critical key aspects to control. The first one is the user involvement during all period long where the acquisition will be performed. A lot of care must be taken in order to prevent users leaving the experiment before the database (DB) is completely build and ready to be used. Second, the scheduling of the acquisition through 6 months from January to June implies a full control of users and data already acquired. Third, the characteristics of the DB have an impact on time and user effort. This means on the one hand, how many users will be involved, and on the other hand, how many days (sessions) will be necessary for each user. If we have in mind to leave the DB open to the scientific community at least 100 users are necessary, and at least some samples are also needed per user. The process obtains 10 samples per user but from five different sessions. In each session, the user will provide two acquisitions (see Figure 1.1 for details). Finally, one of the most challenging tasks for its strong impact on quality are environment conditions. These conditions can affect the quality of the captured images. Thus, environmental conditions such as light, camera position, hand placement, temperature, humidity, among other conditions have to be considered.

1.1.2. Thermography

Thermography is the measurement of temperature variations at some layer surface (i.e. temperature changes in your skin). This layer surface may be from an electric engine or

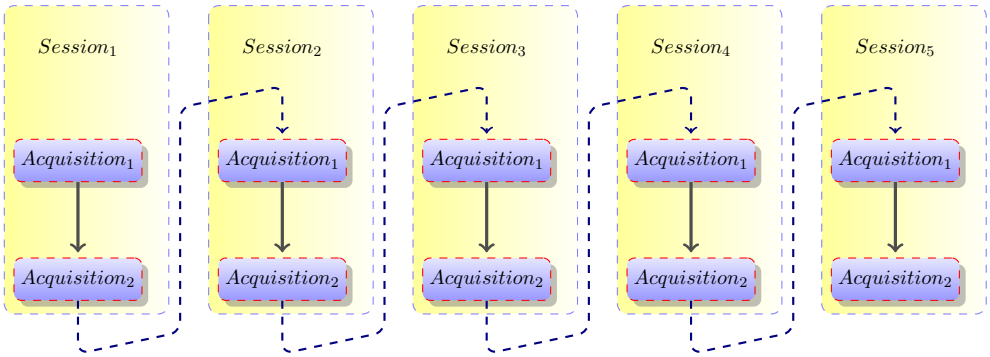

Figure 1.1.: *Acquisition Process.*

an arm muscle. Obviously, both layers are totally different, one made from some metal material and the other from human skin. However, the principles behind both situations are the same.

Thermography is a non-invasive imaging technique that is intended to measure the object layer surface temperature distribution. The infrared radiation from these objects reveals temperature variations by producing brightly colored patterns. Interpretation of the color pattern is thought to contribute to the diagnosis of some problems. An engine that does not work properly, a building not enough well insulated or some healthy physical problem like a vertebral subluxation. In our case, it could represent a heat pattern from a user we would like to identify.

A better presentation of thermography will be described in the chapters ahead (see Chapter 5). Here, it is seen how it looks a thermography from two different body parts, hand and knee (see Figure 1.2 and Figure 1.3)

Figure 1.2.: *Hands*

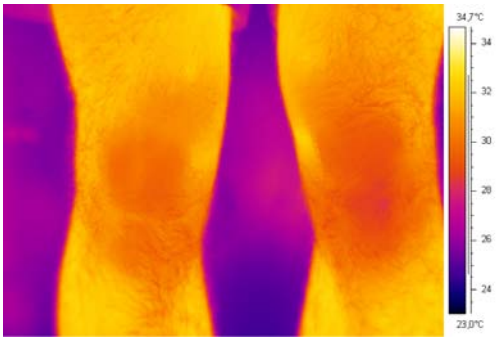

Figure 1.3.: *Knees*

1.1.3. Multimodal Biometrics

The use of different modalities is the easiest way to mitigate poor performance due to noise errors. There is a lot of effort made with unimodal biometrics. However, all current research papers in the field offer some issue related with multimodal biometrics. This work presents different electromagnetic representations by using different sensors (VIS, see Figure 1.4, NIR, see Figure 1.5, and TIR, see Figure 1.6),and different modalities. These modalities are coming by using different extraction algorithms (hand, palm and fingers). This wide range of possibilities points out the use of different fusion schemes to properly integrate them.

Figure 1.4.: *VIS Hand Image*

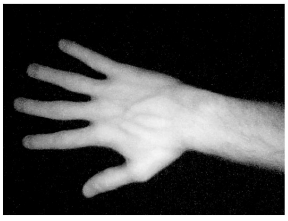

Figure 1.5.: *NIR Hand Image*

Figure 1.6.: *TIR Hand Image*

Broadly speaking, we are interested in information fusion. There are several ways to perform fusion in this thesis environment. Through different multispectral sensors (VIS, NIR and TIR), through different feature extraction approaches (Holistic, Geometric and Feature Based), through different classification methods (BDM, LDA, Fisher Discriminant Analysis, KNN, KLNN and Logistic), through different score normalization techniques (mini-max, z-score, hyperbolic tangent, logistic, linear, double sigmoid, and quadrics) and through different fusion methods (product, mean, median, max, min, vote and weighting)

Design of Experiments : `approximate dimension`

$n_{experiments}$ = Sensor × Extraction × Method × Normalization × fusion

$n_{experiments} = 3 \times 3 \times 6 \times 7 \times 7 = 2647$

Figure 1.7 shows how the hand data from the user is obtained from the different sensors and goes through the different stages until reaches the desired ready to analyse data sets.

1.1.4. Hand Base Biometry

There is a clear advantage when deploying recognition or verification using a unique user-friendly biometric system. This is one of the aims of the research done in this thesis. The user has increased confidence in a system where only hand is acquired.

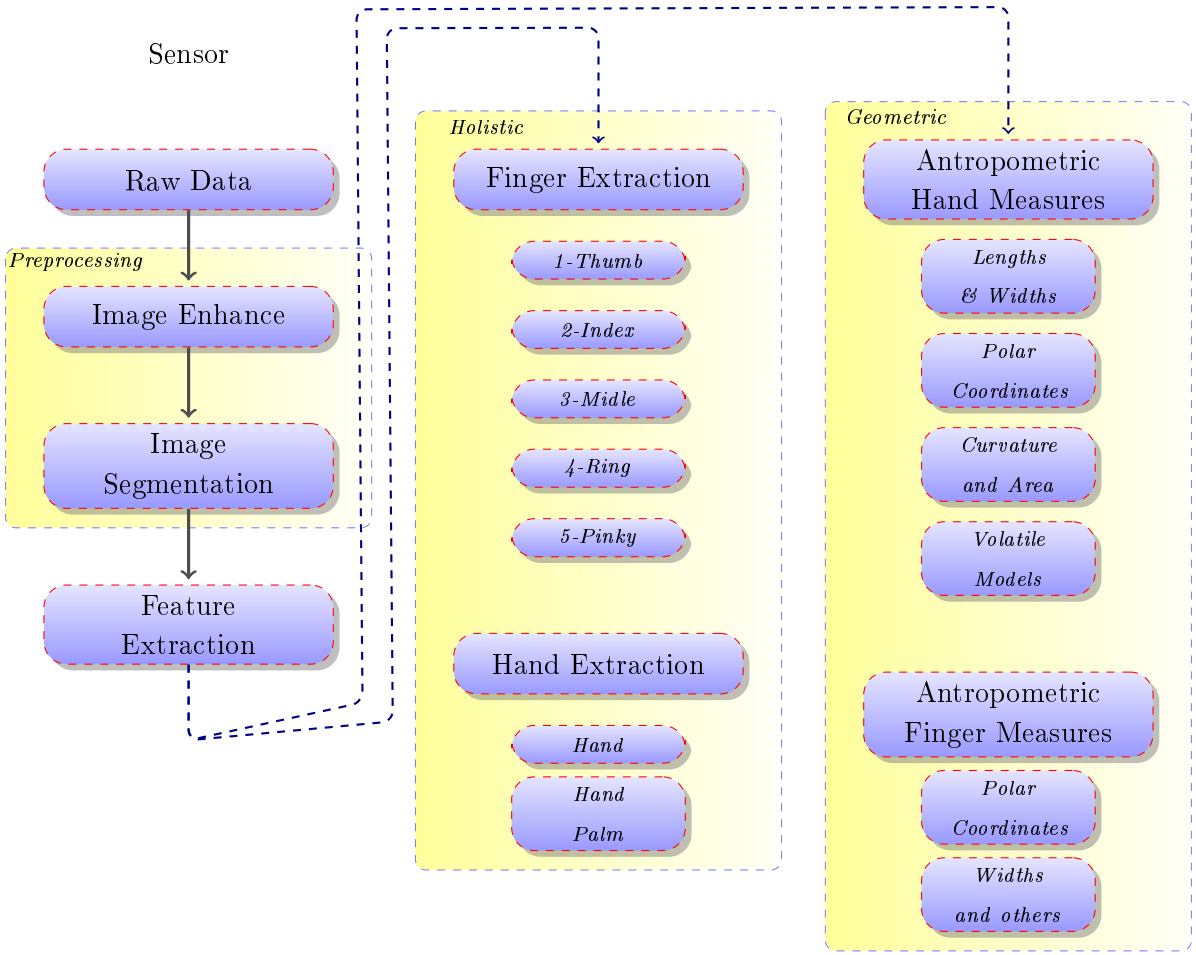

Figure 1.7.: *Extraction Process*

The intention is that the user will not be aware that the system takes three different images from three different sensors at the same time. Additionally, hand is perceived as something not as personal as face or iris, giving a greater confidence against other systems (interested reader can get a look to [188]). Although hand systems are not often installed in high security systems it gives remarkably good performance.

Perhaps, one of the most evident problems with hands is the artificial noise generated by the user itself. This noise can came from wearing watches (or not), wearing bracelets (or not), colored nails or the presence of cuff. Other possible objects present in hands are rings (possible placed at ring finger) These situations increase variability and decrease reliability. The other problem comes from the way the hand is acquired. If the hand is placed in a peg system there is a better image processing algorithm to detect hand shape. If the hand is placed in a free peg system user can hold fingers together making extremely difficult discerning those fingers. Finally, if there is not a flat surface layer that help place the hand and stretching the fingers, so that acquisition is made on air, the variations and situations constitute another issue we here no longer deal with.

1.2. Thesis Objectives

This thesis has a clear field environment related with hand biometric recognition. This statement means all that it can be faced when dealing with hand biometric system: data base construction (experimental design issues, sensor choice VIS, NIR or TIR), image processing techniques (enhancing, edge detection and segmentation), feature extraction (three different approaches: holistic, geometric or feature-based), classification methods (mainly focused on BDM but extended to others like LDA, FDA, KNN or SVM), fusion methods and normalization techniques. Obviously, through this process some statistic ammunition has to be used in order to quantify some of the results obtained. Comprehensive reviews of the state of the art will be described later on.

The following objectives are stated as short as possible:

Thesis Objectives

1 Construction of a multi-spectral hand-based image database

2 Design a suitable segmentation method in order to get the desired region of interest

3 Solve the problems with hand segmentation in all spectrum: **VIS**, **TIR** and **NIR**

4 Design a feature extraction algorithm to apply **Holistic**, **Geometric** and **feature-based** approaches

5 Deploy **fusion methods** to explore the **behaviour of BDM**

6 Analyse the effects of **normalization** over fusion methods and its benefits on performance

A considerable effort has been made to accommodate the thesis objectives so they can be stated as realistic as possible. Nevertheless, as happens in real applications a lot of troubles during the post-processing step have increased the time spent with the overall project. Over these hard ways the research has come out with other interesting innovative solutions to recognition problems, some of them not yet published but ready to be published. Here we describe some of the new contributions this thesis has captured:

Collection of Additional Contributions

1 Development of a New Performance Measure: Pareto Confusion Matrix

2 Gender Recognition Deployment

3 Statistical Analysis over BDM

4 Identification of extremely similar behaviour between BDM and LDA

5 Highlight finger as a reliable modality (improved by normalization and fusion)

6 Diversity Rule appear as the natural optimal selection

1.3. Thesis Applications

Biometric System (BS) is a critical component in every application that is intended to provide services to only validated users. The demanding of security over the current internet era is moving up and increasing primarily because people are truly concerned with this issue and for economic and ethic reasons. Applications running in airport facilities, or sharing resources through the cloud, or granting access to the finance administration (Internal Revenue Services in USA) must be reliable and unconditionally secure.

There is a clear change related with how BS operate nowadays. It is possible to establish identity based on who you are, no matter if it is for something you are (face, fingerprint, iris, retina, etc.) or for something you do (signature, speech, etc.), rather than by what you possess (key, card, etc.) or by what you know (password). Nevertheless, it is weird and suspicious when something classified, is secured over card items or passwords. Among the most challenging problems in pattern recognition, there has been a strong interest in developing advanced biometric system in order to produce good verification and identification results within recognition. Research focused on a single biometric characteristic such as fingerprint, face, iris, hand, signature or voiceprint constitute a strong and usually invariant link between the person and his identity. This approach has been overcome to multiple biometric systems that try to build multi-modal biometric systems in order to integrate multiple schemes from these different characteristics.

This thesis makes a clear step forward making a new multi-spectral database with data prepared to work under three different approaches: Holistic, Geometric and Feature-Based. This work encourages the research and improves the availability of a new database to work with. It is shown and it is improved the reliability of the system combining sensors (VIS, NIR and TIR) with different feature extraction methods to make recognition over hand genuinely appealing to work over high security environments. The system presents a list of advantages that certainly are related with the biometric characteristic we have selected:

The first one comes from the fact, hand, is from the user perspective a non-intrusive method (that is not true with the face or iris). Thus, making the system commercially attractive for an easy market acceptance. The second one comes from costs related with the hardware construction. In this case, VIS and NIR sensor are extremely cheap. We mean less than 20 euros. The main drawback comes from the price of TIR sensor, which has decreased over these last years, but it is still an expensive technology. For instance, the sensor used in this thesis costs over 8.000 euros, however, it moves in less than a year and half from 12.000 euros to 8.000 euros. That is not a good new, but currently there is a high pressure on prices for sensors coming from China that forces the price decreasing. That means it can easily reach an acceptable thermographic sensor for less

than a 900 euros currently. If as the thesis figured out only with low resolution images it is possible to afford high performance results the point is to reduce TIR expensive technology as much as possible. The third one comes from the fact the same technology can help authentication and other applications.

1.4. Thesis Publications

This thesis is about the construction of a new multi-spectral hand-based database, its segmentation, its dataset extraction, its analysis and its performance improvement through careful selection of modalities, normalization techniques and fusion strategies. The contributions of this thesis can be classified on work already made public and research already submitted or almost ready to be submitted. Huge amount of results have been generated and becomes an undesired problem in the sense that there is no time to gain further insight. Obviously there is room for further research. The reason becomes clear for the strong implication of many fields that enrich the target of the thesis.

Different published works have been made along side with the research of the thesis. Here we outline those that are already accepted and published.

1.4.1. Indexed Journals

Xavier Font-Aragones, Marcos Faundez-Zanuy and Jiri Mekyska 2012. Thermal Hand Image Segmentation For Biometric Recognition. IEEE Aerospace And Electronics Systems Magazine. Editor letter October 2012, to be published in June 2013

1.4.2. Conferences and Workshops

- Xavier Font-Aragones and Marcos Faundez-Zanuy 2012. Hand-Based Gender Recognition Using Biometric Dispersion Matcher. 22nd Italian Workshop on Neural Nets, WIRN 2012, May 17-19, Vietri sul Mare, Salerno, Italy.
- Jiri Mekyska, Xavier Font-Aragones, Marcos Faundez-Zanuy, Rubén Hernández-Mingorance, Aythami Morales, Miguel Ángel Ferrer-Ballester. Thermal Hand Image Segmentation For Biometric Recognition. pp 26-30 45th IEEE Carnahan Conference On Security Technology ICCST'2011, October 18-21, Mataró

1.4.3. Submitted Works

- Xavier Font-Aragones, Marcos Faundez-Zanuy and Jiri Mekyska. A new hand image database simultaneously acquired in visible, near-infrared and thermal spectrums. Gognitive Computation. Ref: COGN-D-12-00376R1
- Xavier Font-Aragones, Marcos Faundez-Zanuy. Data Fusion for Hand Image Biometric Recognition. 23th Italian workshop on Neural Nets, WIRN'2013, May

1.4.4. Ready to Submit Works

- Results on Finger and Hand Geometric Fusion. To be sent to the *Special Issue on Multibiometrics and Mobile-biometrics: Recent Advances and Future Research.*
- Results on BDM and Fusion. To be sent to the *Pattern Recognition*

1.5. Thesis Organization

The thesis is organized in five different parts.

√ Part One: Thesis Motivation and Goals. Here we describe the introduction and the main objectives of the thesis.

√ Part Two: Thesis Background. This part is related with all the key fields where it is necessary to dig into in order to understand the strengths of the thesis work. It gives a brief introduction over all aspects this thesis has faced. This includes the following chapters: Introduction to biometrics (chapter 2) that will give a general overview of a biometric system. It will follow a Performance Metric Chapter (chapter 3). This chapter is essential for a clear understanding of the performance of a system usually used in Pattern Recognition literature. It will show the different ways to evaluate a biometric system. Then it will follow a chapter related to fusion and normalization. So chapter 4 introduces the concepts of fusion and how to consolidate evidence through combining different sources of information. In chapter 5, we introduce thermography, the basic principle behind and how to work with thermography. The last chapter of this part will be related to hand base biometric system state of the art.

√ Part Three: Thesis Development. Here, we highlight the main developments of the thesis. Chapter 7 takes a look into the information theory and the way our database has been build. From chapter 8 to chapter 10 is covered the preprocessing steps needed to obtain an accurate hand segmentation. All these chapters cover feature extraction process (from holistic and geometric perspective) and data generation as well. Chapter 11 consider a different issue linked with gender recognition. This chapter takes into account the datasets obtained from recognition purpose and tries to apply in a different context, gender recognition.

√ Part Four: Thesis Results. Two chapters examine the main results obtained from the study of our database with the segmentation methods described in part two. Chapter 12 shows results throughout holistic data while chapter 13 include geometric data. Both chapters show the importance of a correct selection, from normalization and fusion strategy. Performance measurements are made from the two possible recognition operations, identification and verification. Chapter 13 finish with our proposed performance measure we have called Pareto Confusion Matrix.

√ Part Five: Thesis Conclusions and Future Extensions. The last part of the thesis enumerates the main results and substantial contributions of this research. Obviously some previously presented results will be summarized and powerful conclusion came to light, such as the diversity rule. Because optimal solutions have been used, reader can be aware that our results are good as any of the state of the art and in some configurations surpass best results. Chapter 14 finish with some of the possible future extensions.

Part II.

Thesis Background

Chapter 2.

Introduction to Biometrics

Chinese Proverb

The journey of a thousand miles begins with one step.

Overview

National Security is a major issue in USA and other western countries. In this context, biometric systems are defined as autonomous systems ready to acquire biometric samples from users, extracting data from physical or behavioural traits, and then building a reliable model (template) in order to be used for ensuring granted access to granted users. Systems that, once the model has already been built, can compare biometric data from any user. The biometric data saved in the model (template) is then used to make a decision through a matching score and generate an authentication result. This chapter gives insight in the context of biometric systems.

Contents

2.1. Introduction

The easiest way to obtain biometrics definition is through any public internet dictionary. There, we can find the following two simple and clear definitions (see Definition 2.1) :

Definition 2.1: Biometrics

Biometrics refers to methods for uniquely recognizing or verifying a person based upon a physical characteristic or behavioural traits. Biometrics identifies the person by what he is, rather than by what he knows not what he has.
Science involving the measurement and analysis of unique physical or behavioural characteristics (as fingerprint or voice patterns) especially as a means of verifying personal identity.

Biometrics has been used since men first steps in history. It is an important and critical issue for survival. We must recognize our family, neighbours our closed group that provides security. All these operations were performed through visual face recognition. But still today face recognition is the usual approach to person identification. Other characteristics like voice or signature can be used for this purpose. Either way, biometrics evolves along side with technological research. It is a hot topic, and an issue for permanent improvement and encouragement for national agencies. For instance, the Annual National Security Innovation Competition (NSIC) for college students is designed to stimulate interest in national security related innovations, sponsored by the Science and Technology Division of the Department of Homeland Security (USA). Other competitions spread worldwide in order to test new methods and systems related with biometric systems.

Biometric technology is improving, but it is government agencies who are still carrying the load. Industry is under the government steps. A clear example of this is the testimony of Deputy Assistant Secretary for Policy Kathleen Kraninger, Screening Coordination, and Director Robert A. Mocny, US-VISIT, National Protection and Programs Directorate who quote [104]:

"Biometrics have increased our Nation's security and the security of nations around the world to a level that simply did not exist before. Biometrics are affording us greater efficiencies, making travel more convenient, predictable, and secure for legitimate travelers. Biometrics are enabling people to have greater confidence that their identities are protected, and in turn decision-makers are more certain that the people they encounter are who they say they are."

In the next section we will examine biometric systems and their usual operation modes, the major biometric characteristics, as well as major advantages and disadvantages. We will finish with a section about their applications.

2.2. Biometric Systems

Essentially, a biometric system is a system intended to solve biometric problems. To put it in another way, a biometric system is a system designed to provide a solution to

Table 2.1.: *Comparison between Physiological and Behavioral traits*

	Disadvantages	Advantages
Physiological	could be time consuming	nonalterable
	could be uncomfortable	difficult to forge
Behavioral	high variations	user friendly
	very affected by user state	less expensive

authentication problems, or more generally, to pattern recognition problems. There are some good references addressing general **pattern recognition** problems. In [213] and [202] the problem is faced from a statistical point of view. Others like [21] put the accent in machine learning. A straightforward view of biometrics can be found at [91].

The problem of biometric identification has been widely addressed [154]. Different applications deal with reliable identification and/or verification approaches that represent the methods for authentication. In this context, biometric recognition turns to automatic identification of an individual by using certain personal attributes [93]. These can be split into two groups: physiological, such as face, fingerprint, iris, hand and finger geometry and behavioural [234] such us signature or key stroking (see Table 2.1). We can represent a general biometric system (see Figure 2.1) where the three operation modes are depicted.

The next subsections present the typical operation modes one can find in biometric systems. The first one, which is a must, is Enrolment. It must be deployed so that the system can work properly. It can be understood as a data base collection step where templates are saved in order to be used for Identification and Verification. Then a description of these two usual modes, Identification and Verification, will follow.

2.2.1. Enrolment

Enrolment is the first process needed in order to operate correctly. In these stages validated or legitimated users will proceed to give a sample (generally an image from its hand, face or another information like a recorded speech or a signature). The designers of the system will require them for some further samples to improve the recognition abilities of the system. This acquisition step is critical for its later impact in the recognition and verification operation modes. The way the acquisition is made depends largely on the way we collect biometric information from the user.

This thesis has been working with an enrolment of two and a half sessions (the training data). That means 5 samples per user (see chapter 7 section 1 to 3). With the help of

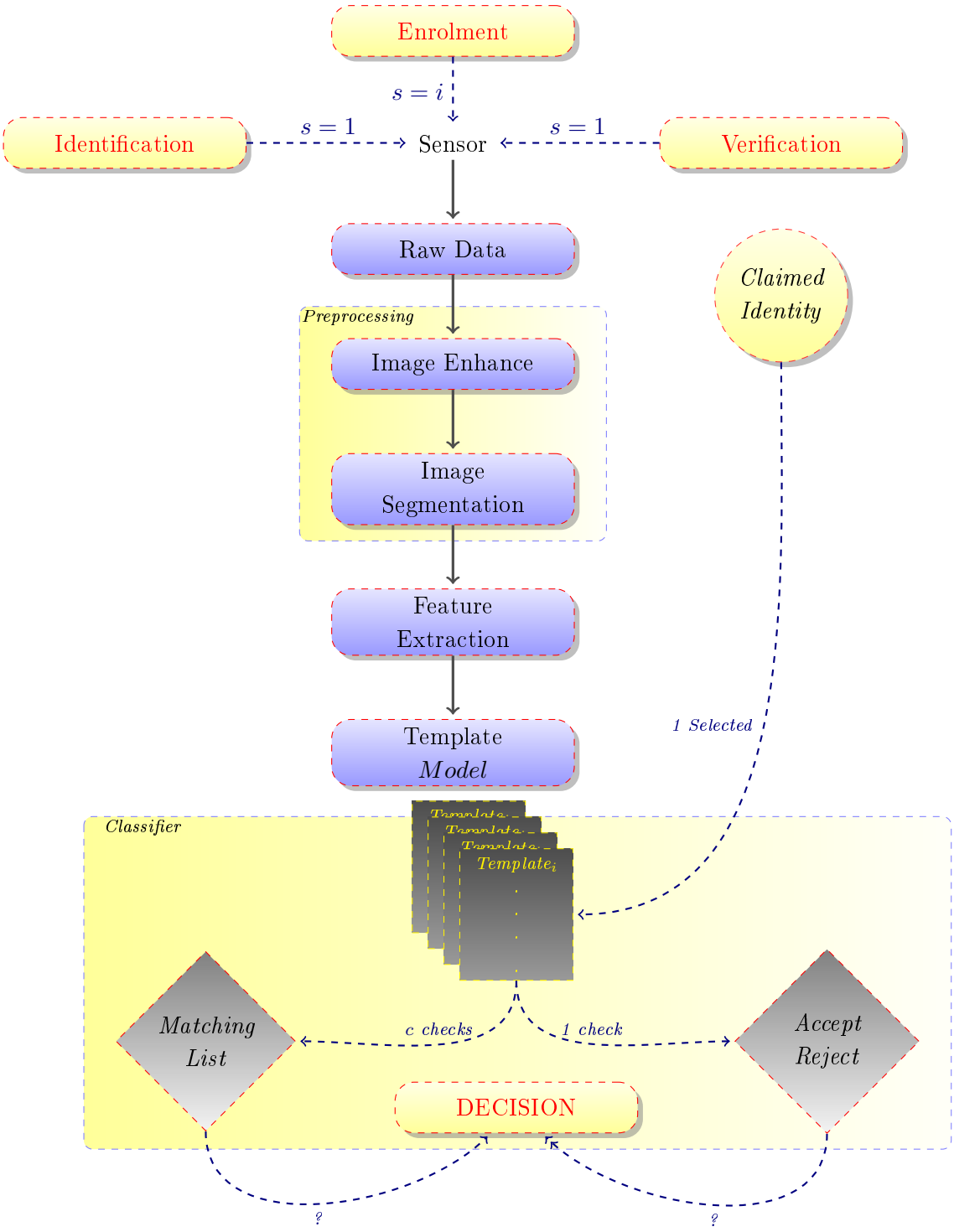

Figure 2.1.: *Biometric System.*

three different sensors (VIS, NIR and TIR) in the same acquisition session three images are taken at the same time.

As shown in Figure 2.1 (central part) the enrolment begins with the user showing (or giving) the sensor the desired biometric characteristic. All biometrics systems start with the user in front of a sensor (device) that makes the data capture. This sensor obtains the raw data (voice sample, face or hand image) that is delivered to the signal preprocessing unit. The main idea behind this step is to make the data useful for the goals of the system, reduce image noise, improve contrast, and detect edges. Thus, we achieve the main objective of keeping those features relevant to make a successful comparison. The feature extraction module carries out this work. With the help of a model and a reasonable sample size, a template model is generated.

2.2.2. Identification

Identification is the hardest recognition problem. Here, a sample from the user is given as a biometric characteristic (needed for the system) Once acquired, the system makes a guess over one of the previously enrolled users. Sometimes this guess does not belong to any of the legitimated users. In these situations, the system gives a different output: user unauthorized.

Recognition problems are challenging because, once the template from the user is obtained, it must be compared with all the database templates. At first sight, it does not seems, at all, a challenging problem, but if you think for a moment of the F.B.I. fingerprint database, then something becomes clear. Scalability, computation costs, strategies to segment templates, hash methods and DB indexing approaches become a must rather than a need.

In Figure 2.1 (left side) it is showed how the system operates in identification mode. It is supposed that the template database has been correctly generated in the enrolment mode, otherwise no identification is possible. Thus, the user who wants to be recognized offers their biometric trait/s to the sensor to proceed in the same way as enrolment. However, no template is saved in the template data base. This template is needed in order to proceed to compare with the c possibles data base templates. We suppose there are c possible authorized users. In case the system can give a result of an unidentified user, then the system accounts for $c+1$ template. What the system generates is a list of c or $c+1$ scores between the user to be identified and the total number of templates. This procedure, called classification, takes the matching score list and selects the user related with the higher score.

2.2.3. Verification

Verification is another common operation mode of biometric system. In this case, the user gives a sample (in the same way as in identification mode), but the user provides an additional information to the system. This additional information represents a claimed identity from which the system will make the comparison. Thus, the user template is compared with the claimed identity template.

Verification system does not have problems related to computation times. The right side of Figure 2.1 shows the way verification is deployed.

Whatever the operation mode used, the system will give a measure of similarity between the generated user template and the saved data base template. This measure, usually called **score**, is employed in order to make a decision that may represent a rejection or an acceptance. Here the final decision is made through the help of a previously defined threshold η. The decision is built with a simple comparison between the score and the threshold η. If score is greater than η the final decision will be *Accepted*, otherwise it will be *Rejected*.

2.2.4. Recommended Properties

There are certain recommended properties desirable for any biometric characteristic [31]. One of these properties is universality, which means that all users have to own this characteristic. Using face recognition, it is clear all examples (users) follow this common sense rule, but in other situations it could represent a serious drawback. Let us imagine index finger recognition. What would happen if, by accident, some of the legitimate users in the system lost the finger in a domestic accident?. Obviously, the system should change in order to be more robust to such situations, otherwise this unfortunate user will not be recognized any longer. There are other characteristics that are also recommended and should be taken into consideration [4] such as performance and elusiveness.

Different authors suggest a list of desirable biometric characteristics. This recommendation is circumscribed to unimodal biometric system for any trait under consideration. Here, we briefly show them (see [31] and [4] for further details).

The complete list of biometric characteristics:

1 **Universality**: user accessing the system should posses the trait

2 **Uniqueness**: trait sufficiently different across user population

3 **Permanence**: invariant over time

4 **Measurability**: acquisition possible

5 **Performance**: to match applications requirements

6 **Acceptability**: accepted by the users of the Biometric System

7 **Circumvention**: refers to the ease with which the trait can be imitated using artifacts

It is important to keep in mind that all these items are suggested in a uni-modal environment. For example, two traits with some desired characteristics not present may, in a multi-biometric system, work perfectly well. That is one of the interesting points this thesis addresses when working with thermographic finger traits. No one should at all work with fingers for their thermoregulation properties, but taking into account 5 fingers and fusioning them the system could be surprisingly improved.

2.3. Biometric Characteristics

A great number of biometric characteristics used by different applications can be found. Although our main interest is linked with hand-based recognition system, here an easy overview of the most common biometric modalities is shown.

2.3.1. Face

Face is, per-se, the most common biometric feature used by human beings to recognize one another (see [239]). The high amount of information coming from face, say eyes, nose, lips, face shape, mouth, relation between them, helps biometric recognition systems to use face for security and surveillance applications. As we will also find later on with hand-based biometrics, the two ways we can approach recognition is through geometric conditions, based on location and distance between the main face characteristics, or by dealing with a holistic approach taking the whole image to proceed with the recognition. Systems have big problems with illumination conditions, face orientation, use of glasses, beard or any other element that increases variability. By dealing with real environmental conditions, the performance of the system decreases. If we take a look at commercial face

recognition solutions we will find a great coincidence between the conditions imposed by vendors and the difficulties enumerated above.

Figure 2.2.: *Faces from AR DB ex.1*

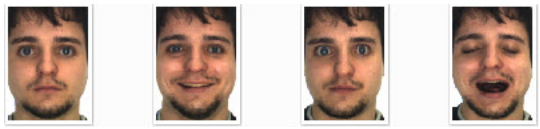

Figure 2.3.: *Faces from AR DB ex.2*

Nevertheless, researchers have a full number of face data base in order to improve and test face recognition systems. Figure 2.2 and also Figure 2.3 show a partial sample from the AR-face [130] publicly available.

There are many different face recognition approaches that deal with eigenfaces, fisherfaces and other variants (for further details see [113]) Other methods use 3D approaches as in [203] and on local Gabor in [161]. Another database called FERET database is used in [157] where fusion methods are also applied to improve the overall system.

2.3.2. Hand-Based System

Here again we can find two different approaches to deal with recognition. Geometric approach or holistic approach. The first one takes measures of hand geometry while the other one deals with image information using, for example, DCT2 or PCA.

Hand Geometry

Hand geometry modality is far from being used by humans to recognise people. The reason was presented previously, because face is enough for us and for human interaction. However, hand has a number of distinctive characteristics that make it interesting for recognition applications. Lengths and widths of fingers (thumb, index, middle, ring and pinky) as well as wrist and shape of the hand are used by many commercial applications. Hand-based system has a great advantage over other systems. The cost of the hardware is extremely affordable, and the conditions required to work in suitable operations are easy to accomplish. Hand-based system is also a non intrusive system and well accepted by final users. The main disadvantage of hand geometry is that it cannot be scaled to a big hand database, mainly because hand geometry was found not to be very distinctive. Other disadvantages are the following: it may not be invariant during the growth period; users can wear watches, jewelry or bracelets.

Palmprint

As we can find with fingers, palm has a number of patterns that are distinctive for every person (see [235] for a full coverage of palmprint technologies). Thanks to the greater

area available, ridges and valleys can be found and used to discriminate individuals. Still better, palmprints are expected to provide better performance than fingerprints. The reason comes from the kinds of different information we can obtain: geometric information, finger print and palmprint. All that information can be combined to improve the performance of the biometric system.

Here we represent some samples in Figure 2.4 from the Biosecure Data Base [83] and in Figure 2.5 from the Thesis Data base.

Figure 2.4.: *Palmprint ex.1*

Figure 2.5.: *Palmprint ex.2*

It is worth mentioning how both palmprints have been taken. The first one using a high resolution scanner (Figure 2.4) and the second one using the fixed optical sensor of a thermographic camera (Figure 2.5). Thus, one sample has been taken below the hand (with a scanner) and the second one through an optical sensor placed above the hand. This apparently similar approach gives an absolutely different result for the way hand is placed on the surface (one case flat hand with palm down, the other one turned on so palm is up).

Dorsalprint

The other side of the hand can also be used in order to obtain discriminative information from the user. Applications involving vein pattern identification have been proved quite reliable, and ready against spoofing attacks. Nevertheless the palm side has been used many more times than the dorsal one. This thesis is working with the insights of this kind of biometric characteristic. Here we show two different representations from the same user at the same time. Figure 2.6 shows the NIR hand image while the Figure 2.7 shows the VIS side.

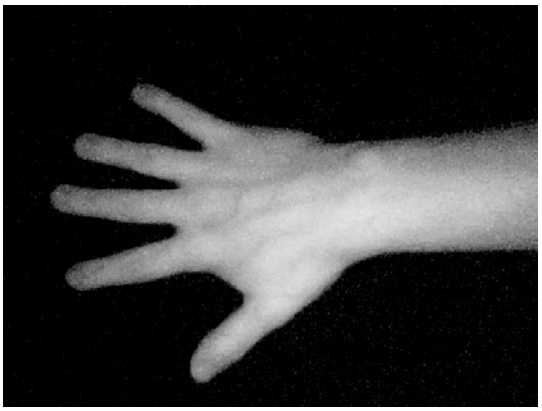

Figure 2.6.: *NIR sample*

Figure 2.7.: *VIS sample*

If the hand image has enough resolution an option is to further segment the hand in order to obtain fingers' images. Then each of these fingers can be used separately as different modalities, or combined with fusion methods when needed.

2.3.3. Fingerprint

The fingerprint is the pattern of ridges and valleys known as minutae points on the surface of a fingertip, whose formation is already determined since birth (see [127]). Systems using fingerprint have been proved to be very accurate (in identification), mainly for being highly discriminative and general invariant through life span. Fingerprint recognition systems have been successfully used for forensic applications with great success. Even with a larger data base (more than a million users) the system is quite reliable. However the main disadvantage (in identification operation) is the great number of computational effort necessary to obtain results in reasonable time. Here comes to light one well known problem related with the dimension of the problem. Algorithms suitable to deal with a 100 or 1000 user problem can not be at all applied to a 10 000 000 user problem.

In order to improve further a fingerprint system it is possible to use more than one fingerprint (ten prints used in Integrated Automated Fingerprint Identification System IAFIS maintained by the FBI) to allow a large-scale identification operational use.

In Figure 2.8 and Figure 2.9 two samples from BiosecureID data base are shown. Fingerprint is one of the most widely used biometric characteristics that works under two usual approaches: minutiae-based or correlation-based approach.

2.3.4. Iris

The iris (see examples from Figure 2.10 and Figure 2.11) is the eye region responsible for controlling the size of the pupil. Bounded by the pupil and the sclera, iris has a

Figure 2.8.: *Finger Print ex.1*

Figure 2.9.: *Finger Print ex.2*

complex texture that carries highly discriminative information. Even iris of identical twins are different (also found in fingerprint and other modalities) Performance of iris system has a very low False Accept Rate (FAR), however the False Reject Rate (FRR) tends to yield high rates [114]. Many of the problems iris system must address comes from segmentation [74] (*FAR and FRR defined in Chapter 3*).

The entrance in high secure facilities tends to use this modality, not just for the low FAR but for the ability to detect a fake iris and the ability to detect liveness through hippus movement.

The major drawback of this kind of biometric system is low user acceptance.

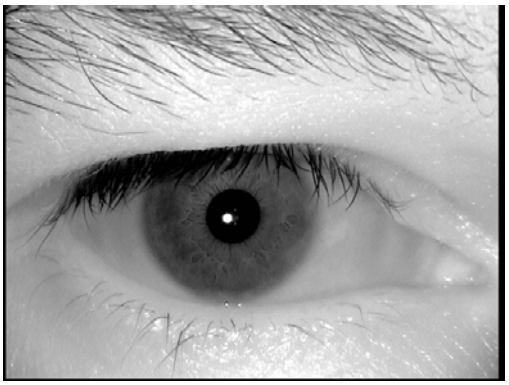

Figure 2.10.: *Right Iris*

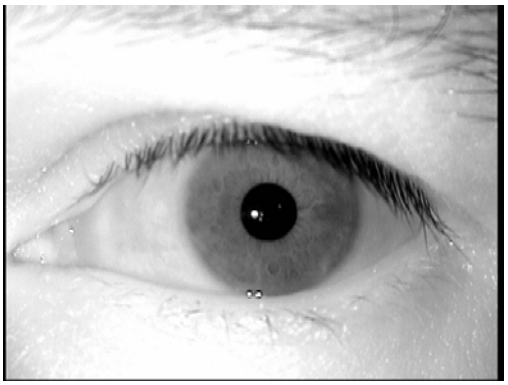

Figure 2.11.: *Left Iris*

2.3.5. Retina

The retina is a light-sensitive tissue lining the inner surface of the eye (see Figure 2.12). Its reliability relies on the uniqueness of the pattern of blood vessels lining the retina (see Figure 2.13) To acquire this data the system uses an incandescent light beam and a sensor obtains a capillary pattern by measuring reflected light. The use of the retina as a biometric trait, is usually led to high security access control.

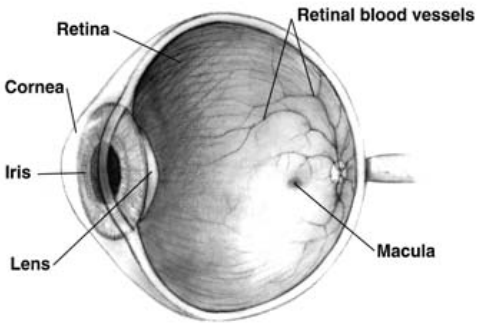

Figure 2.12.: *Human Eye. From NIH National Eye Institute*

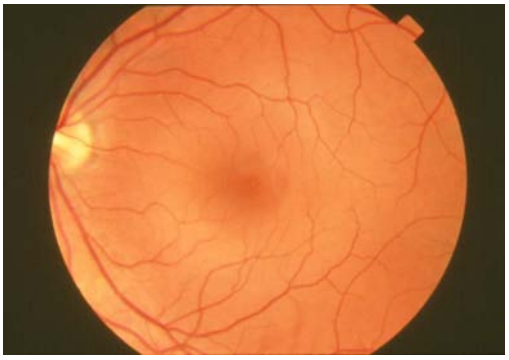

Figure 2.13.: *Retina vessels. From NIH National Eye Institute*

2.3.6. Keystroke

This biometric trait uses the characteristics every person has when typing on a computer. It is an example of a behavioural modality. Every user is supposed to have a pattern that defines how words are being used, or other values that can be monitored, such as time between words, velocity and other related issues. The most interesting thing about this trait is that a user that has been logged in a software system can be continuously verified.

2.3.7. Signature

The signature has been used for decades as a way to verify the persons identity [208], for example through many bank operations. It is understood the way a person signs is taken as unique and enough to identify himself. For this reason has been widely accepted not just in business operations but also in government, and legal environments. Some official identification documents use a signature as one of the secure elements present in them. There are, however, some problems related with the high variability of the signature within the same person. And the physical and emotional conditions can affect further this signature even without being aware of that. The major weakness of this biometric is

the easiness from with which professional forgers to reproduce a signature that fools the system. Nowadays the signature is also commonly used in logistic companies (FedEx, UPS,) that through a PDA or tablet asks for a signature of the owner of the parcel. It is worth mentioning [50], where different approaches are tested such as vector quantization (VQ), nearest neighbor (NN), dynamic time warping (DTW) and hidden Markov models (HMM) and [53] where BDM is used as method.

Handwritten

It is another way to use handwriting, [82] presents an on-line recognition method for hand-written characters.

2.3.8. Voice

Voice can be seen as a combination of physical (see vocal tracts, mouth, nasal cavities, lips) and behavioural modality (like healthy conditions, emotional state). Voice recognition is currently one major area of interest, thanks to the mobile proliferation. Applications always have to deal with noise from communication channel. A survey can be found in [27], and [176] uses a distance measure based on a fast approximation of the Kullback–Leibler (KL) divergence for Gaussian mixture models (GMM).

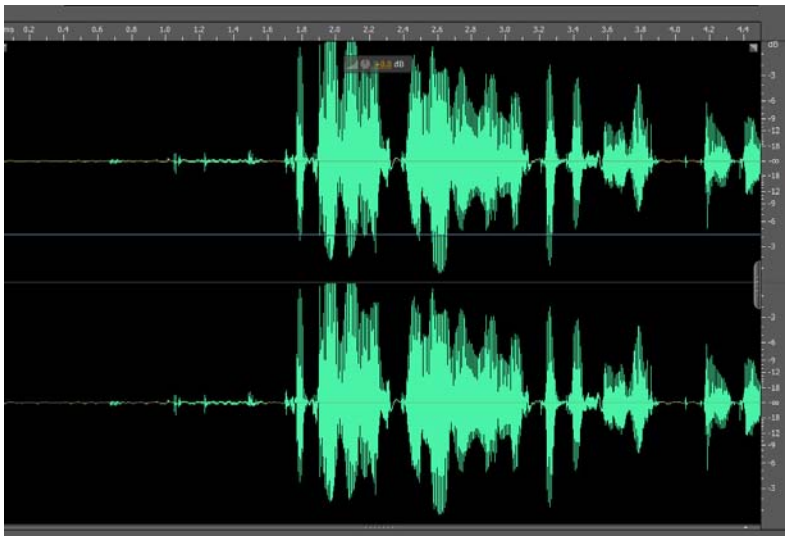

Figure 2.14.: *Voice Left and Right Channels*

Table 2.2.: *Comparison of Biometric traits through biometric characteristics*

	Biometric	Universality	Accuracy	Stability	User Acceptab.	Cost	Circumvention
1	Face	H	L	M	H	L	L
2	Fingerprint	M	H	H	H	L	L
3	Voice	M	L	L	H	L	L
4	Iris	H	H	H	L	H	H
5	Signature	L	L	L	H	L	L
6	Gait	M	L	L	H	L	M
7	**Palm-print**	M	H	H	M	M	M
8	**Hand geometry**	M	M	M	M	L	M

H: High ; M: Medium ; L: Low

Source: Adapted from [93]

2.3.9. Comparison Between Biometric Traits

It is interesting to point out how different biometric modalities can be compared. The first straightforward comparison is through biometric characteristics. For each pair of modality and characteristic we suggest three different levels (see TABLE 2.2). Something interesting appears when observing hand characteristics, because palmprint and hand geometry give different measures (and fingerprint as well). So using multi-modal biometric system can help improving the perception of system individually. That means, two weak biometric characteristics can become a strong one if combined properly. By taking advantage of these different modalities each of individual characteristics shown in Table 2.2 are outperformed.

2.4. Biometric Applications

The quick technology improvements have made possible to find biometric applications in many areas (see [1]). Biometrics can be used for:

Table 2.3.: *General Pattern Recognition Applications*

	General Field	Application	Input Pattern
1	Biometric Recognition	Identification	Face, Hand
2	Machine Learning	Searching for key patterns	Multidimensional Data
3	BioInformatics	Searching for key patterns	DNA sequence
4	Text and Web mining	Automatic Classification	Text and log data

Source: Authors' elaboration

- Citizen identification: Mainly for government agencies
- Physical Security: In some strategic facilities such as airports, ports, military sites.
- Surveillance: To monitor or control some individuals
- Business Transaction: provide authentication for retail ATM or Point sale
- Network Access: securing resources in the net or cloud
- Voting: increasing political engagement in election process
- Law enforcement: drivers license, guns control
- Identification Documents: Passports, VISA

Depending on the applications the main markets come from Government, Transport, financial, health care and from law enforcement. Thus, biometric applications will be omnipotent for security, privacy, protection and to enhance services. This list can be spread if taken into account general pattern recognition problems (see Table 2.3). Because Recognition problems are classification problems the list can be easily increased. Gender recognition, for example, illustrates an application that could be added to the list.

If we take a look at some of these biometrics market trends (see TABLE 2.4) fingerprint recognition including AFIS is dominant: approximately 2/3 of biometric market. The global market for various biometric technologies is poised for sustained growth throughout the forecast period. This market is estimated at 5 billion USD in 2010 and is expected to reach a value of nearly 12 billion USD by 2015. Face, iris, vein, and voice recognition biometric technologies together form the second largest segment. This sector is worth an

Table 2.4.: *Biometric Market Trend (in Milion USD)*

		2009	2010	2011	2012	2013	2014
1	Fingerprint	971	1,380	1,740	2,064	2,422	2,827
2	AFIS/Live Scan	1,309	1,489	1,816	2,154	2,525	2,965
3	Iris	174	287	360	480	578	730
4	**Hand geometry**	**62**	**62.8**	**63.7**	**68.2**	**76**	**85**
5	middleware	275	327	413	525	625	732
6	face	390	510	675	848	1,097	1,417
7	voice	103	109	113	136	167	189
8	vascular	83	102	132	172	199	235
9	others	54	85	107	131	154	184
10	Total	3,422	4,356	5,423	6,581	7,846	9,368

Source: Adapted from [2]

estimated 1.4 billion USD in 2010 and is expected to reach 3.5 billion USD in 2015, a compound annual growth rate (CAGR) of almost 20 percent. For further details see [2].

Biometrics is used across the world but with a high interest alongside transportation sector. The reason has been previously commented and in TABLE 2.5 it is seen how biometrics traits are used across the world within different transportation sectors. What is clear is that biometrics is a growing field with many possible applications.

Table 2.5.: *Biometrics Used Across the World within different modes of Transport*

	Aviation	Rail	Maritime	Highway	Mass Transit
North America	Face,Iris ↕ Finger ⇑	Face,Iris ↓ Finger,Voice ↕	Face,vascular ↕ Iris ↕ Finger ⇑	Finger ↕ Iris ↓	Face ↓
Middle East	Face,Finger ↑ Iris ⇑	∽	Iris ⇑	∽	∽
Central and S. America	Finger ↑	∽	Finger ↓	Iris,Face ↓ Finger ↓	Iris,Face ↓ Finger ↓
Europe	Iris ⇑ Soft Biom. ↑	Face ↕	Hand ↑	Finger ↑	Face ↓
Africa	Finger ↑	∽	∽	∽	∽
Asia and Pacific	Face ↑ Finger ⇑	Finger ↑	Face,Finger ↑	Iris ↓ Finger ↕	∽

⇑: Widespread Use ↑: Moderate Use ↕: Niche Use ↓: I+R

Source: Adapted from [132]

Chapter 3.

Performance Metrics

Goethe

Knowing is not enough; we must apply.
Willing is not enough; we must do.

Overview

In order to properly compare biometric systems it is necessary to define some performance metrics. In this chapter we present the most useful performance measures always present in biometric journals. A good understanding of measures gives a deeply insight of the strengths and weaknesses of the biometric system.

Contents

3.1. Introduction to System Performance

To have a better judgement on how a system operates in its different ways it is important to define measures for the quality of that system. That means defining performance measures becomes a key issue in the comparison and understanding of different systems.

There are some certainties as it comes to biometric systems. The first one is that any biometric system will fail. This is not a Murphy's Law, but a fact. The other one is that

it is hard to find out the true theoretical error rates. A stronger and deeper implication when dealing with performance measures is that they will be dependent measures. That is, they depend hardly on some factors such as threshold η (which means where the decision boundary is placed) and how the training and test data are designed.

As a general rule, it will be desirable to have data sets that exhibit very low intra-class variation, that is, variability between samples from the same user, and high inter-class variation, that is, variability between all samples.

In the next sections we present a collection of measures that have been developed in order to obtain an objective criterion for biometric system performance. Because it is well understood that biometric systems can operate in verification and identification mode we describe the performance measures for each of these situations.

Another interesting issue to keep in mind is that although it is possible to obtain two samples from the same user, there will not be a perfect match. There always exists same level of dissimilarity, perhaps very low but there exists. If the system is aware that there is 0 dissimilarity between templates, and this situation is taking place in a verification or identification step, that could perfectly represent a clue for an attack over the system. Once detected, the system can warn in some predefined way.

3.2. Verification Performance Measures

This section discusses performance in the context of a binary response. Thus, the system only has two possible outcomes to predict a **YES** or **POSITIVE** class for a verified user, or a **NO** or **NEGATIVE** class for a rejected user. From a statistical point of view, this situation perfectly matches test theory or hypothesis testing. Usually, a test requires a clear statement of a null hypothesis, which is generally associated with the default situation. For instance, in a bank access point, the verification question stated: *is that really you?* H_0 say yes (in the law environment we always suppose that the accused is not guilty). The other hypothesis, called alternative hypothesis H_A, is the hypothesis related with the negation of H_0. Two types of errors are present: type I error and type II error.

A type I error, also known as an error of the first kind, occurs when the H_0 is true but it is rejected. This error may be related with what we call **false positive**. False positive is also commonly called a false alarm. A type II error, also known as an error of the second kind, occurs when the H_0 is false but it is accepted as true. Here we have the same association calling this error as a **false negative**. Because the objective of a test is rejecting a H_0, it is not true that, when we fail in rejecting this hypothesis, we prove it is true. Failing to reject a null hypothesis does not prove it true.

The next performance measure definitions work under the construction of two densities. Both densities work under a random variable called match score. A match score is a

measure of the similarity between two templates. The larger the score, the better to say they are from the same user. It is possible to define genuine users, as those who come from the same template user, and impostor as those who do not. If there are c possible enrolled users, it turns out there are c possible template models. If we have a list of test samples per user ns_i , we will obtain a matrix score SC with a $(c \times ns_i) \times c$ size. In order to understand how the distribution of genuine and impostor is built let's take a look at how scores are linked with genuine or impostor group. This is represented by the following matrix:

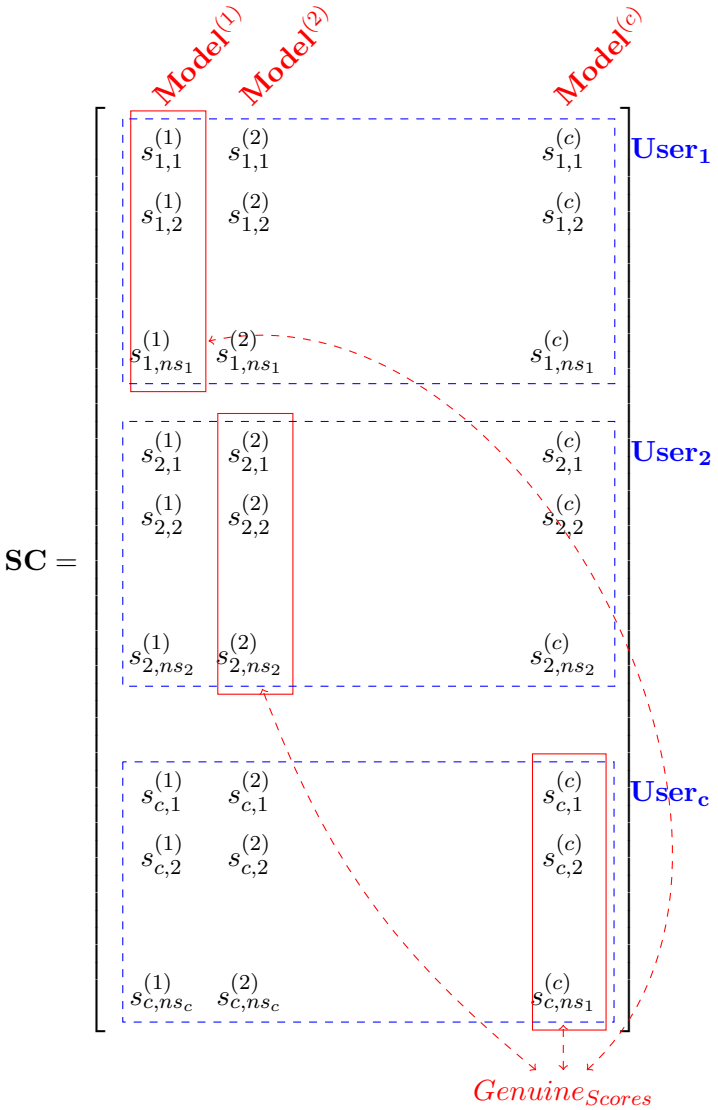

where $s^{(i)}_{j,k}$ refers to the matching score between the sample k from user j with the data base template model i.

- Genuine Density: This density is associated with the scores from genuine users.
- Impostor Density: This density comes from the scores from impostor users.

In order to estimate both densities, we use any statistical procedure to represent the shape of both distributions [122] [102]. In the Figure 3.1 are shown the true densities functions from genuine and impostors. It is easy to figure out the relation between the threshold η and the performance values of FAR and FRR that will be defined in this section.

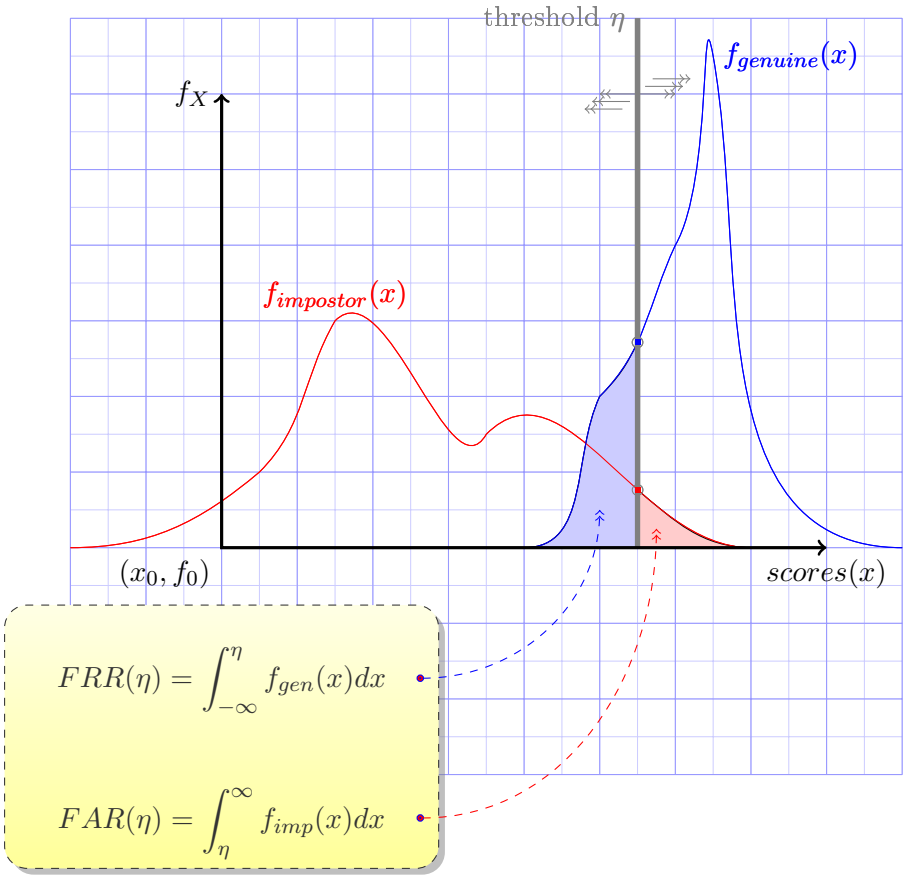

Figure 3.1.: *Genuine and Impostor Distributions.*

Each performance measure has a clear relation with η. Once threshold has been fixed, the values for FRR and FAR will be perfectly defined. Any change on the value of η will make FAR decrease and FRR increase or vice versa but never do both measures increase or decrease simultaneously.

Definition 3.1: Error Rate (ER)

Error Rate is the proportion of observations for which the model incorrectly predicts the class with respect to the actual class. We estimate this value as the ratio between the misclassification number and the total number of observations.

The most basic performance measures are shown in Figure 3.1 which are formally defined below:

Definition 3.2: False Accept Rate (FAR)

False Accept Rate (FAR) is the proportion that a user making a false claim about his identity will be verified as that false identity. (Sometimes written as False Match Rate: FMR)

$$FAR(\eta) = \int_{\eta}^{\infty} f_{imp}(x)dx$$

FAR characterizes the strength of the matching algorithm. It is possible to estimate FAR as:

$$\widehat{FAR} = \frac{\text{false acceptance}}{\text{false attempts}} = \frac{\#Sc_{imp} > \eta}{\#imp}$$

Definition 3.3: False Reject Rate (FRR)

False Reject Rate (FRR) is the proportion that a user making a true claim about his identity will be rejected as himself. (Sometimes written as False Non Match Rate: FNMR)

$$FRR(\eta) = \int_{-\infty}^{\eta} f_{gen}(x)dx$$

FRR characterizes the robustness of the algorithm. One way to estimate FRR is through this:

$$\widehat{FRR} = \frac{\text{false rejections}}{\text{true attempts}} = \frac{\#Sc_{gen} < \eta}{\#gen}$$

Observe how FAR and FRR can be changed through threshold (see Definition 3.2 for FAR and Definition 3.3 for FRR). If η moves through higher scores (see Figure 3.1) then FAR decreases, but at the same time FRR increases.

Depending on the application we want to make our system to work with, we can have interest in FAR or FRR. The higher the FRR, the less convenient the application will be. Why? Because more subjects are incorrectly recognized and therefore subject to denial of service. Thus it is possible to write $Convenience = 1 - FRR$. In a similar fashion FAR is used to measure the security of the system. Similarly, we write $Security = 1 - FAR$.

Security environments like military facilities work under very low FAR, while convenient and forensic applications work under low FRR.

Sometimes it can be interesting to work with a measure related to FRR. The Genuine Accept Rate (GAR) is the fraction of genuine scores exceeding the threshold (see [18]). $GAR = 1 - FRR$

Definition 3.4: Equal Error Rate (EER)

Equal Error Rate (EER) is the operating point where $FAR = FRR$

$$\int_{\eta}^{\infty} f_{imp}(x)dx = \int_{-\infty}^{\eta} f_{gen}(x)dx$$

Many biometric systems use the EER as a summary measure. It is the point where FAR and FRR have the same value (see Definition 3.4). However, keep in mind that two biometric systems with the same EER does not mean equal biometric systems (a clear picture of this situation in Figure 3.10).

3.2.1. Precision, Sensitivity, Specificity

Sometimes, instead of working with FAR and FRR, it is defined Precision, Sensitivity and Specificity. Common definitions in medical and pharmaceutical research tests. Our intention is to make clear that terms are isomorphic to the biometric definitions.

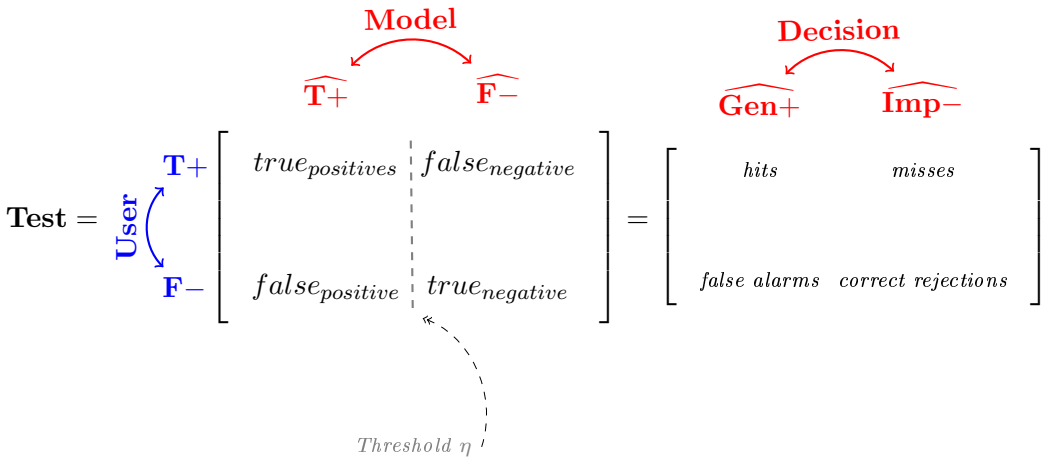

Precision is equal to the ratio of number of true positives to the total number of predicted positives (true and false positives). That is : $precision = \frac{TP}{TP+FP}$

Sensitivity = True positive rate (TPR) reads as percentage that an authorized person is admitted : $sensitivity = \frac{TP}{TP+FN}$ then it follows $FRR = 1 - TPR$
Specificity = True negative rate (TNR) reads as percentage that an unauthorized person is correctly rejected: $specificity = \frac{TN}{TN+FP}$ then it fallows $FAR = 1 - TNR$

A good system should have both low FRR (high sensitivity) and low FAR (high specificity). However, there will be always a trade-off between both measures. Decreasing one means increasing the other. Here it is possible to see the x axis as a score that represents a measure of closeness or difference between two templates. This measure has to be introduced and usually represents a measure of similarity (usual interpretation as shown in Figure 3.1). However, it may be possible to have scores where high values mean distance within templates. In this sense, higher values should be associated with impostor distribution.

From a statistical point of view, verification can be stated as a hypothesis testing problem. Nevertheless we cannot know the associated distribution when null hypothesis is held. Thus, the basic definition of the hypothesis is straightforward:

- Null Hypothesis: two samples match (it means Genuine person)
- Alternative Hypothesis: two samples do not match (it means Impostor person)

Another way to deal with this approach is to think of a characteristic vector from the person CV_{person} let abbreviate as C_p and another one from the template $CV_{template}$ let abbreviate as $\widehat{C_p}$. If there is a metric defined between characteristic vectors, let say $SC(C_p, \widehat{C_p})$ we redefine our hypothesis testing problem as:

Table 3.1.: *Verification Measures Overview*

Concept	Equivalence	Definition
TPR	True Positive Rate	positive users correctly classify as positive
	Hit Rate	
	Recall	
	Sensitivity	
FNR	False Negative Rate	positive users erroneously classify as negative
	FRR	
FPR	False Positive Rate	negative users misclassified as positive
	FAR	
TNR	True Negative Rate	negative users classify as negative
	Specificity	
Precision	Positive Predictive Value	positive users classified as positive
	$\frac{TP}{TP+FP}$	
Accuracy	Predictive Accuracy	users correctly classified
	Identification Rate	
	$\frac{TP+TN}{TP+FN+FP+TN}$	
ER	Error Rate	users incorrectly classified
	$\frac{FP+FN}{TP+FN+FP+TN}$	

- Null Hypothesis: $\widehat{C_p} \geq \eta$ (it means Genuine person)
- Alternative Hypothesis: $\widehat{C_p} \leq \eta$ (it means Impostor person)

The reliability of the SC depends on various factors. Among them

- Biometric modality
- Equipment (sensor) used
- Quality of the aquisition data process.
- Quality of the preprocessing step.
- Quality of the extraction and definition of the characteristic vector.
- Algorithm (where metric is formally defined)
- Genuine and Impostor sample size.

For these reasons SC will never be equal from the same live biometric of the same person. In case there would be a perfect match, that is we get the highest possible score, this certainly might point out an attack. On the other hand the lowest possible score between two quite different characteristic vectors will never be reached.

As an illustrative example we show, from two different data sets which are coming from the VIS geometric data (called *vecGeomVISHand1* and *vecGeomVISfing1* from Hand and thumb finger), how genuine and impostor densities look like. In Figure 3.2 and Figure 3.3 it is possible to see how genuine distributions are plotted in blue, and in the right side where score values are higher. Different data set can have different placement over the score axis as it can be seen on both representations.

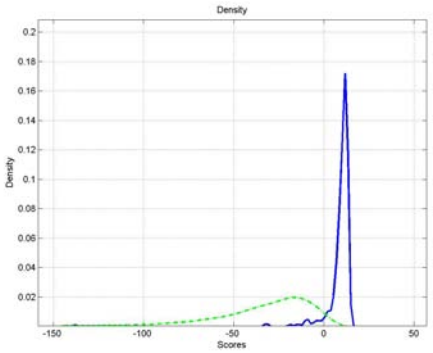

Figure 3.2.: *Genuine (blue) and Impostor (green) from Hand VIS Geometric data Set*

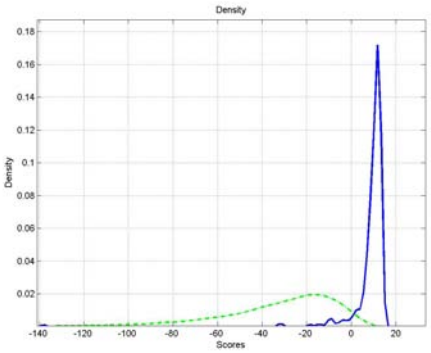

Figure 3.3.: *Genuine (blue) and Impostor (green) from Thumb VIS Geometric data Set*

As soon as we compute the values of FAR and FRR as a function of the threshold η it is possible to represent both values along side η (see Figure 3.4 and Figure 3.5). The resulting plots are useful to easily compute the threshold η where the values of FAR and FRR are equal. This point is called EER previously defined in Definition 3.4 and can be shown enlarging the Figure 3.4 in the Figure 3.6.

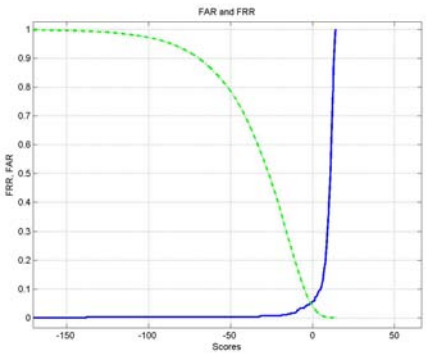

Figure 3.4.: *FAR (green) and FRR (blue) from Hand VIS Geometric data Set*

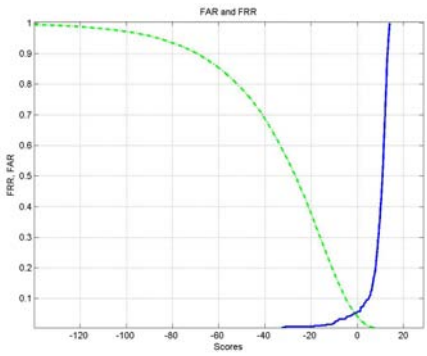

Figure 3.5.: *FAR (blue) and FRR (green) from Thumb VIS Geometric data Set*

3.2.2. The ROC and DET curve

As far as we can compute FAR and FRR for a given threshold η, we can estimate all possible FAR and FRR values depending on the threshold. It means we are going to obtain a function $FAR(\eta)$ and $FRR(\eta)$ that can be mapped in the [0,1] range. In Figure 3.9 the FAR and FRR it is represented as a function of threshold (η) and it is also possible to plot $FRR()$ vs $FAR()$ parametrized by η. The last of these representations is called the Receiver Operating Characteristic (ROC) curve [43]. Operating points can be specified by a threshold (see Figure 3.10). In this Figure, it is clear that both systems have the same EER but depending on the operating point one of them can give better performance.

There are some properties associated with ROC curve.

- Each point on ROC represents different tradeoff (cost ratio) between false positives and false negatives
- Slope of line tangent to curve defines the cost ratio
- ROC Area represents performance averaged over all possible cost ratios
- If two ROC curves do not intersect, one method dominates over the other

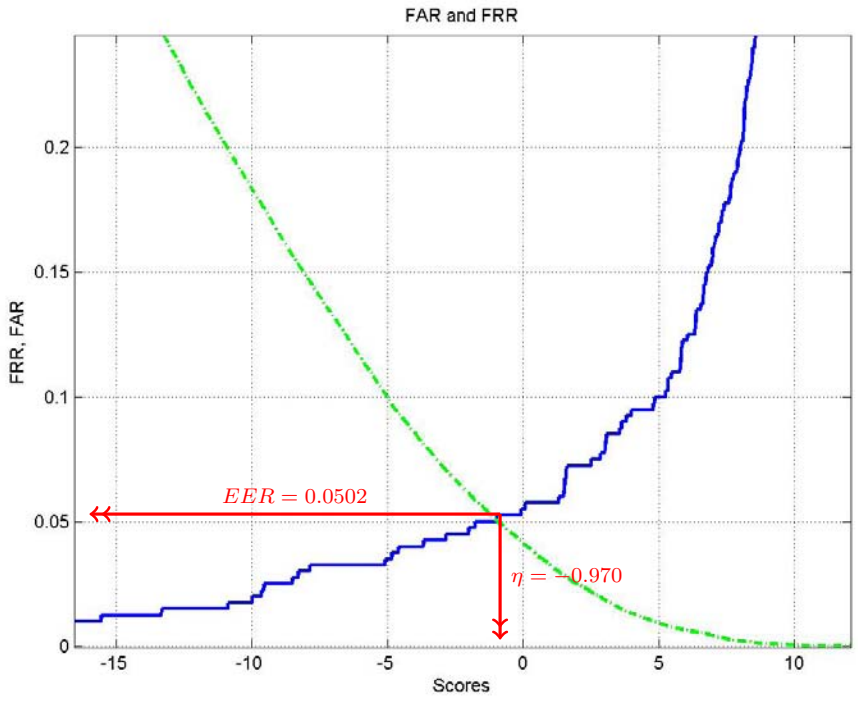

Figure 3.6.: *FAR (blue) and FRR (green) from Hand VIS Geometric data Set and the corresponding threshold and EER values*

- If two ROC curves intersect, one method is better for some cost ratios, and the other method is better for other cost ratios (see Figure 3.10)

At this point we plot two ROC curves related to the same previous examples. In Figure 3.7 and in Figure 3.8 the different trade off between FAR and FRR can be seen.

There are other ways of representing ROC curves. Another useful one, plots correct Reject Rate (1 - FRR) vs FAR. GAR vs FAR plot can be used to compute the area under the curve. This measure can help with the following appreciation according to the area computed:

- 1.0: perfect prediction
- 0.9: excellent prediction
- 0.8: good prediction
- 0.7: mediocre prediction
- 0.6: poor prediction

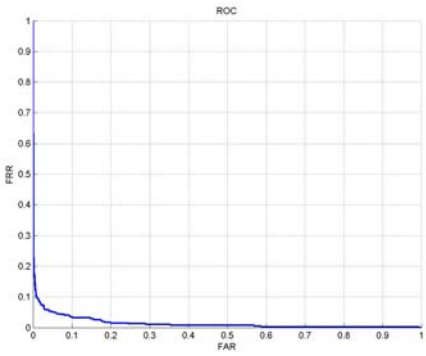

Figure 3.7.: *ROC curve from Hand VIS Geometric data Set*

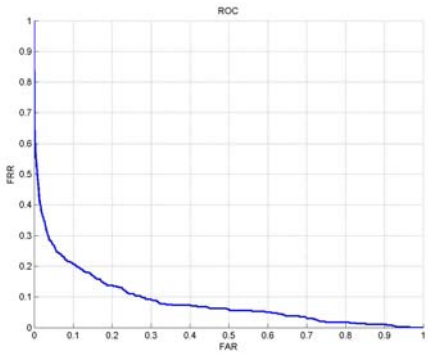

Figure 3.8.: *ROC curve from Thumb VIS Geometric data Set*

It is also possible to define one of the axis being on a non-linear scale using, for instance, a logarithmic scale. When both axis are in their standard normal deviates, yielding trade-off curves that are more linear than ROC curves, then curves are called Detection Error Tradeoff (DET) [129]. DET helps in reading and highlights the differences between different systems in critical zones (see Figure 3.13).

In general the ROC curve provides a complete specification of a single biometric matcher performance. It shows a trade-off between FAR and FRR over a broad range of thresholds. When different biometric matchers have to be compared, the best matcher depends on its operational point.

The ideal situation, happens if the proposed matcher is the one which always has better performance than the other one. In this situation the decision of the best matcher is straightforward. However, most of the cases fall into this category of representations, where at some point one matcher is better than the other one, but worse in the other side of the point.

There are other single point performance measures some times used:

Definition 3.5: D-prime

D-prime measures how well the genuine density function and the impostor density function are separated in standard deviation units.

$$d' = \frac{|\mu_{gen} - \mu_{imp}|}{\sqrt{\sigma_{gen}^2 + \sigma_{imp}^2}}$$

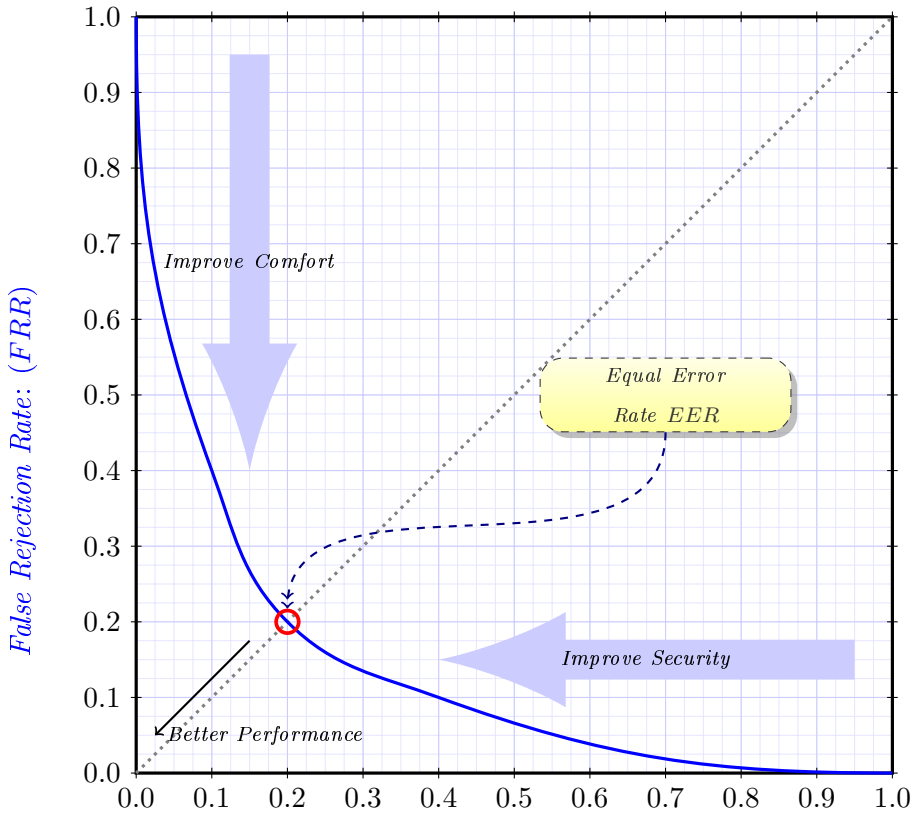

Figure 3.9.: *ROC curve (FRR vs FAR).*

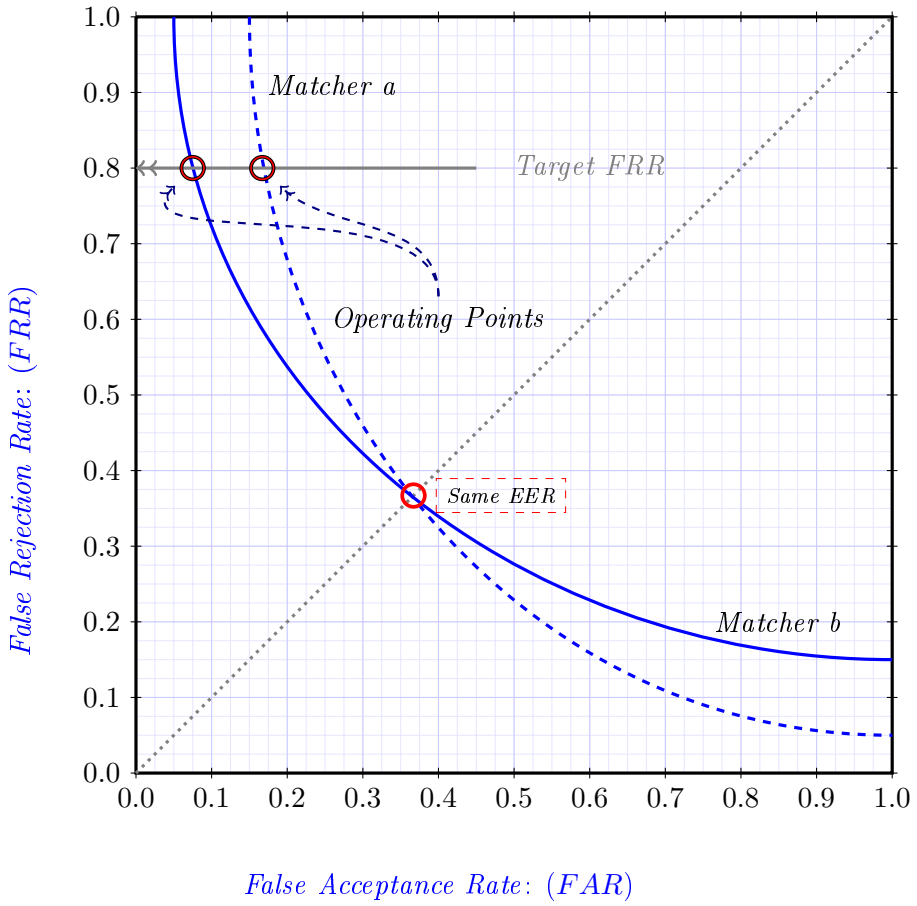

Figure 3.10.: *Same EER different Operating Points.*

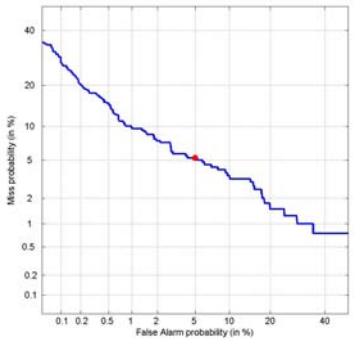

Figure 3.11.: *DET curve from Hand VIS Geometric data Set*

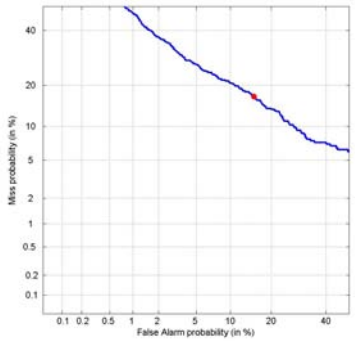

Figure 3.12.: *DET curve from Thumb VIS Geometric data Set*

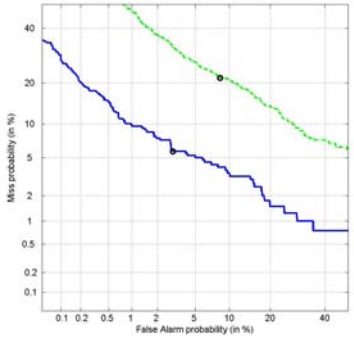

Figure 3.13.: *DET from two model performance. Hand VIS Geometric data Set vs. Thumb VIS Geometric data Set*

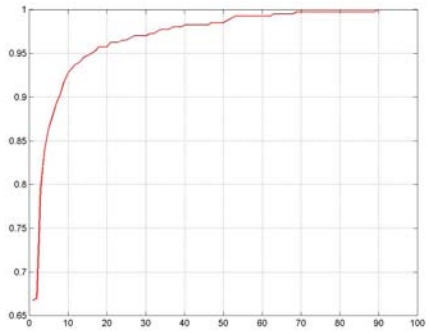

Figure 3.14.: *Example of a Cumulative Match Characteristic from Hand VIS Geometric data Set*

Definition 3.6: Detection Cost Function (DCF)

The Detection Cost Function is a trade-off between FAR and FRR from a practical point of view, where some of errors have different importance.

$$DCF = C_{FAR} \times FAR \times P_{gen} + C_{FRR} \times FRR \times P_{imp}$$

where C_{FAR} and C_{FRR} are costs of false acceptance and false rejection respectively and P_{gen} are the associated prior probability that the user will be a genuine user. For simplicity take $C_{FAR} = C_{FRR} = 1$ and also $P_{gen} = P_{imp} = \frac{1}{2}$

3.3. Identification Performance Measures

Verification is a simpler process than identification. In verification, the user biometric characteristic vector is compared only to the template he claims for, thus only a single match score is obtained. However, in identification operation, the biometric system needs to compare the biometric characteristic vector with all the templates present in the data base. If it is supposed to have c enrolled users, then c match scores will be obtained. Here, it is possible to differentiate two alternatives. The simple one is called closed world identification, where the biometric system always make a decision over one of the c possible enrolled users. This situation sometimes is far from reality where we can have an attempt to identify an unenrolled user. This second option, known as open world identification works with $c+1$ classes. In this last approach the biometric system has to consider another template associated to the reject option (user not enrolled)

In this thesis we only deal with closed world, where the input biometric feature vector is compared against the c templates in order to obtain the best match. The system reports the identity of the template corresponding to this best score.

Definition 3.7: Identification Rate

The identification rate gives us a measure of the ratio of successfully input biometric feature vectors mapped to the correct identity with the total number of attempts. In this computation it is understood that the question asked to the system is: does the best score correspond to the correct identity? It is possible to write as R_1, meaning account for the first top scores

Definition 3.8: Cumulative Match Characteristic (CMC)

Cumulative Match Characteristic (CMC) curve plots the rank-k identification rate against k. Rank-k R_k is the same of the previously identification measure. If R_1 accounts for the first top scores, when using R_k identification rate answer the question does the best k scores correspond to the correct identity?

The CMC has a relation to ROC, see [173] and an example of a CMC function is in Figure 3.14

3.4. Confusion Matrix

A confusion matrix also known as an error matrix shows the predicted values versus the actual results in a table. It can show results as a percentage or as a count. Thus, it can be used either by verification or by identification operation modes. In the case of verification the confusion matrix presents a binary classification (genuine and impostor), in the case of identification it will be a c case classification. The main drawback of this tool is when the number of classes is big enough, say, above a hundred of classes. In this context, confusion matrix is not practical because we can have more than a hundred or thousand users making it impossible to read.

The Pareto Confusion Matrix

This is one of the thesis contributions not initially intended for. In order to improve readability, and obtain only information from the users that fail in the authentication process, we have defined a new performance technique called: ***Pareto Confusion Matrix***. The idea behind is just to show the worse users and forget the correctly classified users. This can dramatically reduce the original confusion matrix, from a hundred rows to just ten percent.

We present here two different ways of visualizing the Pareto Confusion Matrix. Both ways work under the same assumptions and only differ in the distinctive element:color or size. If a geometric data set is used we have a hundred user classes, which means $c = 100$. The commonly used confusion matrix works as a matrix with a dimension equal to $c \times c$ so we drastically reduce this dimension. We present the resulting performance matrix in the two possible ways in Figure 3.15 and in Figure 3.16. The problem with user $U58$ that is incorrectly classified with user $U81$ three times and with $U90$ once is clearly highlighted. By taking advantage of this innovative way of presenting data, the new matrix has a dimension of 4×6.

The reason to present two graphical solutions is only to fit user requirements and to report conveniently. Both graphics keep the focus on the worst user scenario. In the color approach, the tile with the highest red color is linked with the worst identified user. As red intensity decreases so do user problems. Each tile also shows the number of misclassified attempts. The size approach uses a box, with lengths proportional to the errors. Here, again the number of misclassified attempts is showed.

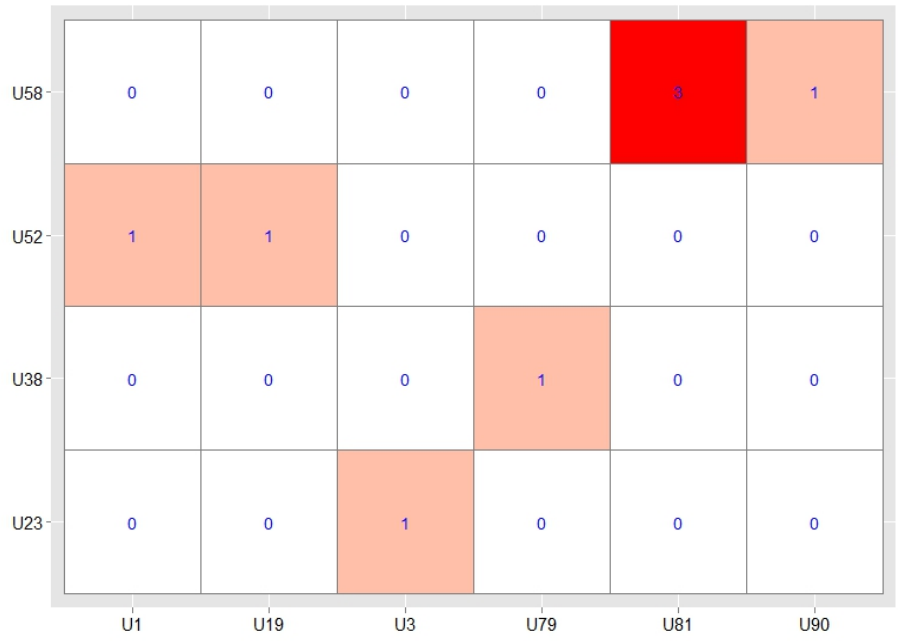

Figure 3.15.: *Pareto Confusion Matrix. Color Option*

It turns out, however, that sometimes there are many incorrectly classified users. Thus, there is an increase in the PCM dimension. We can overcome this drawback by working specifically with the worst users or by projecting the PCM so that we forget the decision axis (x-axis in the matrix). This approach can be seen in Figure 3.17 and in Figure 3.18.

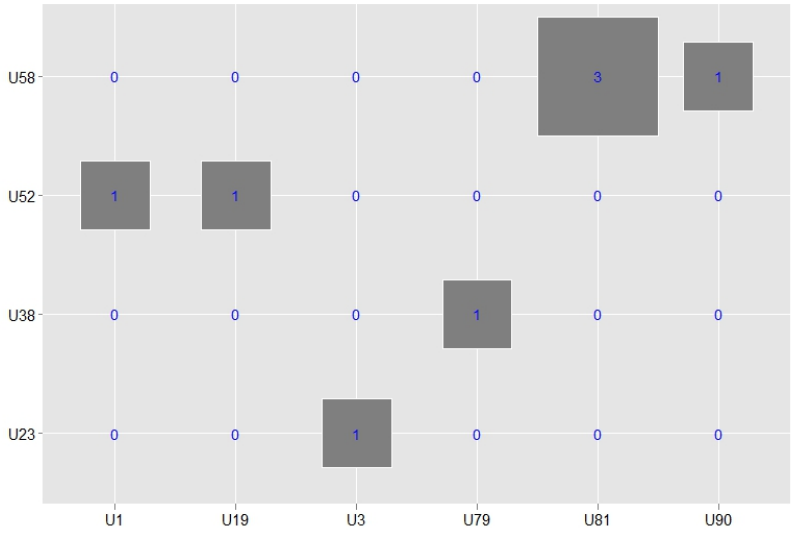

Figure 3.16.: *Pareto Confusion Matrix. Size Option*

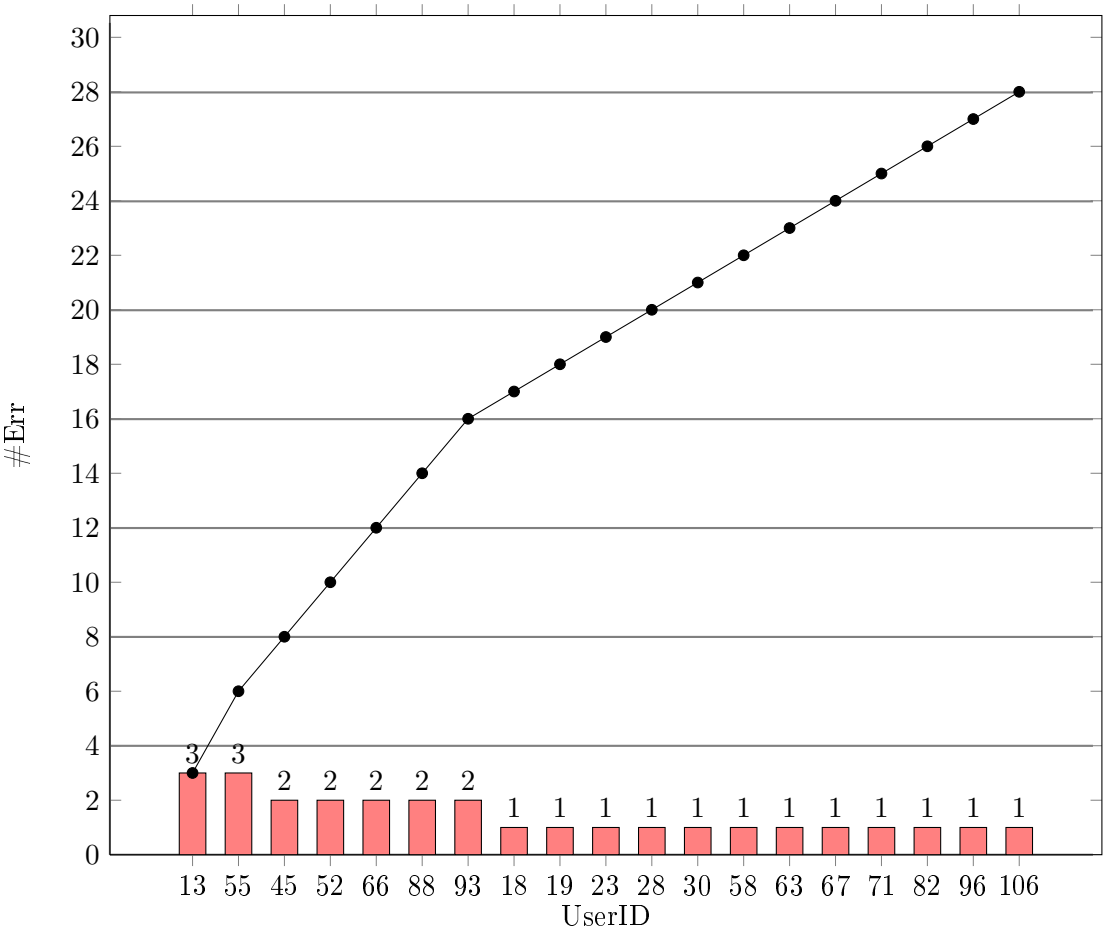

Figure 3.17.: *Pareto Accumulative Representation for Hand VIS Geometric Data*
Y axis shows the number of errors (misclassified users) and X axis the user identifier (users that fail)

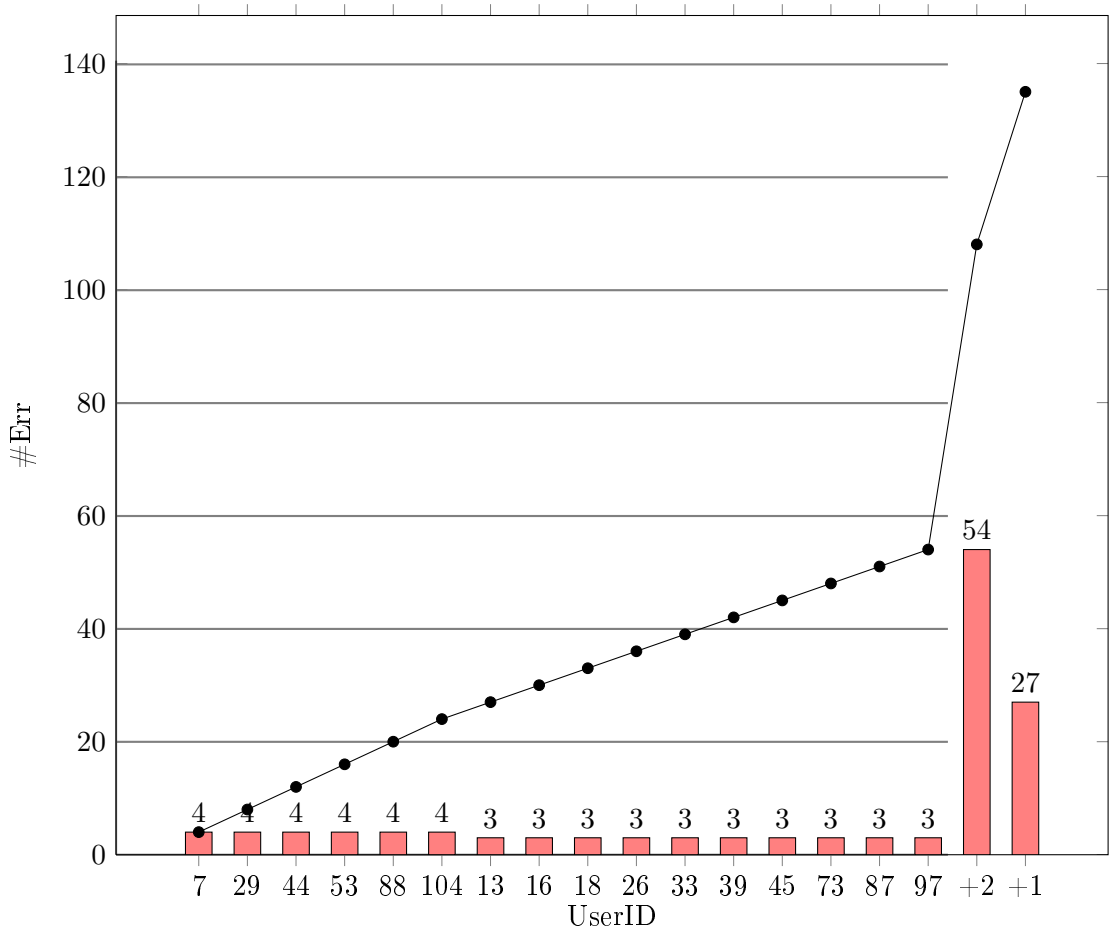

Figure 3.18.: *Pareto Accumulative Representation for Thumb VIS Geometric Data*
Y axis shows the number of errors (misclassified users) and X axis the user identifier (users that fail)

Chapter 4.

Combining Classifiers and Biometrics Fusion

unknown

Experience is not what happens to you;
it is what you do with what happens to you.

Overview

Recently there has been a lot of interest in multi-modal biometric systems. The idea behind biometric fusion is quite clear: to improve uni biometric systems and to obtain highly accurate and reliable systems. The major strength of these systems rely on the capacity to use more information, which can be from different sources such as different classification methods, and different biometric traits among others. Broadly speaking, the terms fusion and combining can be found in any field of research in an attempt to consolidate evidence for supporting better decisions.

Contents

4.1. Introduction

The idea behind combining different sources of information is always to improve decisions. Classifier fusion schemes have been treated with full extension and detail in some books ([6] and [108]), and in some journals([182], [37] and [187]) In our context, where we look for a better authentication performance system, this approach can lead us to :

- A complementary information not available when using one single biometric characteristic.
- A multiple sensors which can increase reliability.
- A selection of cheaper sensors that can be better than using one high sensitive sensor (extremely expensive).
- An improvement of biometric performance. It is supposed to happen when the information present in the system is wisely mixed.
- Avoiding the non-universality problem. One user can have a hand injury but the other modalities will be still present.
- Increasing system flexibility. System can use any piece of evidence instead of only one.
- Reducing noise. As we increase the number of pieces of evidence, noise should decrease.
- Being used as a hash method for huge biometric database in identification problems. One easy-to compute modality is used as an access to the database. This capacity to prune can help drastically reduce the computational time costs.
- More robust system. This robustness helps preventing any of the available attacks a system can suffer (at least can be highly reduced). It will be extremely difficult for an intruder to violate the requirements of systems.

It turns out this approach change a little bit the initial paradigm already seen. Instead of looking for the best classifier method (trying to develop more sophisticated ones) or by looking for the best set of features or by improving data extraction methods, now we can move on our efforts by looking for the best set of classification methods [98] and the best way to combine them.

As it has been stated by other researchers a long time ago describing in some sense this new approach *"to solve really hard problems, we'll have to use several different representations ... and ... we should work at a higher level of organization and discover how to build managerial systems to exploit the different virtues and evade the different limitations of each of these ways of comparing things"* (see [137])

Our research thesis takes a clear bet on that direction, since we are working with three different representations (VIS, NIR and TIR) and from each of these we might be able to generate almost a huge number of different data sets.

4.2. Source of Evidence

When dealing with multi biometric systems, different sources of information are possible. Here we describe some of these options:

- Multiple sensors. Using a VIS, NIR and TIR camera sensor.
- Multiple Modalities: Face, Hand Geometry, Signature.
- Multiple Instances: Left and Right hand. Dorsal and Palm hand.
- Multiple Samples: helps improving estimation of statistical measures such as variance.
- Multiple Representations: DCT2, PCA, Perimeter representation in Hand-Based analysis.
- Multiple Algorithms: LDA, BDM, KNN, SVM.

When the biometric system uses different modalities, this system is called Multi-modal Biometric System. From this point, however, we just focus on general multi biometric system and refer to them as hybrid systems. It means they can involve any of the options described. Whatever the option chosen, this general framework fits the approach to solve difficult pattern recognition problems involving large class sets and noisy input with the help of some subset of the different sources described above. Here we detail some of the different sources of evidence.

Multiple Sensors

Using different sensors helps introducing a new source of information without increasing the time to proceed to the acquisition process. Imagine a face or a hand acquired by a single CCD optical sensor. This information, with a wavelength ranging from 0.4 to 0.7 μm is the same as those we use for recognition through our optical system. The incorporation of another electromagnetic spectrum can be very useful, cheap and without cost for the user. Adding a NIR image that spans approximately between 0.7 to 1.1 μm of the same face or hand is straightforward. The same CCD used in solid state cameras are also sensible in the NIR range of frequencies. So it is enough to make same arrangements dropping the NIR filter and replacing it by a VIS filter (see Figure 7.1). Another sensor,

not without cost, is adding TIR images. This Thermal Infrared (TIR) is especially interesting with sub-band of Far InfraRed (FIR) spectrum that goes from 3 μm to 14 μm. In Figure 7.2 it is possible to see a professional camera from a vendor that costs approximately 8.000 euros.

Figure 4.1.: *Commercial Thermographic Camera. Model Testo 882-3*

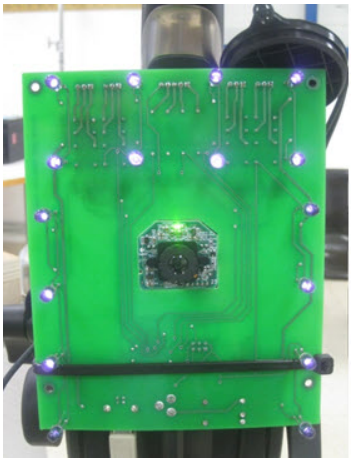

Figure 4.2.: *Own Disegned NIR camera with Infrared Leds*

Multiple Modalities

Using different modalities has become a practical and commonly used approach to improve performance. The reason lies on the fact that different modalities give absolutely different information, say, for example, face, hand (see Figure 4.3) and signature (see Figure 4.4).

Figure 4.3.: *Palmprint*

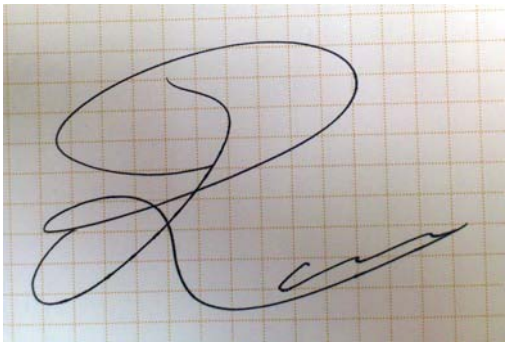

Figure 4.4.: *Signature*

Multiple Instances

The use of multiple instance, [6], like left and right eye or left and right hand can give us better evidence over the whole identification process. However, the effectiveness of multiple instance is not higher than adding new modalities. Sometimes it is difficult to categorize how dorsal (see Figure 4.5) and palmar (see Figure 4.6) information are multiple instance or multiple modalities. However from an strictly definition point they come from multiple instance.

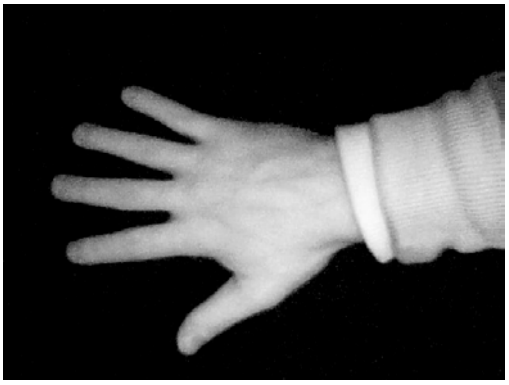

Figure 4.5.: *Dorsal print*

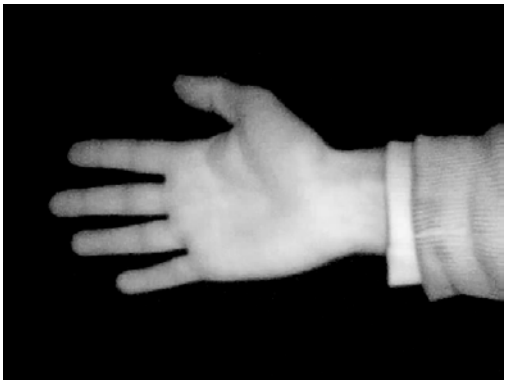

Figure 4.6.: *Palm print*

Multiple Samples

The use of multiple samples has been applied since first biometric systems. Samples acquired by the same sensor and by the same user helps improving estimation of variation within user. Samples should be captured in different sessions in order to drop possible correlation effects. Databases with a high number of samples help more than with low number, because there is room to design the way it is deployed by testing and training.

Multiple Representations

There are many ways to deal with the approach in order to build the characteristic vector. Always there is a need to reduce dimensionality and for this reason methods like Discrete Cosine Transform (DCT), Principal Component Analysis (PCA) or Multidimensional Scaling (MDS) can be used to reduce and better represent raw data.

DCT2: Discrete Cosine Transform (DCT) has emerged as the de-facto image transformation in most visual systems. DCT has been widely deployed by modern video coding standards, for example, MPEG, JVT etc. Its main properties are decorrelation, energy compaction, separability, symmetry and orthogonality. Some examples using DCT are found in [240] and [146].

PCA: Principal Component Analysis has been widely used to reduce the feature vector dimension. The objective is to figure out a way to reduce the number of variables to some components (or factors) with a minimal loss of information. This is done through eigenvectors and eigenvalues that help in finding directions with the largest variance and subsequently project the data on it. Some practical examples can be seen in [11] and [217].

MDS: Multidimensional Scaling is based on another well known mathematical principle known as perceptual mapping. The construction of this perceptual map is based on obtaining similarity among instances as close as we can by using less dimensions than initially.

To illustrate this effect, let us suppose we acquire an initial hand image with a typical resolution of 640×480 pixels. It is not a high resolution image but provides an easy way to make clear the course of dimensionality, because working with this raw image means 307200 variables (one for each pixel). Thus, the effect of representation can be seen in Figure 4.7 where a DCT2 has been applied and a vector with lengths from 100, 250 and 500 are enough to discriminate a hand shape. An improvement in perception is shown in Figure 4.8 where the DCT2 dimension has increased to 1000, 1500 and 2000 and better judgement is made as we raise the length of the DCT2 vector. However, increasing this vector does not guarantee any improvement in authentication performance.

Multiple Algorithms

Different algorithm methods can be used in order to improve biometric performance. The strongest performance requirements imposed by many applications can enable us use different algorithms, say, experts to solve the problem. An integration scheme is always required to fuse the information churned out by the individual algorithms. Many times the approach to pattern recognition problems was to introduce a new and sophisticated method (algorithm) to solve some specific problems. In other situations the approach was to simply modify or extend an existing and well-known method to make it more robust, quick, and better for the new faced problem. Here we present a set of well known classification algorithms that will be used all trough the thesis.

According to the Oxford English Dictionary, classification is defined as: *The action of classifying or arranging in classes, according to common characteristics or affinities; assignment to the proper class* The classification is then, a process that tries to assign class labels to object (user). In reality, users are represented by sets of measurements taken on various aspects of form, structure and content and called characteristic vector.

Discriminative Methods: This methods usually have a common approach. Involves finding a variate, which is no more than a linear combination of independent variables that will discriminate best between objects in the previously defined groups. In other words, discriminant analysis is concerned with the relationship between a categorical

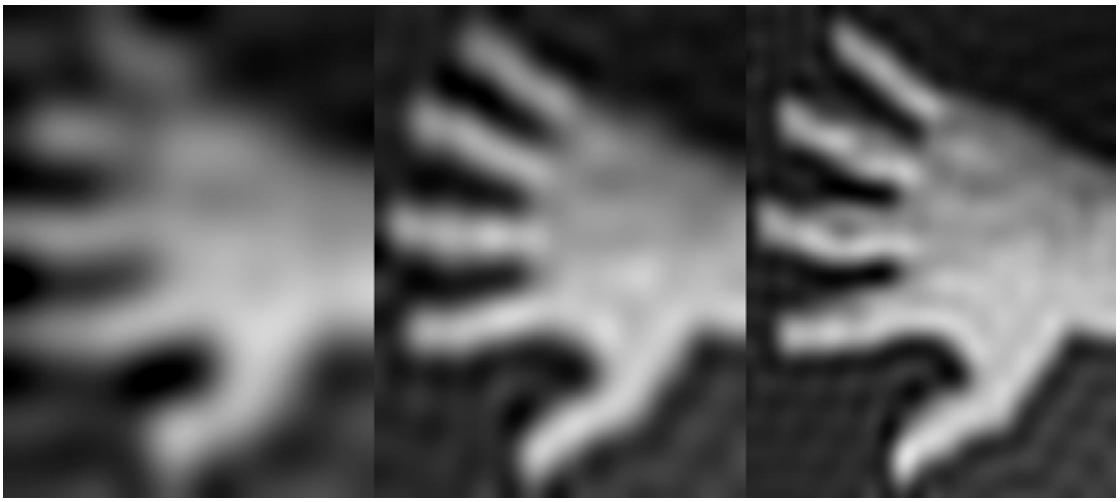

Figure 4.7.: *DCT2 with only d=100, 250 and 500 components*

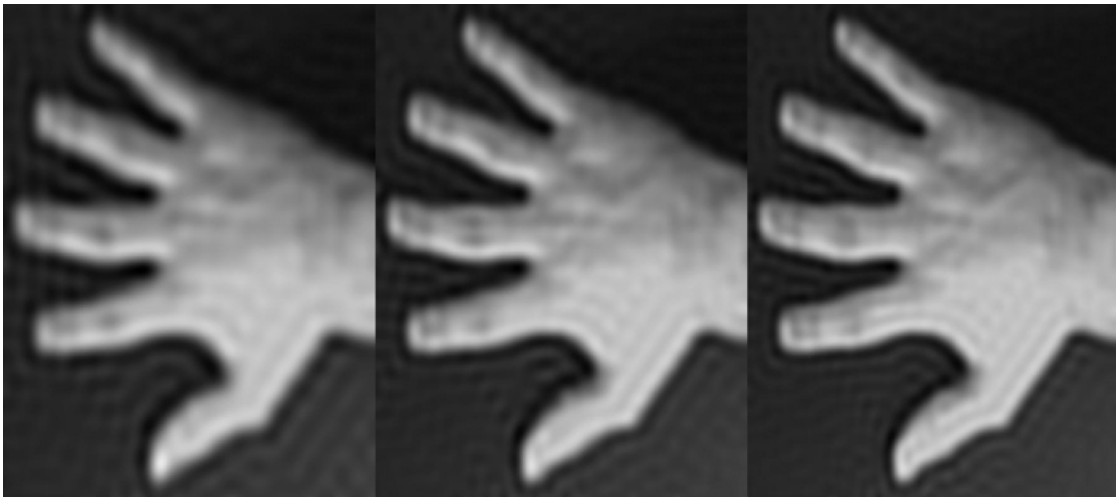

Figure 4.8.: *DCT2 with only d=1000, 1500 and 2000 components*

variable (user identification labels, gender class label, and so on) and a set of interrelated variables (finger length, finger width, and so on). The groups are always known a priori (we have c groups-users or $c+1$ to represent unenroled case) and it means the construction of c discriminative functions (one for every class).

Fisher Algorithm: The method was first introduced in [56] and has been used and improved since then. It tries to solve the following objective:

$$J(w) = \frac{w' S_B w}{w' S_W w} \tag{4.1}$$

where S_B stands for "between classes scatter matrix" and S_W for "within classes scatter matrix". The definition of both covariance matrices are as follows

$$S_B = \sum_c N_c (\mu_c - \overline{x}) (\mu_c - \overline{x})' \tag{4.2}$$

$$S_W = \sum_c \sum_{i \in c} (x_i - \mu_c) (x_i - \mu_c)' \tag{4.3}$$

where N_c is the number of cases in class c and

$$\mu_c = \frac{1}{N_c} \sum_{i \in c} x_i \tag{4.4}$$

$$\overline{x} = \frac{1}{N} \sum_i x_i = \frac{1}{N} \sum_c N_c \mu_c \tag{4.5}$$

A good solution is one where the class means are well separated, measured relative to the variances of the data assigned to a particular class. Because the total scatter matrix S_T can be computed as $S_W + S_B$ it is possible to interpret the main objective as maximizing the total scatter of the data while minimizing the within scatter of the classes.

Fisher DA is similar to LDA except that it builds a linear boundary without assuming that all classes have equal boundaries. When all classes have equal covariance matrices then the boundary is the same as in LDA. And an important property of Fisher DA boundary is determined by maximizing the ratio between class variation and within class variation, similar to maximizing the signal to noise ratio.

Linear Discriminant Analysis. Examples of the relation between some of these methods can be seen in [52]

Biometric Dispersion Matcher. As it has been stated in the first chapter, BDM trains a discriminant classifier that distinguishes between two groups:

- E: Equal groups are pairs from the same user (same class)

- U: Unequal groups are pairs from different user (different class)

$$g(\delta) = \frac{1}{2}\delta' \left(S_U^{-1} - S_E^{-1}\right)\delta + \frac{1}{2}\ln\left(\frac{|S_U|}{|S_E|}\right) \tag{4.6}$$

$$S_E = \xi(c-1)\sum_{i=1}^{c}\sum_{j,l=1}^{ns}(x_{ij} - x_{il})(x_{ij} - x_{il})' \tag{4.7}$$

$$S_U = \xi(c-1)\sum_{i,k=1}^{c}\sum_{j,l=1}^{ns}(x_{ij} - x_{kl})(x_{ij} - x_{kl})'; i \neq k \tag{4.8}$$

where $\xi = \frac{1}{cm^2(c-1)}$ and if $g(\delta) \geq 0$ then $\xi \in E$, indicating the two patterns belong to the same user.

Logistic Regression. This method is linked with regression methods but with a subtle change. The response variable is no longer a real variable, otherwise it is a factor (variable category)

Support Vector Machine. This method is based on a modifying data process by changing its representation. Tries to define a region, called margin, as big as possible that separates classes without there being any points inside. This margin is built with the help of support vectors. SVM are some of the most used methods in pattern recognition problems and machine learning as well. In [218] SVM is applied as a classification method but using LDA for dimensionality reduction and feature extraction.

K-Nearest Neighbour: This is also one of the most used methods for its simplicity and easy to program. The way it works is straightforward, once you define the number of classes K and the metric used as a dissimilarity measure. The method assigns the template to the closest neighbour according to the previously defined metric.

Generative Methods: This methods try to fit probability density to samples from each class. To obtain posterior density estimates, Bayes theorem is used extensively.

4.3. Fusion Architecture

There are important issues that must be faced in order to correctly design a fusion method. By fusion architecture we mean how to determine the information that should be consolidated. This consolidated information can take place in different stages of the authentication process (see Figure 4.9) From top to bottom the first step to consolidate data is from the acquisition step where sensors take data from the user. Called sensor level fusion or data level fusion has one advantage over the remaining steps: it takes information as it is, without extraction or any other dimension reduction technique. The next step to consolidate information is from feature level. Feature level fusion can be

done by concatenating feature vectors from different sources. However, some authors represent a middle step between sensor and feature level. In [41] a fusion scheme is made over covariance matrices. The other steps are from results stage. So score, rank and decision level fusion are consolidating information from the classifier model. Depending on how this result is obtained, so it should be the fusion strategy to be applied. If we deal with the matrix score, then is straightforward to apply fusion at score level. If the results are in ranks, then rank level fusion is the option. And, finally, if the model makes a decision, then, the recommended approach is decision level fusion. Last three fusion schemes are called fusion after matching (see [6] and [182]).

4.4. Fusion Approaches

There are different approaches to perform fusion. From the whole recognition process it is possible to realize that a fusion can be performed from different stages. From the top layer of recognition (data acquisition) to the last layer (decision) it can be possible to define fusion strategies at that specific level. Here we describe some of this approaches

Figure 4.9 shows the recognition process and where it is possible to perform fusion. In the right upper side of the Figure there are the two first fusion schemes: Sensor and Feature level fusion. In the left central side there are three additional schemes that work once the match is already computed. Here are depicted the following fusion levels: Score, Rank and Decision. The next subsections describe an overview of methods.

4.4.1. Sensor Level Fusion

Sensor level fusion is deployed on the top layer of recognition process. This fusion is performed before calculating the model and the match scores. Here we can work with the construction of a unique image coming from three different sensors, say VIS, NIR and TIR. There are many research studies consolidating this kind of information. For instance, two 2D views to build a 3D view.

4.4.2. Feature Level Fusion

This approach looks as an easy way to integrate information coming form different feature vectors. The application of a concatenation over the whole feature vectors available could be interesting, easy and straightforward. However, it should be taken with some care due to possible weaknesses. The first one comes from the increased dimensionality of the resulting vector. Size of the individual feature vectors and the number of features to be integrated can make unrealistic (course of dimensionality) working with this situation. The second one comes from the fact that there is no coherent representation of the whole new characteristic vector. Imagine an individual vector representing finger lengths and

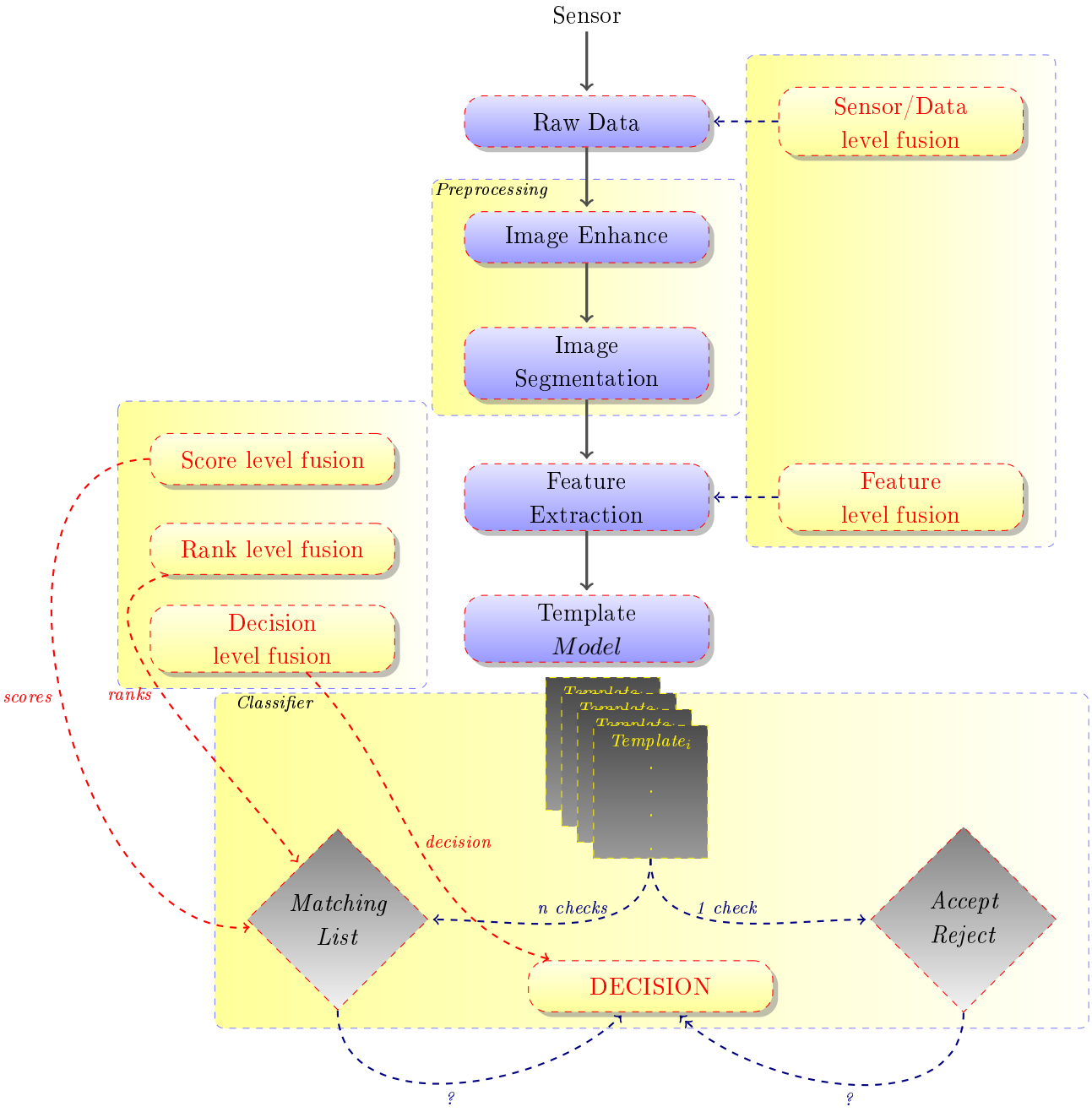

Figure 4.9.: *Biometric System and where Fusion can be applied.*

widths in pixels, and another vector representing finger lengths and widths as well but in meters. When concatenating, the first part would be clearly overweighted against the second one. Thus, concatenation has to be used with care and perhaps applying some normalization approach.

Other ways of looking at feature level fusion mean improving template information. Imagine the template currently uses lengths and widths. We have lengths from a VIS sensor, then we obtain another vector from a NIR sensor and finally from a TIR sensor. We could just use a simple mean to improve the length and width template.

Examples of feature level fusion will be found in [177], [228], [230] and in [97] comparing parallel and serial strategy.

4.4.3. Score Level Fusion

Trying to integrate multiple sources of evidence looks a wide option space through the different places where we can take a look into. One of the most promising fusion schemes comes from Score Level, where every matcher gives us the number that, later on, will be used to deploy the decision. In this sense, it seems to be better to work with score level than with other fusion schemes. The main point is to keep a look at the research done in this field. Almost 80 percent of the research with fusion takes this approach to improve biometric system performance. However, some challenging issues must be addressed in order to make the fusion operative. Issues are listed in the following points:

- The scores can represent, either a similarity measure (like results coming from BDM or LDA) or a dissimilarity measure (like distance). Before performing fusion it is advisable to put scores in an homogeneous way.
- The scores can be mapped in different scales range. If using distance we may have cm. or km. lengths so the scale linked to cm. will be overestimated when fusing. Here again should be advisable to work with this problem making scales comparable.
- The scores can be related to one another. It means, one matcher gives practically the same linear information than other matcher. This undesired situation should be avoided, at least if the fusion method applied is based on independence assumptions.
- The scores may be following quite completely different density functions. If the method states a gaussian distribution as an assumption, then, again, some kind of correction must be performed.

Some of these approaches can be seen in different papers: [75] exploits finger-vein pattern and improves performance through score level fusion. Other authors take into account quality measures to improve fusion [133], [13] or based on error rate minimization

[200]. Others work hand in hand with SVM methods such as [73] or in the design side [174].

Assumptions and General Rules

Assumptions usually stated to perform the following score level fusion rules are: from a Bayesian perspective, statistical independence. This assumption, allows us to rewrite the joint density function as a product of marginal conditional densities. Generally when dealing with fusion from different modalities (hand and face) it gives us uncorrelated scores. However, in other situations coming from multiple evidences like those coming from different algorithms (BDM, LDA or Fisher), usually tend to be correlated. That is obvious because all these methods come from the same linear discriminant family.

The general classification problem can be stated as follows:

Let Y be a raw data vector coming from a sensor. Let X be a feature vector understood as a pattern template used to authenticate, classify or whatever similar concept we have in mind. Let's suppose there are c different groups or users labeled as w_i with $i = 1, \ldots, c$. Let us suppose we have D different classifiers (or models). Then, from a Bayesian decision theory the input pattern X should be assigned to the class w that has the highest posterior probability. That is:

$$\text{if } P(w_k|x_1, \cdots, x_D) \geq P(w_i|x_1, \cdots, x_D)\ \forall i \in c \Rightarrow X \rightarrow w_k \tag{4.9}$$

The posterior probabilities in (4.9) can be expressed in terms of the conditional joint probability using Bayes rule. If we assume, independence across the D feature vectors, then it is possible to express the joint probability density as a product of marginal conditional densities (4.10).

$$p(x_1, \cdots, x_D|w_i) = \prod_{j=1}^{D} p(x_j|w_i) \tag{4.10}$$

The usual techniques from score decision fusion, are: product, mean, median, max and min rule. Assuming in all cases equal prior probabilities:

- Product Rule:

$$\text{if } \prod_{j=1}^{D} P(w_k|x_j) \geq \prod_{j=1}^{D} P(w_i|x_j)\ \forall i \in S \Rightarrow X \rightarrow w_k$$

- Mean Rule:

$$\text{if } \frac{\sum_{j=1}^{D} P(w_k|x_j)}{D} \geq \frac{\sum_{j=1}^{D} P(w_i|x_j)}{D}\ \forall i \in S \Rightarrow X \rightarrow w_k$$

- Median Rule:

$$\text{if } med_{j=1}^{D}\left[P(w_k|x_j)\right] \geq med_{j=1}^{D}[P(w_i|x_j)]\ \forall i \in S \Rightarrow X \rightarrow w_k$$

- Max Rule:

$$\text{if } \max_{j=1}^{D}\left[P(w_k|x_j)\right] \geq \max_{j=1}^{D}\left[P(w_i|x_j)\right]\ \forall i \in S \Rightarrow X \rightarrow w_k$$

- Min Rule:

$$\text{if } \min_{j=1}^{D}\left[P(w_k|x_j)\right] \geq \min_{j=1}^{D}\left[P(w_i|x_j)\right]\ \forall i \in S \Rightarrow X \rightarrow w_k$$

4.4.4. Rank Level Fusion

Rank level refers to an identification measure. For this reason it is a technique to improve identification rates trough a way to consolidate the rank coming from multiple sources of evidences.

Highest Rank Method

The easy way to apply rank level fusion is with a simple math function to identify the highest rank computed by different sources. Because the highest rank corresponds to the minimum value, the function to be used is *min*. To improve the strength of this method a minimum number of different sources is recommended. However we can find ties between them, which we can break them randomly.

Borda Count Method

This is another simple method to consolidate information. A single sum of the ranks of the different sources, tells us the lower the sum the better the evidence against this identity.

Logistic Regression Method

A generalization of the previous method applying a weighted sum. Weights can be estimated through a logistic regression model.

4.4.5. Decision Level Fusion

The decision level fusion is supposed to happen in the final layer of the pattern recognition process. This means, the decision made for any of the single biometric sources is available. We can find many research publications facing fusion in this way. In [7] a brief survey is presented and in [227] a recognition through decision level fusion.

AND, OR operators

Applying AND an OR operators over the final decisions can give us an easy method to integrate the full set of biometric decisions. The AND gives us a decision when all individual biometric decisions agree with the result. The OR operator gives us a decision as long as one biometric decision matches with the template. It is advisable to note that when AND is applied the FAR decreases while FRR increases. Similar behaviour happens but in the other direction when using OR operator, since FRR decreases and FAR increases. However using both operators degrades the overall performance.[!Ref]

Majority Voting

This is the most popular decision level fusion. It follows a democratic account, making the final decision where the majority of the individual decisions agree.

One way to improve majority voting is by applying a weighted scheme. The weight related to each of the individual biometric results is proportional to the ones with better performance.

4.4.6. Other Strategies

Strategy fusion comes from trained rules: Some classifiers should have more relevance on the final result. This is achieved by means of some weighting factors that are computed in the following way:

$$Comb = \alpha D_{VIS} + (1 - \alpha) D_{TH}$$

The effect of correlation between different biometric matchers should be avoided in order to expect better results when fusing, otherwise it is not at all sure to achieve any improvement in performance [108].

Some authors came up with a strategy that put weights on every matcher. This is called Matcher Weighting and is straightforward to apply once we obtain the score and the EER of each D classifiers. Thus

$$\sum_{j=1}^{D} W_j SC_j$$

where W_j in inversely proportional to EER. If the EER of the classifier j is r_j then

$$W_j = \frac{1/\sum_{j=1}^{D} \frac{1}{r_j}}{r_j}$$

With this we ensure weights sum up to 1. The idea behind reinforcing those matchers with better performance offer several variations. Some of them in a similar way, and others change the focus from matcher to user.

4.5. Normalization Techniques

In occasions, before trying to apply a fusion technique, it is necessary to homogenise scores [96]. Any fusion normalization technique can be viewed as a function that maps the scores from $\mathbb{R}$ to the $[0, 1]$ interval. The design of such function is absolutely open to the researcher.

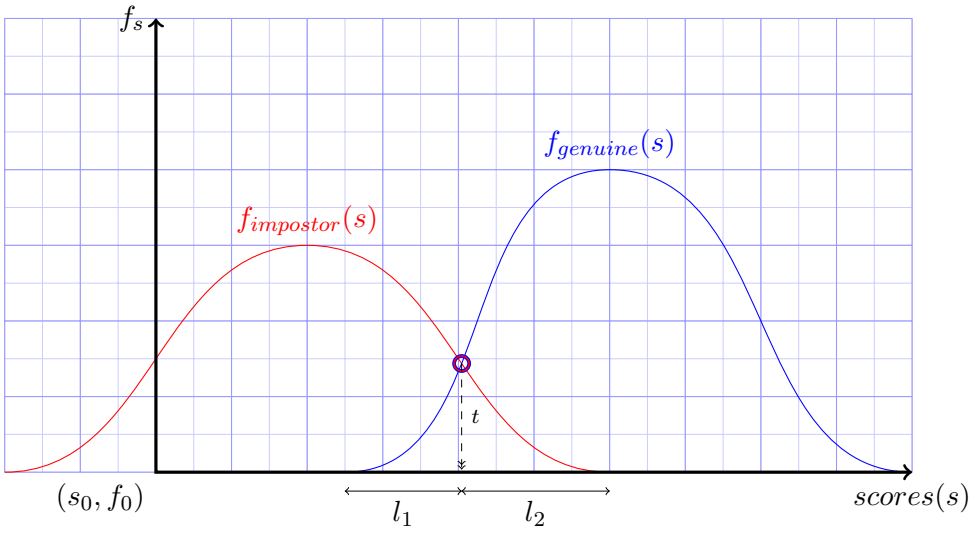

Figure 4.10.: *Genuine and Impostor Distribution. Key points for normalization techniques*

Let us define the following variables:

- S: Set of scores (total set, note that $S = S_{gen} \cup S_{imp}$).
- S_{gen}: Set of genuine scores.
- S_{imp}: Set of impostor scores.
- t: intersection point between densities f_{gen} and f_{imp}
- l_1: overlapping left to the t point. FRR zone
- l_2: overlapping right to the t point. FAR zone
- $w = l_1 + l_2$ represent total overlap region

Note that all variables are depicted in Figure 4.10

The Min-Max method maps the row scores to the $[0, 1]$ range. There are other variants similar to this one using median and median absolute deviation.

$$S_N = \frac{S - \min(S)}{\max(S) - \min(S)} \tag{4.11}$$

The z-score or normalized-score maps the row scores to a new range that do not guarantee the $[0, 1]$ range. The reason is because there are two operations inside this transformation. The first one consists of centring the new scores in the 0, thus mean is discarded. And the second operation discards the possible units and lets deviation score in 1. However, both mean and deviation are sensitive to the presence of outliers.

$$S_N = \frac{S - \text{mean}\left(S_{gen}\right)}{\text{std}\left(S_{gen}\right)} \tag{4.12}$$

The Hyperbolic Tangent is one of the robust methods that minimize the effect of outliers. The k parameter needs to be tuned to get good results. Values 0.01 and 0.5 give good results.

$$S_N = \frac{1}{2}\left\{\tanh\left(k\left(\frac{S - \text{mean}\left(S_{gen}\right)}{\text{std}\left(S_{gen}\right)}\right)\right) + 1\right\} \tag{4.13}$$

In the illustrations labelled Figure 4.11 and Figure 4.11 it can be seen the effect of the transformation described in (4.13) with parameter k equal to 0.2 and 0.5

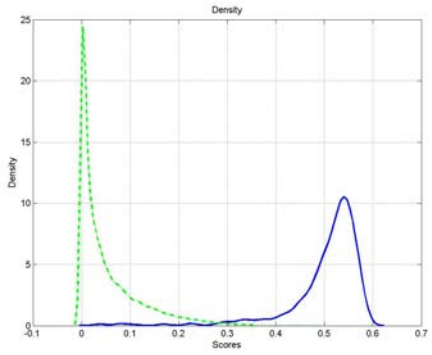

Figure 4.11.: *Genuine (blue) and Impostor (green) $k = 0.2$*

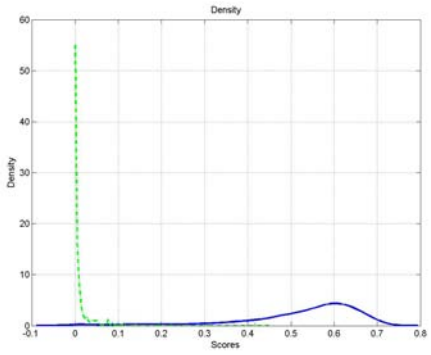

Figure 4.12.: *Genuine (blue) and Impostor (green) $k = 0.5$*

At this point, it is possible to think of two directions. The first one defining a predefined k parameter that will be used later on with whatever situation the system has to faced. The other one, is optimizing some quality function and uses this value as the best for that situation. If we have an original genuine and impostor distribution like that showed in Figure 4.13 we can compute the Dprime measure and see the maximum values close to 0.24 (see Figure 4.14) However this situation can be absolutely time consuming and the usual approach tries to test with some predefined k values.

Linear Transforming Mapping that defines clear boundaries under the minimum of genuine scores S_{gen} and over the median value of S_{gen}. At this point transformations

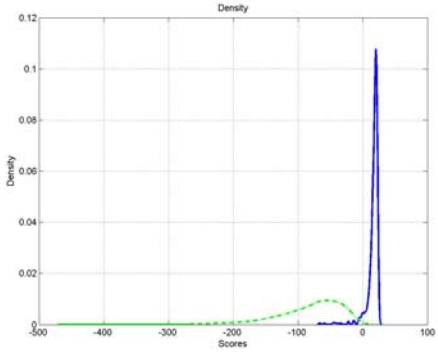

Figure 4.13.: *Initial Densities*

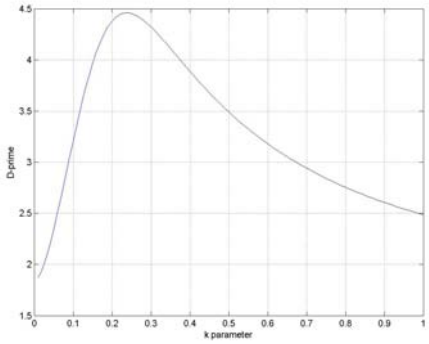

Figure 4.14.: *D-prime against k*

ensure new score values of 0 or 1.

$$S_N = \begin{cases} 0 & S \leq \min(S_{gen}) \\ \frac{S - \text{mean}(S_{gen})}{\text{mean}(S_{gen}) - \min(S_{gen})} & \min(S_{gen}) < S \leq \text{mean}(S_{gen}) \\ 1 & \text{mean}(S_{gen}) < S \end{cases} \tag{4.14}$$

There are times where the transformation can represent a backward step (see Figure 4.16). In other situations it is necessary to apply a readjustment over the scales (see Figure 4.15). This can be fully interpreted across the way genuine and impostor distributions are plotted or can be quantitatively stated. One measure to quantify separability between genuine and impostors are D-prime that gives 1.53 for linear transformation and 1.84 for z-score.

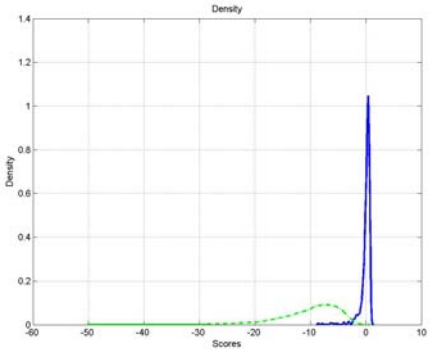

Figure 4.15.: *Genuine (blue) and Impostor (green) Z-Score Normalization*

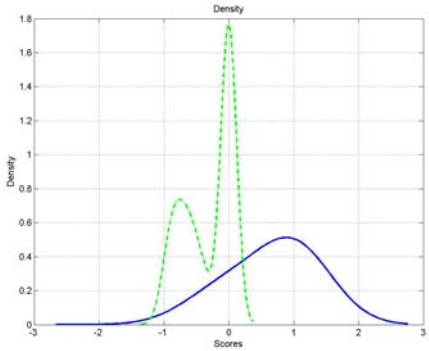

Figure 4.16.: *Genuine (blue) and Impostor (green) Linear Transformation*

Double Sigmoid Mapping performs a common normalization technique through a sigmoid function but this time linked with previously defined overlapping measures: t,

l_1 and l_2.

$$S_N = \begin{cases} \frac{1}{1+e^{-2\left(\frac{S-t}{l_1}\right)}} & S < t \\ \frac{1}{1+e^{-2\left(\frac{S-t}{l_2}\right)}} & S \geq t \end{cases} \tag{4.15}$$

Quadric Mapping taking as a reference point t

$$S_N = \begin{cases} \frac{S^2}{t} & S \leq t \\ t + \sqrt{(1-t)(S-t)} & S > t \end{cases} \tag{4.16}$$

Logistic Mapping with two parameters that can be taken with care to make score normalization scheme work properly. Instead of finding this parameters, one option is to use some predefined values, such as $\alpha = 99$ and $\beta = \frac{4.597}{t}$

$$S_N = \frac{1}{1 + \alpha e^{-\beta S}} \tag{4.17}$$

Linear and Quadric Mapping. In this case the linear mapping is applied for values close to the intersection point t and outside the transformation takes a quadratic form.

$$S_N = \begin{cases} \frac{S^2}{t-\frac{w}{2}} & S \leq t - \frac{w}{2} \\ S & t - \frac{w}{2} < s \leq t + \frac{w}{2} \\ t + \frac{w}{2} + \sqrt{\left(1 - t - \frac{w}{2}\right)\left(S - t - \frac{w}{2}\right)} & S > t + \frac{w}{2} \end{cases} \tag{4.18}$$

One of the major drawbacks of these approaches comes from the fact that the estimation of the genuine score density is not reliable enough. The reason becomes clear as the data coming from both groups (genuine and impostor) are absolutely different.

Chapter 5.

Thermography

Sir Winston Churchill

Success consists of going from failure to failure without loss of enthusiasm.

Overview

Temperature has been proved to be a very good indicator of health. Basically because human beings are homoeotherm and it is essential to keep a constant body temperature to survive. For a proper operating function of our body we need to maintain a constant temperature. If this temperature moves upward or downward, then it could be read as a clear indication of probable illness. Temperature has been also proved as a very good measure for insulation in engineering and architecture. Temperature helps in mechanical and electrical engineering in order to detect failure.

Contents

5.1. Introduction to Thermography

Temperature has been utilized since almost 4000 years ago. There, in 1600 BC fever was diagnosed in ancient Mesopotamia [185] and 500 years later Hippocrates used to determine the health of patients. However, thermal imaging is based on a principle stated in 1800 AD when William Herschel discovered infrared rays. Later in 1840 Sir John Herschel produced the first infrared thermogram using a method that he called evaporography. It took almost a century before M. Czerny built the first evapograph, which was the first one working infrared device. That was in 1929 just a few steps ahead of Second World War Conflict. The first infrared line scanner was developed in 1946 by military. The image last one hour to process. In 1954 infrared scanners took 45 minutes to process. By 1960 the time to obtain, process an image was reduced to 5 minutes.

The first commercial versions were derived from military and was not until early 90's when high resolution infrared Focal Plane Arrays (FPA) provided hundred of images per second.

What is temperature? Temperature can be defined as a measure of the average kinetic vibrational energy of the molecules of a substance or object. Through this way objects emit a distribution of electromagnetic radiation that is uniquely related to the object temperature. This is the key fundamental principle that makes thermographic devices detect infrared energy emitted from any object.

5.2. Thermographic Physical Principle

The basic thermographic physical principle is based on a well known field called thermodynamics and heat transfer. Some knowledge of thermodynamics laws are convenient in order to get the most of thermographic images. Detection of radiation, emissivity and atmospheric transmittance can be seen in detail in [77]. The infrared radiation is emitted by all materials above 0 degrees kelvin or -273 degrees C. This infrared energy is proportional to their temperature. Infrared cameras convert the emissions into an electrical signal by the image sensor (microbolometer) and displayed as a color heat image called thermography.

- **The Zeroth Law of Thermodynamics**: If two objects, say A and B, are separately in thermal equilibrium with a third object, say C. Then A and B are also in thermal equilibrium with each other.
- **The First Law of Thermodynamics**: Heat that flows to or from one object must go somewhere. Energy must be conserved, can not be created or destroyed, only changed from one form to another.
- **The Second Law of Thermodynamics**: The entropy of a system which is not

in equilibrium will move to an entropy that let the system in equilibrium. In other words, heat will flow from hot areas to cool areas until equilibrium is reached.

- **The Third Law of Thermodynamics**: The entropy of a system approaches a constant value as the temperature approaches zero. This state is called zero entropy.

When a professional thermographer looks at an image like those showed in Figure 5.1 and in Figure 5.2 he should realize the radiated energy is only seen from the first tenth of a millimetre of the surface of that object.

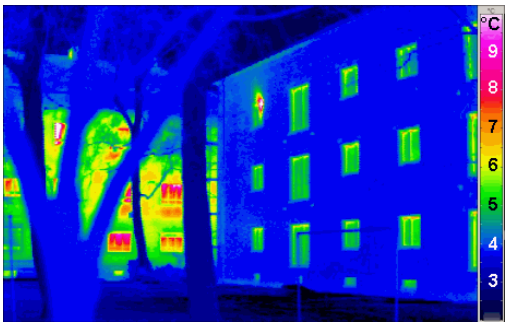

Figure 5.1.: *Building Insulation*

Figure 5.2.: *Electrical fault*

Some suggested questions arise. Is the surface material a conductor or an insulator? How far does the energy have to travel to get the surface? What does the temperature difference really mean? Although interpretation can seem straightforward, it is not. Temperature measurement acquired by the thermographic camera actually reads three sources of thermal energy. That is: energy emitted (by the object itself), energy reflected and energy transmitted. The important measure comes from emitted energy source.

5.3. Electromagnetic Spectrum

The electromagnetic spectrum helps us to easily locate where the thermographic spectrum bands are, the near infrared bands and the visual bands as well. It is a chart of energy which describes the full range of known electromagnetic radiation types (see Figure 5.3). We could find waves from low frequencies radio waves as long as $> 1000m$ down to high frequencies such as gamma rays $\frac{1}{1000000000}m$.

Since electromagnetic radiation, especially the infrared one, is emitted by all objects based on their temperatures, according to the black body radiation law, it is possible to see living beings and warm objects with or without visible illumination. A particularly interesting sub-band of FIR spectrum lies from $3\mu m$ to $14\mu m$, called Thermal Infrared (TIR), which humans experience every day in the form of heat or thermal radiation.

This special band of the spectrum presents two important windows called Mid Wave IR (MWIR) comprised of the range between 3 and $5\mu m$, and Long Wave IR (LWIR), which lies in the range between $8\mu m$ to $14\mu m$. Between them a blocked band exists due to the contamination by solar reflectance and water steam absorption.

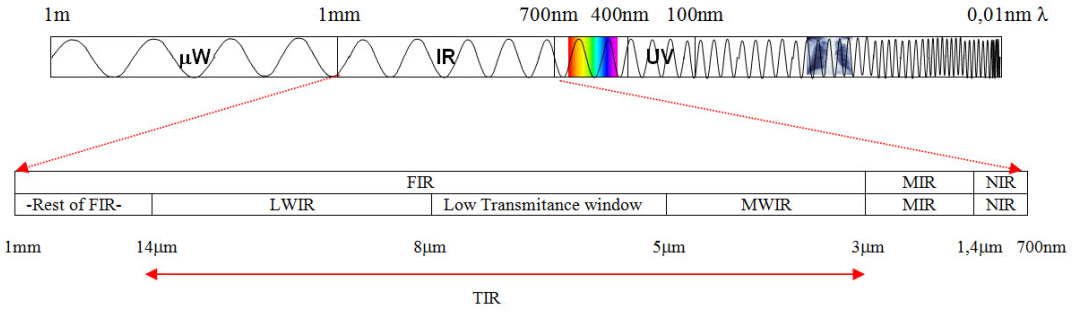

Figure 5.3.: *Electromagnetic Spectrum*

5.4. Skin's physiology

The use of thermography in military and engineering applications is always linked with a high knowledge of the object we are interested in. It could be a tank or a car engine. In the same way, for a better understanding of the applications we are involved with, a basic knowledge of the underlying surface is essential. This means the skin. In security applications this issue is some times forgotten and usually underestimated. From a medical and healthy perspective this issue is absolutely essential. In this section we describe the basic structure and function of the (human) skin. This knowledge gives us clues to the experimental results we will face later on.

5.4.1. Skin structure

The skin is composed of three different layers. The first one is the epidermis, which we usually see with our eyes and may have different textures and colors depending on age, gender or other factors. Under this layer there is the second layer called the dermis, which contains the connectivity tissue, blood vessels and nerves. The third and last layer of skin is the hipothermis, which is fixed with muscle fascia and contains adipose tissue. A clear color view of skin components can be seen in Figure 5.4 where the three basic layers that will be briefly described are shown.

Epidermis

This component of the skin is the thinnest one. In some cases, it is possible to see under this thin layer, almost translucent, the blood vessels and pink hue underneath it (see Figure 5.4). The epidermis provides a barrier to the outside world protecting the body the threatened environment. It has no blood vessels, so all its nutrients come from the dermis. Its basic cell is called keratinocytes.

Dermis

This layer offers a protective function along side the epidermis, and helps retain water and nutrients. It is worth mentioning the most interesting function that affects the quality and the understanding of TIR images called thermoregulation. Dermis helps regulate the temperature of the body. Nevertheless, the heat of the body comes from metabolism and muscles exercise, and it is lost at peripherical parts, especially through the dermis skin. So the dynamics of surface temperature distribution is governed by blood flow in this layer, heat conduction from deeper blood vessels and sweat evaporation from surface. The dermis is composed of connectivity tissue, amorphus matrix (colagen, elastin, glicoproteins, and other elements) and, between them, glands and nerve system. Many blood cells circulate through the dermis, most of them involved in the immune function of the skin, allergic reactions, and body defences against infection and tumor surveillance. Some of these cells are monocytes, macrophags, dermodendrocytes, and mast cells. There is a great vascular interconnection within this layer that makes it difficult for blood flow to be blocked. The walls of the blood vessels are the thickest in the deeper dermis section and the thinnest in the superficial one.

The skin has a regulation system to allow blood to be shunted away from superficial dermis. These shunts are called glomus bodies and drive blood from arterioles to venulles and contain muscle cells which are innervated by nerves of the sympathetic nervous system. Extremities such as finger, toes, ears and nose contain the highest number of these shunts.

The skin is extremely sensitive to temperature change. With high accuracy our body can detect variations in temperature of 0.1 C and when variations with respect our body temperature (approximately 36 C) increase, for instance in summer season, our body engine tries to lose heat through the skin. It is in this layer where heat produced by the body core is pushed away through the cutaneous vascular system in order to transfer heat to the outside. As temperature rises again, more blood flows increases in dermis. When environment conditions go in the other direction, decresing the temperature (i.e. winter season), our skin preserves temperature by decreasing blood flow by reflex vasoconstriction. Between 5 and 10 % volume cardiac output goes to through skin but can rise up to 7 times in extrem hot conditions or to 0 in extrem cold conditions.

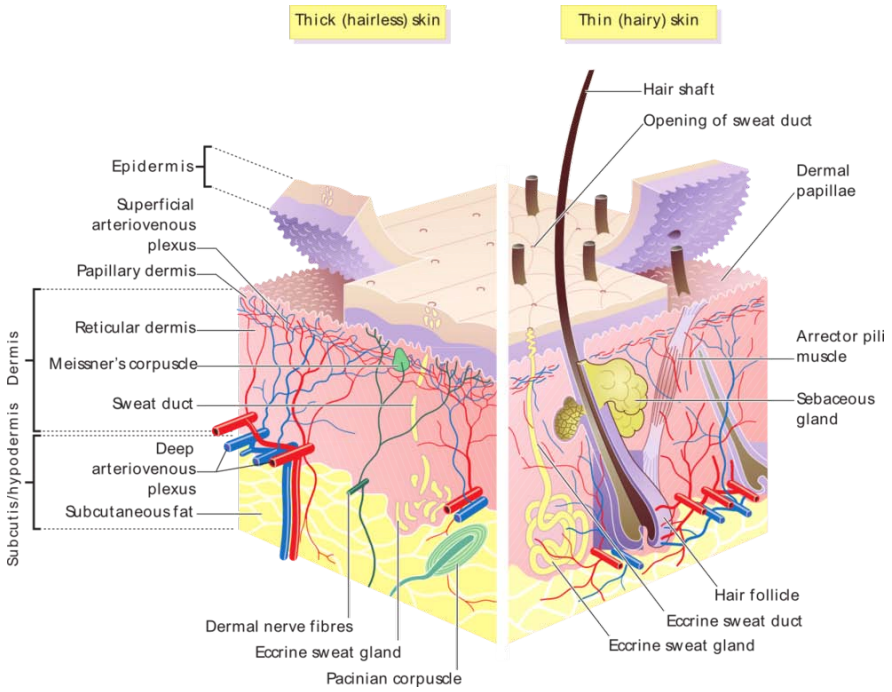

Figure 5.4.: *Skin Layers*

Hypodermis

The last layer of the skin, mainly composed by adipose tissue contains the areas where we can find hair roots, sweat glands, nerves, vessels and lympha. Obviously, this skin component has a function related to anchoring with the muscle fascia layer. Heat loss is also induced by evaporation through sweating. Hair follicles are innervated by extensively branched nerve fibers.

5.5. Applications

The knowledge of skin provides us with a clear insight of its function and structure, and its deep relation with heat which can be monitored with thermography. If thermogaphy images are acquired for training and these sessions were performed in winter and we proceed to test the system with thermographic images made in summer the heat patterns of the same person will be completely different from those taken during training. We can see this interpretation in Part IV.

Here we illustrate another example that comes from sport field. In a continued exercise of going up and down a staircase (>50 steps), we obtain an image of two completely different users. We called one of them trained (or runner trained), and the other one as no trained. Is the response of the knee heat pattern different from one another? See

both images in Figure 5.5 for the no runner user and Figure 5.6 for the runner user. It is easy to appreciate a clear homogeneous heat pattern for the trained user, while from the no trained user there is an obvious view of vain pattern.

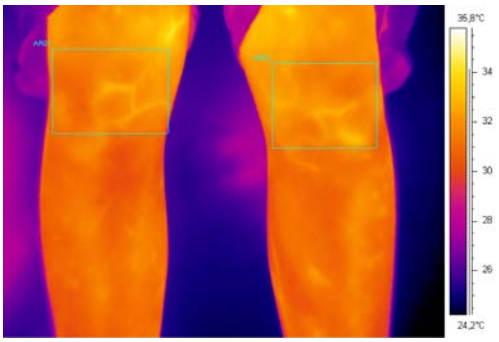

Figure 5.5.: *No runner knees*

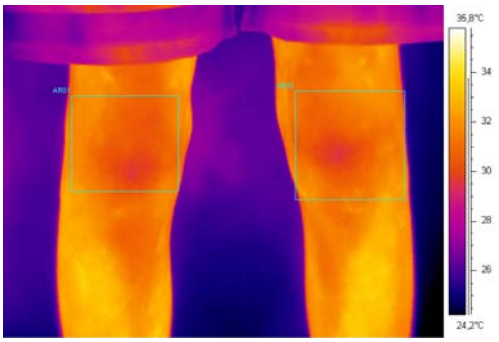

Figure 5.6.: *Runner knees*

What happens is that in intense exercise and also during heat exposure, skin blood flow can increase to provide better and greater heat dissipating capacity. These properties combined with increased cutaneous circulation (as previously described) operate as an exceptional radiator. There is another factor that helps in this process and that usually plays the role jointly, sweating. With sweat the skin surface increases the heat dissipating process. Here it is not well appreciated but the mean temperature of both left and right knees from trained user and untrained user is greater than 2 degrees C. That means that the untrained user needs further circulation in order to decrease the effort made by the knee. This is quite similar to what happens with engines.

The next figures show a hand pair from a user where there is also a clear difference between them in resting conditions. In Figure 5.7 it is possible to appreciate a completely different effect from the one that has been described with knee. When there is an exposure to cold environment, the skin surface almost eliminates blood circulation and for this reason the skin becomes an efficient insulator. The main goal is to keep our body warm and that is exactly what skin thermoregulation does. However, here, with the same environmental conditions, one user has cold hands while the other one does not (Figure 5.8).

There are many examples of thermographic uses. Here we describe some of them from a reliability and safety perspective.

From a medical perspective Table 5.1 shows some of the most common thermographic applications.

From a medical perspective, thermographic images help many times with relative temperatures rather than absolute temperatures. Thus, it is necessary to know the standard difference mean values to correctly estimate the differences from same body areas (see Table 5.1).

Table 5.1.: *Thermographic Medical Research Applications*

Application	
Breast cancer detection	Vertebrae (nerve problems/arthritis)
Diabetes	Endocrine Disorders
Fever screening	Locomotors Disorders
Dermatological applications	Skin Problems
Diagnosis of rheumatic diseases	Respiratory dysfunctions
Vascular and Heart operation	Lymphatic dysfunctions
Gynecology	Reproductive disorders

Source: different sources

Table 5.2.: *Temperature differences of various body sides*

Body segment	Mean temperature difference (°C)
Forehead	0.12
Cheek	0.18
Chest	0.14
Abdomen	0.18
Arm (biceps)	0.13
Palm (medial)	0.23
Foot (dorsal)	0.30
Finger-tips average	0.38
Toe-tips average	0.50

Source: adapted from [111]

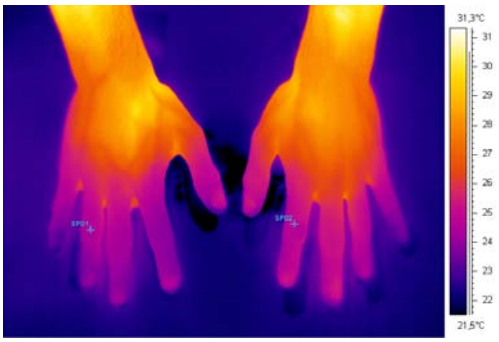

Figure 5.7.: *Cold Hands*

Figure 5.8.: *Warm Hands*

As stated in [131] different studies recommend some standardized procedure in order to acquire thermographic images for medical uses. Among them we can find average room temperature and acclimation time as shown in Table 5.3. The reason, minimize changes in cutaneous temperature due to environmental conditions or muscle activity. When thermographic is deployed in non medical environment this care is no longer needed and in occasions no longer possible. For instance, as a biometric device it is not possible to wait for users to stand up for 15 minutes or more in order to proceed with recognition. Thus the image has to be taken immediately, otherwise no user gives credit to the biometric system in use.

With thermography we can work in two different ways. The first one is through absolute temperatures. This approach, sometimes called quantitative approach is commonly used when we can get an accurate temperature at a specific point. This benchmark is used to obtain fairly accurate temperature measures at any point. The other one is through relative temperatures. This option, called quantitative option, is generally used to identify different heat patterns within the same patient. For example, in order to identify breast cancer, what comes to light is a clear temperature difference between the two breasts. However, in both cases the real issue is how accurate one needs to be in measuring temperatures. This approach is also used in electrical maintenance where it is enough to identify a point or area that is hotter than that from neighbourhood. Table 5.4 shows different applications in the field of reliability and sustainability engineering.

Table 5.3.: *Medical Thermography Experimentation*

Study	Experimental Conditions	
	room temperature (°C)	Acclimation time (min)
Diabetic neuropathy	25	5
Thermoregulation	24	10
Shoulder impingement syndrome	20	15
Facial telethermography	22	15

Source: adapted from [111]

Table 5.4.: *Uses in Electrical and Engineering Applications*

Equipment	Predictive and Preventive Maintenance	
	A	B
Electrical		
	Motor control centers	Transformers
	Substations and Switchgear	Drives
	Overhear Power Lines	UPS
	Terminal Strips	Power Cables
Non Electrical		
	Identify damaged insulation	or refractory
		or build up roofs
	Verifying cooling tower efficiency	or condense coil
		or convection heater/cooler
	Analyse building heat loss	or temperature profiles

Source: adapted from [178]

Chapter 6.

Hand-Based Biometric Systems

James M. Barrie

The secret of happiness is not in doing what one likes,
but in liking in what one has to do.

Overview

Here it is presented a complete background of the hand as a biometric trait. Unlike fingerprint, hand is not unique and means not discriminative enough for identification. However when combined with other individual features, hand biometric systems can perform quite well in verification environments. In this chapter we highlight the state of the art in hand recognition. Through the different approaches, biometric system can deal with some of the many features hand offers. That is, fingerprint (although is treated as an own biometric characteristic), palmprint, dorsalprint, hand geometry and so forth. We detail its main advantages and disadvantages as well as its performance.

Contents

6.1. Introduction to Hand Biometric Trait

Hand is defined as the part of the body at the end of the arm, consisting of five fingers and a palm. The join between the forearm and the hand is called wrist. The five fingers are called: thumb, index finger, middle finger, ring finger and pinky finger (see Figure 6.1). There are three mainly approaches to hand characteristics: Fingertips, palmprint and hand-shape geometry. From an anatomical point of view hand has two sides: dorsal which is not generally used and palmar which is extendedly used.

Palmar side is the preferred to extract the desired characteristics. From palm side hand we can extract: fingertips, palmprint and hand-shape geometry measures (see Figure 6.1).

Hand, as other physiological characteristics remain equal after certain age. Hand biometric devices perform quite well in controlling granted access instead of card passes that can be forgotten or stolen. It is easy to use and is non-intrusive. Hand biometric device usually works under the following schema: A person's hand is placed on a surface and the system through a sensor (VIS sensor) measure and analyse the hand structure, the hand shape and any other interesting measure significantly enough to help identify users. Then the system can compute hand proportions using lengths and widths, skin surface like creases and ridges and perform any other computation to extract a strong feature vector.

Some of the disadvantage hand biometric system can face are: injuries, jewellery, bracelets, rings and watches. In the first case the solution is in some way direct because it is only necessary to update the system with the new (injured) hand. Another option is to design a policy that regularly perform an automatic update of the user templates. In the other situation, the easy solution is to avoid this undesired items. That means the system warns and asks the user to take off their ornaments. However when this solution is not acceptable the system should allow to improve this variability of the hand images.

Thorough the next sections and mostly in Part IV the convention used for finger's names are described in Table 6.1. It is recommended to remember briefly that finger bone segments (carpals) are named phalanges and are divided by three segments called:

- Tip segment: Distal phalanx
- Middle segment: Middle phalanx
- Bottom segment: Proximal phalanx

The palmar side of the hand (the palm) has a cushiony surface and the back side of the hand (dorsum) is bonier and has thicker veins than the palmar side.

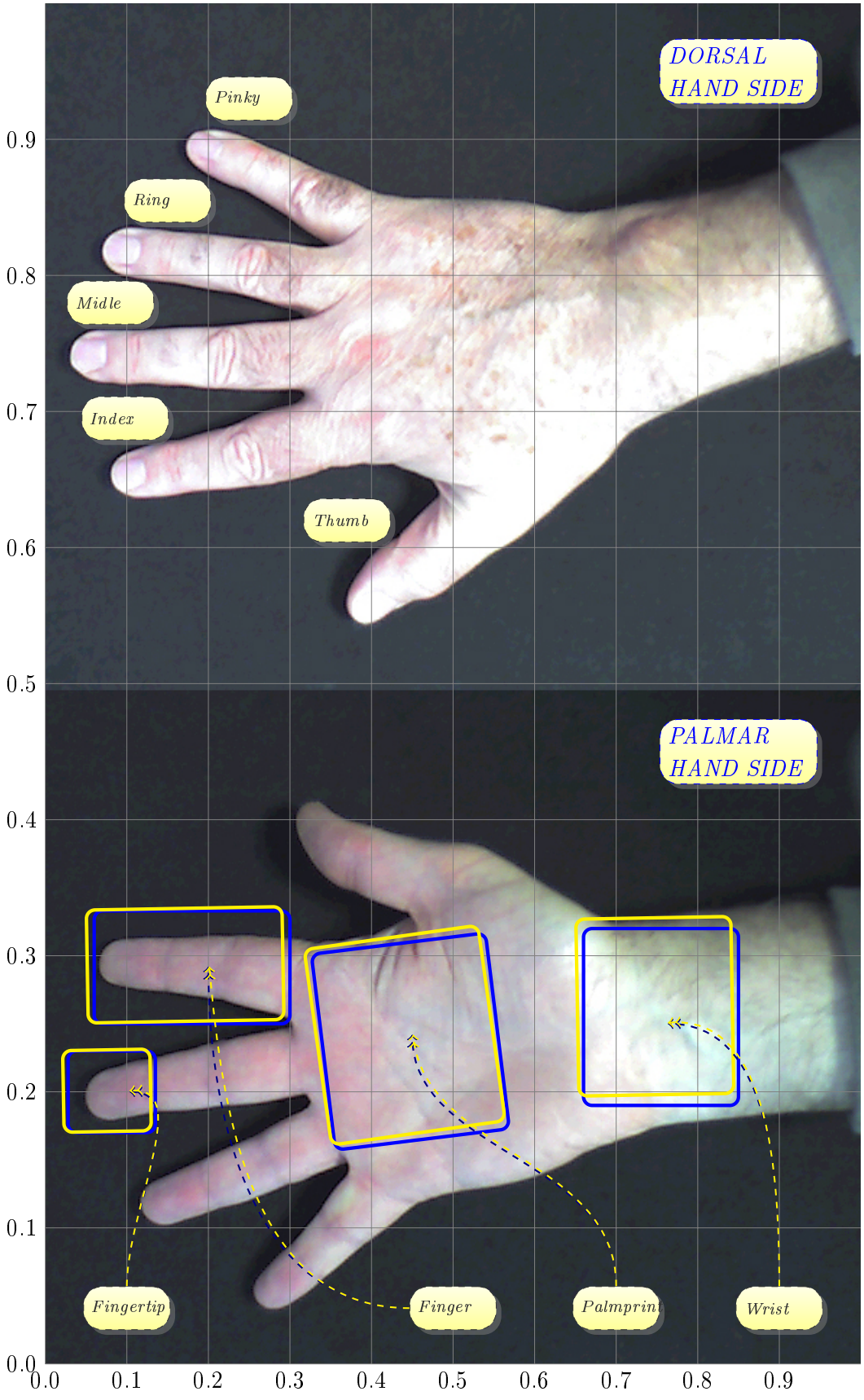

Figure 6.1.: *Dorsal Hand Side and Palmar Hand Side.*

Table 6.1.: *Finger's Name*

Finger	Regular name	Medical name
1	Thumb	Pollex
2	Index finger (also known as pointer finger, fore finger)	Digitus Secundus Manus
3	Middle finger	Digitus Me'dius
4	Ring finger	Digitus Annula'ris
5	Pinky (also known as baby finger)	Digitus Mi'nimus Ma'nus

6.1.1. Fingertips

As it was already described in Chapter 2, fingerprint recognition is the most used feature in biometric systems. They have been strongly used for almost a 100 years. The main reason comes from law enforcement utilization. As it has been stated before fingerprint has good biometric characteristics.

Some commercial application go a step further with fingerprint recognition. For instance, the business Lumidigm [119] (awarded from US Army) developed a sophisticated technology that uses multiple spectrums of light and polarized techniques to extract characteristics from both the surface and the subsurface of the skin. We can realize the importance to work with different source of data in order to improve the quality and performance of the system. Lumidigm uses different wavelengths of visible light that interact with the skin in different ways, enabling significantly enhance data acquisition.

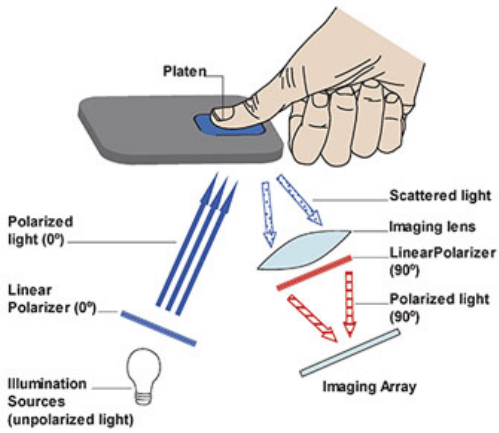

Figure 6.2.: *Lumidigm Technology*

With this technology his biometric system is ready to see beyond fingerprint ridges. The foundation of this structure is beneath the skin surface, in the capillary beds and other sub-dermal structures. The main advantage of this procedure is that although surface fingerprint can be obscured with dirt, wear or moisture the inner fingerprint lies undisturbed and mainly unaltered beneath the surface. Both informations combined adequately produce reliable results.

We no longer talk about this modality because it is off the scope of this thesis.

6.1.2. Palmprint

Palmprint recognition is another important characteristic of the hand. The truth is that it takes many of the ideas behind fingerprint. There exist many useful information to be used such as: Minutiae features, Delta point features (defined as in fingerprint), Wrinkle features, principal line feature and geometry features.

Resolution plays an important role and has to be defined accordingly with the application main objective. We could have two palm images one coming from a 640×480 and the other coming from a 3510×2550. It is possible to appreciate in Figure 6.3 and in Figure 6.4 this situation. Without a high quality scanner palmprint performance will decrease drastically. It will not be possible to extract the high amount of information on the hand surface. In [8] it is showed how to use palmprint to identification process. The idea behind many of the palmprint identification follow this steps:

- Palmprint acquisition
- Key points identification
- Apply filter, i.e. Gabor filter and merge (in case of some filters)
- Obtain a feature vector.
- Use some metric, i.e. Hamming distance

The results obtained in [8] are certainly accurate when verification is used (see Table 6.2).

Many of the research made in this specific area are sometimes circumscribed in Hand image. An example of this can be found in [12]. Here the authors work under an integrated system that combines palmprint image information with hand geometric information. The results are shown in Table 6.3. The performance criterion used in this table is based on finding the threshold that gives the minimum sum of FAR and FRR.

Figure 6.3.: *Palm from a* 640×480 *image*

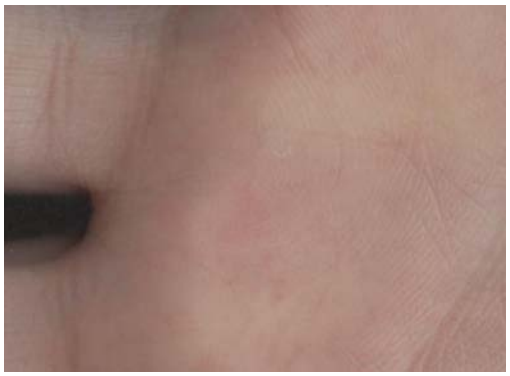

Figure 6.4.: *Palm from a* 3510×2550 *image*

Table 6.2.: *Genuine and False Acceptance Rate with Different threshold values*

Threshold	FAR (%)	FRR (%)
Verification		
0.317	1.2×10^{-5}	7.77
0.324	1.3×10^{-4}	6.07
0.334	1.0×10^{-3}	4.15
0.350	1.0×10^{-2}	2.32

Source: adapted from [8]

6.2. Hand Image

The approach of hand biometric system through hand image is something challenging. The reason became clear when it is a must to obtain some desirable image characteristic. In this situation it is necessary to take off with image processing algorithm arsenal in order to extract that feature. Examples have been described in the previous section when talking from palmprint focus.

Image analysis strategies appear to be the first ingredient when dealing with hand images. The starting point is always a raw data coming from a sensor (usually a digital CCD). This data is far from being perfect, though. Coming from many general situations the raw data needs to be enhanced and improved in order to highlight some key image features. Examples of this efforts in segmentation can be found in [147] and in [22].

One of the common approach to hand recognition is through a normalization procedure that enables the hand to be correctly compared. That means the template becomes

Table 6.3.: *Performance Scores for total minimum error*

	FAR (%)	FRR (%)	Decision threshold
Palmprint	4.49	2.04	0.9830
Hand geometry	5.29	8.34	0.9314
Fusion at Feature Level	3.74	1.91	0.9853
Fusion at Score Level	0	1.41	0.9840

Source: adapted from [12]

invariant to rotation or translation. Here there is no assumption on the table in the sense described in [10] where authors suppose hand were always completely extended in a tensed position (commented in the next section). Using normalization approach as in [47] helps reducing this assumptions. One of the common assumptions with hand, is related with ring and watches. If the system allow them to be used, then it is clear user can have it in one attempt but not in the other (the system will not know). This issue put pressure on the biometric system because it will make it less reliable and less high secure. It is a challenge to let the system remove finger artifacts. In Figure 6.5 it is seen how authors proceed to eliminate this undesired conditions.

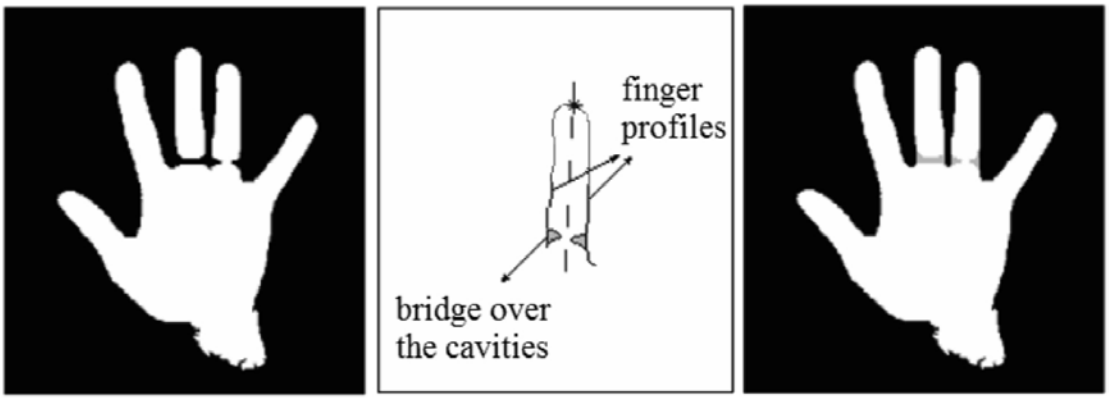

Figure 6.5.: *Biometric Verification/Identification based on hands natural layout [10]*

The approach presented in [47] has to considered for its originality. The main point is hand normalization. That means to develop an efficient hand segmentation method that enable to register the fingers in the desired directions. In order to identify directions it is used the binary hand/finger image through the larger eigenvector of the inertia matrix. As a simple overview of the tasks ready to deploy a list shows a sense of the computation

effort to accomplish the desired goal:

- Segmentation of the hand
- Hand rotation
- Hand translation
- Finding finger axes
- Ring artifacts removal
- Wrist completion
- Estimation of finger pivots (metacarpal-phalanx joints)
- Rotation and translation of fingers to the standard predefined orientations

They present four different feature extraction processes. Three of them deal with two different kinds of the hand image. The first one as it is, called *shape* and the other one transformed to enhance skin texture called *appearance*. The extraction methods were Independent Component Analysis (ICA), Principal Component Analysis (PCA), Axial Radial Transform (ART) and weighted Haussdorff distance. You can observe some of the results in Table 6.4

Table 6.4.: *Identification performance of feature types with different number of selected features (populationsize : 458)*

Feature type	Number of features			
	40	100	200	400
ICA_{shape}	94.32	97.67	98.4	97.31
$ICA_{appearance}$	95.41	98.25	99.49	99.36
PCA_{shape}	96.01	96.97	97.19	97.16
$PCA_{appearance}$	96.27	97.91	97.99	97.91
ART_{shape}	94.18	95.78	95.63	95.05
$ART_{appearance}$	95.92	97.38	97.67	97.60
Distance transform	93.38	95.49	95.71	95.99

Source: adapted from [47]

Other possible solutions, perhaps somehow a little more elaborated work under different feature extraction algorithm. In this context we can find zernike moments (complex polynomials that form a complete orthogonal set over the interior of the unit circle). In [16] they develop a new efficient computation of high order zernike moments. What is interesting is the way they analyse single finger performance and compare with respect to the whole hand. Later they perform fusion at feature level. In Table 6.5 it is shown the performance of the system in verification results in one of the proposed variants. When using fusion strategies the results decrease significantly, because EER stand at 0.044% in majority voting technique and in 0.052% in weighted sum.

Table 6.5.: *Performance of different parts of the hand for verification*

	Hand	Fingers				
	Palm	Thumb	Index	Middle	Ring	Pinky
#Feautures	256	121	121	121	121	121
EER (%)	2.05	3.62	0.93	1.28	1.62	1.77
TAR (%)	96.9	92.2	99.2	98.3	97.3	96.9

Source: adapted from [16]

TAR = True Acceptance Rate

6.3. Hand Geometry

There have been an enormous number of published papers in the direction of hand geometry. When the biometric system turns its main interest into geometrical features, then something easy come to light. This means, dealing with lengths and widths of fingers, angels or any other interesting measure easy to imagine and easy to understand. Something easy to understand makes it ready to be used and applied. There is something still more advantageous: computational efficiency.

There is also another issue concerning business related applications. With the help of some standards it is possible to develop efficient and reliable operative biometric hardware [196] ready to be used in *verification* mode. In Figure 6.6 it is shown a currently hand reader to grand access control.

In [10] it is shown a system based on three main components. The first one called Natural Reference System (NRS). That NRS basically defines a coordinate system based on thumb and middle finger. This hypothesis is far to be certain in real operation modes

Figure 6.6.: *Biometric Hand Reader 2700USD*

because thumb has a long range of movement (scope variation). To be precise the thumb has movement through two joins: the metacarpal-phalanx and the trapezium-metacarpal. Nevertheless the authors state that it is perfectly reasonable when hand is placed in an extended position. The second point is using polar coordinates instead of the usual euclidean ones. The use of polar coordinates it is something already used by other authors. The last component of this article is the use of the two hands. That means acquiring right and left hand and enabling correlating measures between them.

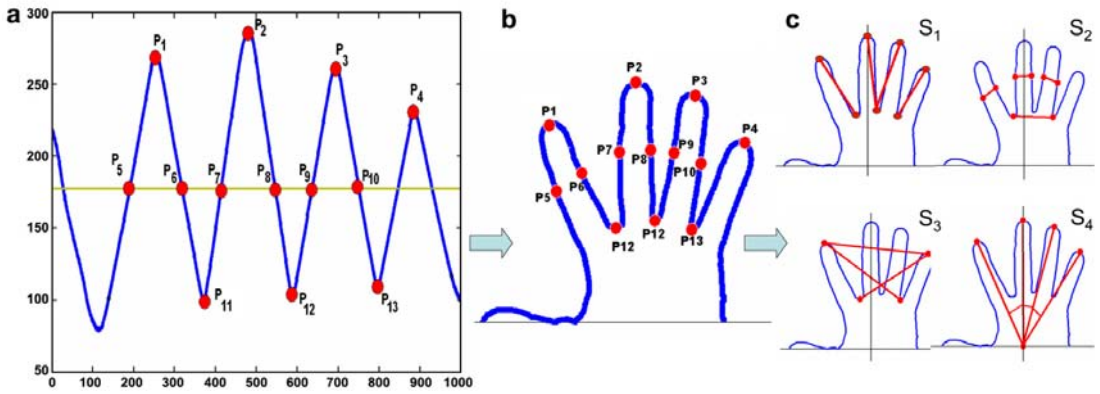

Figure 6.7.: *Biometric Verification/Identification based on hands natural layout [10]*

Recently developments try to mitigate some of the requirement usually hand biometric systems have. Among them the hand surface that can come with a peg system or without. In [66] is presented a Contact-free hand geometry-based identification system. Its main contribution is perhaps the infrared illumination they use in order to enhance hand image quality. However the results are far to be considered outstanding (FAR = 1.85%) whereas

Table 6.6.: *Performance Scores for from two feature vectors [10]*

	M1	M2
(a) Verification		
FAR (%)	1.30	1.36
FRR (%)	1.28	2.58
(b) Identification		
Candidates 1(%)	97.6	95.0
Candidates 3(%)	99.0	98.0
Candidates 6(%)	99.5	98.7

Source: adapted from [10]

they consider effective for practical verification applications.

6.4. Other Hand Approaches

In this section we try to help the reader to put some recently research that is not easy to fit with either hand image or hand geometry approach. For this reason we describe two possible group of contributions: combining or integrating information from hand image and hand geometry and another option where the hand present a non visible sensor to acquire the image. In this last option is possible to make room for NIR and TIR hand images.

6.4.1. Combining Hand Approaches

One of the most straightforward improvements when dealing with hand is to mix both approaches. This means combining in some way image information with geometric information. We can see this kind of approach in some articles as in [172]. In this paper authors present a multibiometric system based on finger geometry, knuckle print and palmprint features. The multimodal system then integrates all this information using a fusion scheme at decision level.

The fingers used in this paper are: pinky, ring, midle and index. Thumb has been discarded and the system performs with both FAR and FRR lesser than 1%.

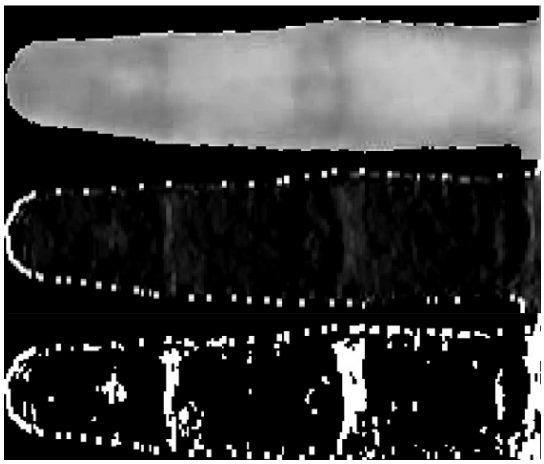

Figure 6.8.: *Knuckel print detection and binarization [172]*

6.4.2. NIR and TIR Approaches

Many interest has began to come from other electromagnetic bands, such as NIR and TIR. Using NIR sensors help obtaining information coming from the vein capillarity system. Some work has been done in this direction as it is shown by recently published papers and from industry. However TIR approach is much harder to find in indexed articles related to biometric security systems.

As it is stated in [78] vein recognition appears to be making real headway in the market and the reason become clear as it has already been shown in [119]. Other examples of the interest in vein pattern can be found in [99] and in [223]. Some of this approaches also play with fusion strategies in order to improve performance [209]. The main significant advantage of finger vein and hand vein approach over traditional biometrics lie in low-risk forgery, noninvasiveness, noncontact and robust to spoff attacks [227].

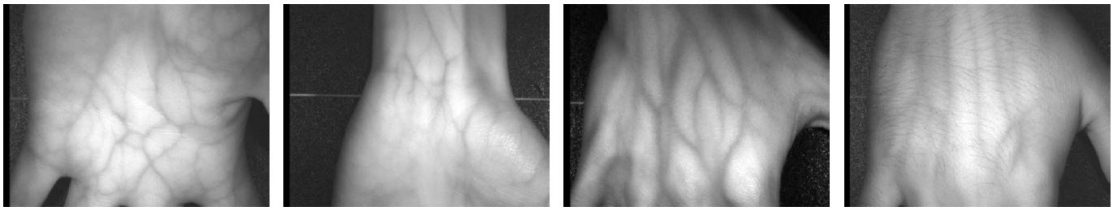

Figure 6.9.: *NIR images from palm, wrist, dorsal without hair and dorsal with hair [212]*

Some of the results showed are in occasion outstanding but difficult to reproduce. For example in [212] the biometric system used achieves a FAR = 0% and FRR = 0% for all testing set. However other authors obtain results far from this one. In [75] they use a hand vein biometric system comprising of dorsal and palmar vein. Both modalities are

integrated through a fusion score level schema that perform reasonable well. The results are presented in the Table

Table 6.7.: *Performance on vein pattern [75]*

	FAR (%)	FRR (%)
Dorsal hand	0.92	0.83
Palmar hand	1.20	2.87
Fusion hand	0.02	0.35

Source: adapted from [75]

6.5. Biometric Data Base

In [14] it is shown a survey on hand recognition systems. There, different strategies are compared with the help of the University of Nevada at Reno (UNR) and the University of Notre Dame (UND) hand databases.

In this section we briefly describe some known multi biometric data base. There are aspects to be considered when working with a data base. One of these could be information related to user socio-graphic or discriminant characteristic factors, such as gender, age, race or others. However, multi biometric data base are more concern in acquiring a wide range of different user features, no matter if are from behavioural or physiologic. Here, face plays a central role because with no exception the proposed data base always have face as a modality to work with. The reason for this huge interest with face is evident, but the aim of this section is take a look at the multi-modal data base who has Hand as a modality [83].

- BiosecurID [83]: This database was collected at six different sites in an uncontrolled environment trying to simulate a real operative scenario. The traits to be considered are: speech, iris , face, signature, handwriting, fingerprints, hand and keystroking.
- BIOSECURE [155]: The most relevant information from this database is its length. With 1000 users the database consider three different scenarios. Here the following data is available: face, fingerprint, hand, iris, signature and speech
- MyIDEA [76]: It includes face, audio, fingerprints, signature, handwriting and hand.

- BIOMET [60]: Five different modalities are present in this database: audio, face (2D and 3D), hand, fingerprint and signature.
- SmartKom [195]:Four different modalities: fingerprint, hand, signature and speech.

Table 6.8.: *Database Most Relevant Modalities*

Multimodal DB	Users	Fa	Fp	Ha	Hw	Ir	Ks	Sg	Sp
BiosecureID	400	√	√	√	√	√	√	√	√
BIOSECURE	700	√	√	√		√		√	√
MyIDEA	104	√	√	√	√			√	√
BIOMET	91	√ *	√	√				√	√
SmartKom	96		√	√				√	√

Source: adapted from [83]

Fa=Face; Fp=Fingerpint; Ha=Hand; Hw=Handwriting

Ir=Iris; Ks=Keystroking; Sg=Signature; Sp=Speech

Reader can suggest a detailed description on hand database. This will be addressed thorough chapter 7.

6.6. Hand Biometric Conclusions

We conclude this section in a sense of awareness into performance results. It is not possible to represent a fair performance table with identification and verification values for any of the modalities and strategies presented in this chapter. Nevertheless we will present a final table sorting the best modality and method to compare easily. Performance of hand base systems vary strongly as it has been seen with vein pattern approaches. Classification of hand base system is quite difficult because some *uncontrolled* factors have a sharp effect on performance.

Some of this factors are described briefly:

- Hardware Device: How user interact with the system (i.e. peg free)
- Sensor Device: The quality of the sensor, say 1 Mpx or 5 Mpx.
- Dataset size: The number of users and the samples per user is usually referred to as dataset size. The way we define the training set and the test set is key.

  - Training Set
  - Test Set

- Timescale: Data base are build within a short period of time, say a month, a semester or a year. There is no example of long term acquisition data base.
- Test Conditions: It is not the same laboratory conditions where the environment is in a certain way controlled than a real operation mode.
- Demographics: Most research is carried out at colleges and universities. This reduce the heterogeneity of the database since many hand samples come from students or academic staff. Accounting for race, age and gender distribution is also important.
- Number of attempts: It is possible that the system under consideration has a poor results because the captured image is not good enough. If we account for another attempts, then the system can work correctly for that user.
- New Enrollments: Does the biometric system need to rebuild when new users are enrolled.
- Identification Operational Mode: Does the system check for non enrolled users. (note: this point is close to Dataset size)

The need to follow some standard is advisable (ANSI INCITS 396-2005)

Table 6.9.: *Hand Shape System*

Ref.	Year	Pop. Size	Sampl. Person	Features Used	Similarity measure	Performance
[121]	1997	100	8	F l/w thickness(17)	Bayes aposteriori class prob.	$_{(3)}0.0012$
[181]	1999	50	5-10	F l/w aspect ratios(16)	Mahalanobis distance	$_{(1)}0.01 -_{(2)} 0.17$
- [95]	1999	53	2-15	H cc (120-350 contour p.)	Mean alignment error	$_{(1)}0.01 -_{(2)} 0.06$
[184]	2000	20	10	F l/w, ratios thickness, dev.(25)	Euclidean, Hamming, GMM	$_{(3)}0.05$
[215]	2002	22	12-15	F l/w(13) Fingertip coord.(50-90)	GMM prob. ratio of hit points	$_{(1)}0.022 -_{(2)} 0.111$
[26]	2004	70	10	Geometric features (30)	Nearest box (Linfinit)	$_{(1)}0.01 -_{(2)} 0.03$
[151]	2004	110_g 399_i	7	F l/w, palm width(24)	Normalized Euclidean distance	$_{(1)}0.01 -_{(2)} 0.001$
[206]	2005	51	10-20	H cc, angles(51-211 contour p.)	Log-Likelihood	$_{(3)}0.002$
[140]	2005	96	10	F l/w (21)	ratio min/max	$_{(3)}0.03$
[216]	2005	223	5-8	Shape indices (3D surface curv.)	Normalization corr. coeff.	$_{(3)}0.09$
[231]	2006	458	3	H cc (2048) ICA on bin.image(458)	Modified Hausdorff L1, cos. dist.	$_{(3)}0.015$
[15]	2006	40	10	Zernike moments + PCA (30)	Euclidean	$_{(1)}0.01 -_{(2)} 0.02$
[9]	2008	470	6-8	Non-landmark based geometric	Normalized sum of feature dev.	$_{(1)}0.0045 -_{(2)} 0.034$
[139]	2008	20	10	F l/w (3 fingers) (40)	SVM score	$_{(3)}0.034$
[16]	2009	100	10	F + Palm(861)Zernike M.	Euclidean	$_{(3)}4.38 \times 10^{-4}$

F l/w:Finger lengths/widths

H cc: Hand contour coordinates

$_{(1)} = FAR$ - $_{(2)} = FRR$ $_{(3)} = EER$

Source: adapted from [42]

Part III.

Thesis Development

Chapter 7.

Hand Database Construction

Groucho Marx

Before I speak, I have something important to say.

Overview

The construction of a new Hand Database is a challenging process. Here we describe how this new multispectral hand database called *Tecnocampus* has been built. It will be described the main advantage and disadvantages, and how to exploit it in an efficient way. All the images have been acquired with three different sensors (visible, near infrared and thermal). This database consists of 100 people acquired in five different acquisition sessions, two images per session, and palm / dorsal sides. The total amount of pictures are 6.000 and are mainly developed for hand-image biometric recognition purposes.

Contents

7.1. Hand Database

Generally any biometric data base is a precious commodity. The reason become clear for scientific community where using public data base can be used to compare methods in

a standardized way. Biometric databases are a milestone for algorithmic improvements. They let researchers to check competing alternatives on the same experimental data, making the comparison feasible. Although several databases exist for biometric hand recognition, to the best of our knowledge this is the first multi-session and multi-modal spectral database that addresses three different spectrums

7.1.1. The Thesis Hand Database

The thesis proposal takes a road through the construction of a multispectral hand image data base. To the best of our knowledge is the first one that covers three different wavelengths. For each person the data to be recorded will be the following:

- ★ **Visible** (VIS), the portion of the electromagnetic spectrum that is visible to the human eye. It has been acquired using the visible camera incorporated in Testo 882-3 thermal camera. We have acquired visible images with a 640x480 pixel resolution.
- ★ **Near InfraRed** (NIR) is inside the band called infrared (IR) that is characterized with longer wavelengths (range from $700nm$ to $1.4\mu m$). It has been acquired with a specially adapted webcam, in a similar way to our previous work for face images. The spatial resolution is 640x480 pixels
- ★ **Thermal Infrared** (TIR) is especially interesting sub-band of Far InfraRed (FIR) spectrum that goes from $3\mu m$ to $14\mu m$. We have used the testo 882-3 thermal camera, which provides a 340x240 pixel resolution. It is four times higher than our previous face database.

These three wavelengths data coming from the same hand could increase the performance of any biometric system because it reduces noisy data problems, poor error rates and the ability to conduct different system attacks like spoofing. As it will be demonstrated in the next session, these spectral bands provide complementary information.

Table 7.1 summarizes the main characteristics of the most popular existing hand databases. As can be checked, this is the first multi-spectral and multi-session database.

7.2. Acquisition Scenario

The acquisition over the VIS and TIR data will be through a commercial thermal camera (see Figure 7.2) called testo 882-3. Although the camera is intended for TIR image analysis it also provides a visible image with a limited quality sensor (automatically the camera obtains both TIR and VIS images). The main characteristics of this camera are the following:

Table 7.1.: *Main characteristics of the existing databases. Column "Contact" indicates whether the hand was touching a desk or whether the hand was acquired contactless. Column "Variations of Hand" indicates, whether the hand was always in the same position or whether it was rotating*

Name	Population Size	Involved Hand	Samples per User	Contact	Colour	Image Size	Variations of Hand
$GB2S_1$ [189]	50	both	3	no	C	1600x1200	yes
$GB2S_2$ [189]	5	both	15	no	C	1600x1200	yes
$GB2S_3$ [189]	5	both	24	no	C	2048x1536	yes
$GB2S_4$ [189]	3	both	100	no	C	1280x1024	yes
UST [5] [192]	287	both	10	no	BW	1280x960	yes
IITDelhi [107]	235	both	7	no	BW	800x600	no
GPDS [54]	150	right	10	yes	BW	1403x1021	no
HGC2011 [125]	46	right	10	yes	C	685x494	yes
Bologna [153] [152]	270	both	3	yes	C	526x381	yes
Bosphorus [231]	1031	both	3-6	yes	C	526x382	yes

Source: Author's search

- ★ Thermal image resolution: 320×240 pixels.
- ★ Spectral sensitivity: 8 to $14\mu m$.
- ★ Thermal sensitivity (NETD) < 0.06°C at 30°C
- ★ Geometric resolution (IFOV): 1,7 mrad.
- ★ Thermal detector type: silicon microbolometer uncooled, temperature stabilized.
- ★ FOV: $32° \times 23°$; focal distance: 15mm; fixed aperture: f/0,95

We have used a second external camera to obtain the NIR data (See Figure 7.3). In this case we have built a NIR camera using a webcam changing the default optical filter for a couple of Kodak filters for IR. We have also used a printed circuit board with 16 infra-red LEDs that provide the infra-red illumination (see Figure 7.3)

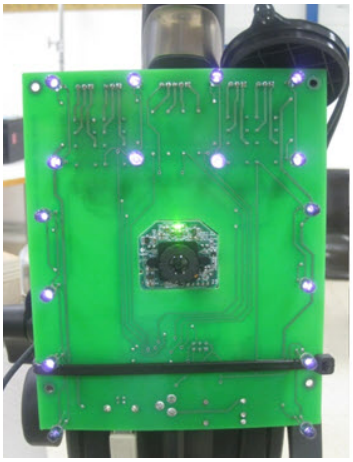

Figure 7.1.: *IRcamera*

Figure 7.2.: *testo 882-3*

In order to alleviate the variability on the way the users present their hand we have used a kind of removable mask/template that can be seen in Figure 7.6. Users had to put their hand in a neoprene surface (in Figure 7.5) with the help of a hand mask (figure 7.6). Hand mask is a way to indicate the approximate hand and finger position in a more convenient way than pegs, because database acquired with pegs contain the pegs in the final image and our mask is removed before image acquisition (see in Figure 7.7). Once the hand is placed the mask is removed and the three images (VIS, NIR, TIR) are shot. The same process is repeated with the palmar hand side, but using the mask in the opposite position (flip up to down). This process provides images like those shown in figure (dorsal and palm), which emphasizes the most relevant areas for recognition purposes. We have used the neoprene surface because it has lesser thermal

Figure 7.3.: *Lab conditions: Sensors View*

Figure 7.4.: *Lab conditions: Horizontal View*

Figure 7.5.: *StepProc1*

Figure 7.6.: *StepProc2*

Figure 7.7.: *StepProc3*

latency and in this way we alleviate the annoying effects that appear with other surfaces, which provide higher residual heat when the hand is lifted.

Once the first acquisition is finished (no more than a minute) the user takes a soft dice, which is pressed several times in order to change hand heat conditions. This step was carried out in less than 30 seconds so that when finished, the user proceeds again with the second acquisition. For each session a total of 12 hand images were captured per user. Figure 7.8 shows the first acquisition of a user (dorsal and palm images for the three spectrums.

7.3. Database characteristics

The multispectral hand image database consists of 100 users. Each user has been acquired in 5 different recording sessions (see Figure 7.9). In each session two acquisitions were performed of each face (palm and dorsal image). The time span for the whole database acquisition was 6 months. From January to June users were acquired in five sessions. These sessions were separated from each other with a delay of at least 4 weeks. Any time

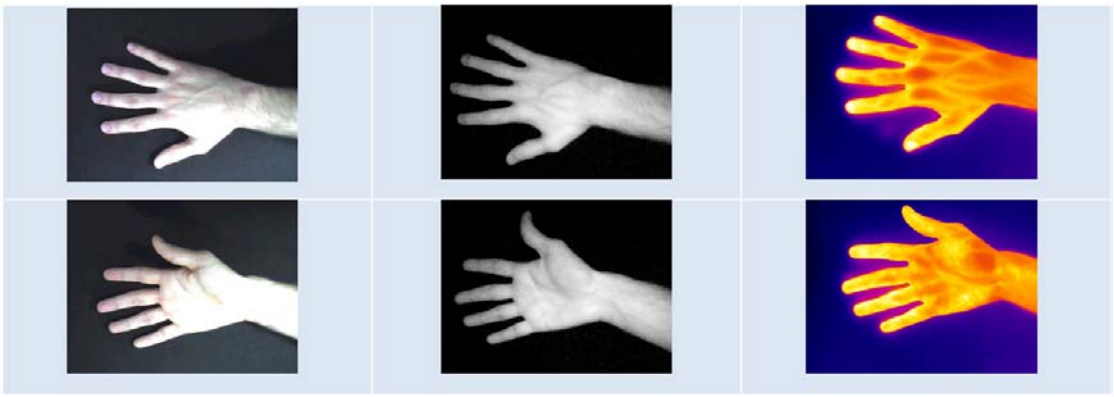

Figure 7.8.: *Acquistion's Images*

a user proceed with a session two acquisitions were done. The first one was done without any special requirement. The second one was done just after the first one but with a slightly small hand exercise (flexing and stretching hand pressing a soft dice). This hand exercise helped to change hand thermal conditions.

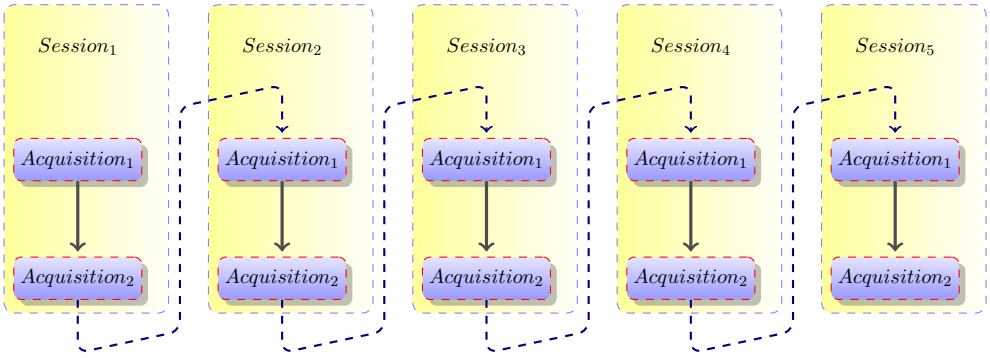

Figure 7.9.: *Acquisition Process.*

Data Base Numbers

100 users x 5 sessions x 2 acquisitions x 3 spectral ranges x 2 sides (palm and dorsal images)

Total Number of images = 6.000

Different samples from the same user can be seen in Figure 7.10. In the VIS spectrum (first raw) appreciable differences are coming from lighting conditions, hand and finger positioning and orientation. From TIR (second row) a clear different heat pattern is present. The environment affects through humidity and temperature as well as the user

conditions (if it is stressed or relaxed). Finally NIR spectrum is shown in the last row of Figure 7.10.

Worth to mention that the existence of two sides of the hand can help researchers to decide which part of them is most suitable for biometric recognition purposes. We assume that with a segmentation method hand could be split to obtain the regions of interest: fingers, wrist, palm or other hand zones.

Figure 7.11 shows images from different users where some problems are detected. The major challenge comes from the fact that many users present some kind of difficult issue. It is hard to deal with sleeves (casts shadows), rings, colored-nails and cold fingers. We will call this database *Tecnocampus* due to the faculty (Escola Universitaria Politecnica de Mataro - Tecnocampus) where it has been acquired. Table 7.2 summarizes the main characteristics of the hand database.

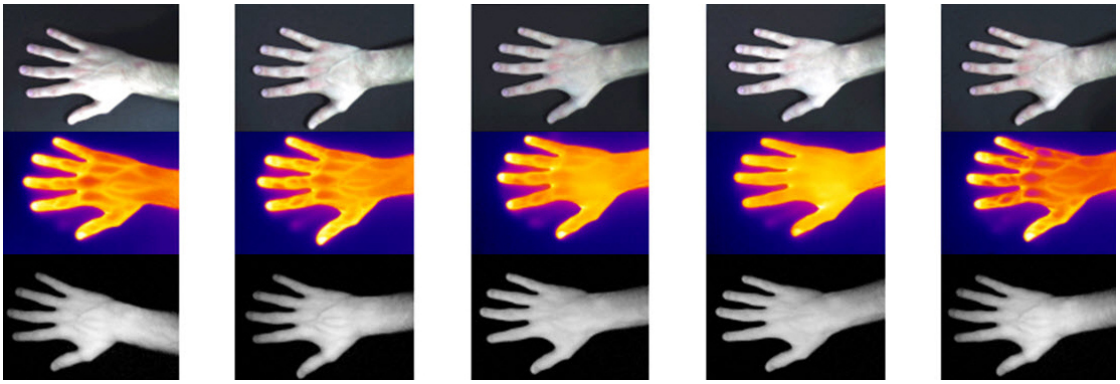

Figure 7.10.: *Sample Acquistion's Images from the same user (Dorsal Side) in VIS, TIR and NIR*

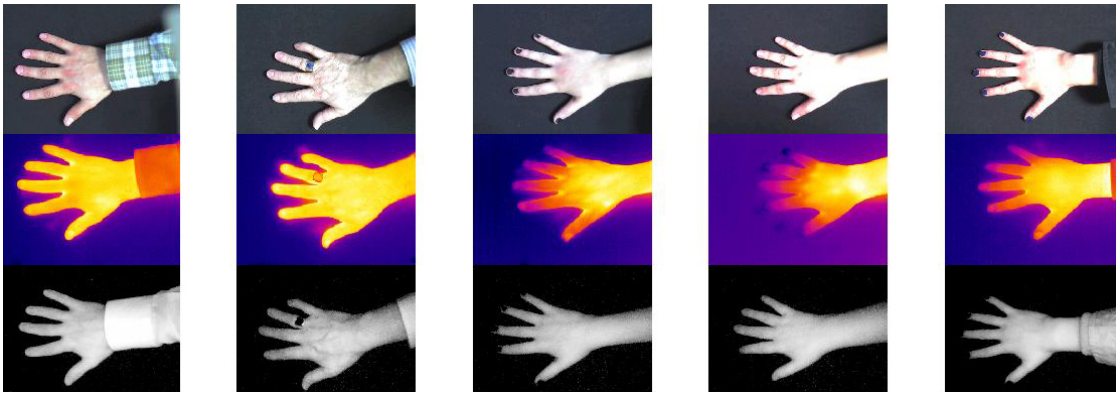

Figure 7.11.: *Sample Acquistion's Images from different user (Dorsal Side) in VIS, TIR and NIR*

Table 7.2.: *Main characteristics of the Tecnocampus database*

	VIS	NIR	TIR
Sensor	Testo 882-3	Logitech WebCam	Testo 882-3
Resolution	640 x 480	640 x 480	320 x 240
Number of Users	100	100	100
Samples per User	10x2	10x2	10x2
Dorsal Side	YES	YES	YES
Palm Side	YES	YES	YES
Total Number of Images	2000	2000	2000

7.4. Information theory analysis

Information theory is a mathematical tool to measure the amount of information provided by a given source as well as the amount of redundant information/ new information when evaluating a couple of sources of information. WE have used this same analysis for the case of faces [1] and on-line handwritten text [14].

From an information theory [15] point of view we can establish these following measurements:

7.4.1. Entropy

Considering that the random variable X consists of several events x, which occur with a probability $p(x)$, the entropy $H(X)$ can be calculated according to equation:

$$H(X) = -\sum_{x \in X} p(x) \, log_2 (p(x)) \tag{7.1}$$

Entropy measures the information contained in a message (in our case will be an Image) as opposed to the portion of the message that is determined (or predictable).

7.4.2. Conditional Entropy

The conditional entropy (or equivocation in communication theory) quantifies the remaining entropy (i.e. uncertainty) of a random variable Y given that the value of a second random variable X is known. It is referred to as the entropy of Y conditional on X, and is defined as:

$$H\left(Y|X\right) = -\sum_{x\in X}\sum_{y\in Y} p\left(x,y\right) log_2\left(p\left(y|x\right)\right) \tag{7.2}$$

7.4.3. Joint Entropy

The joint entropy of two random variables X and Y measures how much entropy is contained in a joint system of these two random variables. It is defined as

$$H\left(X,Y\right) = -\sum_{x\in X}\sum_{y\in Y} p\left(x,y\right) log_2\left(p\left(x,y\right)\right) \tag{7.3}$$

7.4.4. Mutual information

The mutual information $I(X;Y)$ of two random variables X and Y (representing two images in our case) is defined as:

$$I\left(X;Y\right) = \sum_{y\in Y}\sum_{x\in X} p\left(x,y\right) log_2\left(\frac{p(x,y)}{p\left(x\right)p(y)}\right) \tag{7.4}$$

where $p(x,y)$ is the joint probability distribution function of X and Y, and $p(x)$ and $p(y)$ are the marginal probability distribution functions of X and Y respectively Intuitively, mutual information measures the information that X and Y share: it measures how much knowing one of these variables reduces our uncertainty about the other. For example, if X and Y are independent, then knowing X does not give any information about Y and vice versa, so their mutual information is zero. At the other extreme, if X and Y are identical then all information conveyed by X is shared with Y: knowing X determines the value of Y and vice versa. As a result, in the case of identity, the mutual information is the same as the uncertainty contained in Y (or X) alone, namely the entropy of Y. Mutual information quantifies the dependence between the joint distribution of X and Y and what the joint distribution would be if X and Y were independent. Mutual information is a measure of dependence in the following sense: $I(X;Y) = 0$ if and only if X and Y are independent random variables. This is easy to see in one direction: if X and Y are independent, then $p(x,y) = p(x)p(y)$ and therefore

$$I\left(X;Y\right) = \sum_{y\in Y}\sum_{x\in X} p\left(x,y\right) log_2\left(\frac{p(x,y)}{p\left(x\right)p(y)}\right) = \sum_{y\in Y}\sum_{x\in X} p\left(x,y\right) log_2\left(1\right) = 0 \tag{7.5}$$

Mutual information can also be expressed as:

$$I(X;Y) = H(Y) - H(Y|X) = H(X) + H(Y) - H(X,Y)$$

The next diagram (see Figure 7.12) helps to explain the relation between these different definitions

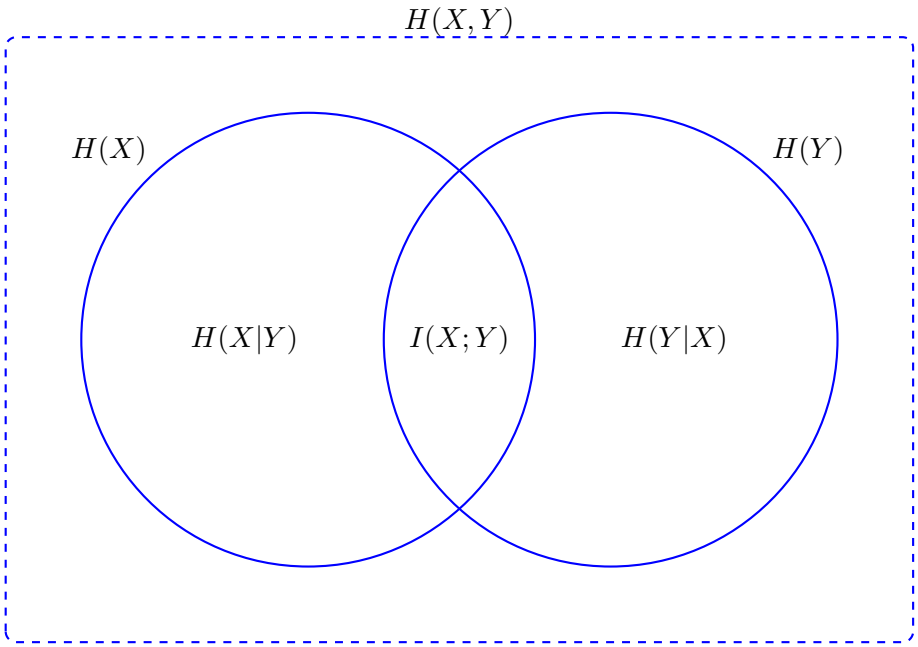

Figure 7.12.: *Relation between different information theory measurements.*

7.4.5. Normalized 2D cross-correlation

Cross-correlation is a measure of similarity of two signals as a function of a time-lag applied to one of them. It is possible to calculate a two-dimensional cross-correlation $c(u, v)$ according to the formula [16]:

$$c\left(u,v\right) = \sum_{x \in X} \sum_{y \in Y} f\left(x,y\right) t\left(x-u, y-v\right) \tag{7.6}$$

where f is the image and t is the feature positioned at u, v. The disadvantage of the two-dimensional cross-correlation is that the range of $c(u, v)$ is dependent on the size of t and it is not invariant to changes caused by changing of illumination conditions across the image sequence. These disadvantages are suppressed by normalization of image and feature to unit length which is used in normalized 2D cross-correlation $\gamma(u, v)$ defined by

$$\gamma\left(u,v\right) = \frac{\sum_{x,y}\left[f\left(x,y\right) - \bar{f}_{u,v}\right]\left[t\left(x-u,y-v\right) - \bar{t}\right]}{\left\{\sum_{x,y}\left[f\left(x,y\right) - \bar{f}_{u,v}\right]^2 \sum_{x,y}\left[t\left(x-u,y-v\right) - \bar{t}\right]^2\right\}^{0.5}} \tag{7.7}$$

Table 7.3.: *Experimental entropies for dorsal and palm images in each spectrum*

$H(X)$	VIS		NIR		TIR	
	Mean	Std	Mean	Std	Mean	Std
dorsal	5.34	0.46	4.06	0.43	5.40	0.22
palm	5.28	0.49	3.92	0.41	5.30	0.25

Source: Author's

where $\bar{t}$ is the mean of feature and $\bar{f}_{(u,v)}$ is the mean of $f(x,y)$ in the region under the feature. This measure is interesting because we should take into account that information theory measurements do not take care of pixel position. They consider the statistical properties of the pixels regardless of their distribution inside the image. This is not the case with cross-correlation that certainly considers pixel positions

7.5. Experimental Results

Based on information theory we have studied the relations between several pairs of images (TIR=thermal, NIR= Near Infrared, VIS= Visible). Table 7.3 shows the experimental entropies for each kind of image and table 4 the joint, mutual and maximum cross-correlation results. These results have been obtained using the whole Tecnocampus database

Table 7.3 reveals that TIR spectrum contains slightly higher level of information that VIS one and higher than NIR. This result is different from the experimental results of [48], which revealed higher level of information for NIR and VIS. However it should be emphasized that [48] used a Testo 880-3 thermal imager, which provides lower resolution and lesser thermal sensitivity. In addition, the distance from the camera to the object is smaller in the case of hands than for faces, as well as the degree of information, which is almost limited to the hand contour for the hand images, and is more reach for VIS and NIR in the case of face images. Another nice property of TIR images is that they show lesser standard variation. In principle, this is a good result (higher amount on information and smaller variation along the 2000 evaluated images than the other sensors).

Table 7.4 reveals that the higher mutual information is obtained when evaluating pairs of images of the same kind (dorsal or palm) and sensor, which corresponds in a biometric system application to the combination of several consecutive snapshots of the same hand. In this case the highest mutual information value is 1.66 (dorsal) and 1.55 (palm), which corresponds to the TIR sensor. The highest joint information, which is 10

bit, corresponds to VIS and TIR dorsal information. This result indicates that it seems more convenient to fuse different sensors than different sides of the hand, because the available information is higher. Nevertheless, the combination of palm and dorsal images contains similar information (9.84) when using a TIR sensor. In addition, this maximum joint information value is lower than the one we reported in [48], which was 12.20 bit.

In the first column we mark with bold numbers those situations where maximum joint entropy is obtained when combining different sensors. It can be observed that this situation is always obtained when one of the sensors is thermal. This seems to indicate that thermal sensors offer high potential for biometric recognition. Looking at the maximum normalized crosss-correlation between images obtained with different sensors and side of the hand we obtain the highest values (see 9th column of Table 7.4) when combining VIS and NIR sensors. This is probably due to the fact that VIS-NIR are closer to each other than VIS-TIR.

Table 7.4.: *Experimental results when combining two sensors*

Cond.	$H(X,Y)$		$I(X,Y)$		$H(X\|Y)$		$H(Y\|X)$		max_γ	
	Avg	Std	Avg	Std	Avg	Std	Avg	Std	Avg	Std
X=Y=D										
X_{VIS}, Y_{NIR}	8.44	0.66	0.94	0.14	4.39	0.44	3.10	0.41	**0.85**	0.06
X_{VIS}, Y_{TIR}	**10.00**	0.51	0.73	0.10	4.60	0.42	4.67	0.21	0.75	0.05
X_{NIR}, Y_{TIR}	8.88	0.51	0.59	0.07	3.48	0.42	4.80	0.21	0.77	0.06
X_{VIS}, Y_{VIS}	9.51	0.78	1.17	0.28	4.16	0.48	4.18	0.50	0.85	0.06
X_{NIR}, Y_{NIR}	6.86	0.65	1.26	0.26	2.82	0.44	2.78	0.43	0.91	0.04
X_{TIR}, Y_{TIR}	9.13	0.44	**1.66**	0.36	3.73	0.37	3.73	0.39	0.88	0.06
X=Y=P										
X_{VIS}, Y_{NIR}	8.28	0.67	0.93	0.14	4.37	0.47	2.98	0.40	**0.85**	0.06
X_{VIS}, Y_{TIR}	**9.86**	0.54	0.73	0.12	4.56	0.43	4.56	0.24	0.78	0.05
X_{NIR}, Y_{TIR}	8.67	0.52	0.55	0.08	3.38	0.42	4.74	0.24	0.79	0.05
X_{VIS}, Y_{VIS}	9.40	0.81	1.16	0.26	4.13	0.47	4.10	0.50	0.85	0.06
X_{NIR}, Y_{NIR}	6.72	0.63	1.12	0.24	2.81	0.44	2.78	0.41	0.89	0.04
X_{TIR}, Y_{TIR}	9.05	0.42	**1.55**	0.29	3.75	0.33	3.74	0.34	0.89	0.05
X=D,Y=P										
X_{VIS}, Y_{NIR}	8.50	0.66	0.74	0.10	4.60	0.44	3.17	0.39	**0.82**	0.06
X_{VIS}, Y_{TIR}	**9.84**	0.53	0.79	0.11	4.54	0.44	4.50	0.24	0.75	0.05
X_{NIR}, Y_{TIR}	8.68	0.51	0.69	0.10	3.38	0.42	4.60	0.23	0.78	0.05
X_{VIS}, Y_{VIS}	9.75	0.76	0.85	0.14	4.49	0.40	4.42	0.46	0.81	0.06
X_{NIR}, Y_{NIR}	7.21	0.69	0.78	0.13	3.30	0.44	3.13	0.40	0.86	0.04
X_{TIR}, Y_{TIR}	9.81	0.36	0.88	0.13	4.52	0.22	4.42	0.25	0.85	0.06

Chapter 8.

VIS Preprocessing and Feature Extraction

Pablo Picasso

Action is the foundational key to all success.

Overview

This chapter highlights some of the necessary steps to obtain reliable feature vectors when dealing with hand visual images. Once image is read, an important pre-process has to be performed to find the region/s of interest. Some additional steps have to be made in order to decompose the initial hand in its main components, fingers and palm. In this sense, image segmentation plays an important role before the application of classification methods.

Contents

8.1. Characteristics of the VIS raw data

As it has been described in the previous chapter all VIS images have a resolution of 640×480 pixels. Depending on the application this resolution could not be enough (i.e.

extract fingerprint). The quality and characteristics of the image define the techniques to be applied in order to correctly segment the image.

The work presented here will not dig into image quality measures, because it is not the main objective of the thesis. However, it is advisable to check a simple an straightforward image histogram. They basically represent the tonal distribution in an image. This representation (see Figure 8.1) helps to value the tonal distribution at a glance, where x axis represents tonal variation from black areas in the left, to the white areas in the right of the axis and Y axis represents the number of pixels in that particular tone.

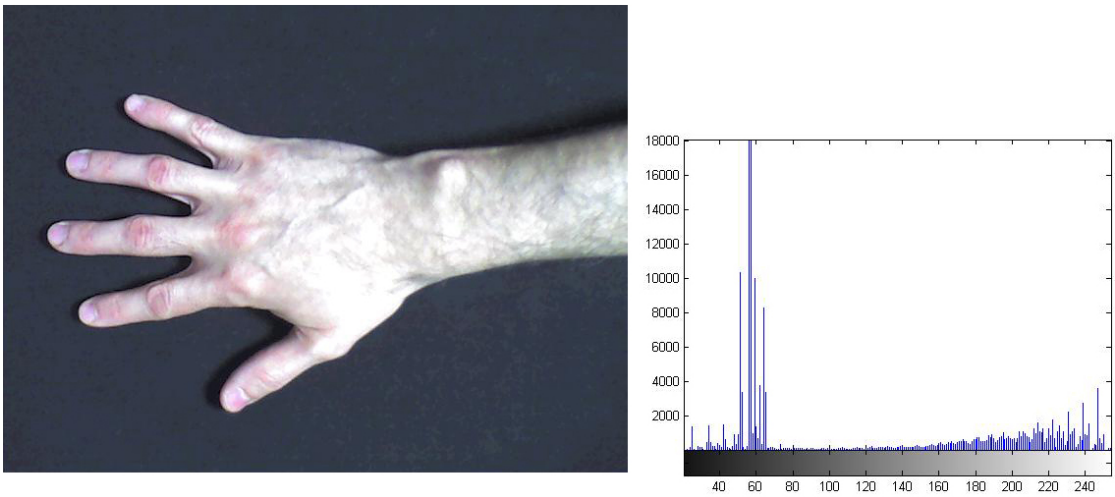

Figure 8.1.: *Hand Sample Image (Dorsal Side) in VIS an its associated histogram*

What is clear when analysing the histogram from Figure 8.1 is that there are two main differentiated areas. The left side, representing the black surface (the neoprene) and the right side representing the hand. However when the distribution is concentrated in the most right side means the image is overexposed (burned). In other words, it looks like a white spot and it is not worth to extract texture surface.

The reason for this lack of image quality has one main reason: Thermographic cameras are not intended to shot high VIS quality pictures, instead high quality thermographic images. A webcam actually would have provided better quality images.

8.2. Hand Segmentation

Image segmentation is a division of the image data into regions in such a way that region **R** contains the pixels of the silhouette of object **O** in the real world. Image segmentation is based on three principal concepts: Detection of discontinuities, Thresholding or Region Processing. Many research is conducted on this field and topics such as

- Automatic segmentation algorithms

  - Clustering approach
    * Analyzing the distribution of pixel features
    * Thresholding (binarization) on the gray value (Otsu)
  - Edge-based approach
  - Region merging and growing
  - Hybrid optimization approach
- Interactive segmentation methods

and many others. There are some general references such as [170] and [163] where fundamentals on image processing are well covered.

8.2.1. Watershed Transform

The idea behind watershed transform is to interpret each pixel's grey level as an altitude. Different approaches may be employed to use the watershed principle; here we just describe one of them. Two steps are necessary in order to segment hand, that is, marker extraction and watershed transform. Reader can ask why it is necessary the marker extraction and just keep going straight to watershed transform. The main reason is because the direct application of the watershed segmentation algorithm generally lead to over-segmentation of an image due to noise and other local irregularities. This can render the result to be virtually useless. The first step tries to extract the hand from the background. Depending on the background this process can be easy or extremely difficult. With this idea a two clustering problem face the first step and incorporating a preprocessing stage designed to bring additional knowledge into the next step. The second step uses the morphological gradient from grey level. The main aim of the this segmentation algorithm is to find watershed lines [207].

8.2.2. K-means

The main goal of the segmentation process is to separate two main different regions. Once this is clear, a simple approach can be tested. With this idea a K-means clustering algorithm with $k = 2$ can be applied. However this easy approach can give some undesired holes or other irregularities. Then it is advisable to perform some morphological operators.

8.2.3. Skin Detection

Sometimes when the image is good enough, this approach turns out to be interesting to detect skin [159]. Obviously, there are many other applications related to skin detection such as person detection, face detection [22], face tracking and hand tracking as well. In

fact, the human skin has some color properties that can be explored in order to segment human characteristics such as face or hand. The color spaces primarily used to detect human skin are RGB (Read, Green and Blue), HSV (hue, saturation, value) and YC_bC_r. RGB is perhaps the most used color space to represent images and one of the rules to determine whether a pixel is skin or it is not. However, some drawbacks are present. Between them, high correlation between channels, significant perceptual non-uniformity and mixing of chrominance and luminance data.

YC_bC_r is another colour space with some interesting characteristics. First, it reduces the redundancy present in the RGB and second it works under statistically independent components. The representation stores the luminance information as a single component (Y), and the chrominance information is stored as two colour-difference components C_b and C_r.

Other colour spaces are suitable for skin detection but two of such rules have been tested coming from RGB and YC_bC_r color spaces (see Equation (8.1) and Equation (8.2)) The way the rule from Equation (8.1) is deployed can be seen in Figure 8.4. Although one could stand for a correct skin detection there are many samples where the skin identification does not perform well. It is not a problem from the rule itself but from the image. In other words, the colour properties from our hand data base are no quite well represented by the described rules. One possible solution came up immediately in the sense to generate a better decision rule that fit the real sample data. This is not the intention, because many other segmentation methods use other variants [231] better for our images.

$$\begin{gathered}
\text{R} > 95 \text{ and G} > 40 \text{ and B} > 20 \text{ and} \\
\max(\text{R,G,B})\text{-}\min(\text{R,G,B}) > 15 \text{ and} \\
\text{abs(R-G)} > 15 \text{ and R} > \text{G and R} > \text{B} \\
\text{or} \\
\text{R} > 220 \text{ and G} > 210 \text{ and B} > 170 \text{ and} \\
\text{abs(R-G)} <= 15 \text{ and R} > \text{B and G} > \text{B}
\end{gathered} \tag{8.1}$$

$$\begin{gathered}
\text{Cb} >= 77 \text{ and Cb} <= 127 \\
\text{or} \\
\text{Cr} <= 133 \text{ and Cr} >= 173
\end{gathered} \tag{8.2}$$

The result of both rules can be deployed in the same user as an example of what areas are identified as skin. What is clear is that in Figure 8.2 all hand areas are marked as skin as a result of applying Equation (8.2). However there are some though issues. The

rule also marks as skin areas far from hand and to be precise they are in the neoprene surface layer. This behaviour was not punctual on few users but general. That is the reason to discard the rule. In the other representation, see Figure 8.3, it shows hand areas are marked as skin but many hand areas are not detected as skin. The application of (8.1) guarantee that all points marked are inside the hand. What is clear is that neither rule works perfectly well, but we use the RGB rule as an additional information to improve the step of thresholding.

Figure 8.2.: *handP1S1VIS1skinYCbCr*

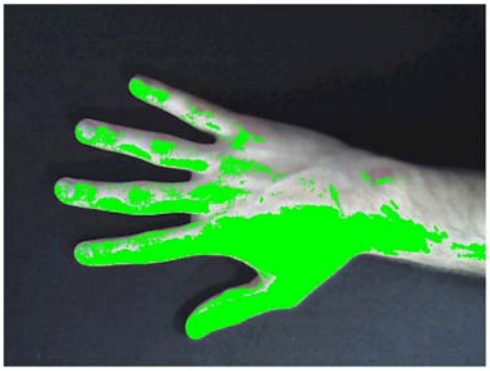

Figure 8.3.: *handP1S1VIS1skinRGB*

Figure 8.4.: *HandSegmExempP30S9step3*

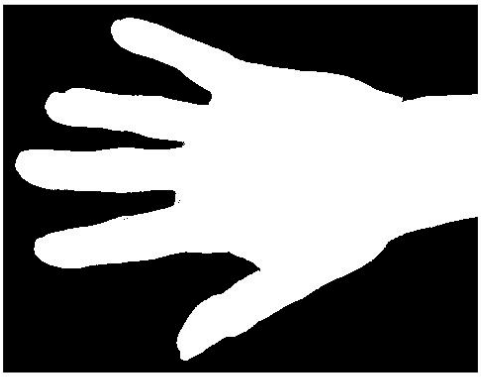

Figure 8.5.: *HandSegmExempP30S9step4*

8.2.4. Otsu's Method

The approach finally deployed in this thesis in order to segment hands has been a method based on thresholding. Using the image histogram one can find an optimal threshold. In general, a good threshold can be selected if the histogram peaks are tall, narrow, symmetric, and separated by deep valleys. As it has been seen in the histogram from Figure 8.1 there is a clear separation but not with deep valleys.

Using prior knowledge for segmentation such as the area or size of the objects present in the image one can improve performance. Otsu's segmentation is based on region homogeneity and region homogeneity can be measured using variance. Otsu's method selects the threshold by minimizing the within-class variance. However this method has some threads: does not work well with variable illumination, assumes that the histogram of the image is bimodal, breaks down when the two classes are very unequal.

According to the experimental results obtained the threshold for the segmentation method has been chosen empirically as:

$$\frac{95}{255}$$

8.2.5. General Segmentation Approach

In this subsection it is shown the basic backbone of the developed hand segmentation steps (see Listing 8.1).

It is worth mentioning the way it is overcome the set of image problems through a moving average process. First, it helps with non smoothly boundaries, and second it overcome ring and other artefacts present in users hand. Thus, moving average have been deployed successfully during the segmentation process. What it is clear with our hand database is that needs some noise reduction technique in order to avoid the hand looks pretty abrupt and useless. In Figure 8.6 it is shown the effect of wrong illumination conditions. This kind of effects are hard worst when there is a ring or other artefact such as bracelets. In this representation horizontal and vertical blue lines show the center of mass for this image and red line is linked to the major directional component.

The solution proposed is a moving average filter, quite common in time series analysis. The most easy one is the simple moving average (see Equation (8.3)) but give better results the exponential version of the formula. The exponential moving average also known as exponentially weighted moving average for the way it computes the new values as weights that decrease exponentially. In Equation (8.4) there is the recursive version of the formula.

$$x_t^* = \frac{1}{k}\sum_{i=0}^{k-1} x_{t-i} \tag{8.3}$$

Listing 8.1: VIS Segmentation Steps

```
% Read Image from path
I=imread(pathVIS11);
% Skin Detection
[infoCSkin]=findSkin(I,15,0);
% Threshold, from experimental tests
defThr = 95/255;
% Converts the grayscale image gI to a binary image
Shape=im2bw(gI,defThr);
% Perform Morphological Op.
[Shape,I]=morphCorrectOp(Shape,I);
% Mask Definition
MaskBin = zeros([480 640]);
contour=getContour(MaskBin);% Extract Contour
% Smooth contour operation through Moveng Average
parExp=10;
cRF=movavg(contour(:,2),parExp,e);
rRF=movavg(contour(:,1),parExp,e);
BW1 = roipoly(rgb2gray(I), cRF, rRF);
for i=1:3
    I(:,:,i)=double(K(:,:,i)).*BW1;
end
% I correspond to the masked image
% BW1 is the mask
```

$$\begin{cases} x_1^* = x_1 \\ x_t^* = \alpha x_t + (1-\alpha)\, x_{t-1}^*; \text{for } t \geq 2 \end{cases} \tag{8.4}$$

In Figure 8.7 it is showed the same hand's mask following the method developed for this thesis. Here hand has been smoothed and obviously some fine details have been lost. Nevertheless, some major hand characteristics remain invariant such as length and width measures from hand or finger. Results will show that finger widths and hand geometric measures are highly discriminative (see Chapter 11). This indicates that the filtering process has not removed useful information to correctly identify or verify a user.

One decision has to be made for the k value of the exponential moving average. As a trade-off between preserving the original silhouette which result in low k values and remove noise from highly corrupted images with high k values. The rule followed is taking a low k value, say $k = 10$. This measure helps in keeping mainly the original hand shape while it is smoothing a little bit the general hand shape. Results are satisfactory when no major problems are present (like rings).

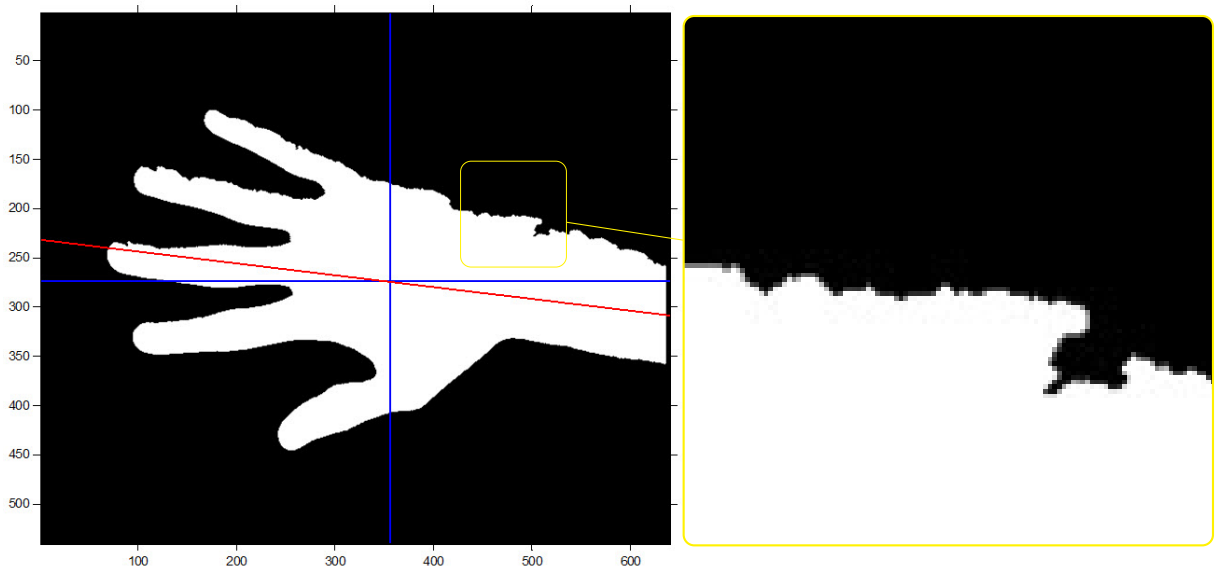

Figure 8.6.: *Hand Sample Mask without MA. Abrupt shape mask*

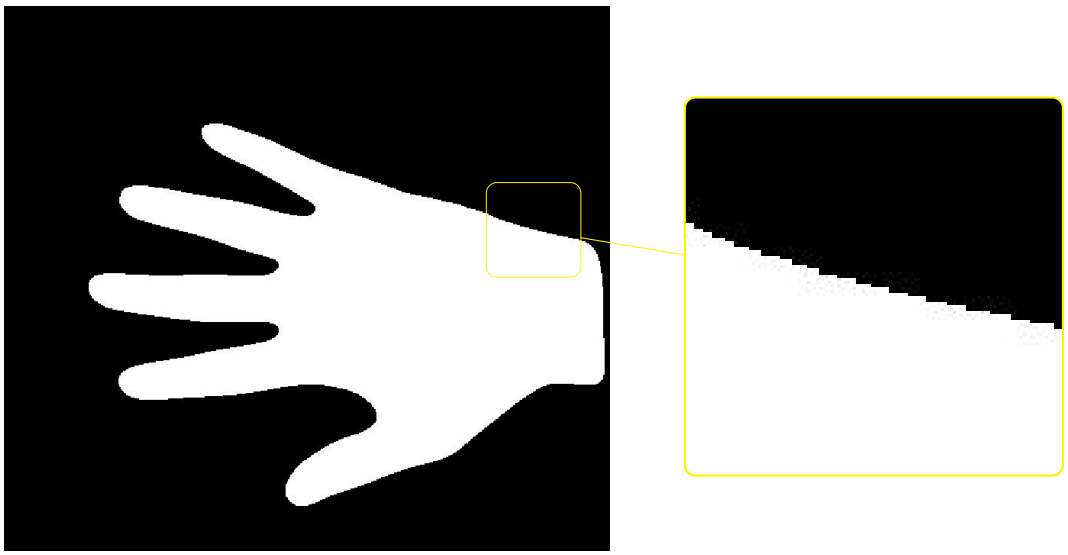

Figure 8.7.: *Hand Sample Mask with Exponential MA. Smoothed shape mask*

8.3. Finding Hand Key Points

The main hand key points are those who define the fingers' position: say tips and valleys, and it is also possible to add the wrist points (cuff will cause problems, though). The detection of tips and valleys are solved thanks to a distance function from a reference point. This reference point could be a point located in the center of the wrist. There are some strategies to find the reference point. If hand has no predefined orientation, let say has free orientation (rotation) the method proposed in [231] is advisable. They use the larger eigenvector of the inertia matrix with the wrist line to find the intersection point.

Once there is a reference point throughout wrist line it is possible to compute all distance from the contour. What this distance function is going to shows is some maxima and minima (see Figure 8.8). Optimum points correspond to the finger key points: tips and valleys.

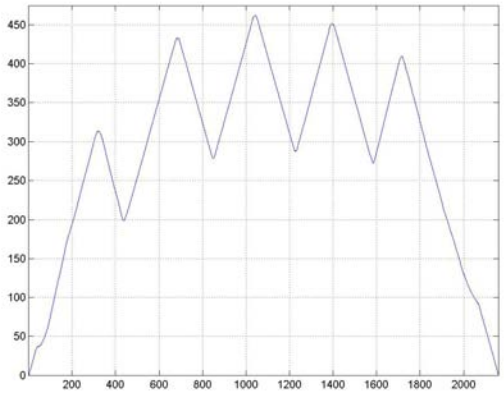

Figure 8.8.: *Radial distance function for Hand Key Points Detection*

There are some ways to compute the unknown key points depicted in Figure 8.10. These points are called valley points and depending on its vertical location are specified as up or down points. Thus the three unknown points are, pinky up valley point, index down valley point and thumb down valley point. One way, and perhaps the easy one to came up with is to join a line between finger valleys from ring finger. The intersection point between this line (that goes through ring up and down valley points) and the contour identifies one of these unknown points. This process can be repeated for the other unknown values (see Figure 8.11). For example, the intersection between the line coming from index up and thumb up valley points give another unknown point. Keep in mind that this point is slightly different from that represented in the previous Figure. This strategy has been used in [66] while a more sophisticated one comes from [47]. In this article its proposed a similar distance from the tip to the known valley point and to

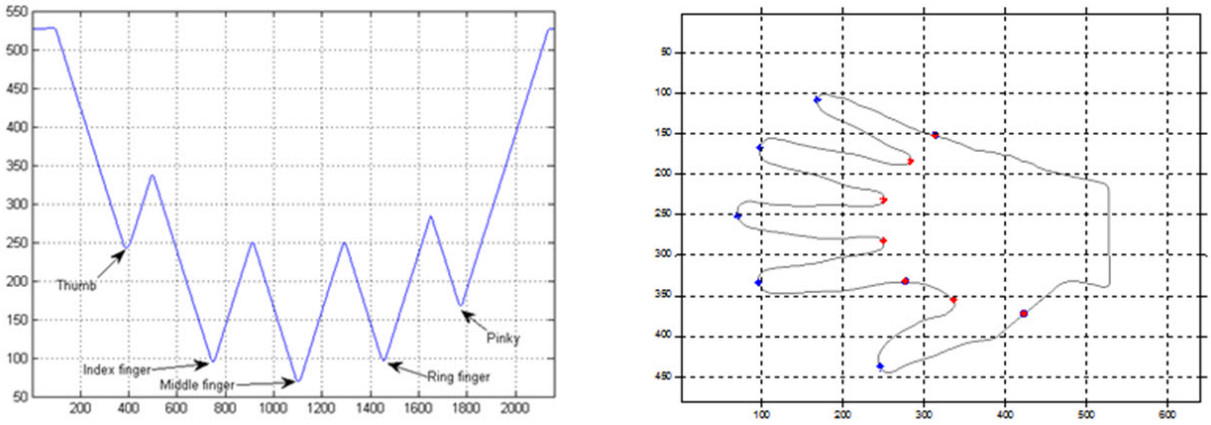

Figure 8.9.: *Hand Key Points Detection*
Left Figure: Y axis is linked with the X axis of the right image

the unknown point. The idea is to preserve some similar distance from valley points to the tip point (see Figure 8.12). The advantage of this method relays on its flexibility to adjust the distance. With the help of a fixed parameter Δ_i it is possible to increase or decrease the distance used to locate the unknown valley points.

Once identified the hand key points it is possible to segment fingers. In Figure 8.14 it is showed how to obtain fingers or proceed to a more sophisticated process like finger registration [47, 231].

8.3.1. Finger Segmentation

In order to properly segment fingers and use them as an individual modality the following process is described .

- Locate finger key points through minima and maxima radial distance function
  - Tip finger points (the farthest points or maxima points)
  - Up and down valley points (the minimum points)
- Create a Mask for that finger
  - Use the whole hand contour to locate the desired finger
  - The initial point corresponds to the down valley point of that particular finger
  - Then take all points from here (down valley point) to the up valley point. (Observation: The tip finger point will stay in this Mask)
  - Create a Mask from these specific obtained points.

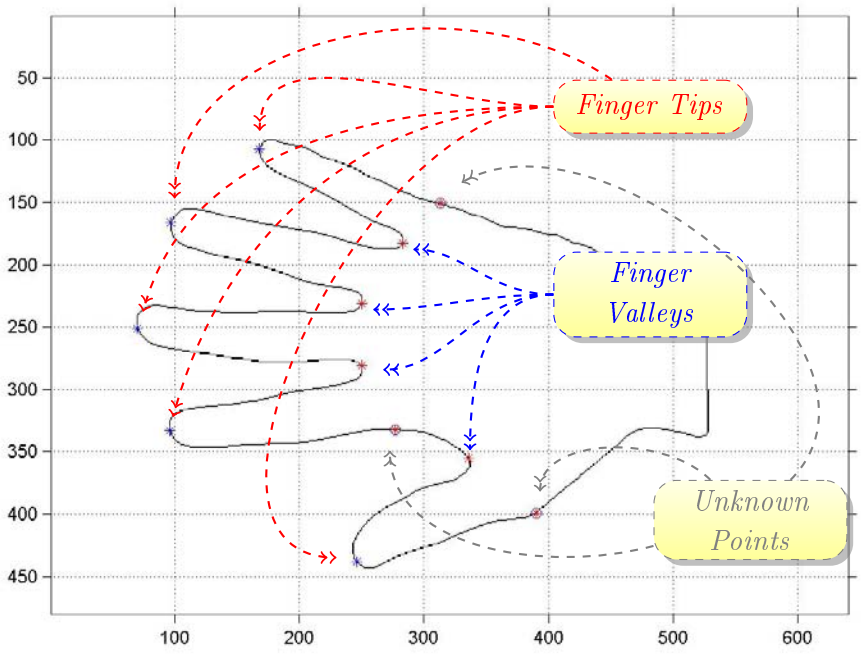

Figure 8.10.: *Extreme points. The tip and valley come directly from maxima and minima points from the radial distance function. The unknown points, however are located in a no optimum place (neither minima or maxima values) and it must be figured out how to compute them*

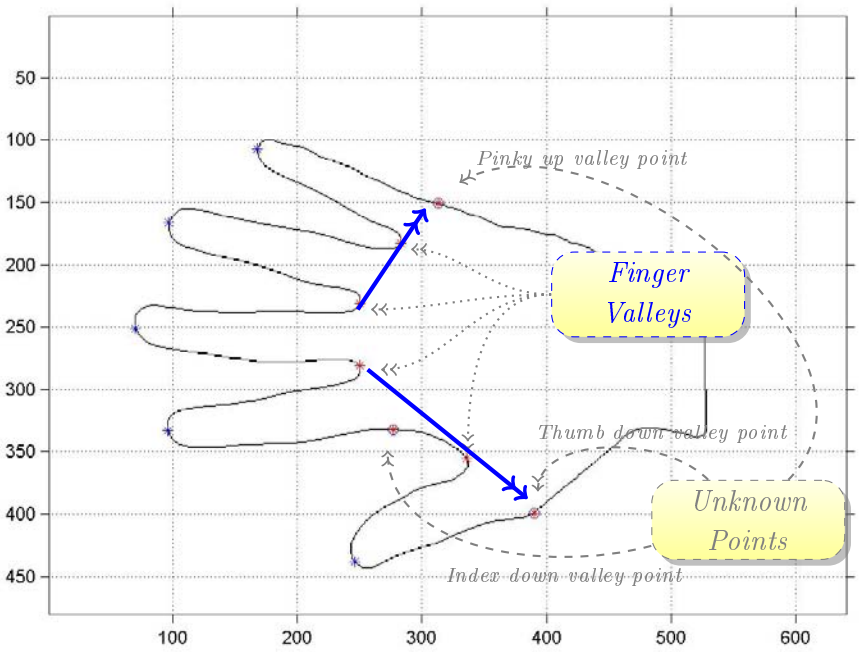

Figure 8.11.: *Unknown Points Identification. From two well known valley points it is obtained the unknown points through an intersection between this line and the finger contour.*
From up and down ring valley points a line is generated. This line helps locate the Pinky up valley point when it goes through hand contour and an intersection point is found.

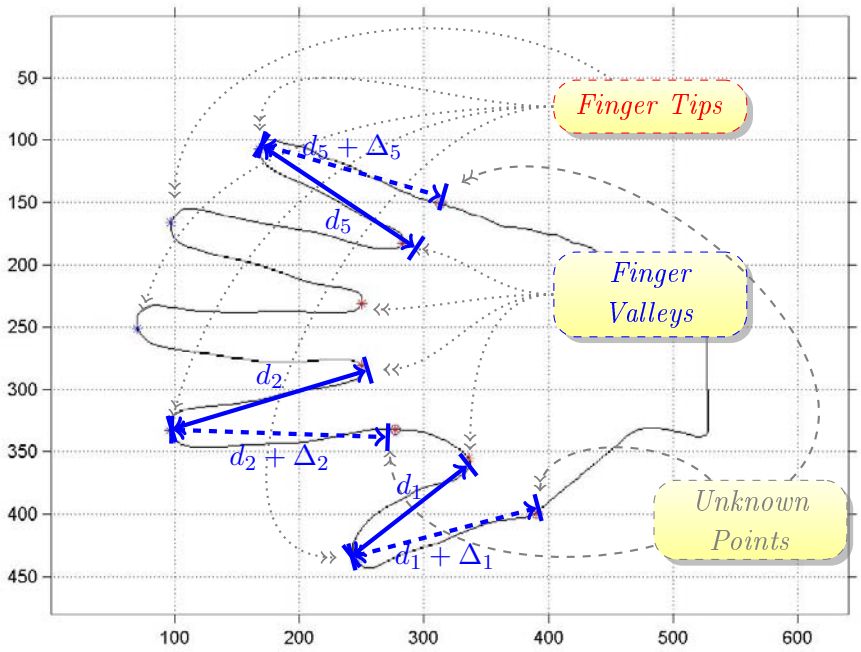

Figure 8.12.: *Unknown Points Identification. From two well known points it is computed a distance, used to figure out the location of the unknown valley point.*
For instance, $\Delta_5 = 0$ would be a right decision because the distance between up and down valley points are practically the same. That is not the case with Thumb down valley, so the $\Delta_1 > 0$

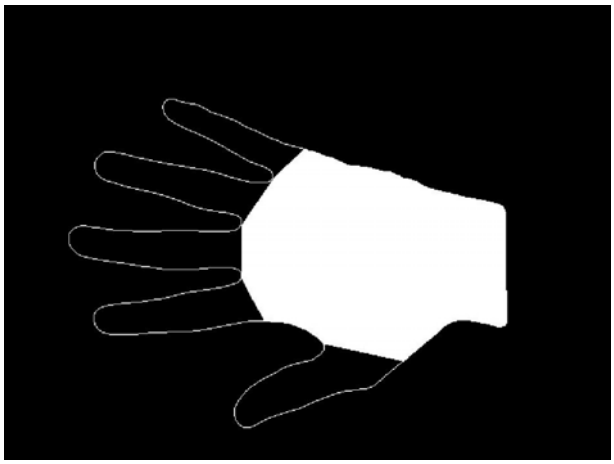

Figure 8.13.: *Finger Segmentation*

- Apply the mask over the image to obtain the finger
- Compute eigenvectors
- Compute angle and center of mass
- Rotate (to an horizontal position)
- Translate (to the center of the image)

Listing 8.2: Finger Segmentation

```
for i=1:nFingers
    %Compute eienvectors from finger inertial matrix
    cmpF=comptF(I,keyPoints);
    %Compute the orientation angle
    cmpFangle=arctan(v1,u1);
    %Rotate the finger to ensure horizontal place
    imrotate(fI,cmpFangle);
    %Translate the finger to the center of the image
    imtranlate(fI,par);
    %Save the finger
    save(fI)
end
```

Listing 8.3: Detailed Finger Segmentation

```
II=zeros(300,300);%New immage Gray
%%%%%%%%%%%%%%%%%%%%%%%%%%%%%%%%%%%%%%%
% Computation of the eigenvectors from finger inertial matrix
[center,e1]=findDirection(FINGER);
[r,c]=find(FINGER);
opts.disp=0;
[e2,h]=eigs(cov([r c]),1,lm,opts);
e2=sign(trans(e1)*e2)*e2;
e1=e2;
%%%%%%%%%%%%%%%%%%%%%%%%%%%%%%%%%%%%%%%%%%%%%%
% Compute angle and rotate to a horizontal position
angle1=atan(e1(2)/e1(1))*57.2957795;% 1 rad= 57.2 degree
if (angle1>0)
    angle2=90-angle1;
else
    angle2=-(angle1+90);
end
B = imrotate(II,angle2,bicubic,crop);
%%%%%%%%%%%%%%%%%%%%%%%%%%%%%%%%%%%%%%%%%%%%%%%%%%%%%%%

%%%%%%%%%%%%%%%%%%%%%%%%%%%%%%%%%%%%%%%%%%%%%%%%%%%%%%%%%%%%%%
%     Translation from centerB to centerN
[centerB,e1B]=findhanddirection(uint8(B));
centerN=[150 150];
trans=centerB-centerN;
[Mrrz,Mccz]=find(B);% rows and columns of elements different from 0
IIN=zeros(300,300);%New immage Gray
dimNI=length(Mrrz);%dimension of finger
for i= 1 : dimNI
    nprow=round(Mrrz(i)-trans(1));%new row index coordinate
    npcolumn=round(Mccz(i)-trans(2));%new column index coordinate
    IIN(nprow,npcolumn)=B(Mrrz(i),Mccz(i));
end
%%%%%%%%%%%%%%%%%%%%%%%%%%%%%%%%%%%%%%%%%%%%%%%%%%%%%%%%%%%%%%%
```

8.4. Holistic Approach

The holistic approach is performed using the Discrete Cosine Transform (DCT). Other approaches for extraction and dimensionality reduction are possible, for instance, Principal Component Analysis (PCA) or Multidimensional Scaling(MS). DCT has an interesting property that makes the method preferred over Discrete Fourier Transform (DFT). DCT always obtains real valued coefficients. Both methods transform the original signal to a transform domain. The very first coefficients refer to the signal's lowest frequency, and usually carries the major strength in terms of representative information. The last coefficients represent the contra-position situation. In this case components of the signal

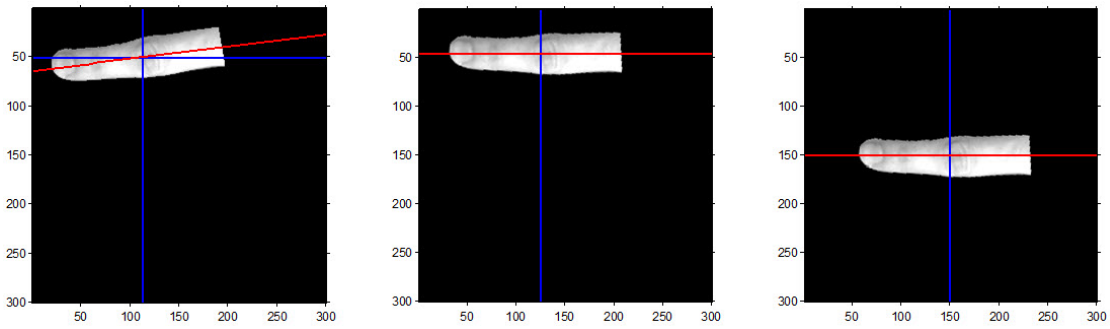

Figure 8.14.: *Finger Normalization.*
The process standardize angle orientation and position

that have the higher frequencies. These frequencies represent thin image details.

The main objective of these methods is to reduce the curse of dimensionality while keeping the important information. This reduction has other side effects that are also desirable such as simplify complexity, reduce noise, enhance computation costs and improve accuracy. All image information has been processed through Equation (8.5) and then saved as a component' vector. Thus, each hand and finger image has been reduced to a single vector of 2.000 frequency components length. The 2.000 value has been chosen arbitrary from hand analysis and has been kept from finger as well.

$$C(u,v) = \alpha(u)\,\alpha(v) \sum_{x=0}^{N-1} \sum_{y=0}^{N-1} f(x,y) \cos\left[\frac{\pi(2x+1)u}{2N}\right] \cos\left[\frac{\pi(2y+1)v}{2N}\right] \tag{8.5}$$

For $u, v = 0, 1, 2, ..., N-1$ and $\alpha(u)$ and $\alpha(v)$ defined as

$$\alpha(i) = \begin{cases} \sqrt{\frac{1}{N}} for i = 0 \\ \sqrt{\frac{2}{N}} for i \neq 0 \end{cases} \tag{8.6}$$

The reduction done in each image analysis has been always the same. No matter the original source size because the characteristic vector will be evaluated just before classification in order to use only those component discriminant enough for recognition. For instance, the normalized hand has a dimension of 640×480 pixels. Applying the DCT2 formula (Equation (8.5)) it is obtained a matrix with the same image dimension. That is a 640×480 frequency component matrix. For the properties of DCT2 the component selection has been made sorting the frequency components by zigzag as it is shown in Figure 8.15.

For recognition application less than 500 components had been enough, but for later analysis it was kept 2000 components. The resulting vector is seen in Figure 8.16.

$$\begin{bmatrix} x_{11} & x_{12} & x_{13} & x_{14} & \dots \\ x_{21} & x_{22} & x_{23} & x_{24} & \dots \\ x_{31} & x_{32} & x_{33} & x_{34} & \dots \\ x_{41} & x_{42} & x_{43} & x_{44} & \dots \\ \dots & \dots & \dots & \dots & \dots \end{bmatrix}$$

Figure 8.15.: *Zig Zag Extraction process from DCT2*

$$\begin{bmatrix} x_{11} & x_{12} & x_{21} & x_{31} & x_{22} & x_{13} & x_{14} & x_{23} & x_{32} & x_{41} & \dots \end{bmatrix}$$

Figure 8.16.: *DCT2 resulting vector*

8.4.1. Hand Data Extraction

Hand can not be processed directly. The finger and hand orientation vary from sample to sample within the same user. The solution is to normalize hand. To normalize hand through a process called registration ensures that the fingers follow some predefined standard orientation and location. The final result of the registration process can be seen in Figure 8.17. Two different views from hand and the central part of the hand are shown. The first view is the standard enhanced VIS image and the other one correspond to a texturized version (from PCA).

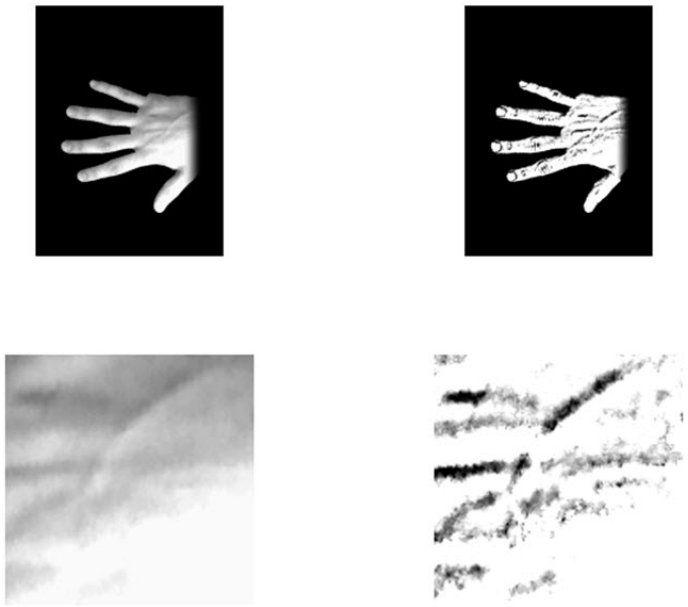

Figure 8.17.: *Hand and PALM images*

The data sets saved from Hand data extraction are viewed in Listing 8.4

Listing 8.4: VIS Hand and Palm extraction

```
%XXX Aquisition XXXX
%X Palm Square (Vis and Text) and Hand (Vis and Text)
%X 11 12 13 14
getHandVIS{11,sample}=getDCT2img(NormPalmVIS,dComp);
getHandVIS{12,sample}=getDCT2img(NormPalmTEX,dComp);
getHandVIS{13,sample}=getDCT2img(NormHandVIS,dComp);
getHandVIS{14,sample}=getDCT2img(NormHandTEX,dComp);
%XXXXXXXXXXXXXXXXXXXXXXXXX
```

8.4.2. Finger Data Extraction

All fingers' VIS information have been saved within a MATLAB object. In Listing 8.5 it is shown the way VIS fingers are processed and saved. Thanks to MATLAB object all data sets are easily reload to deploy recognition.

Listing 8.5: VIS finger extraction

```
%XXX Aquisition XXXX
dComp=2000; % DCT2 Length

%X Finger Factorization 1:5 DirectVisual
for ii=1:5
            getFinger=extractFinger(gI,FINGER{ii});
            getHandVIS{ii,sample}=getDCT2img(getFinger,dComp);
end
%XXXXXXXXXXXXXXXXXXXXXXXXX

%XXX Aquisition XXXX
%X Finger Factorization 6:10 TextureVisual
for ii=1:5
            getFinger=extractFinger(gITXT,FINGER{ii});
            getHandVIS{ii+5,sample}=getDCT2img(getFinger,dComp);
end
%XXXXXXXXXXXXXXXXXXXXXXXXXX
```

The total amount of files coming from holistic analysis are summarized in Table 8.1. There, it is possible to appreciate the 4 data files coming from hand and 10 data files coming from fingers.

Table 8.1.: *Hand Holistic Data Files.*
The whole Visual Holistic Data Set with 2000 DCT2 components

Id. Name	Type	Name	Option
getHandVIS1	Finger	Thumb	
getHandVIS2	Finger	Index	
getHandVIS3	Finger	Middle	
getHandVIS4	Finger	Ring	
getHandVIS5	Finger	Pinky	
getHandVIS6	Finger	Thumb	TXT
getHandVIS7	Finger	Index	TXT
getHandVIS8	Finger	Middle	TXT
getHandVIS9	Finger	Ring	TXT
getHandVIS10	Finger	Pinky	TXT
getHandVIS11	Hand	Central	
getHandVIS12	Hand	Central	TXT
getHandVIS13	Hand	Hand	
getHandVIS14	Hand	Hand	TXT

TXT: Texture

8.5. Geometric Approach

The geometric approach presents some innovative solutions to conduct recognition. First will be introduced the hand geometric features and later on the finger geometric features as it has been described previously for holistic approach.

8.5.1. Hand Geometric Features

This subsection describes the different extraction process that has been deployed using the complete hand. A number of data sets have been generated (see Table **??**).

Table 8.2.: *Hand Geometric Data Files from VIS images*

Id. Code	File Name	Based on
visHG1	vecGeomVIS15	lengths and widths from hand key points
visHG2	vecGeomVIS18	lengths and widths from hand and finger
visHG9	vecGeomVISHandcurv3	EMA(3) + Curvature + DCT
visHG10	vecGeomVISHandcurv4	EMA(10) + Curvature + DCT

vecGeomVIS15

The idea behind this data set is compute distance from finger tip points to valley and mid valley points. The characteristics of these vectors are summarized in three main sections. *The first section* takes into account the finger tips points to compute distance from here to valley points. These valley points can be located at valley points, or somehow between them, *down*, *up*, *middle* and *midEIG*. These last two points are not strictly valley points, but mid points between the former ones. Thus, middle point is the mean point from *down* and *up* valley points, and *midEIG* is the intersection point between the major finger eigenvector and the line between *down* and *up* valley points. *The second section* of components compute all possible distance from *midEIG* adding the hand mean point (*handmid*). *The third and last section* compute components at first sight perhaps not obvious for person recognition but might be a help in gender recognition problems. This last set of components are distance difference between middle finger and the other ones (for further details it has been showed a Matlab Listing 8.6)

In Figure 8.18 the components of vecGEomVIS15 data set are seen in two images. The left one corresponds to the components described before as from the first section, while the right one links with the second section.

vecGeomVIS18

This data set joins information coming from finger widths and finger properties. Actually it is coming from finger extraction data set called **vecGeomVISfingWidth10** and from other image region computations. In this case the vector has five different sections, each of them associated with one of the five possible fingers (from thumb to pinky). So, each section has finger area, finger perimeter, major axis length, minor axis length plus an additional information coming from finger width data set. Thus, twelve components for section gives a total of 58 components. A description can be found in Listing 8.7

This data file is looking for a good balance between finger widths (8 measures) and an additional finger measures (area, perimeter and length of the major and minor axis).

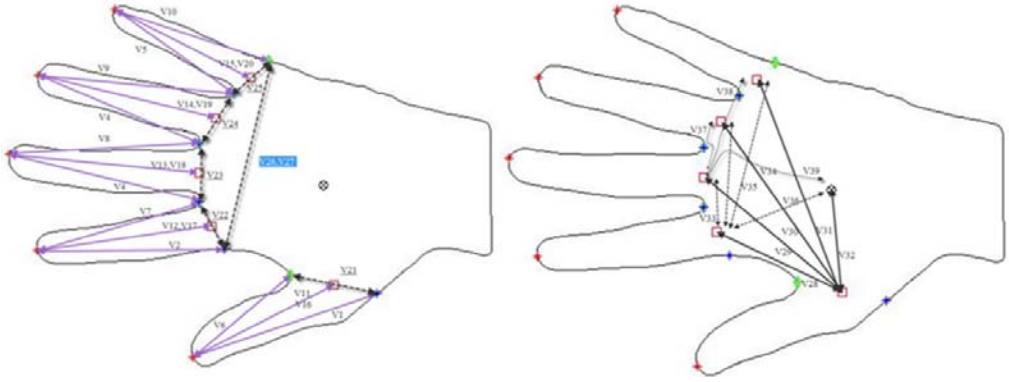

Figure 8.18.: *Lengths and widths measures from Hand Extraction Data File* ***vecGeomVIS15***

vecGeomVISHandcurv3 and vecGeomVISHandcurv4

These two subsets are the best representatives among other curvature subsets. They all work under the assumption of a hand contour. There is no normalization performed in order to correct some finger orientations, uniquely a simple transformation through a base change (see the effect in Figure 8.19). Curvature is a simple idea (used also in [16]) that trays to model variations within a curve that in our case is the hand contour (perimeter).

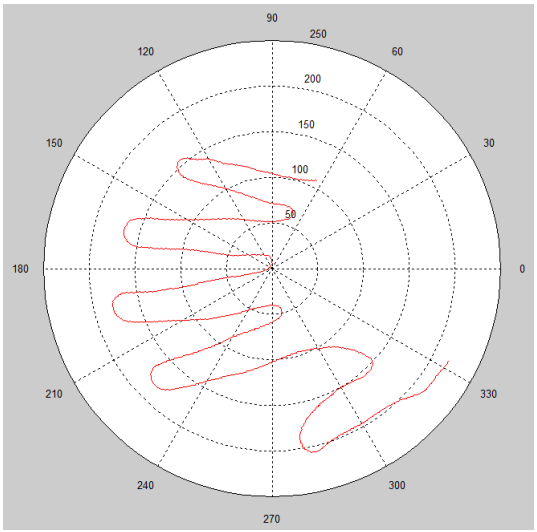

Figure 8.19.: *Hand Perimeter*

Let us define the following definitions: Let x_t be the coordinate in the x-axis in the t position, and let y_t be the coordinate in the y-axis in the t position. Then it is possible to define the following two operators $\bigtriangledown x_t$ and $\bigtriangledown^2 x_t$ as:

$$\bigtriangledown x_t = \frac{x_t - x_{t-1}}{y_t - y_{t-1}} \qquad \bigtriangledown y_t = \frac{y_t - y_{t-1}}{x_t - x_{t-1}} \tag{8.7}$$

$$\bigtriangledown^2 x_t = \frac{\bigtriangledown x_t - \bigtriangledown x_{t-1}}{\bigtriangledown y_t - \bigtriangledown y_{t-1}} \qquad \bigtriangledown^2 y_t = \frac{\bigtriangledown y_t - \bigtriangledown y_{t-1}}{\bigtriangledown x_t - \bigtriangledown x_{t-1}} \tag{8.8}$$

Both $\bigtriangledown x_t$ and $\bigtriangledown^2 x_t$ can be interpreted as an estimation of the first and second derivatives of x (and y respectively).

Then, the final curvature definition stands for:

$$Curv = \frac{\bigtriangledown x_t \times \bigtriangledown^2 y_t - (\bigtriangledown y_t \times \bigtriangledown^2 x_t)^2}{(\bigtriangledown^2 x_t + \bigtriangledown^2 y_t)^{2/3}} \tag{8.9}$$

Equation (8.9) can be seen as an instantaneous rate of change of the slope of the tangent with respect to arc length. The curvature is very sensitive to noise whether it came from x_t or from y_t. For this reason, it has been left a free parameter that allows to reduce noise through an exponential moving average. The goal is to increase the curvature reliability applying an Exponential Moving Average to both x_t and y_t. In the data sets described in this section parameter has been set to 3 and 10 respectively. These two possibilities generate the following two data sets (see Figure 8.20 and Figure **??**).

The final step in order to work under the same characteristic vector has been to apply a DCT. The DCT coefficients are saved and define the user feature vector for *vecGeomVISHandcurv3* and for *vecGeomVISHandcurv4*.

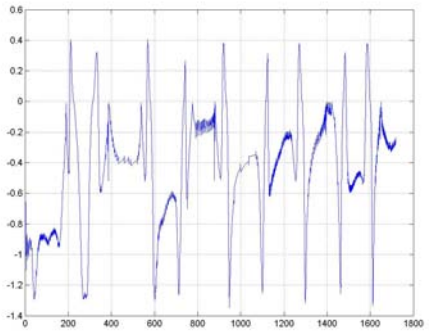

Figure 8.20.: *Curvature Exp(3)*

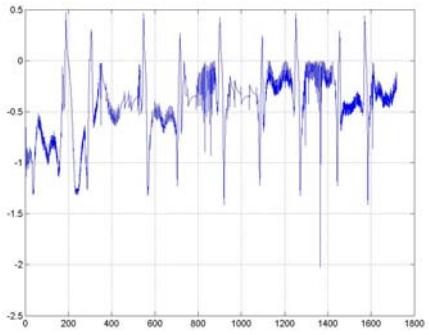

Figure 8.21.: *Curvature Exp(10)*

Polar Coordinates

It is straightforward to use polar coordinates for recognition. Actually there have been saved for comparison or for later research. Nevertheless will be used within finger data sets.

8.5.2. Finger Geometric Features

With the same idea as previously exposed in the last subsection it is presented the extraction data sets for each of the 5 fingers. A total of 7 data sets have been obtained for analyse and are also described in Table 8.3.

Table 8.3.: *Finger Geometric Data Files*

Id. Code	File Name	Based on
visFG1	vecGeomVISfingWidth10(:,:,ki)	10 measures + trimming
visFG2	vecGeomVISfingWidth25(:,:,ki)	25 measures + trimming
visFG3	vecGeomVISfingWidth50(:,:,ki)	50 measures + trimming
visFG4	vecGeomVISfingWidth200(:,:,ki)	200 measures + trimming
visFG5	vecGeomVISfingWidth200DCT(:,:,ki)	DCT(Width200)
visFG6	vecGeomVISfingPol(:,:,ki*2-1)	Polar C.: Theta + DCT
visFG7	vecGeomVISfingPol(:,:,ki*2)	Polar C.:Rho + DCT

It has already been shown in previous bibliography a lot of good results are obtained through finger widths. There is a clear interest in discover the effect of the width when the number of widths alongside fingers varies in length (10, 25, 50 and 200). There is a clear view of how data is depicted depending on these dimensions (see Figure 8.22).

Finger Width

Five different data sets have been generated taking into account finger widths. However, all width characteristic vectors have been trimmed in order to increase performance and to reduce possible noisy effects. If we take as an example the data set *vecGeomVISfingWidth10* that initially had 10 width fingers measures, actually has eight width measurements. The first width of the vector which are under the tip finger point has been removed. The last width measurement (tail of the vector) has also been removed. The main reason to conduct this cut over the beginning and the ends of the finger width measures is to discard wrong widths (noisy effect).

Another different way to deal with width characteristic vectors is through a DCT. It does not has sense with a vector of reduced dimension, but it does with longer vectors such as *vecGeomVISfingWidth200*. For this case a DCT has been applied and a DCT coefficient vector has been obtained. We called this vector *vecGeomVISfingWidth200DCT*. Nevertheless, the 200 it is not an indication of the number of DCT components, instead from the

original widths measurements. The length of the vector has been fixed to 100.

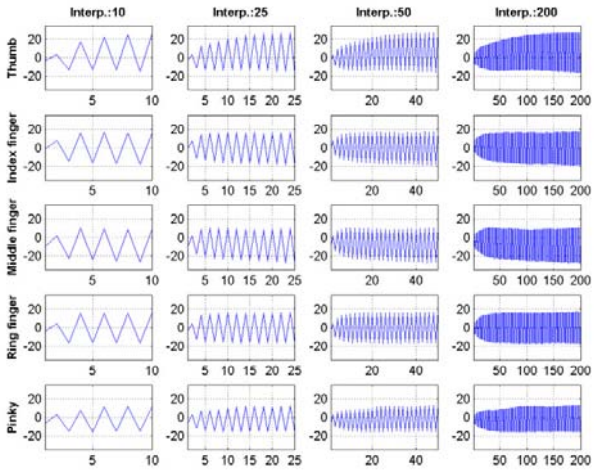

Figure 8.22.: *Finger Widths Data Sets. In rows the five fingers from Thumb to Pinky and in Columns from 10 measurements finger widths to 200.*

Polar Coordinates

Polar coordinates have been used as a characteristic vector as well. Thus, for each finger a couple of data files have been generated. The first one takes into account the θ (angle from a fixed direction $\theta = arctan(x, y)$) and the second one takes into account the ρ (distance from a fixed point $\rho = \sqrt{x^2 + y^2}$). In each case, the first 200 components of the DCT have been computed.

Listing 8.6: Info vecGeomVIS15

```
% First Part of Measures: finger lengths
%lFing1TipValdw, lFing2TipValdw, ..., lFing5TipValdw, lFing1TipValup, ...
% to see the distances of the first finger
%    dw  up    mid    midEIG
dist=[1,  6,   11,      16] = % F1 Thumb
dist=[2,  7,   12,      17] = % F2 Index
dist=[3,  8,   13,      18] = % F3 Midle
dist=[4,  9,   14,      19] = % F4 Ring
dist=[5, 10,   15,      20] = % F5 Pinky
%total distances 5 finger * 4 long = 20 values
numDIST2=[21.f1;22.f2;23.f3;24.f4;25.f5;26.d(f2f5);27.palmW]
%width base finger 1 x 5 + hand width x 2
%numDIST2= [wFing1ValdwValup, wFing2ValdwValup, ... , wFing1ValdwFing5Valup, wHand1, wHand2]
%%%%%%%%%%%%%%%%%%%%%%%%%%%%%%%%%%%%%%%%%%%%%%%%%%%%%%%%%%%%
% Second Part of Measures: Distance from fingers to midle of the hand
numDIST3=mxEIG;% %1 X 15 [28 29 30 31 32 33 34 35 36 37 38 39 40 41 42]
% Compute distance from Hand Center to midleFinger points
%                midEIGf2     midEIGf3       midEIGf4        midEIGf5         handmid
%1           0   137.5817(28) 178.3118(29)  203.8805(30)  221.5888(31)   138.5625(32)
%2   137.5817           0      56.1982(33)  104.0190(34)  147.5077(35)   220.0980(36)
%3   178.3118    56.1982             0       51.5678(37)  100.6700(38)   228.6579(39)
%4   203.8805   104.0190      51.5678               0      51.0866(40)   221.4200(41)
%5   221.5888   147.5077     100.6700        51.0866               0     205.9366(42)
%w   138.5625   220.0980     228.6579       221.4200       205.9366            0
%%%%%%%%%%%%%%%%%%%%%%%%%%%%%%%%%%%%%%%%%%%%%%%%%%%%%%%%%%%%
% Third Part of Measures: Finger length differences
difDits1=midle - index % midval    43
difDits2=midle - ring  %           44
difDits3=midle - thumb %           45
difDits4=midle - pinky %           46

difDitsE1=midle - index %  midEIG  47
difDitsE2=midle - ring %           48
difDitsE3=midle - thumb %          49
difDitsE4=midle - pinky %          50
```

Listing 8.7: Info vecGeomVIS18

```
%XXX Aquisition DATA antropometrics XXXX
%X Hand Measures widths 8 + 4 image measures
%X 4+8 4+8 4+8 4+8 4+8 Compute area of interest and widths of fingers
newFingQM=[];
for ii=1:5
    D = regionprops(Fing{ii}, area, perimeter,MajorAxisLength,MinorAxisLength);
    vectIMG0=[D.Area D.Perimeter D.MajorAxisLength D.MinorAxisLength];
    bb1=fingerTS{2}{ii,1,1}(2:end-1);%Compute finger Width and discard extreme values!
    newFingQM=[newFingQM vectIMG0 bb1];
end
getHandVIS{18,cara}=newFingQM;
```

Chapter 9.

NIR Preprocessing and Feature Extraction

Stephen Covey

Effective leadership is putting first things first. Effective management is discipline, carrying it out.

Overview

In this chapter we explain the basic pre process steps to segment NIR hand images. NIR images can be extremely noisy, for this reason it is important to mitigate or remove its effect. NIR imaging are playing an increasingly important role in many recognition applications and in many research fields as well. Even though NIR is invisible for human eye, its properties are close to those of VIS. The origin of NIR comes from physicist W. Herschel in early 1800, since then technological improvements have rise NIR to leading-edge scientific and industrial endeavours in many fields.

Contents

9.1. NIR Images

Many of the work needed to segment the NIR hand has already been described in the previous chapter. However, some specific problems must be addressed when facing NIR images. Perhaps the most important ones are the presence of noise and lack of definition with many edges. Is it true that with the help of a professional NIR camera and good illuminations these problems would be gone (at least partially). Because the thesis works with a home-made camera, with a reduced cost ($< 20 Euros$) a battery of image processing techniques are necessary in order to improve the final region of interest.

The approach has taken two different roads. The first one means identifying correctly the hand Mask. That is, the binary image used to obtain the desired region of interest (the hand). So it is not necessary to keep attention with the details inside the hand like vein patterns. Here, the focus is to obtain a clear binary Mask. The second road consider the enhancement of the hand, basically the presence of vein patterns (quite common in dorsal view).

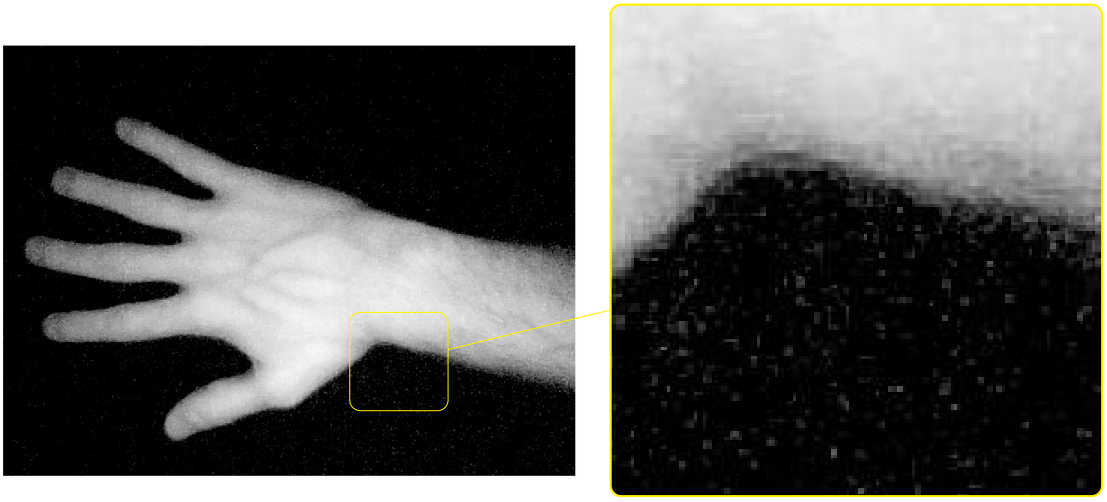

Figure 9.1.: *NIR original image. Visualization of noise disturbance.*

The details related to this approach are described in Listing 9.1

Is it possible to appreciate the effects of this approach in the set of Figures from Figure 9.2 to Figure 9.9.

The complete description of techniques and tools available for image enhancement and segmentation can be found in [170], in [163] and many others. In summary it is applied a nonlinear filter to reduce *salt and pepper* noise preserving the edges (*wiener2*). Then a Gaussian smoothing that is a low-pass filtering, which means that it smooth or blur the image suppressing noise and also small fluctuations. The filter called *unsharp* actually

Listing 9.1: NIR prepocessing steps

```
%XXXXXXXXXXXXXXXXXXXXXXXXXXX
%X NIR Preprocessing Steps
%%%% MASK identification
nIR=imread(pathIR11);
I3=enhanceLog(nIR,10,0);
nIRf = medfilt2(I3);
J = wiener2(nIRf, [3 3], 10);
h = fspecial(gaussian,[3 3],5);gauf=imfilter(J,h,replicate);
H = fspecial(unsharp);sharpened = imfilter(gauf,H,replicate);

defThr = 95/255;% defaoult threshold
BW1=im2bw(sharpened,defThr);
MASK=morphcorrect(BW1,nIR);

%%%% Image Enhancement
JJ = histeq(nIR);
JJJ = imadjust(JJ,stretchlim(JJ),[]);
%XXXXXXXXXXXXXXXXXXXXXXXXXXX
```

creates a filter for sharpening the image so it can improve edge detection. Once finished with this step it is possible to obtain a pre-Mask. This pre-Mask could be used directly but has been pre-processed in the same way VIS images have also been processed. It means, with the help the Exponential Moving Average filter. The difference between both masks can be seen in Figure 9.6 and in Figure 9.7.

On the other hand, there are the image enhancement process shown in the following Figures, Figure 9.8, and in Figure 9.7

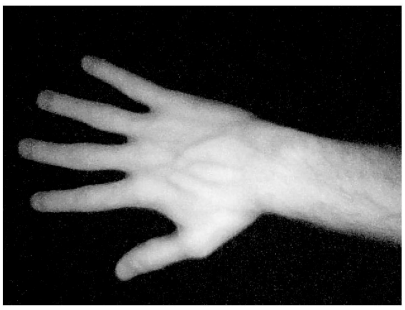

Figure 9.2.: *Initial NIR image*

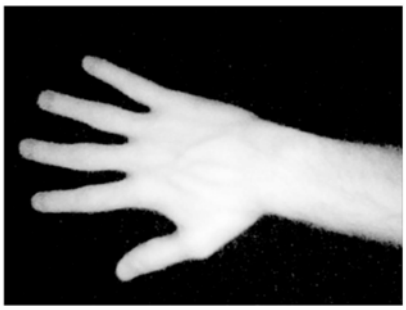

Figure 9.3.: *Log and Weiner Filter*

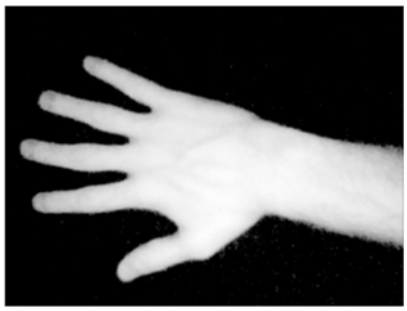

Figure 9.4.: *Gaussian Filter*

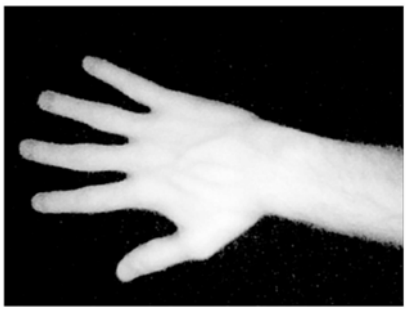

Figure 9.5.: *Sharpening Filter*

Figure 9.6.: *Initial Binary Mask*

Figure 9.7.: *Final Binary Mask*

9.2. Holistic Data

The way data sets from NIR data are obtained comes straight the same way described for VIS images. In Table 9.1 shows the main data sets generated in the holistic approach.

9.3. Geometric Data

Some of the geometric data collected for NIR images are quite similar to those coming from VIS images. Anyway, it is presented here the list of data files coming from the geometric approach that deal with the whole hand (see Table 9.2).

9.3.1. vecGeomNIRHandcurv3 and vecGeomNIRHandcurv4

It is not our intention to repeat the steps already described in chapter 8 with VIS images. Here it is only pointed out the effects to represent in the same figure the curvature of

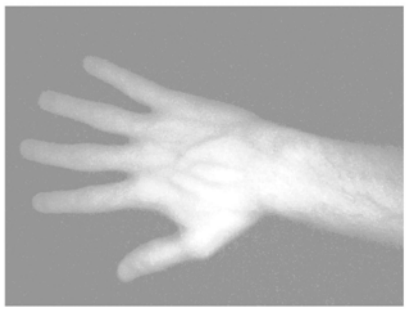

Figure 9.8.: *Histogram Equalization*

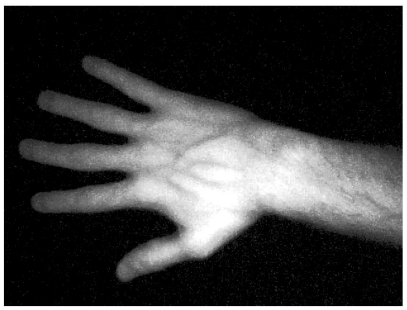

Figure 9.9.: *Grayscale Adjusted*

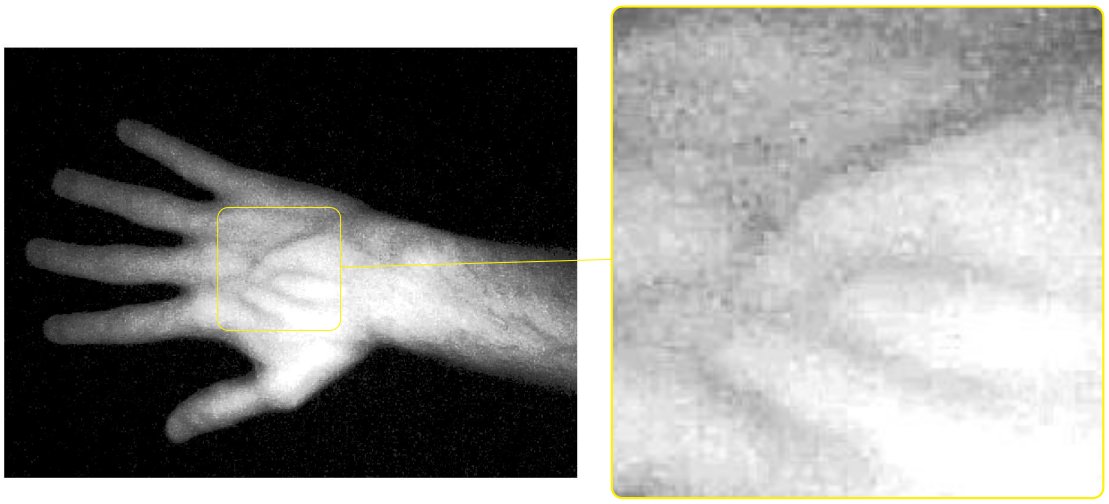

Figure 9.10.: *NIR Enhanced Image. The image still present a deep blur effect.*

two samples from the same user and compare (visually) with those of different users. It turns out, that there is some interesting behaviour that makes sudden changes (regime switching) highly correlate with that from same user. In Figure 9.11 and also in Figure 9.12 one can observe how both colors follow similar shape and curvature in the important points like regime switches.

It is obvious what is going to happen when curvature are coming from two different users (see detail in Figure 9.13 and in Figure 9.14). In these situations there is no any match between curvatures. This is only a visual example and it is left for results the detailed performance of this data sets.

Table 9.1.: *Hand Holistic Data Files.*
The whole NIR Holistic Data Set with 2000 DCT2 components

Id. Name	Type	Name	Option
getHandNIR1	Finger	Thumb	
getHandNIR2	Finger	Index	
getHandNIR3	Finger	Middle	
getHandNIR4	Finger	Ring	
getHandNIR5	Finger	Pinky	
getHandNIR6	Finger	Thumb	TXT
getHandNIR7	Finger	Index	TXT
getHandNIR8	Finger	Middle	TXT
getHandNIR9	Finger	Ring	TXT
getHandNIR10	Finger	Pinky	TXT
getHandNIR11	Hand	Central	
getHandNIR12	Hand	Central	TXT
getHandNIR13	Hand	Hand	
getHandNIR14	Hand	Hand	TXT

TXT: Texture

Distribution Measures Related to Gray Intensity

One of the main problem related with measures coming from the IR spectrum is the possible interferences. These drawbacks can be overcome with a suited infrared light (with a wavelength of 850-900 nm). However, emitted radiation from environment will remain unless lab conditions discard them. In our case neither case have been considered. To mitigate this drawback several data sets linked with gray intensity have been defined.

The idea behind gray intensity is that it gives some information related to temperature. Obviously this view it is not exact but will be used later on with thermographic images, where there is a clear link between both measures. Thus, an histogram and some descriptive statistic such as interquartile range (IQR), some specifics quantiles (at probabilities 0.025, 0.250, 0.500, 0.750 and 0.975), standard deviation and mean measures will be used.

The three data sets used are the following:

Table 9.2.: *Hand Geometric Data Files from NIR images*

Id. Code	File Name	Based on
nirHG1	vecGeomNIR15	lengths and widths from hand key points
nirHG2	vecGeomNIR18	lengths and widths from hand and finger
nirHG9	vecGeomNIRHandcurv3	EMA(3) + Curvature + DCT
nirHG10	vecGeomNIRHandcurv4	EMA(10) + Curvature + DCT

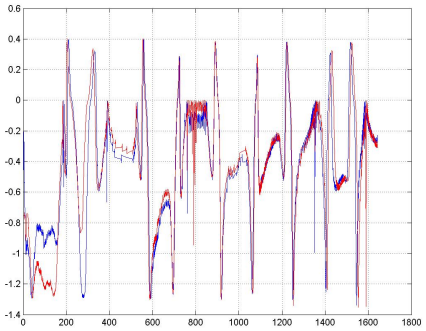

Figure 9.11.: *Curvature from Exp(3) and two samples from the same user*

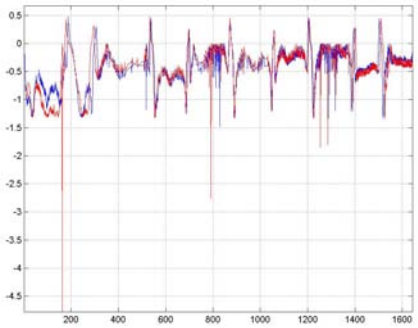

Figure 9.12.: *Curvature from Exp(10) and two samples from the same user*

- ★ getNIRqtyM: this data file takes each of the segmented fingers and compute the histogram, the quantiles, the mean, the IQR, and the standard deviation (see Listing 9.2).
- ★ getNIRqtyMpalm: this data file takes the same information but from the central part of the dorsal hand.
- ★ getNIRqtyMhand: this data takes into account all hand information. Thus the histogram and the other measures come from the whole hand.

It is important to highlight that this three data files where designed to be implemented with TIR images. It is with this images where environmental conditions can produce a huge effect on the object (hand) emittance radiation.

9.3.2. Finger Geometric Data

With the same idea as previously exposed in the last subsection it is presented the extraction data sets for each of the 5 fingers. A total of 7 data sets have been obtained

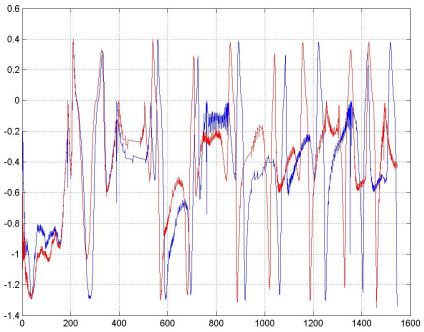

Figure 9.13.: *Curvature from Exp(3) and two samples from different user*

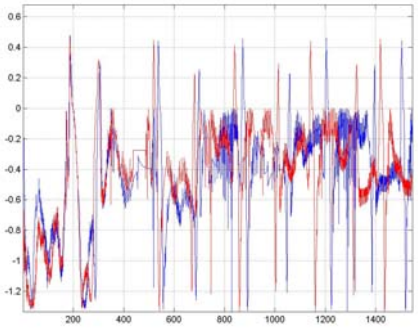

Figure 9.14.: *Curvature from Exp(10) and two samples from different user*

to analyse and are also described in Table 9.3.

Table 9.3.: *Finger Geometric Data Files from NIR images*

Id. Code	File Name	Based on
nirFG1	vecGeomNIRfingWidth10(:,:,ki)	10 measures + trimming
nirFG2	vecGeomNIRfingWidth25(:,:,ki)	25 measures + trimming
nirFG3	vecGeomNIRfingWidth50(:,:,ki)	50 measures + trimming
nirFG4	vecGeomNIRfingWidth200(:,:,ki)	200 measures + trimming
nirFG5	vecGeomNIRfingWidth200DCT(:,:,ki)	DCT(Width200)
nirFG6	vecGeomNIRfingPol(:,:,ki*2-1)	Polar C.: Theta + DCT
nirFG7	vecGeomNIRfingPol(:,:,ki*2)	Polar C.:Rho + DCT

The Finger Approach

This is one of the thesis contributions: Fingers provide better performance than the whole hand.

Listing 9.2: Info getNIRqtyM

```
%XXX Aquisition XXXX
%X Finger Factorization 1:5 DirectVisual
getIRqtyM=[];
for ii=1:5
    getFinger=extractFinger(gI,Finger{ii},0);
    getHandIR{ii,cara}=getDCT2img(getFinger,dComp);
    %%%%%%% Analyse
    ggg=uint8(getFinger);% get scale into (0,255)
    gggAn=ggg(find(ggg>1));% Select only pixels inside MASK (MASK = 0)
    [countsIR,xIR] = hist(double(gggAn),[5:10:245]);
    quantAn = quantile(double(gggAn),[.025 .25 .50 .75 .975]); % Summary of x
    meanAn=mean(double(gggAn));
    iqrRAn=iqr(double(gggAn));
    stdAn=std(double(gggAn));
    getIRqtyM=[getIRqtyM countsIR quantAn meanAn iqrRAn stdAn];
end
%XXXXXXXXXXXXXXXXXXXXXXXXX
```

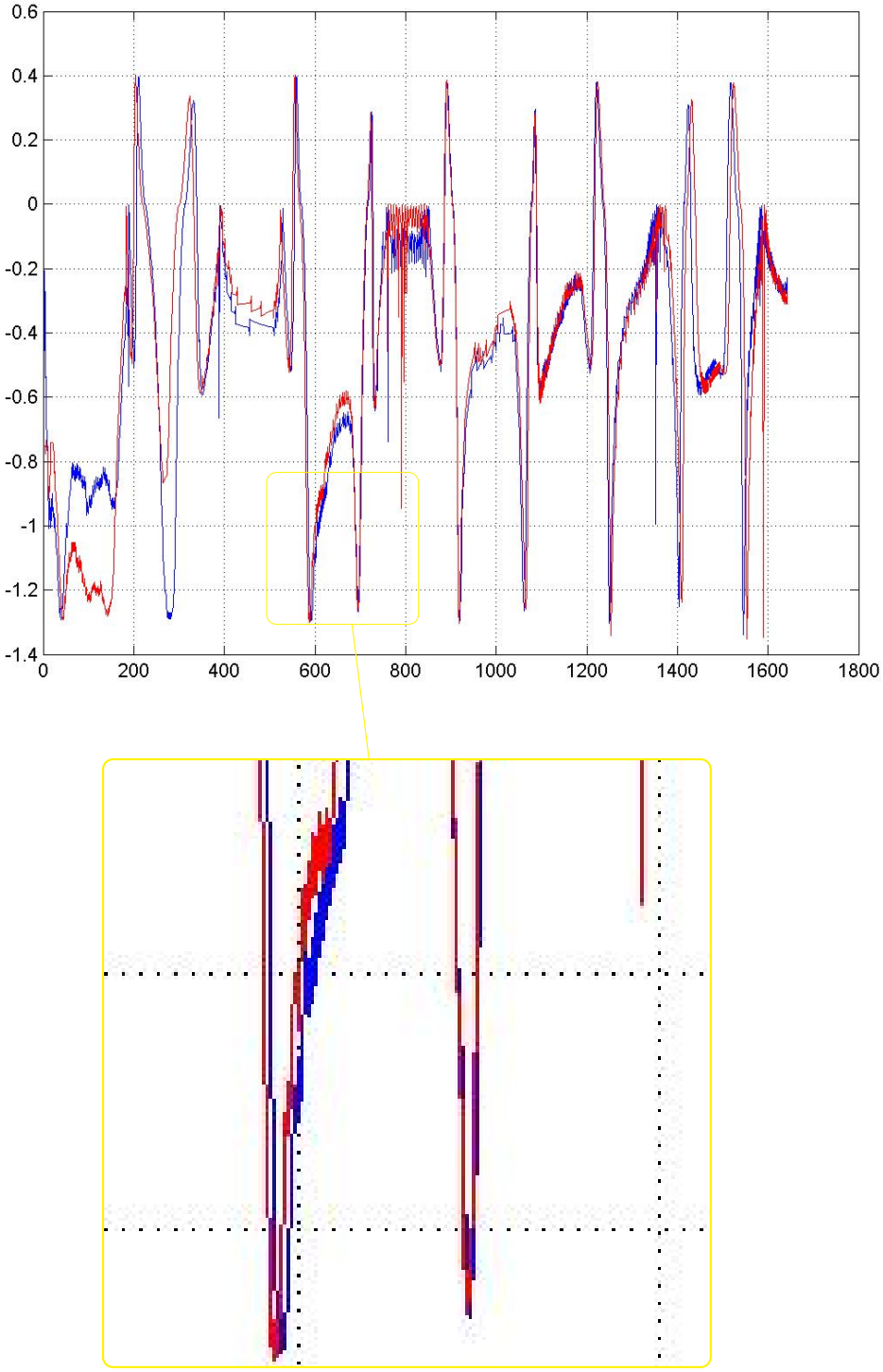

Figure 9.15.: *Curvature example from vecGeomNIRHandcurv3. The image draws the curvature from two different samples from the same user.*
Colours red and blue are used to represent curvature from both sample 1 and 2. A clear match between samples is showed in the magnification portion of the figure

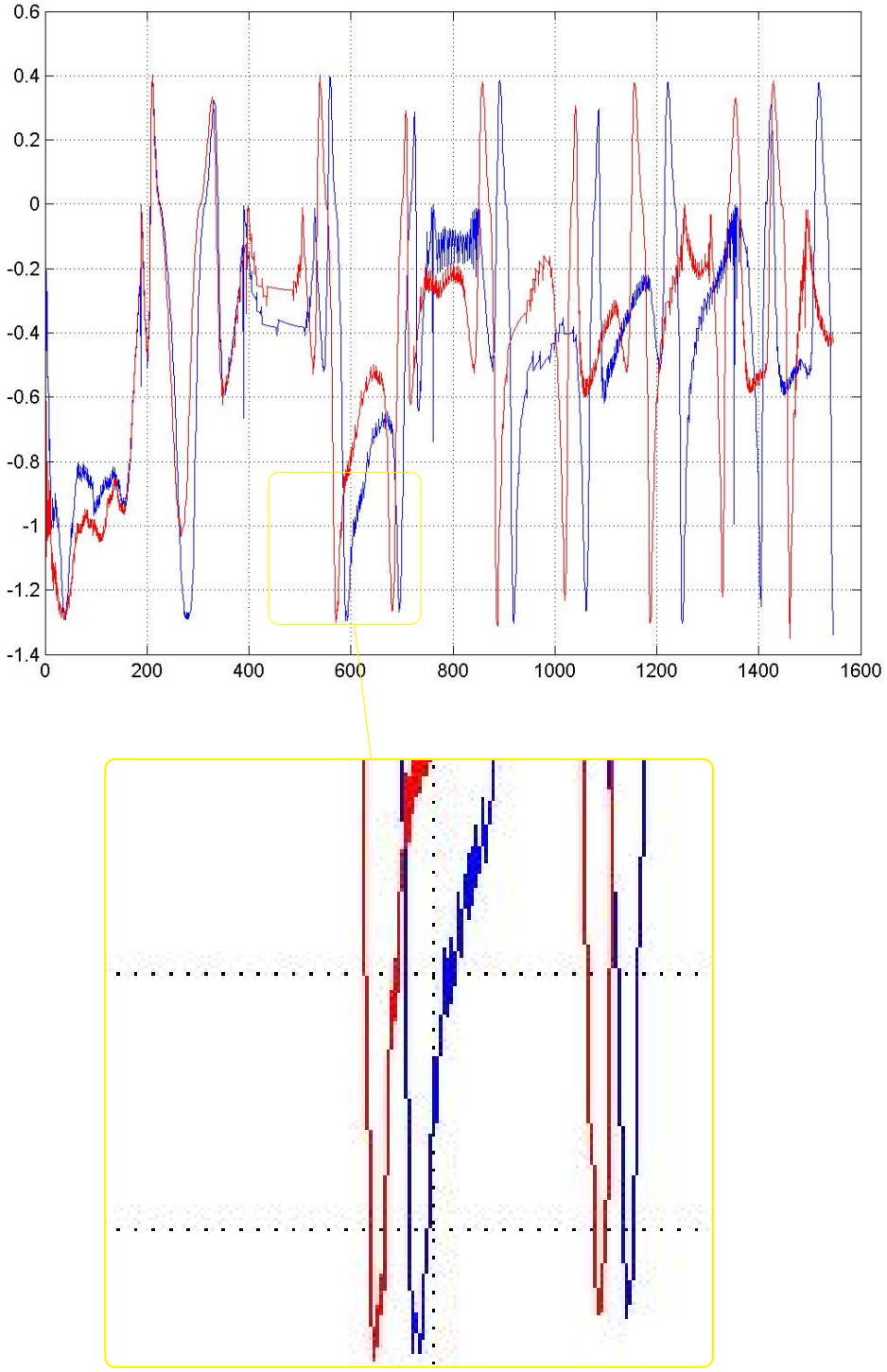

Figure 9.16.: *Curvature example from vecGeomNIRHandcurv3. The image draws the curvature from two different samples from different users.*
Colours red and blue are used to represent curvature from both users 1 and 2. There is a clear mismatch between curvatures in some of the minimum points showed in the magnification portion of the figure

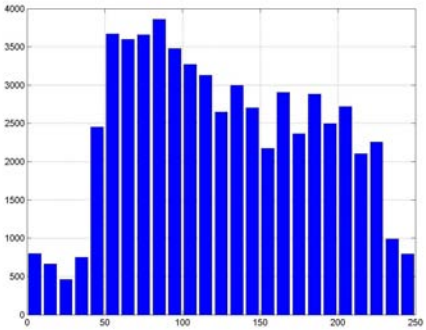

Figure 9.17.: *Gray intensity Histogram from Hand. Default histogram bandwidth*

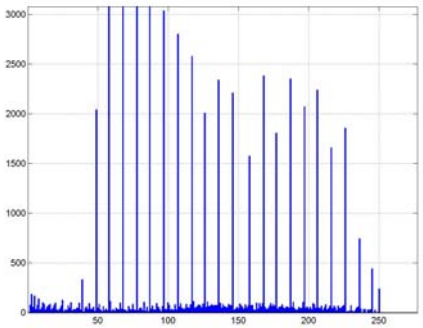

Figure 9.18.: *Gray intensity Histogram from Hand. Extreme low histogram bandwidth*

Chapter 10.

TIR Preprocessing and Feature Extraction

Unkown

Too many people go through life waiting for things to happen instead of making them happen.

Overview

TIR images present some remarkable characteristic: Environment can affect the hand heat pattern. This important fact already described in chapter 5 does not give at first sight good feelings. However thermographic images bring some clue related with improving security reliability.

Contents

10.1. TIR Images

Thermographic images or what is also called infrared thermography has gained huge interest in many fields. This fields goes from industrial applications coming from electrical

maintenance and sustainability, medical applications that has been already described in chapter 5 to military and secure applications. The work presented in this thesis tries to study and analyse the hand TIR images for recognition processes.

Here it is presented a novel approach for biometric recognition based on hand images obtained by a thermographic camera that contains a VIS and TH sensor. One major drawback to use this technology is its cost that could range from $10,000 to $50,000. However, this kind of technology is improving and we think that in the near future the price of these devices will be significantly lower. This research has been performed by a professional TESTO 882-3 camera. The main characteristics of this camera are its thermal image resolution: 320 x 240 pixels, its visible image resolution: 640 x 480 pixels and its thermal sensitivity (NETD) $<$ 0.06 C at 30 C. Fig. 1 shows the physical aspect of this camera.

If VIS and NIR hand images present some challenges when segmentation is needed, for TIR images the challenge is still greater than that. The main reason comes from a series of really metabolic regulation process within the body that in some persons make the heat pattern from hand fingers close to the heat pattern form the surface. In this context mitigate one of the major drawback when dealing with hand images is the main objective of this chapter.

The general expected hands view from a user through the whole acquisition process can be seen in Figure 10.1. In this 10 images row, appears to be clear the difference heat pattern between the whole hand and the neoprene surface.

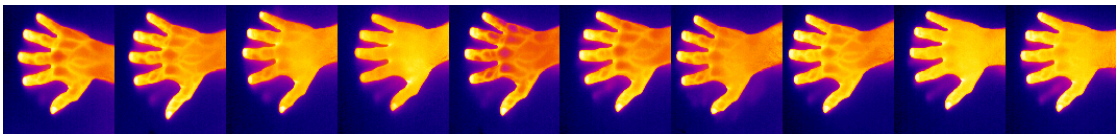

Figure 10.1.: *Complete Set of TIR Hand Samples (Acquisition from the same user)*

However in many situations this clear difference will not be seen.

10.2. Segmentation Method

Image segmentation is typically used to locate objects and boundaries in images. More precisely, image segmentation for TH hand image is the process of assigning a label to every pixel in that image such that pixels with the same label share a desired characteristic (pixel from the user hand). While the segmentation process seems quite strightforward with warm hands (we see a clear heat pattern in Figure 10.1) it is not clear when dealing hand images with cold fingers (see Figure 10.2).

Segmentation methods over this cold hands does not give good results because methods discard the cold areas. The problem is persistent, even thought using more sophisticated

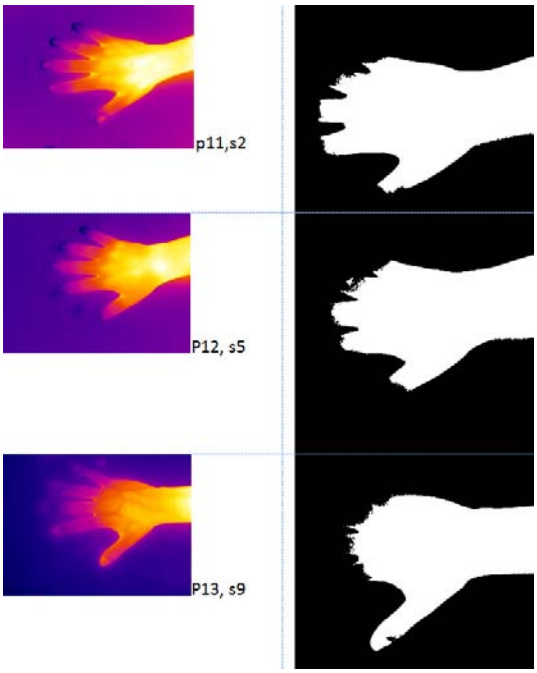

Figure 10.2.: *Wrong segmentation examples with Cold Finger*

methods. Methods based on the active shape models have been used with good results. This method is able to segment the hand directly in TH spectrum, using the basic ASM ("Active Shape Model" Segmentation with Optimal Features [63]). Each model (considering thumb down) was trained on a data set which consists of 50 labeled grayscale images of hand in TH spectrum. The hand was described by 27 landmarks as can be seen on Figure 10.3

During the segmentation, the initial pattern was placed to the center of mass of the hand and consequently it was adjusted to the actual hand shape in 150 iterations. This high number of iterations was selected, because the images are processed off-line and the segmentation accuracy is more important than the overall duration. The disadvantage of this method is a dependence of segmentation accuracy on the suitable training database. Moreover this method usually fails when segmenting the hands with cold areas (see Figure 10.4). Actually a lot of useful techniques have been tested [147], but neither produce accurate results in presence of cold fingers.

In order to avoid this drawback we propose a method that uses the VIS segmented image. This process based on empirically found settings takes advantage of the thermographic camera, which provides two images at the same time: VIS and TH. With this information, it is possible to find the relation between these two images, i.e. find the mutual translation, rotation and scale.

The detailed steps to perform the TIR segmentation are as follows:

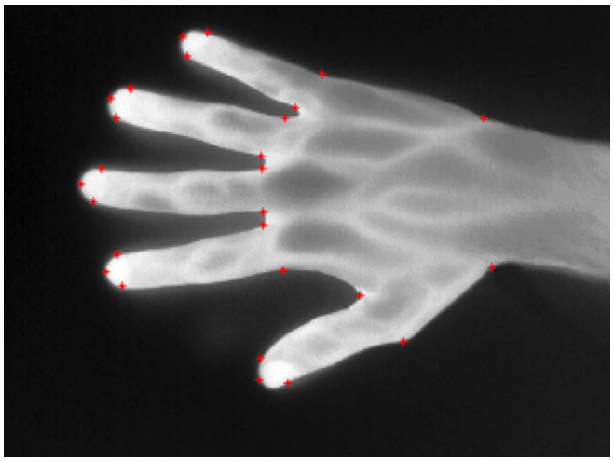

Figure 10.3.: *Landmarks layout* ***ASM***

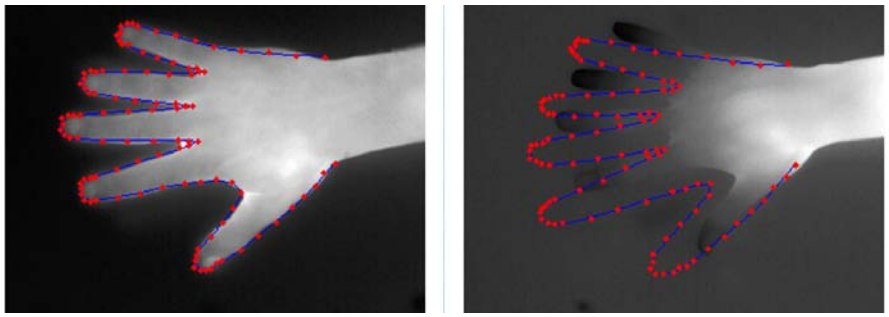

Figure 10.4.: *Active Shape Modelling Fail with cold fingers* ***expASMv1***

1.- First, the VIS image was binarized using the method described in chapter 8.

2.- The VIS binary mask was transformed in order to be applied to the TIR image mask using the correct rotation, translation and scaling parameters. (see Figure 10.5)

Step two can be made empirically, because lab conditions, and the camera was fixed during all acquisition sessions, or by means of a more universal method based on the image registration. In this case to find the best rotation, translation and scaling settings it is possible to use an optimization function based on the simplex search method [110]. In our conditions, the first method outperformed the second one. As soon as TH images present cool areas the goodness of this method comes to light (see Figure 10.5).

It is important to point out that the main relevant information present in TH images that is not contained in VIS ones is the heat pattern distribution related with the vascular pattern (commonly referred to as vein pattern) on the hand surface rather than the hand contour. Thus, this is the proposed procedure to extract this information removing the background information.

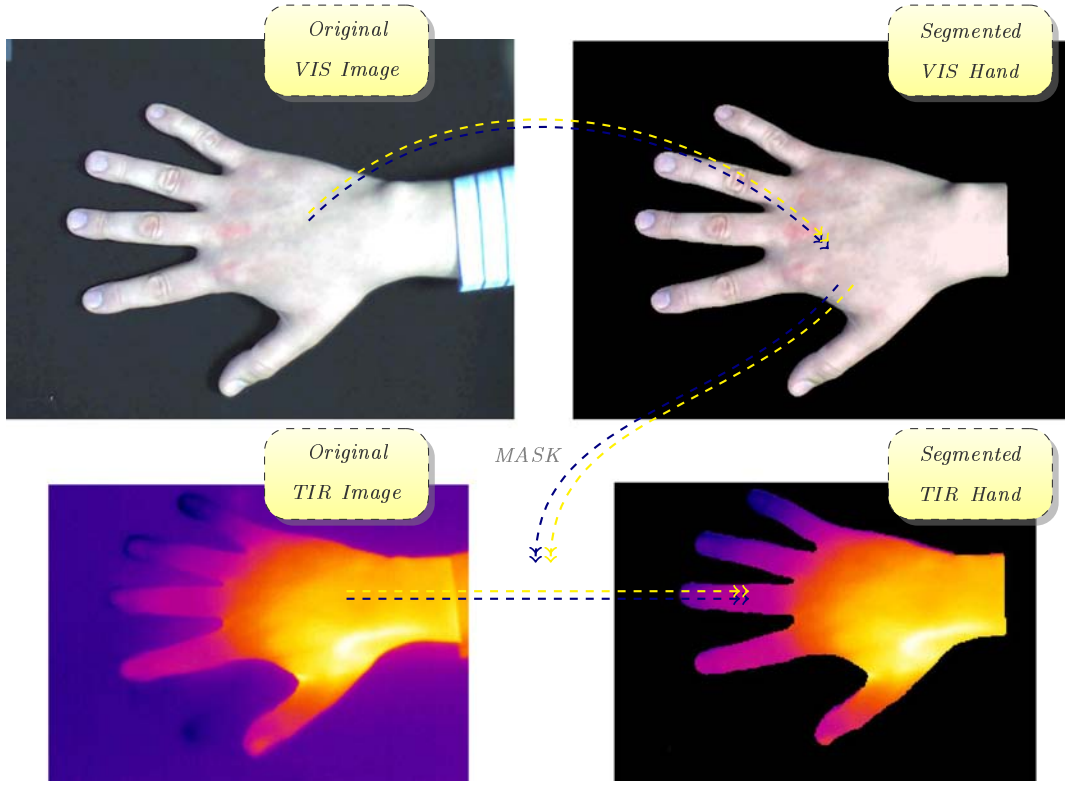

Figure 10.5.: *TIR segmentation Process. The original VIS image is used to build a MASK. This MASK is used to segment the TIR image avoiding the problem of cold finger.*

10.3. Holistic Data

In this section we repeat what has already been described in previous section. The set of data sets coming from TIR images once the segmentation process has been correctly deployed. In Table 10.1 there are the generated data sets from the holistic approach.

Table 10.1.: *Hand Holistic Data Files.*
The whole TIR Holistic Data Set with 2000 DCT2 components

Id. Name	Type	Name	Option
getHandTIR1	Finger	Thumb	
getHandTIR2	Finger	Index	
getHandTIR3	Finger	Middle	
getHandTIR4	Finger	Ring	
getHandTIR5	Finger	Pinky	
getHandTIR6	Finger	Thumb	TXT
getHandTIR7	Finger	Index	TXT
getHandTIR8	Finger	Middle	TXT
getHandTIR9	Finger	Ring	TXT
getHandTIR10	Finger	Pinky	TXT
getHandTIR11	Hand	Central	
getHandTIR12	Hand	Central	TXT
getHandTIR13	Hand	Hand	
getHandTIR14	Hand	Hand	TXT

TXT: Texture

10.4. Geometric Data

Geometric data collected from TIR images are through the same approach that those from VIS and NIR images. Table 10.2 shows the geometric data coming from TIR hand images. The extraction data sets for each of the 5 fingers are described in Table 10.3 as well.

Table 10.2.: *Hand Geometric Data Files from TIR images*

Id. Code	File Name	Based on
HG1	vecGeomTIR15	lengths and widths from hand key points
HG2	vecGeomTIR18	lengths and widths from hand and finger
HG9	vecGeomTIRHandcurv3	EMA(3) + Curvature + DCT
HG10	vecGeomTIRHandcurv4	EMA(10) + Curvature + DCT

Table 10.3.: *Finger Geometric Data Files from TIR images*

Id. Code	File Name	Based on
tirFG1	vecGeomNIRfingWidth10(:,:,ki)	10 measures + trimming
tirFG2	vecGeomNIRfingWidth25(:,:,ki)	25 measures + trimming
tirFG3	vecGeomNIRfingWidth50(:,:,ki)	50 measures + trimming
tirFG4	vecGeomNIRfingWidth200(:,:,ki)	200 measures + trimming
tirFG5	vecGeomNIRfingWidth200DCT(:,:,ki)	DCT(Width200)
tirFG6	vecGeomNIRfingPol(:,:,ki*2-1)	Polar C.: Theta + DCT
tirFG7	vecGeomNIRfingPol(:,:,ki*2)	Polar C.:Rho + DCT

10.5. Additional Measurements for Improvement

One of the main problems with thermographic data is its dependence on user condition and environment. Because all acquisition were obtained in different months, and with completely different environmental mean temperatures (ranges were from 10 ^oC to 20 ^oC from January to June), research effort has been made in order to correct this drawback. Obviously this is not the desired situation, but weather environment lab conditions clearly were not under control. In order to reduce this effects, this thesis have test two different approaches. All these work is based on the distribution of gray levels. One of them, and perhaps the most intuitive use a difference measure, instead of the direct value. For a formal description let us define the following count distribution for each one of these hand modalities: thumb, index, middle, ring and pinky finger, and central hand area and the whole hand called $F_1, F_2, F_3, F_4, F_5, C_h$ and H_x respectively.

$F_i = [F_{i,1}, F_{i,2}, \ldots, F_{i,l}]$ $C_i = [C_{i,1}, C_{i,2}, \ldots, C_{i,l}]$ $H_i = [H_{i,1}, H_{i,2}, \ldots, H_{i,l}]$

The distributions used to classify are computed as a difference between the modality and a reference distribution measure which comes from one of this distributions as well. Thus, the new data generated came from the following operation:

$$F'_{1,i} = F_i - C_i F'_{2,i} = F_i - H_i F'_{3,i} = F_i - F_1 F'_{4,i} = F_i - F_2 F'_{5,i} = F_i - F_3$$

It is understood that with this straightforward operations the effect of environmental temperature is removed. The other tested approach is based on different well known distance. These distance has been used in order to properly measure a distance between a target distribution and the real distribution. Kullback-Leibler divergence, Bhattacharyya distance and Lukasky-karmowski metric have been used.

Kullback-Leibler divergence is a non-symmetric measure that computes how far two probability distributions are from each other. One of this distributions is called the true or model distribution (P_x) and the other one is called approximation distribution(Q_x).

$$d_{KL}(P_x, Q_x) = \sum_{i=1}^{k} \left[P(x=i) \ln \frac{P(x=i)}{Q(x=i)} \right] \tag{10.1}$$

One of the interesting points related to Kullback-Leibler (KL) divergence is its close relation to information theory measures, such as Shannon entropy.

Bhattacharyya distance is a measure of the distance between two discrete (or continuous) probability distributions.

$$D_{Bhat}(P, Q) = -\ln(B_{coeff}(P, Q)) \tag{10.2}$$

Where B_{coeff} is the Bhattacharyya coefficient related to distribution overlapping and defined as:

$$B_{coeff}(P, Q) = \sum_{x \in X} \sqrt{P(x) Q(x)} \tag{10.3}$$

The last measure tested was the **Lukasky-karmowski metric**. This function defines a distance between two random variables.

$$D_{LK}(X, Y) = \sum_i \sum_j |x_i - y_j| P(X = x_i) P(Y = y_j) \tag{10.4}$$

Do they work?

There is hope for improvement through this computations.

Chapter 11.

Hand Gender Recognition

James M. Barrie

The secret of happiness is not in doing what one likes,
but in liking in what one has to do.

Overview

Here it is presented a complete background of the hand as a biometric trait for gender recognition. Gender recognition has not been widely studied in comparison with person identification. The reason becomes clear, as security applications are by far much more interesting for industry, government agencies and business. However, in the context of human computer interaction, gender recognition could play an important role. There is also an interesting field where gender recognition applications can give some advice with intelligent advertising once your gender is detected.

Contents

11.1. Introduction to Gender Recognition

The process of gender recognition is straightforward for humans. We have been trained for that task since we were children. And this task, sometimes made unconsciously, is important for social activities. Actually, the gender recognition using biometric physiological

characteristics (such as face, hand, human shape) remains a difficult task. The high variability present within genders, whatever the characteristic, makes us use some of the algorithms and methods available in general recognition applications. This chapter presents a gender recognition approach throughout one of the geometric data sets obtained in chapter 8. Identification will be performed with the Biometric Dispersion Matcher classifier. This method is closely related to Discriminant Analysis and works pretty well for linear problems.

11.1.1. Acquisition and Data Extraction

The data for gender recognition comes from the same hand data base presented in chapter 7. Instead of using the person identifier, here it will be used the gender identifier, male or female for identification. The description of the data extraction process has already been made, and for that reason it is highlighted the main components of the data file used for the problem.

Basically the first 20 components (named V1 to V20) correspond to finger length. These lengths are computed from the tip of each of the fingers to the valleys and central part. In some of the arrows depicted two variables can observed. The reason is because we use two similar points that are not distant enough to be appreciate in Figure 11.1. One of them is computed as an average point from the two valleys of the finger. The other one is measured across the intersection point between the eigenvector directions defined by the fingers and the two valley points related to finger. The other group of distances is width (from V21 to V27). The next group (see Figure 11.2) of distances are mix of widths and lengths between the center point of the finger (square points) and the center of the hand. These variables range from V28 to V42. Observe that the last ones have not been represented for clarity purposes.

We have highlighted the variables V26 and V27 because they will be the main variables for gender recognition as we will show in the next section. It is coherent with what people can usually think, the greater the hand (hand width) the higher the chance to be a man.

11.1.2. Data Traits

This section provides the experimental rates of the proposed algorithm. It is important to remark that there is an unbalanced design, because we have more men (68 %) than women (32 %).

In order to observe how BDM works, a test increasing the size of the training set will be performed. Starting with a training set of 27 hands (not necessarily from different users) that was distributed between 18 Men and 9 Women. With these initial conditions we train a BDM. Then a test analysis over the remaining data set is applied. It means

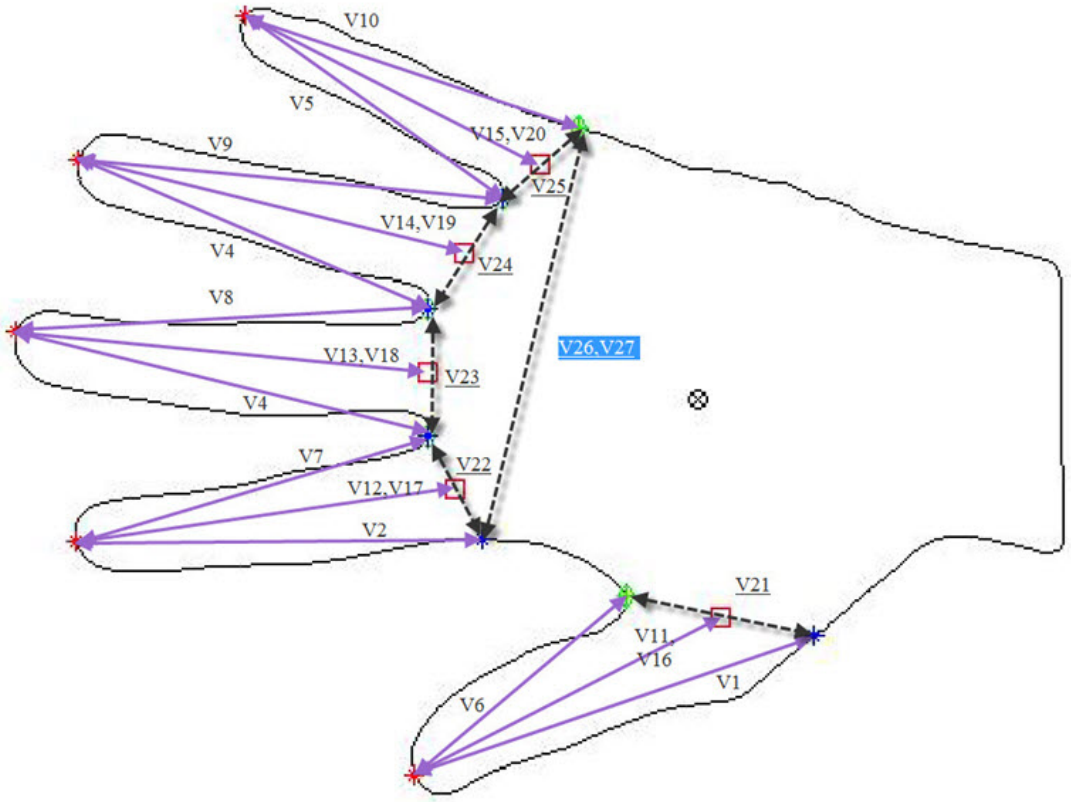

Figure 11.1.: *Lengths and widths measures from Hand Extraction Data File* ***vecGeomVIS15*** *Hand Measures - I*

a total test set of 1013 hands. Then the training set is increased with 36 men and 19 women, and so on until we reach a maximum of 40 % of the total data set.

The main point is that BDM works in each situation presented with the best variables according to its discriminant threshold. Table 11.1 shows how BDM works across the different training data sets. One of the advantages to work with BDM is that it is possible to check how each feature component works. It is presented also in Table 11.1 the 10th most relevant features. As a brief summary:

- Components V26, V27 and V35 related to hand width.
- Components V42 and V34 (V42 not depicted in Fig 3 goes from pinky finger square to the center of the hand), V34 goes from index finger square to the center of the hand.
- Components V33 and V38 equals to the length between index and middle finger (V33) and between index and pinky finger (V38).

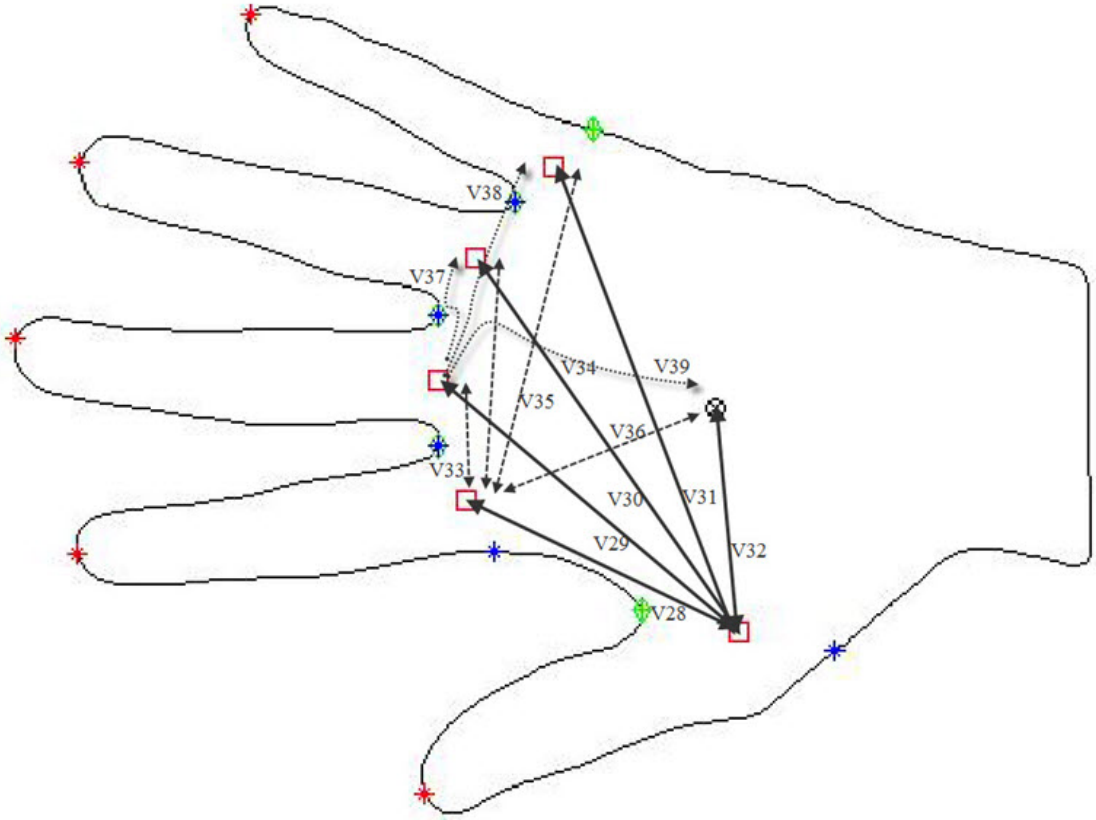

Figure 11.2.: *Lengths and widths measures from Hand Extraction Data File* ***vecGeomVIS15*** *Hand Measures - II*

- Components V1, V11 and V4 lengths from thumb finger (V1 and V11) and from index finger (V4).

Finally it is shown how the different feature components are distributed depending on gender. This distribution gives us a clear understanding of the way BDM discard irrelevant data. For instance, components V27 and V35 (see Figure 11.3) have distributions well separated. It means it will be easier to classify gender according to these feature components. Variables V1 and V4 also show good behaviour (see Figure 11.4)

That is not the case when both distributions are overlapped as the distribution of V48 shows (see Figure 11.5). Across the measurements the mean of men group and women group are the same. Thus, it is not possible to use this feature component (alone) to separate gender.

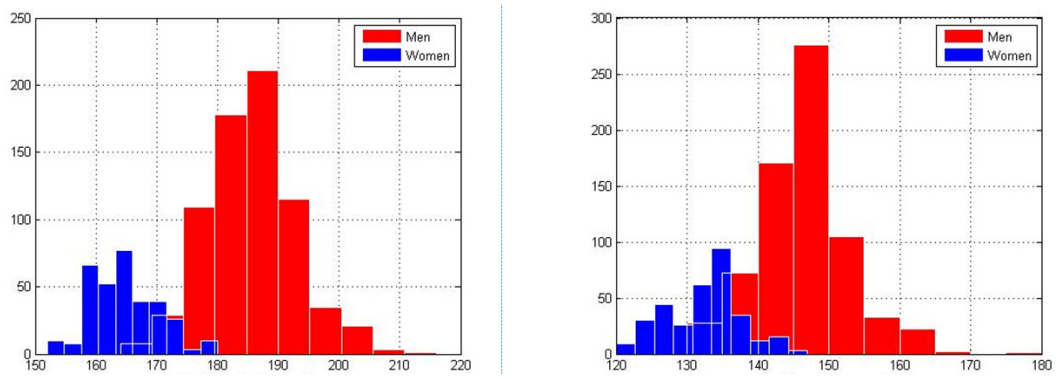

Figure 11.3.: *Distributions for components V27 (left) and V35 (right). There is a clear separation between gender*

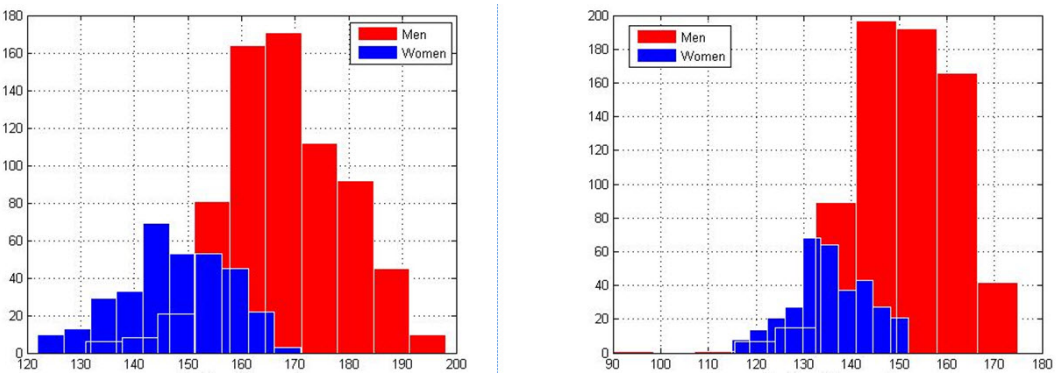

Figure 11.4.: *Distributions for components V1 (left) and V4 (right). Distributions with high discrimination*

11.2. Conclusions about Gender Recognition

These results have proved the reliability to use anthropometric measures of hand images to recognize gender. Performance results are better than those coming from face analysis [120] and are promising when using a combination with some additional information. By means of a fusion algorithm it will be possible to raise identification rates above 99 %. There is a survey on gender recognition for vision approach [148] where it is possible to look at some performance measures quite similar to those results. It has also been proved the suitability of BDM to detect the major feature components. In this context, this classifier contributes to achieve a coherent explanation of which component contain better information for the recognition process.

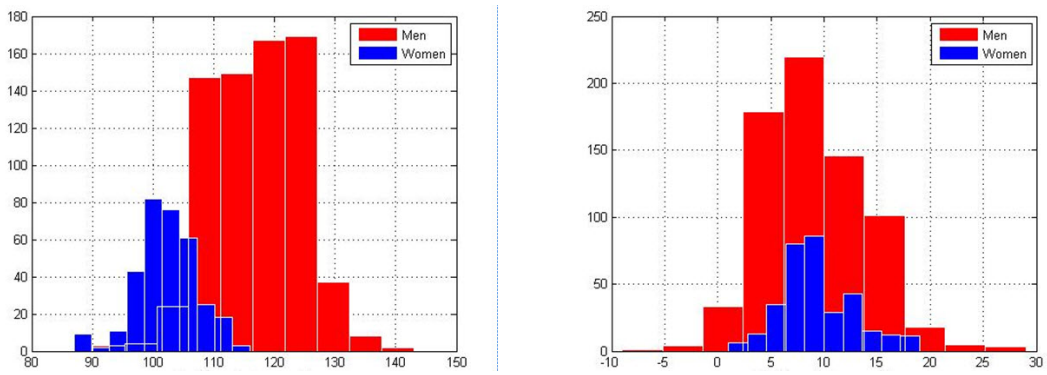

Figure 11.5.: *Distributions for components V42 (left) and V48 (right). Distributions overlapped*

Can Gender Guess, Improve Biometric System?

This is one of questions for further research: would not the performance of the biometric system increase if it knows the gender?

Table 11.1.: *Hand Holistic Data Files.*
The whole Visual Holistic Data Set with 2000 DCT2 components

	Best Discriminative Components										
%Train	1	2	3	4	5	6	7	8	9	10	IDrate
2.5	27	26	34	35	42	33	22	1	11	4	0.9519
5.0	27	26	42	35	1	11	33	22	20	5	0.9189
7.5	26	34	27	35	17	7	2	12	5	20	0.9116
10.0	26	27	35	34	33	38	1	42	23	20	0.9498
12.5	27	26	35	34	42	33	1	11	41	4	0.9516
15.0	26	27	35	34	33	42	1	38	11	41	0.9434
17.5	26	27	35	34	42	33	1	38	11	4	0.9405
20.0	26	27	35	34	42	33	1	41	23	11	0.9639
22.5	27	26	42	35	34	33	1	11	23	41	0.9652
25.0	27	26	35	34	42	33	1	11	23	5	0.9589
27.5	27	26	35	34	1	38	42	33	11	23	0.9575
30.0	27	26	35	34	42	33	1	4	11	19	0.9656
32.5	27	26	35	34	42	1	11	33	4	20	0.9700
35.0	26	27	35	34	42	33	1	41	38	4	0.9748
37.5	27	26	35	34	42	1	33	38	11	4	0.9707
40.0	26	27	35	42	34	1	33	38	11	23	0.9776

Results

Part IV.

Thesis Results

Chapter 12.

Results throughout Holistic Data

James M. Barrie

The secret of happiness is not in doing what one likes,
but in liking in what one has to do.

Overview

This chapter highlight some of the results concerned with recognition problems when data comes from Holistic data files. It is the intention of this work offer a detailed view of performance when multi-spectral data is involved in identification and verification.

Contents

12.1. Holistic Hand Data

The first approach to evaluate the performance of the hand data base and its different data files is with the direct hand. Thus, three different data sets (VIS, NIR and TIR) related with the whole hand will be processed. The hands data files come from the segmentation process described in chapter 8 with the registration option ([47]) to

normalize finger orientation. This approximation can gives a real sense of the capabilities of the data, the segmentation process and the methods involved for recognition.

Two different scenarios have been defined for experimental results. The idea behind each of these scenarios is to treat separately or increasingly the feature vector. Because the characteristic vectors of each of the users has a length of 2000, the possible scenarios are:

- **Scenario A**: chunks of 100 components, each of them taken consecutively from the first component to the last.
- **Scenario B**: chunks increased from 100 to 100 up to reaching 2000

Both scenarios define 20 independent tests. These scenarios or tests are intended to help obtaining performance measurements across the feature vector in this two predefined strategies.

Scenario A:

$$\begin{bmatrix} x_1, \ \dots \ x_{100}, & x_{101}, \ \dots \ x_{200}, \ \dots \ x_{1901}, \ \dots \ x_{2000} \\ x_1, \ \dots \ x_{100}, & x_{101}, \ \dots \ x_{200}, & \dots \ x_{1901}, \ \dots \ x_{2000} \\ & & \\ x_1, \ \dots \ x_{100}, & x_{101}, \ \dots \ x_{200}, & \dots \ x_{1901}, \ \dots \ x_{2000} \end{bmatrix}$$

and **Scenario B**:

$$\begin{bmatrix} x_1, \ \dots \ x_{100}, & x_{101}, \ \dots \ x_{200}, \ \dots \ x_{1901}, \ \dots \ x_{2000} \\ x_1, \ \dots \ x_{100}, & x_{101}, \ \dots \ x_{200}, & \dots \ x_{1901}, \ \dots \ x_{2000} \\ & & \\ x_1, \ \dots \ x_{100}, & x_{101}, \ \dots \ x_{200}, & \dots \ x_{1901}, \ \dots \ x_{2000} \end{bmatrix}$$

12.1.1. Training and Test data sets

Each scenario and chunk will be treated the same way. Data will be split in two parts, one of them for training purpose, and the other one for testing. With the 10 samples acquired the first 5 move to train and the remaining 5 move to test. The way to separate

data is realistic because the training data was actually obtained before the data used for test.

A way to visualize training and test data set through the five session is right here:

$$\underbrace{S_1Ac_1 \quad S_1Ac_2 \quad \| \quad S_2Ac_1 \quad S_2Ac_2 \quad \| \quad S_3Ac_1}_{Training} \quad \underbrace{S_3Ac_2 \quad \| \quad S_4Ac_1 \quad S_4Ac_2 \quad \| \quad S_5Ac_1 \quad S_5Ac_2}_{Testing}$$

So training data consist of 5 acquisitions made on three different session. This represent a 100×5 data set dimension. The same amount of data is ready for testing, with the next 5 acquisitions made from session 3 to session 5. With this assumption and with a single classification method, BDM, it is presented all data from the complete hand.

12.2. Hand Identification Results with VIS, NIR and TIR

The idea is with few data sets (three), but coming from completely different electromagnetic band compare results individually and combined.

12.2.1. Performance from Individually Data Sets

In order to keep an eye on the ability to combine different sources of information, coming at least from three different spectrum, VIS, NIR and TIR it is necessary to observe how well they performed alone. Thus, here we see identification rates from both scenarios.

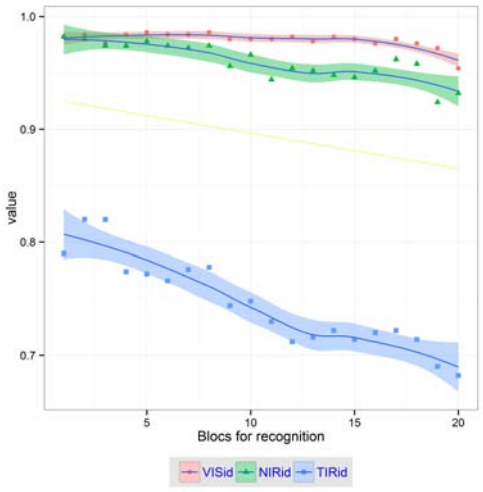

Figure 12.1.: *Identification for Scenario A*

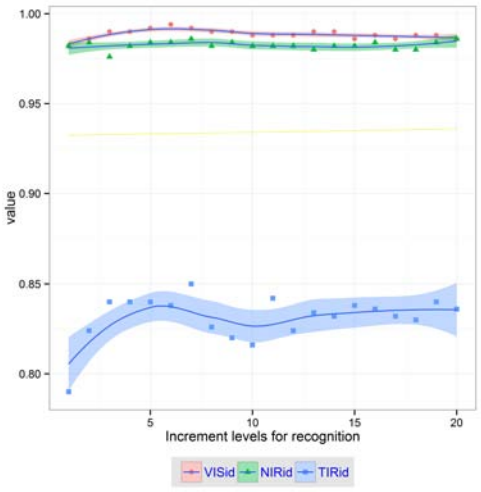

Figure 12.2.: *Identification for Scenario B*

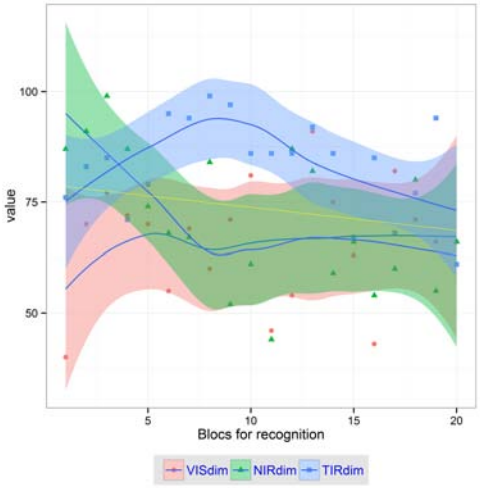

Figure 12.3.: *Selected components - Scenario A*

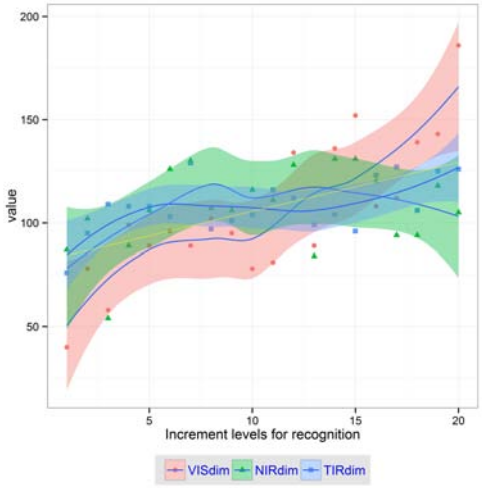

Figure 12.4.: *Selected components - Scenario B*

The scenario A shows a real decreasing performance as chunks are being much further than the first one (see Figure 12.1). That behaviour is reasonable, where the strongest information capacity from DCT usually heads on first components. This downward trend is stronger with TIR data than with VIS and NIR data. Here it is not discussed time performance, however it is clear that all tests use the same computation time. However, that is not happening in scenario B, where the characteristic vectors are successively increased by a 100 components each time. From the first chunk, which has 100 components to the last one, that has 2000 components, the time has been increased heavily as components do. In Figure 12.2 it is seen a function of performance by chunk length. The maximum of this function depends on the data set used, so it is not a predefined length that work well for the different data sets available.

From scenario B, performance does not decrease because each chunk of data add the previous data as well. Noise could affect the performance, however before applying classification BDM method discard those component that are not discriminant or does not help improving performance. VIS and NIR data behave very similar with performance close to each other. The median values for scenario A are, 0.980, 0.960 and 0.737 for VIS, NIR and TIR respectively while for scenario B performance are, 0.988, 0.982 and 0.835 for VIS, NIR and TIR.

Another interesting view of the results through BDM method is the component selection process. Or in other words, the process to discard non-discriminative components. In Figure 12.3 and in Figure 12.4 it is shown the way BDM selects components from both scenarios. From scenario A, there are few variations (median values of 69.5, 67.5 and 85.5 for VIS, NIR and TIR) because all vectors have the same length (100), but from

scenario B that is not happening. It turns out that as we increase the component vector length so do the discarding capacity of BDM. In this case the median of the components finally selected are, 97.5, 106.5 and 107.0 for VIS, NIR and TIR respectively.

12.2.2. Performance from Combined Data Sets

Once all tests have been applied individually to VIS, NIR and TIR data sets it is important to study the different fusion strategies to increase the overall performance of the system. The first key point is the general increased identification performance. The assumptions coming from better performance when combining different source of evidence are now clear. In Figure 12.5 and in Figure 12.6 are shown the four different fusion possibilities, that is VIS+NIR, VIS+TIR, NIR+TIR and VIS+NIR+TIR. Observe that, the strategy to test all possible ways, is certainly a matter of dimension. As we increase the number of possible data sets available, the number of combinations increase exponentially following this well known expression:

$$\sum_{k=2}^{n} \frac{n!}{k!\,(n-k)!}$$

That means for $n = 3$ a very low number, 4 combinations perfectly acceptable. With all combinations ready, it is straightforward to check the best performance across all different tests and scenarios.

For scenario A, the option that combine visible and near infrared gives the best results. Nevertheless, the option that mix all spectrums obtains outstanding results as well, but certainly does not improve VIS + NIR combination. Thus, guided only for this numbers TIR data would not be a reasonable alternative. In Table 12.1 key results are displayed. Increasing performance when results are close to 1 is particularly more challenging and difficult. That is the reason why the performance has increased in 2% approximately from VIS initial value. This percentage doubles (4%) if NIR initial value is taken and if working with TIR data then this value rises to 36%.

For scenario B (Figure 12.6) again the best alternative are displayed for VIS + NIR combination. It is worth mention that increasing the characteristic vector does not seem to increase performance while definitively threatens computation time. From this analysis it comes up a recommendation that few are better than many.

Key values for scenario B are in Table 12.2.

It is possible to see the fusion strategy used for each result in the following figures. As it has been detailed in chapter 4 there are mainly 6 fusion strategies, product (prod), mean, median, max, min and vote. The last one has not been selected as the best in any of the cases treated. Thus, in Figure 12.7 and in Figure 12.8 there is no vote depicted. The main reason is the few data sets combined (at most there are three). These figures have some interesting perspective, where it is possible to appreciate the fusion strategy

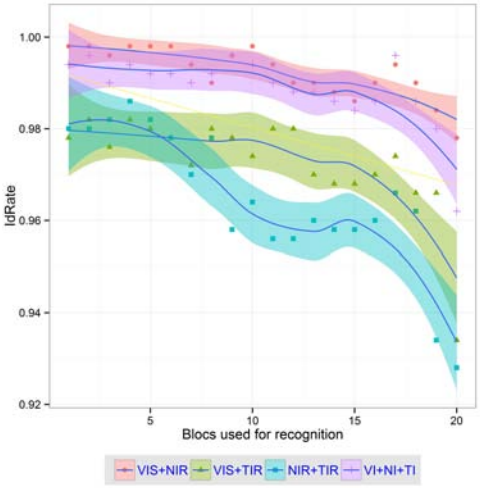

Figure 12.5.: *Fusion for Scenario A*

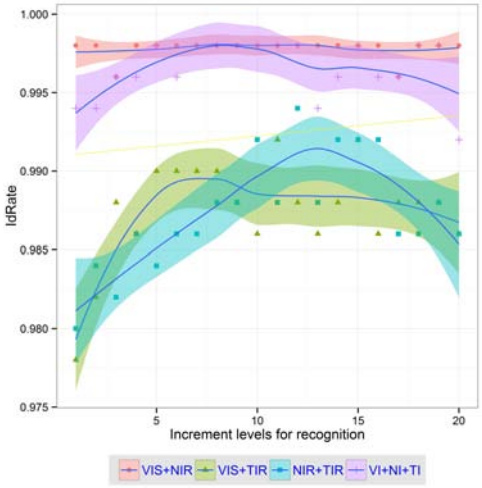

Figure 12.6.: *Fusion for Scenario B*

through each tested combination and scenario. For example, the combination VIS+NIR seems to offer better results when dealing with *max* rule, no matter if it is for scenario A or B. The other combinations basically work quite better with *mean* rule.

As a general overview of the results, and to appreciate the main performance throughout both scenarios box-plot (violin option) have been drawn in Figure 12.9 and in Figure 12.10. It looks like VIS+NIR and VIS+NIR+TIR have similar behaviour and similar top identification performance measurements and the other two much lower. Another important point is the variability of results across the different fusion combinations. Again VIS+NIR combination outperform VIS+TIR and NIR+TIR, while VIS+NIR+TIR option has a slightly worse shape.

From an inspection point of view, it is clear that the combination used affects performance. Nevertheless, to be sure it is advisable to apply a convenient statistical test to ensure

Table 12.1.: *Identification Performance Measures - Scenario A*

	VIS+NIR	VIS+TIR	NIR+TIR	VI+NI+TI
Max	0.9980	0.9820	0.9860	0.9960
Median	0.9940	0.9750	0.9630	0.9900
Sdev	0.0056	0.0110	0.0150	0.0077
	VIS:0.980	*NIR:0.960*	*TIR:0.737*	

Table 12.2.: *Identification Performance Measures - Scenario B*

	VIS+NIR	VIS+TIR	NIR+TIR	VI+NI+TI
Max	0.9980	0.9920	0.9940	0.9980
Median	0.9980	0.9880	0.9870	0.9970
Sdev	0.0006	0.0032	0.0036	0.0018
	VIS:0.988	*NIR:0.982*	*TIR:0.832*	

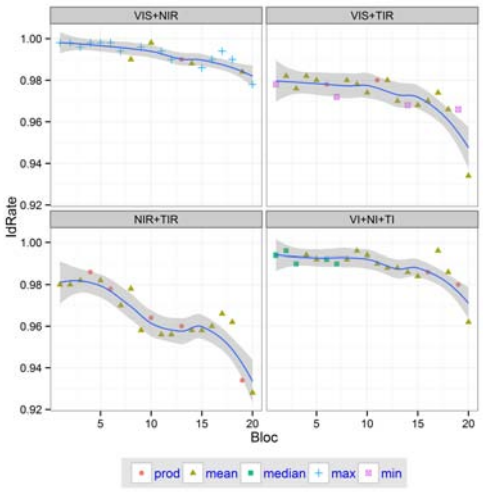

Figure 12.7.: *Fusion Strategies for Scenario A*

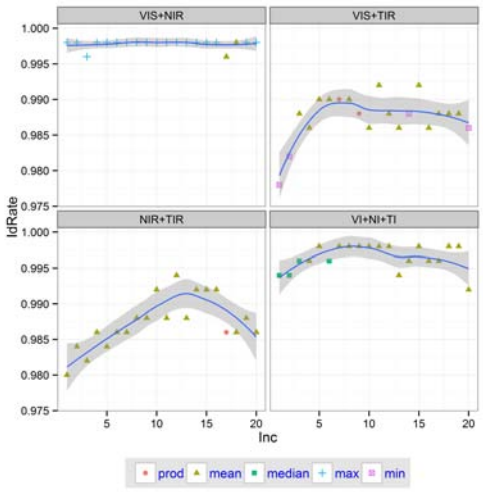

Figure 12.8.: *Fusion Strategies for Scenario B*

this interpretation.

In order to solve this question, and to see if there are significant differences between the four possible combining options it is proposed an ANalysis Of VAriance (ANOVA) test. The application of an ANOVA analysis helps in that direction. Non-parametric approaches like Kruskal-Wallis Rank Sum Test, althought analog to ANOVA will not be used.

Despite the clear box-plot representation, lets define the formal problem that can be applied for both scenarios A and B:

$$\begin{cases} H_o : \mu_{V+N} = \mu_{V+T} = \mu_{N+T} = \mu_{V+N+T} \\ H_1 : \mu_i \neq \mu_j \text{ , for some i and j} \end{cases}$$

Thus, in Table 12.3 it is shown the result of the ANOVA and a conclusion that there are significant differences between combination options. From scenario A the statistic value for test, the *F value* reaches 31, giving a probability lower than 0.00000 (in other words $\leq 10^{-6}$). If we take a look at the scenario B ANOVA test, in Table 12.4 it is shown a grater differences between performance combination options. Here the statistic goes to 92, that lead to a fewer probability value.

These results just confirm what violin diagrams shown: significative differences.

Table 12.3.: *Anova for Effects on Fusion - Scenario A*

	Df	Sum Sq	Mean Sq	F value	Pr(>F)
FUSION	3	0.0103	0.0034	**31.11**	0.00000
Residuals	76	0.0084	0.0001		

Normalization Techniques and Fusion Strategies

The last data that came into light is depicted in Figure 12.11 and in Figure 12.12 for scenario A. The first figure accounts for the number of times different normalization

Table 12.4.: *Anova for Effects on Fusion - Scenario B*

	Df	Sum Sq	Mean Sq	F value	Pr(>F)
FUSION	3	0.0019	0.0006	**92.86**	0.00000
Residuals	76	0.0005	0.0000		

techniques have been selected. To be more precise, it gives the number of times this techniques correspond to optimal solution. As it can be seen the most common technique is the no normalization. It means data keeps its original form without any transformation or mapping. The other options selected for importance are Min-Max and Z-Score transformations.

The second figure (see Figure 12.12) gives a detailed view of the general fusion strategy selected. Best results are coming from the mean technique followed by far from maximum and product rules. This view certainly fit with data showed in Figure 12.7. Readers can be aware that vote strategy does not appear, although used for all tests and scenarios. The reason has to be found in the number of combinations used, not many. Thus vote strategy did not support any optimum value.

When analysing the scenario B, the results are similar. However, some data in Figure 12.13 offers no doubt. It is clear that normalization techniques does not improve performance in this scenario. The main reason comes from the fact data are much more worked. In other words, algorithm takes into account a longer vector that is used to select the best components. By best components it is understood those that show the greatest discriminative power. Results from Figure 12.14 are comparable to those from scenario A.

12.3. Hand Verification Results for VIS, NIR and TIR

Once identification results have been completely analysed, it is time to present results in verification operation. In this case the measurement used is the equal error rate (EER), and as it has been also done for identification, results cover both scenarios described previously, scenario A and scenario B.

12.3.1. Performance from Individually Data Sets

As before, the first thing to obtain is individual verification performance. This gives an initial clue, and if there is room for improvement through fusion and normalization techniques.

In Figure 12.15 it is showed how performance decreases as chunks with less information power are selected. In Figure 12.16 it is seen a function of performance by chunk length. The maximum of this function depends on the data set used, so it is not a predefined length that work well for the different data sets available.

12.3.2. Performance from Combined Data Sets

Once all tests have been applied individually to VIS, NIR and TIR data sets it is important to study the different fusion strategies to increase the overall performance of the system. The first key point is the general increased verification performance.

The assumptions coming from better performance when combining different source of evidence are now clear. In Figure 12.17 and in Figure 12.18 are shown the four different fusion possibilities, that is VIS+NIR, VIS+TIR, NIR+TIR and VIS+NIR+TIR. Reader should be aware with figures from fusion and without. The Y axis has been improved, because in Figure 12.15 range labels go from 0.05 first tick to 0.20 last, and in Figure 12.17 range labels have been shrink to 0.000 first tick to 0.020 last tick. Nevertheless best results are coming from fusion for scenario B. The four strategies can find a minimum optimum below 0.005.

Scenario B for fusion gives an EER percentage quite reasonable going from 0.114% for VIS+NIR, 0.585% for VIS+TIR, 0.293% for NIR+TIR, and 0.196% for VIS+NIR+TIR. These results are slightly better that those coming from scenario A which are 0.130%, 0.918%, 0.646% and 0.260% for VIS+NIR, VIS+TIR, NIR+TIR and VIS+NIR+TIR respectively.

It is possible to see the fusion strategy applied for each result in the following figures: Figure 12.21 and in Figure 12.22. In both scenarios the results are quite similar in the sense of combination strategy deployed. Thus, product rule has been used 71% of the times and median rule 24% of the times. However the median rule has been carried out on VIS+NIR combination instead of being uniformly distributed across the remaining combinations.

As a general overview of the results a violin graph is showed in Figure 12.21 and in Figure 12.22 for scenarios A and B respectively.

One of the most used tools to study the performance of a system in verification mode is de DET (see chapter 3). Here are depicted DET from scenario A and B with the first chunk, or bloc. The first representation (Figure 12.23) shows VIS, NIR and TIR performance, while the second representation (Figure 12.24) shows DET for the four possible combinations.

VIS and NIR shows similar performance, but VIS outperforms NIR. TIR performance is far to be considered as a reliable tool for verification, at least without combining with other modality. When fusion is applied system performance increase and the best results come from VIS+NIR.

12.4. Results on Complete Holistic Data Set

Here, results from the complete holistic data sets will be shown. These results work with the same training data set as before, but with a slightly different approach for test. Instead of defining a unique test data set, it is defined three different tests. These three tests, $Test_1$, $Test_2$ and $Test_3$ correspond right to Session 3, 4 and 5 respectively. Reader will be right if it is aware that $Test_1$ take data that has already been used for training. In fact, half of this Test data have been used for training. Thus, better performance is

expected from $Test_1$ than $Test_2$ or $Test_3$.

Experimentation Diagram:

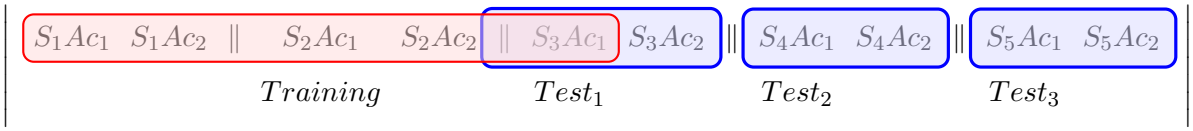

$Test_1$ is carrying out a biased testing. This means performance will be overestimated, and its values will remain higher than for $Test_2$ and for $Test_3$.

Once defined this approach for experimentation it is possible to test different issues that will be detailed in the upcoming subsections.

12.4.1. Methods

In this subsection different classification methods have been deployed in order to study their ability to perform identification problem. Actually the main interest is to compare BDM against other well known methods. The point is to solve some of the questions initially stated in the thesis. For example: Is it BDM better than the other methods? What is expected from spectrum bands?

The list of methods checked are Biometric Dispersion Matcher (BDM), Karhunen-Loeve + Nearest Mean Classifier (KLMN), K-Nearest Neighbour (KNN), Logistic (Log), Fisher and Linear Discriminant Analysis (LDA).

An ANOVA is carried out to find if the method has any effect over the identification rate. It turns out, there is no difference between methods. Significance differences are not enough to conclude one of the methods has a performance mean different from the others. There is no doubt with the results shown in Table 12.5 where the statistic $F - Value$ is too low, and for that reason the probability is too high (0.98). Usually probability values under 0.05 are considered significant, and certainly that is not the case with this data. This conclusion goes in the same direction as goes Figure 12.25.

Table 12.5.: *Anova to Test Method*

	Df	Sum Sq	Mean Sq	F value	Pr(>F)
dfGHL$Method	5.0	0.0608	0.0122	0.1464	0.98
Residuals	12.0	0.9966	0.0830		

If there is any interest to check the effect of the spectrum band on the performance an

ANOVA is also possible and straightforward. In Table 12.6 the statistical $F-value$ rise to 88 and that led to a probability quite low (< 0.0000). The conclusion is again clear, Band has a clear effect on the identification performance.

Table 12.6.: *Anova to Test Spectrum Band*

	Df	Sum Sq	Mean Sq	F value	Pr(>F)
dfGHL$MSpectBand	2.0000	0.9749	0.4875	88.7035	0.0000
Residuals	15.0000	0.0824	0.0055		

A visual representation of the complete distribution of the results between method and Band are shown in Figure 12.25. This representation gives a lot of useful visual information that it is possible to summarize in the following statements.

- √ Identification performance is better in VIS and slightly lower with NIR. Performance decrease significantly with TIR data (verified with ANOVA results).
- √ Performance across methods looks quite similar, however blue methods show a similar behaviour and a little better performance.
- √ The variability of data is more Band dependent than method dependent.
- √ The VIS and NIR distributions are left-skewed, while TIR looks more gaussian. However TIR distributions exhibit a bimodal shape that is generated by the strong performance differences between $Test_1$ and $Test_3$.

In Table 12.7 the median identification performance values with its deviation are shown. This table is a summary of the quantitative information shown in the Figure 12.25. So far it has not came up with a clear experimental results concerning with what is happening with spectrum bands. If reader takes a look at this table for BDM, it is possible to see the decreasing performance across tested bands. An another worthy point, deviation increase drastically from Band to Band going from 0.065 for VIS, to 0.115 for NIR and to 0.336 finally for TIR.

It was previously warned that $Test_1$ that basically was linked with Session 3 offer astonishing results. In Figure 12.25 performance from Session to Session decrease a little bit.

12.4.2. Modalilies

The results detailed for all the holistic modalities are shown in Table 12.8. The best modality for identification purposes in VIS, NIR and TIR is hand. That is not strange,

Table 12.7.: *Identification Performance for different Classification Methods*

	BDM	KLNM	KNN	Log	Fisher	LDA
VIS	0.97(0.065)	0.91(0.120)	0.89(0.115)	0.95(0.095)	0.93(0.085)	0.96(0.067)
NIR	0.92(0.115)	0.80(0.178)	0.73(0.318)	0.86(0.190)	0.89(0.120)	0.93(0.105)
TIR	0.52(0.336)	0.34(0.252)	0.32(0.485)	0.30(0.486)	0.45(0.351)	0.51(0.322)

the complete hand has much more information than a single finger. However, performance alongside Index, Middle and Ring are quite close to Hand, at least in VIS. There is an increasing gap between finger and Hand as soon as spectrum goes form VIS to TIR. Here is what results have shown:

- $\surd$ for VIS $\longrightarrow$ difference equal to 01.3%
- $\surd$ for NIR $\longrightarrow$ difference equal to 06.3%
- $\surd$ for TIR $\longrightarrow$ difference equal to 26.6%

Another warning with these results come up when looking at finger TIR results. There is a gap between NIR and TIR bands. Results drop to half when going from NIR to TIR. The reason for this awkward and awful results could be some of the following:

- $\boxtimes$ The camera's resolution is a quarter of the NIR. It means 320×240
- $\boxtimes$ The effect of thermoregulation and environmental conditions
- $\boxtimes$ Not enough resolution, NITD close to $0.1°C$

The interpretation coming from Figure 12.26 is similar from what has already been described for numeric values. However, in this figure it is possible to detect the real distribution from each of the Bands and Modalities shown.

12.4.3. Finger Fusion

One of the questions this thesis wants to solve concerns the ability of finger to increase hand's performance. In Figure 12.27 it is possible to appreciate how well finger fusion works. This data uses the five fingers instead of trying to figure out which of the fingers is best for the combination approach. Through this straightforward results the conclusions are easy: finger exceeds hand for VIS and NIR but never with TIR.

In Table 12.9 is it highlighted the quantitative results coming from finger fusion within spectrum band.

Table 12.8.: *Modalities*

	Thumb	Index	Middle	Ring	Pinky
VIS	0.870 (0.108)	0.960 (0.060)	0.962 (0.056)	0.965 (0.065)	0.955 (0.075)
NIR	0.827 (0.193)	0.885 (0.151)	0.895 (0.131)	0.893 (0.141)	0.855 (0.161)
TIR	0.445 (0.335)	0.447 (0.289)	0.410 (0.320)	0.488 (0.264)	0.362 (0.279)
	ThumbTXT	IndexTXT	MiddleTXT	RingTXT	PinkyTXT
VIS	0.888 (0.108)	0.955 (0.055)	0.945 (0.075)	0.965 (0.056)	0.935 (0.076)
NIR	0.842 (0.160)	0.883 (0.180)	0.880 (0.175)	0.895 (0.132)	0.850 (0.185)
TIR	0.378 (0.355)	0.442 (0.376)	0.472 (0.335)	0.470 (0.348)	0.352 (0.317)
		centralH	centralHTXT	Hand	HandTXT
VIS		0.708 (0.338)	0.732 (0.372)	0.978 (0.046)	0.975 (0.046)
NIR		0.740 (0.574)	0.718 (0.558)	0.958 (0.073)	0.965 (0.050)
TIR		0.182 (0.369)	0.158 (0.302)	0.755 (0.271)	0.845 (0.176)

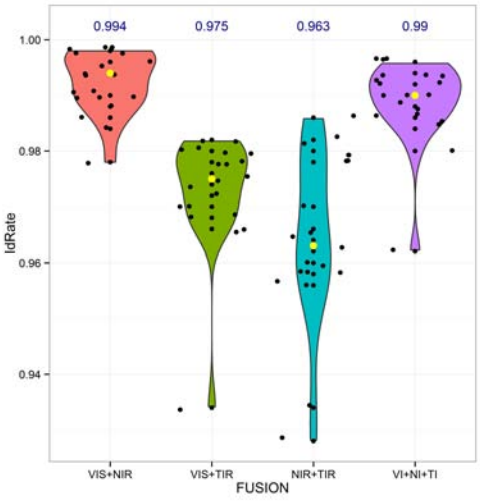

Figure 12.9.: *Fusion for Scenario A*

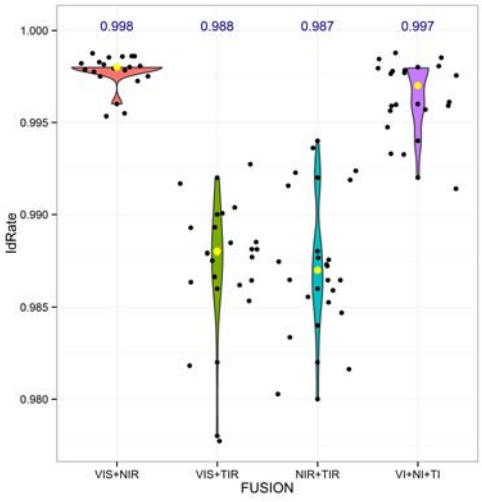

Figure 12.10.: *Fusion for Scenario B*

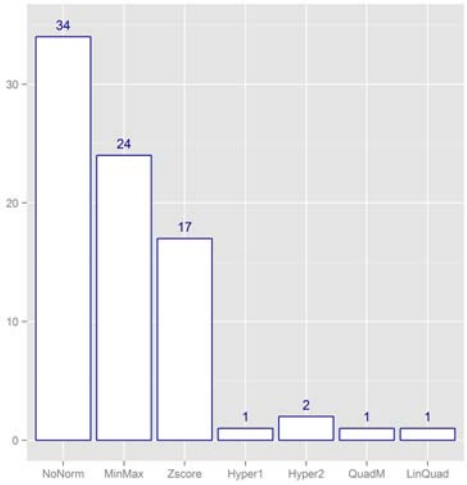

Figure 12.11.: *Normalization Technique Deployed - Scenario A (Y axis = Counting)*

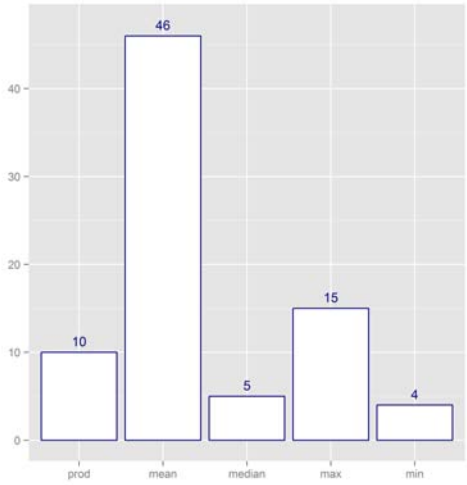

Figure 12.12.: *Fusion Strategy Applied - Scenario A (Y axis = Counting)*

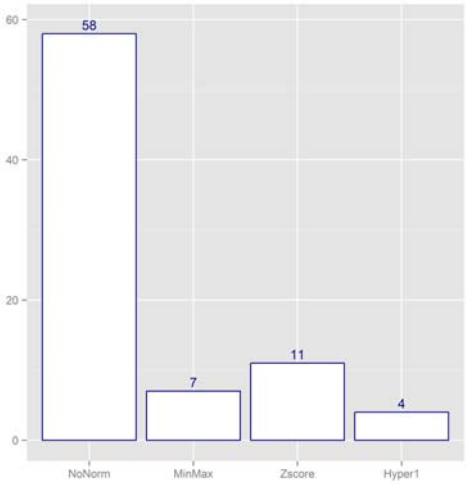

Figure 12.13.: *Normalization Technique Deployed - Scenario B (Y axis = Counting)*

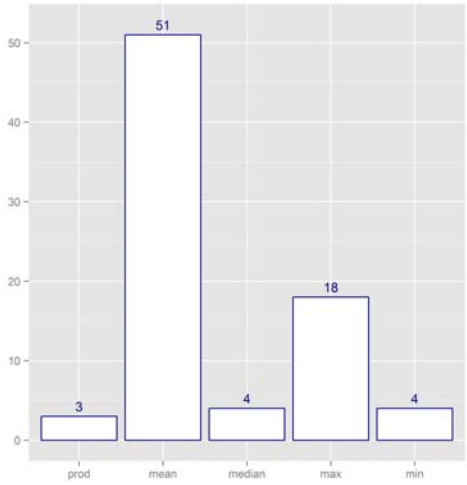

Figure 12.14.: *Fusion Strategy Applied - Scenario B (Y axis = Counting)*

Table 12.9.: *Finger Fusion*

	fFingNN	fFingStd	fFingRang
VIS	1.000 (0.025)	0.985 (0.035)	0.995 (0.015)
NIR	0.975 (0.030)	0.955 (0.135)	0.975 (0.026)
TIR	0.730 (0.190)	0.620 (0.201)	0.745 (0.291)

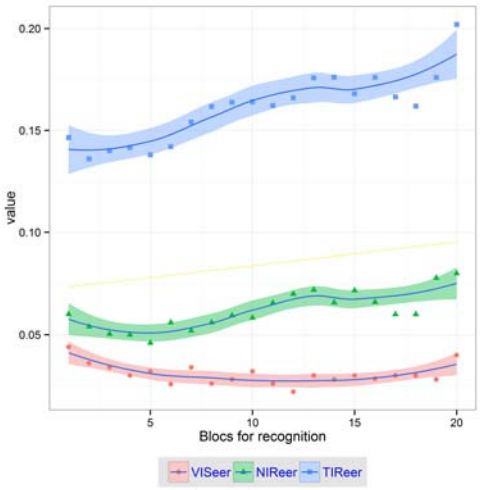

Figure 12.15.: *Verification for Scenario A*

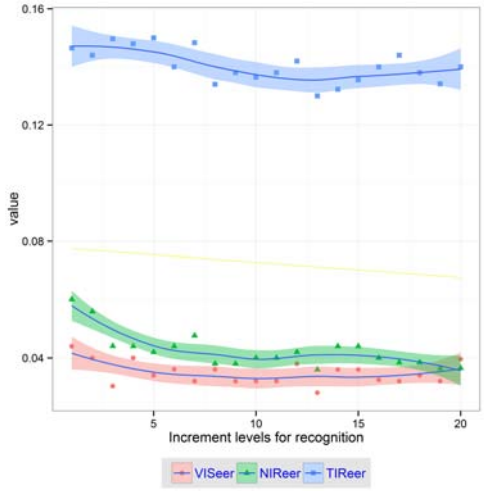

Figure 12.16.: *Verification for Scenario B*

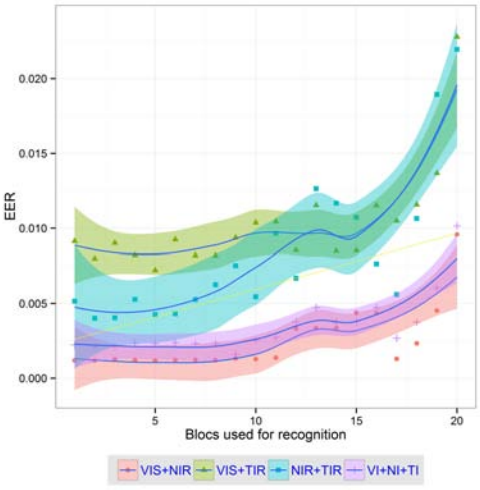

Figure 12.17.: *Fusion for Scenario A*

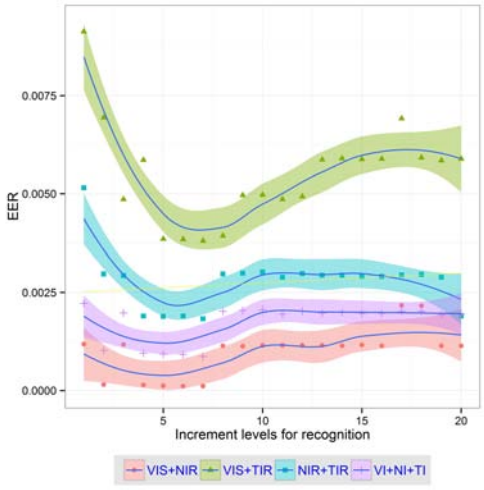

Figure 12.18.: *Fusion for Scenario B*

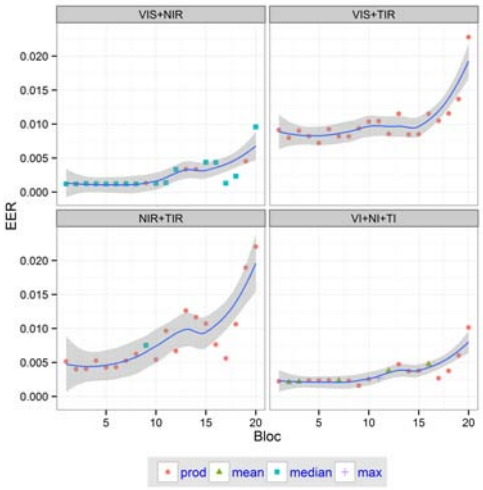

Figure 12.19.: *Fusion for Scenario A*

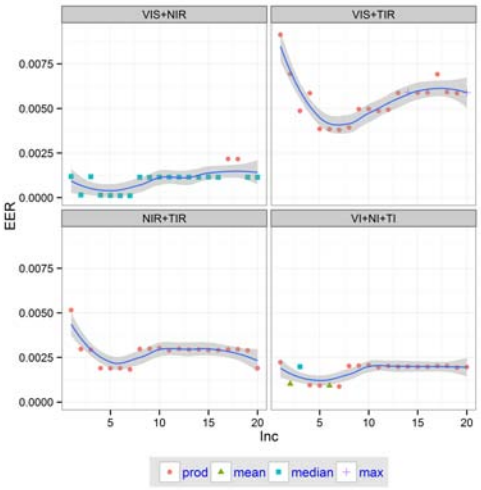

Figure 12.20.: *Fusion for Scenario B*

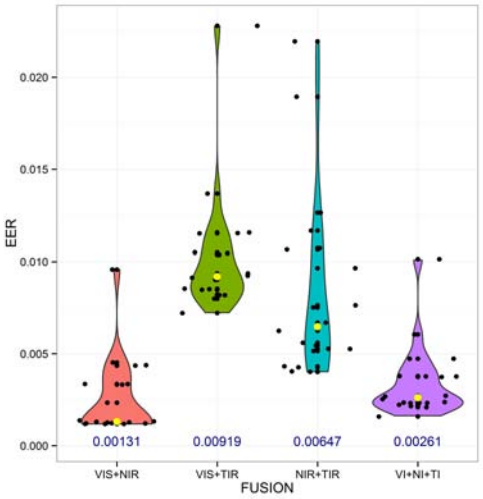

Figure 12.21.: *Fusion for Scenario A*

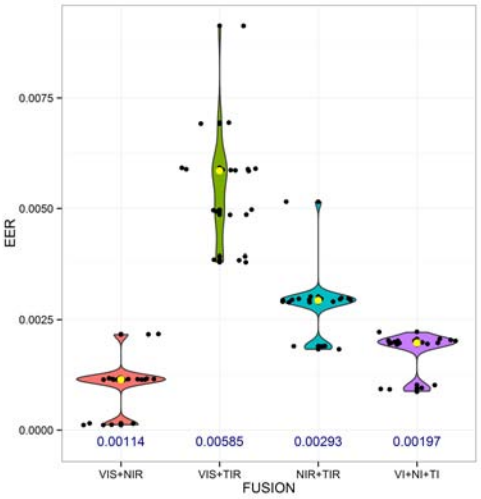

Figure 12.22.: *Fusion for Scenario B*

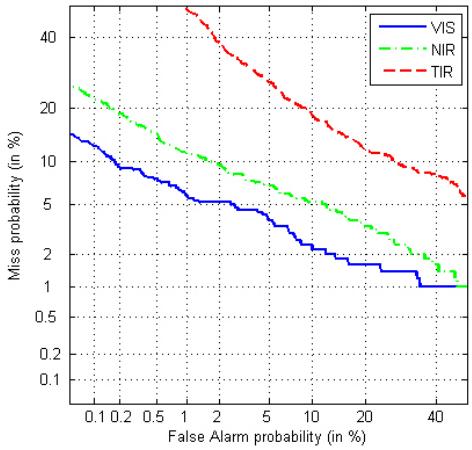

Figure 12.23.: *DET for Hand individual spectrums: VIS, NIR and TIR*

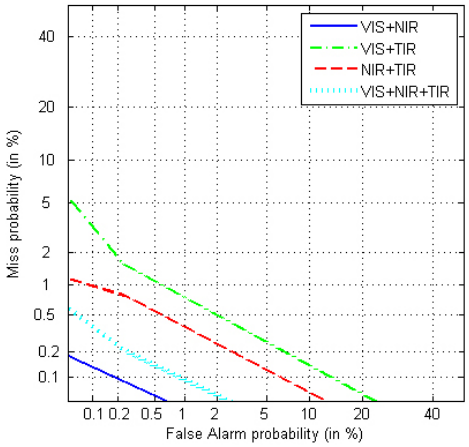

Figure 12.24.: *DET for Hand spectrums fusion: VIS+NIR, VIS+TIR and so on*

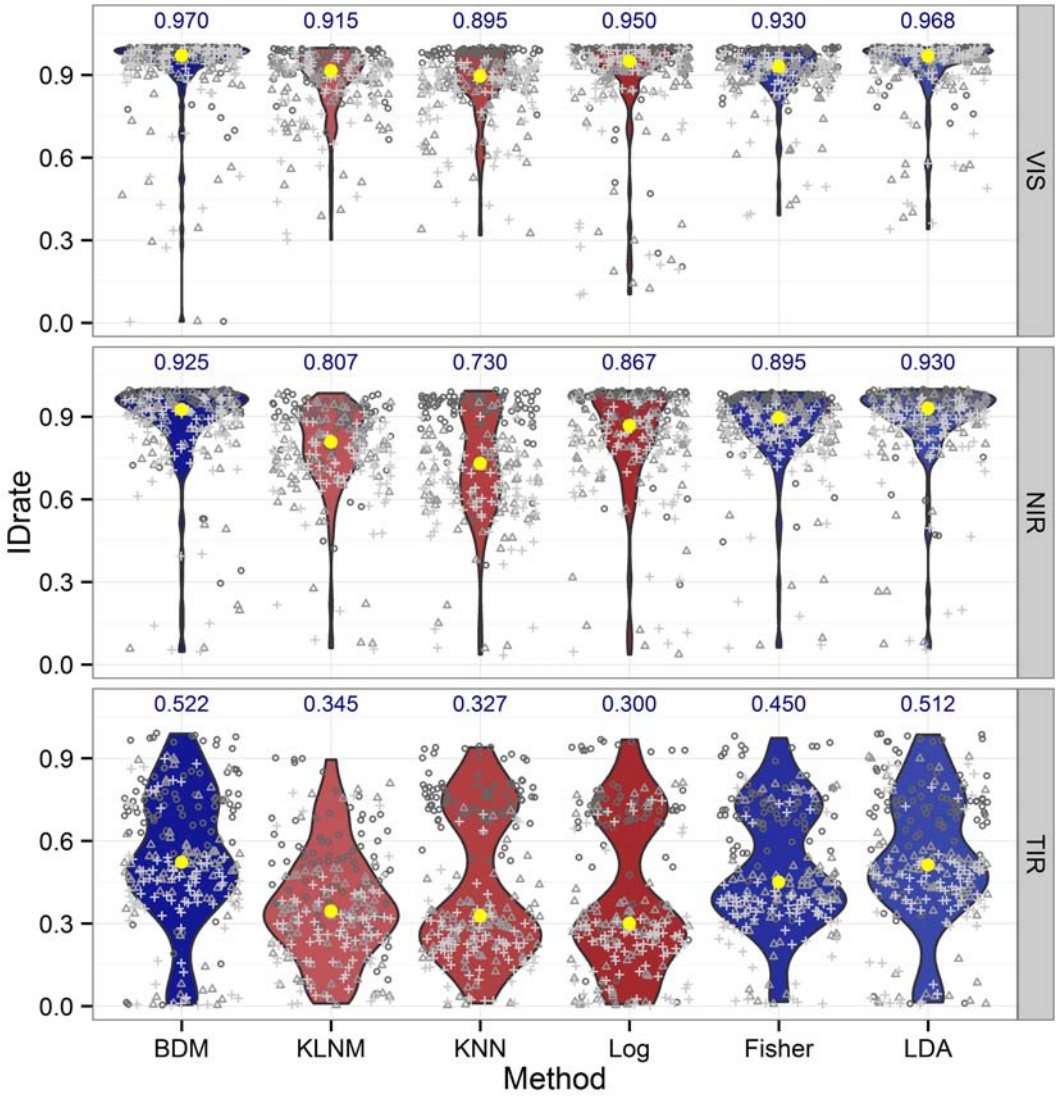

Figure 12.25.: *Identification Performance of classification methods across the three spectrums. Blue color has been used to identify methods close to BDM and red for the other ones. The points in the figure represent identification observation alongside test session. Thus* $\circ = Test_1$, $\triangle = Test_2$ *and* $+ = Test_3$. *Additionally dark points are close to Session 3 while light points are from session 5*

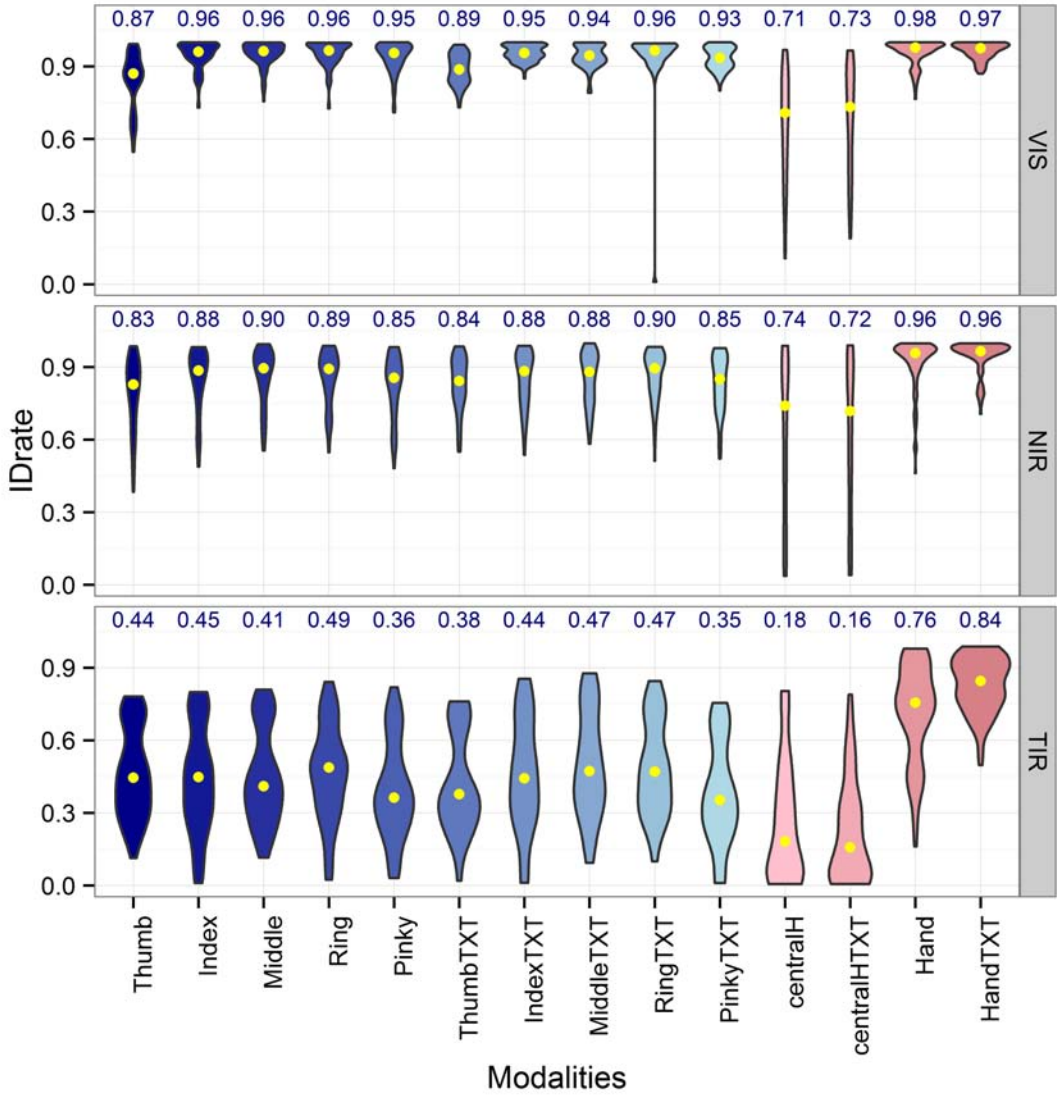

Figure 12.26.: *Identification Performance of the whole holistic data set across the three spectrums.*

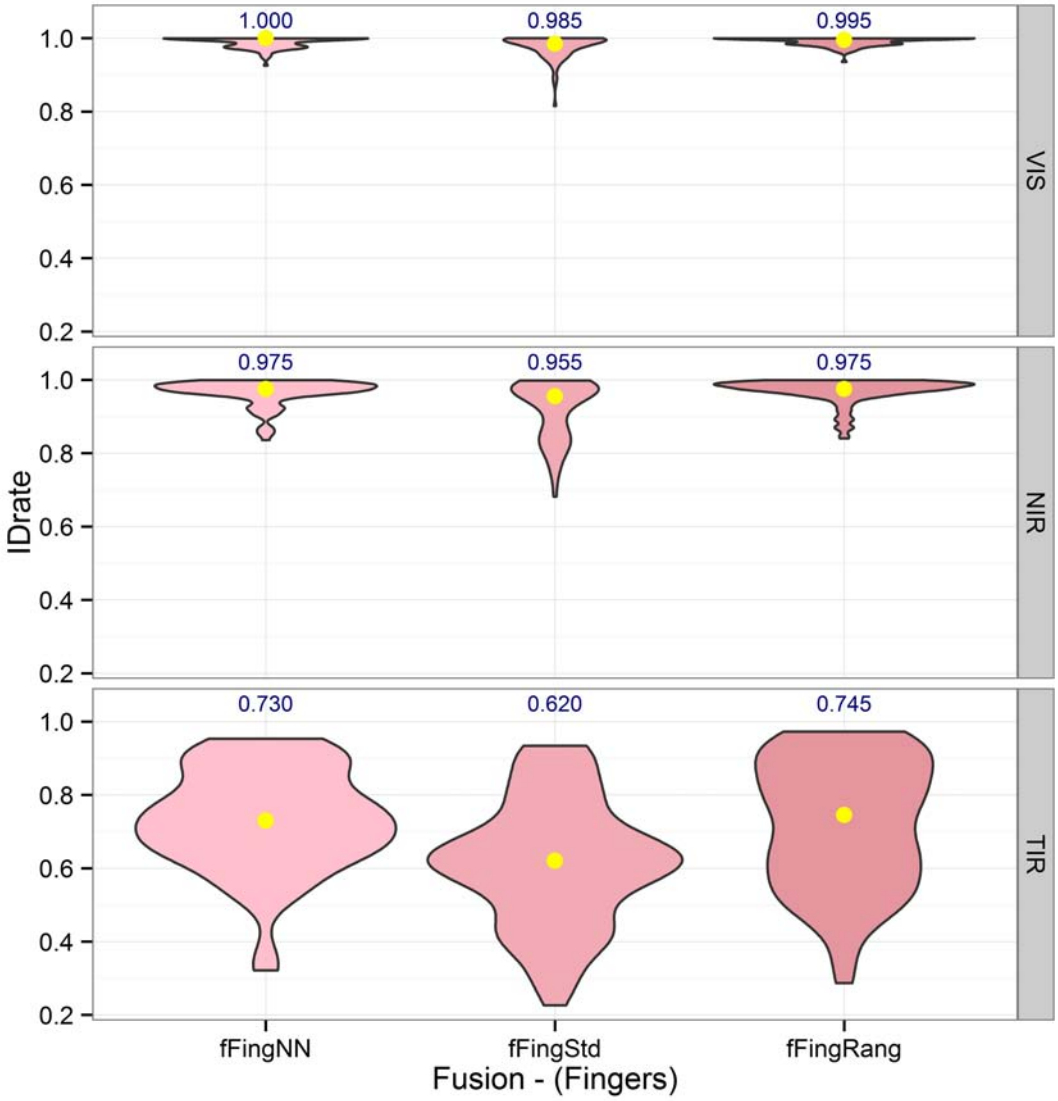

Figure 12.27.: *Finger Fusion. Violin distributions through the fusion finger process related with Spectrum Band.*
The normalization options were no normalization (fFingNN), the z-score (fFingStd) and rang normalization (fFingRang)
VIS hand = 0.98; NIR hand = 0.96; TIR hand = 0.76

Chapter 13.

Results throughout Holistic and Geometric Data

Anonymous

Some people succeed because they are destined to, but most people succeed because they are determined to.

Overview

The purpose of this chapter is offering a clear view of the improvements when the biometric system is combined in a deeper way. In other words, what is going on when the number of different sources to fusion increase. This chapter works under the assumption of a equally distributed training and testing data set (50% for training and the remaining 50% for testing). So the performance from the geometric data will be revealed, first alone and then with the holistic data.

Contents

13.1. Introduction to Holistic and Geometric Results

This chapter analyse results with the approach first stated in chapter 12. It means the full data set is split in two parts:

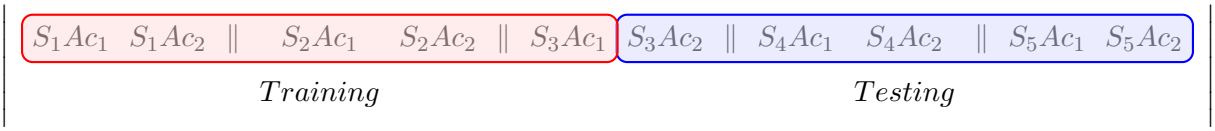

To simplify things, all results have been deployed using the classification method BDM.

13.2. Hand Geometric Data and Hand Holistic Data

The first result it is offered from Hand geometric Data Sets (see Table 13.1). The results are compared with the holistic hand performance. The first point to be highlighted: in identification VIS15g and VIS18g exceed the expectation and become a clear option for identification. That result is quite surprising because by default the usual assumption is holistic data is always more informative than geometric data. Anyway results between VIS and NIR are close to those from geometric data.

Another point to highlight is the data set coming from the curvature which offers a real good performance in identification and in verification as well. Actually Curv3g obtain better performance than NIRh in verification operation.

Table 13.1.: *Identification and Verification Performance Measurements from Holistic and Geometric Data*

	nId	IDrate	EER	SelDim	OrigDim
VISh	1	0.9820	0.0440	40	100
NIRh	2	0.9820	0.0601	87	100
TIRh	3	0.7900	0.1465	76	100
VIS15g	4	0.9880	0.0200	45	50
VIS18g	5	0.9840	0.0220	57	60
Curv3g	6	0.9440	0.0598	73	200
Curv4g	7	0.9220	0.0698	82	200

13.2.1. Holistic and Geometric Fusion Results

Working with the previous data sets is no difficult to explore all possible combinations with two data sets sources. Actually it can be deployed for three and four as well. The total number of combinations are 21, 35 and 35 for 2, 3 and 4 fusion respectively.

Let us begin with two data sets combinations.

Two Combinations

The following two tables, Table 13.2 and Table 13.3 shows the best 6 combinations from identification and verification operation respectively. The best result comes from combining an holistic data set (NIRh) and a geometric data set (VIS18g). Actually three of the best solutions offer this approach. For verification this way to combine data sets increase to four options.

Table 13.2.: *Holistic and Geometric Fusion with Two Data Sets. Identification*

nId	Combin	Norm	Idrate	FirstDS	SecondDS
9	prod	MinMax	1.000	NIRh	VIS18g
1	max	MinMax	0.998	VISh	NIRh
8	max	MinMax	0.996	NIRh	VIS15g
16	prod	MinMax	0.996	VIS15g	VIS18g
4	mean	Zscore	0.992	VISh	VIS18g
13	mean	Zscore	0.992	TIRh	VIS18g

The interpretation of both results' table is the following. Working with two data sets, instead of one, allow the system exceeds individual modality performance.

Three Combinations

If three data sets are selected the following results are obtained (see Table 13.4 and Table 13.5). The main point is that in any of the best combinations showed always there is a mix between holistic and geometric data. For both operations of the system, this way of combining data sets seems to be determinant to obtain a clear improvement of the system performance.

Table 13.3.: *Holistic and Geometric Fusion with Two Data Sets. Verification*

nId	Combin	Norm	EER	FirstDS	SecondDS
9	mean	NoNorm	0.00017	NIRh	VIS18g
1	max	NoNorm	0.00118	VISh	NIRh
8	max	MinMax	0.00115	NIRh	VIS15g
16	prod	MinMax	0.00214	VIS15g	VIS18g
4	mean	NoNorm	0.00317	VISh	VIS18g
13	mean	NoNorm	0.00513	TIRh	VIS18g

Table 13.4.: *Holistic and Geometric Fusion with Three Data Sets. Identification*

nId	Combin	Norm	Idrate	FirstDS	SecondDS	ThirdDS
20	max	Zscore	1.000	NIRh	VIS15g	VIS18g
24	mean	MinMax	1.000	NIRh	VIS18g	Curv4g
2	max	Zscore	0.998	VISh	NIRh	VIS15g
3	max	MinMax	0.998	VISh	NIRh	VIS18g
4	max	MinMax	0.998	VISh	NIRh	Curv3g
5	median	MinMax	0.998	VISh	NIRh	Curv4g

Four Combinations

The last results coming from hand holistic and geometric combination is showed in Table 13.6 and Table 13.7. Both tables use four data sets. For identification, there is again, a clear selection process that offer the best performance. This process means mixing half of the data sets from holistic and the other half for geometric. It is possible to realize the same effect described previously with three data sets. However for verification not necessary half of data sets are coming from holistic and the other one from geometric. Here, there is some combination options that use only one data set (from NIRh) instead of two.

Table 13.5.: *Holistic and Geometric Fusion with Three Data Sets. Verification*

nId	Combin	Norm	EER	FirstDS	SecondDS	ThirdDS
20	max	MinMax	0.00023	NIRh	VIS15g	VIS18g
3	mean	NoNorm	0.00026	VISh	NIRh	VIS18g
23	mean	NoNorm	0.00043	NIRh	VIS18g	Curv3g
24	median	NoNorm	0.00056	NIRh	VIS18g	Curv4g
17	mean	NoNorm	0.00122	NIRh	TIRh	VIS18g
2	max	MinMax	0.00124	VISh	NIRh	VIS15g

Table 13.6.: *Holistic and Geometric Fusion with Four Data Sets. Identification*

nId	Combin	Norm	Idrate	FirstDS	SecondDS	ThirdDS	FourthDS
30	median	MinMax	1.000	NIRh	VIS18g	Curv3g	Curv4g
5	max	Zscore	0.998	VISh	NIRh	VIS15g	VIS18g
8	max	MinMax	0.998	VISh	NIRh	VIS18g	Curv3g
9	median	NoNorm	0.998	VISh	NIRh	VIS18g	Curv4g
10	median	MinMax	0.998	VISh	NIRh	Curv3g	Curv4g
23	median	MinMax	0.998	NIRh	TIRh	VIS15g	Curv4g

13.3. Hand Geometric Data and Finger Holistic Data

Here it is pointed out the improvement of fingers when combining fingers with some of the hand geometric data sets. To offer less variability range and due to the poor thermografic finger performance only fingers from VIS and NIR will be considered. This pruning heuristic allows to reduce the number of data sets to a lower number, 14.

Before presenting the detailed results there are some representations related with verification performance of finger alone and hand geometric measures that will be highlighted in the following figures, Figure 13.1, Figure 13.2, Figure 13.3 and Figure 13.4.

It is perfectly justified the decision to discard TIR fingers data sets. The performance of these modalities are far from be merely poor to became absolutely worthless. The

Table 13.7.: *Holistic and Geometric Fusion with Four Data Sets. Verification*

nId	Combin	Norm	EER	FirstDS	SecondDS	ThirdDS	FourthDS
5	prod	MinMax	0.00032	VISh	NIRh	VIS15g	VIS18g
27	prod	MinMax	0.00049	NIRh	VIS15g	VIS18g	Curv3g
8	mean	NoNorm	0.00053	VISh	NIRh	VIS18g	Curv3g
28	median	MinMax	0.00062	NIRh	VIS15g	VIS18g	Curv4g
9	median	NoNorm	0.00065	VISh	NIRh	VIS18g	Curv4g
30	median	NoNorm	0.00079	NIRh	VIS18g	Curv3g	Curv4g

other data sets shows a completely different performance behaviour. That is the main reason to work only with the following data sets:

- From VIS: The five fingers.
- From NIR: The five fingers.
- Form Geometric hand: the four data sets, VIS15g, VIS18g, Curv3g and Curv4g

With this data, a fully exploratory data analysis is carried out to figure out how well finger operates with hand geometric data.

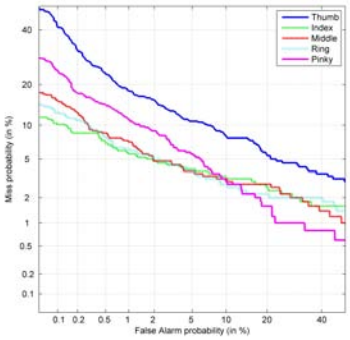

Figure 13.1.: *DET from VIS fingers*

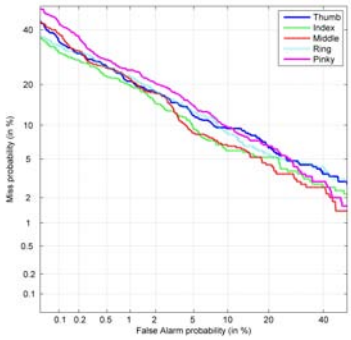

Figure 13.2.: *DET from NIR fingers*

Combining two

The first attempt is combining two data sets. Here again is shown identification in Table 13.8 and verification in Table 13.9. Both tables shown that the best candidates selected

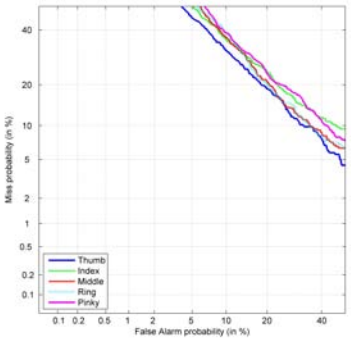

Figure 13.3.: *DET from TIR fingers*

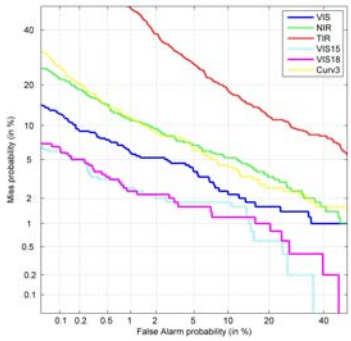

Figure 13.4.: *DET from Hand Geometric*

are always coming from two absolutely different group sets. Holistic group, which comes with DCT component information and Geometric group with length and widths data.

Observe, there is no selection of two modalities coming from the same group. There is always a mix between both groups. In identification the best rates come from combining NIR Thumb finger with VIS18 hand geometric data set. Thus, with the mean combination rule and with no normalization techniques the overall ratio goes to 0.998. The other point to highlight is that the six best combinations shown give a highly performance rate, close to 0.999. In other words, these two data sets obtain a failure every thousands attempts.

Table 13.8.: *Holistic Finger and Geometric Hand Fusion with Two Data Sets (Identification)*

	nID	Comb	Norm	Idrate	FirstDS	SecondDS
1	16	mean	NoNorm	0.998	ThumbN	VIS18g
2	2	mean	ZScore	0.996	IndexV	VIS15g
3	8	prod	MinMax	0.996	MiddleN	VIS15g
4	9	mean	ZScore	0.996	RingN	VIS15g
5	10	mean	ZScore	0.996	PinkyN	VIS15g
6	18	mean	NoNorm	0.996	MiddleN	VIS18g

Reading the verification table (Table 13.9) it is possible to highlight some of the comments made previously. First, the best EER value comes from NIR index finger and VIS15 geometric data file. Using a product rule and a minmax normalization techniques the best combination gives 0.036%. That can be used to say that the biometric system will fail in verification three point six times every ten thousands attempts.

However, the general performance can be reduced by a factor of 10 with the last four

Table 13.9.: *Holistic Finger and Geometric Hand Fusion with Two Data Sets (Verification)*

	nID	Comb	Norm	EER	FirstDS	SecondDS
1	7	prod	MinMax	0.00036	IndexN	VIS15g
2	8	prod	MinMax	0.00038	MiddleN	VIS15g
3	9	max	MinMax	0.00142	RingN	VIS15g
4	10	prod	MinMax	0.00152	PinkyN	VIS15g
5	16	mean	NoNorm	0.00152	ThumbN	VIS18g
6	15	mean	NoNorm	0.00221	PinkyV	VIS18g

combinations displayed. Nevertheless, for these combinations the EER goes from a 0.14% to a 0.22%, and are absolutely at the same level of many published papers.

Combining Three

The second attempt and last with finger and hand information is trough three modalities fusion. Here Table 13.10 shows identification rates close to 1.000 and verification shows results lower than 0.0005 (see Table 13.11).

The selection of a three data sets solution bring a similar interpretation, mix two holistic data sets with one geometric data set. But, there is more. The way holistic data is mixed has to be made properly. This means taking on data set from VIS spectrum band, and the other one from NIR band. This is something to keep in mind when designing a new biometric system focused on hand data.

Table 13.10.: *Holistic Finger and Geometric Hand Fusion with Three Data Sets (Identification)*

	nID	Comb	Norm	Idrate	FirstDS	SecondDS	ThirdDS
1	60	prod	MinMax	1.000	PinkyN	VIS18g	IndexV
2	2	median	QuadMap	0.998	IndexV	VIS15g	ThumbN
3	13	mean	MinMax	0.998	MiddleV	VIS18g	ThumbN
4	55	max	NoNorm	0.998	PinkyV	VIS18g	IndexN
5	69	mean	LinMap	0.998	RingN	Curv3g	IndexV

It is worth mention here, that the results are quite robust. Taking a look at the results, there are no dispersion between the best results. All of them are quite close to

Table 13.11.: *Holistic Finger and Geometric Hand Fusion with Three Data Sets (Verification)*

	nID	Comb	Norm	EER	FirstDS	SecondDS	ThirdDS
1	42	max	MinMax	0.00046	IndexV	VIS15g	IndexN
2	44	median	MinMax	0.00046	RingV	VIS15g	IndexN
3	52	max	NoNorm	0.00046	IndexV	VIS18g	IndexN

each other (0.046% for verification and 99.9% for identification). And that is something really good, because it gives reliability to the system and spread the number of options to be considered.

13.4. Geometric Finger Results

When the full hand is segmented and fingers are segmented as well, it is interesting to study the strengths of finger information alone. Here are shown the results when finger geometric data is used.

Table 13.12 visualize identification rates trough the different finger data sets with respect to the complete set of fingers. The first point to highlight is how the length of width data set affect performance. There is a better identification rates from Width25 than from Width10, and from Width50 than from Width25 as well. However increasing this number too much can force to incorporate noise data, resulting in a worse scenario for identification. That is what happens with Width200. However, when this data goes through a DCT filter results are completely better. This also happens with polar coordinates (see DCT.Pol.Theta and DCT.Pol.Rho).

Some last comments on identification:

- Index and Middle fingers obtain the best performance rates, and close to them ring finger.
- Best width measurements with 50 length vector.
- DCT data sets exceed the other data sets results.

Verification operation mode obtains results quite similar to those from identification results. Table 13.13 shows the EER for any of the possible data sets and fingers studied. Nevertheless, there is a clear difference between the two tables. Results, coming from verification, are less disperse, while the ones which come from identification have a greater variability.

Some point to highlight:

Table 13.12.: *Identification Results for Finger Geometric Data Sets*

	Thumb	Index	Middle	Ring	Pinky
Width10	0.490	0.622	0.666	0.664	0.536
Width25	0.586	0.714	0.730	0.774	0.654
Width50	0.602	0.784	0.808	0.836	0.658
Width200	0.346	0.630	0.682	0.700	0.468
DCT.Width200	0.716	0.860	0.860	0.892	0.766
DCT.Pol.Theta	0.866	0.954	0.910	0.940	0.860
DCT.Pol.Rho	0.778	0.864	0.890	0.912	0.780

- Index, Middle and Ring fingers give EER values close to 5% whatever the data set considered.

Table 13.13.: *Verification Results for Finger Geometric Data Sets*

	Thumb	Index	Middle	Ring	Pinky
Width10	0.114	0.072	0.060	0.072	0.096
Width25	0.106	0.066	0.054	0.050	0.078
Width50	0.102	0.068	0.050	0.056	0.076
Width200	0.142	0.074	0.060	0.066	0.120
DCT.Width200	0.088	0.064	0.048	0.050	0.072
DCT.Pol.Theta	0.074	0.058	0.050	0.054	0.084
DCT.Pol.Rho	0.094	0.090	0.060	0.058	0.108

The dimensional reduction approach trough BDM, can be shown to look at the real length used to deploy recognition in any of its possibilities. Table 13.14 shows the selected components used for recognition.

Some key points revealed on that table are the following:

- First, the number of components used by *DCT.Width200* is very low (between 10 and 15)

- Second, the components selected for the best finger width data set (Width50) are in the range of 37 to 38. This means a 20% dimension reduction over the original data.

Table 13.14.: *Selected Dimension for Finger Geometric Data Sets*

	Thumb	Index	Middle	Ring	Pinky
Width10	7	7	7	7	7
Width25	18	17	17	18	17
Width50	38	37	39	38	36
Width200	57	81	66	89	121
DCT.Width200	12	10	15	12	14
DCT.Pol.Theta	43	54	81	57	80
DCT.Pol.Rho	37	42	36	44	57

Two Combinations

From this data sets that looks far to be considered highly discriminative when properly combined results improve. Here goes the results that in some way exceeds the initial expectation. For identification, Table 13.15 shows the six best combined data sets. The best selection comes from the DCT.Pol.Theta data set with the Thumb and Index finger. For the second best DCT.Pol.Theta data set again this time with fingers Index and Pinky. For this two combinations the percentage of correctly identified persons is 99.4% and 98.8% respectively.

When the question to be solved is in the verification mode Table 13.16 obtain a straightforward and direct response: the best data sets come from DCT.Pol.Theta. From the six best fusion combinations all of them use this data set. And there is more, the best four options use for the first and second data set the same data set. Thus the four best fusion combinations come from DCT.Pol.Theta and the finger pairs used are: (Index, Thumb), (Index, Middle), (Thumb, Ring) and (Index, Ring). The performance are 0.7%, 0.8%, 0.9%, and 1.0% respectively.

However, when the number of different data source, increase to 35, the number of possible combinations increase strongly. Taking a look at how many possible combinations we have to face when combining two data sets from 35? that number is 595. This number increase to 6545 when we look at three combinations, 52360 when we look at

four combinations, 324632 for five combinations and so on. Thus, some care has to be taken to avoid this exponential growth.

Table 13.15.: *Geometric Finger Fusion with two data sets. Identification*

	nID	Comb	Norm	Idrate	FirstDS	SecondDS
1	167	mean	NoNorm	0.994	DCT.Pol.Theta_Thu	DCT.Pol.Theta_Ind
2	363	mean	Hyper1	0.988	DCT.Pol.Theta_Ind	DCT.Pol.Theta_Pin
3	138	mean	MinMax	0.986	DCT.With200_Thu	DCT.Pol.Theta_Ind
4	195	mean	NoNorm	0.984	DCT.Pol.Rho_Thu	DCT.Pol.Theta_Ind
5	360	mean	NoNorm	0.984	DCT.Pol.Theta_Ind	Width50_Pin
6	362	mean	NoNorm	0.984	DCT.Pol.Theta_Ind	DCT.With200_Pin

Table 13.16.: *Geometric Finger Fusion with two data sets. Verification*

	nID	Comb	Norm	EER	FirstDS	SecondDS
1	167	mean	NoNorm	0.007	DCT.Pol.Theta_Thu	DCT.Pol.Theta_Ind
2	349	mean	NoNorm	0.008	DCT.Pol.Theta_Ind	DCT.Pol.Theta_Mid
3	181	mean	NoNorm	0.009	DCT.Pol.Theta_Thu	DCT.Pol.Theta_Rin
4	356	mean	NoNorm	0.010	DCT.Pol.Theta_Ind	DCT.Pol.Theta_Rin
5	350	mean	NoNorm	0.010	DCT.Pol.Theta_Ind	DCT.Pol.Rho_Mid
6	355	mean	NoNorm	0.010	DCT.Pol.Theta_Ind	DCT.With200_Rin

13.5. Holistic Finger Fusion

The last result, that this thesis shows, takes into consideration the five fingers from VIS, NIR and TIR but only with holistic data. The idea is to check if fingers alone improve system performance when combined properly. If they do, the performance related with the whole hand will be questioned.

From Table 13.17 it is revealed some key issues this thesis have made. According to this results, for two finger combination:

- The results obtained are lower than 0.25% EER

- There is always a balanced finger selection between VIS and NIR finger
- There is no TIR finger selection
- The chosen fingers are Index, Middle and Pinky for VIS and NIR (with the addition of Ring finger)

for three finger combination:

- Results obtained are lower than 0.08% EER, for the two best at least.
- Offer two quite different finger selection, although index finger is the main option

for four finger combination:

- Again results are completely low, best results offer EER values from 0.00% to 0.06% EER
- The main finger used to configure the best solution use index finger

for five finger combination:

- EER are in these cases lower than before, obtaining values close to 0.00%
- There is an interesting balance between VIS and NIR finger selection. To be precise three fingers go to VIS and two fingers go to NIR
- There is a common denominator for NIR fingers. That is, Index and Middle fingers are always selected to be part of the best solutions.
- VIS finger selection does not have a single best finger, but Middle finger is always taken as one of them.

So far we have talked in all previous results from two perspectives, verification and identification. Here, the attention has turned on verification. However, results obtained on identification operation are very good as well. For instance, the performance ratio goes to 99.4%, to 99.8% for two and three finger combination and do perfect match for the remaining combinations (four and five finger combination).

Table 13.17.: *Verification Performance for Finger Holistic Fusion with two, three, four and five combinations*

VIS finger					NIR finger					EER
Thumb	Index	Middle	Ring	Pinky	Thumb	Index	Middle	Ring	Pinky	EER
				✓			✓			0.0005
				✓		✓				0.0014
		✓					✓			0.0015
	✓								✓	0.0016
	✓					✓				0.0024
	✓		✓			✓				0.0005
				✓		✓	✓			0.0007
		✓		✓		✓	✓			0.0000
	✓		✓	✓		✓				0.0006
	✓	✓	✓			✓				0.0006
	✓	✓		✓		✓	✓			0.0000
✓		✓		✓		✓	✓			0.0000
✓		✓	✓			✓	✓			0.0001

13.5.1. Pareto Confusion Matrix

Performance measures can fundamentally be used when are clear, readable and give insight of the system. The Pareto Confusion Matrix developed in this thesis goes in that direction. So far, it has not been detailed its implementation neither its usefulness in experimental results. In this section the algorithm is showed in Listing 13.1 and its also used for holistic finger recognition with the Middle finger.

The idea is to use the new performance measure for VIS Middle finger, for NIR Middle finger and also for the fusion of both. What it will not be showed is the standard confusion matrix, because its dimension is large enough to make impossible to write it here. Keep in mind, testing works with 100 users and 5 samples per user, so the resulting matrix is too big and there is no way to be showed. Nevertheless, confusion matrix is useful when its dimension is contained in low dimension. Pareto Confusion Matrix (PCM) solve this problem and helps in the same direction confusion matrix already does.

There are two ways to represent the PCM, the first one is using a heat pattern. That means, basically, to use bright red for the worst scenario and lighter ones for the other ones. Actually there are a graduation of reds according to their error. In Figure 13.5 and Figure 13.6 are shown the PCM for VIS and NIR Middle finger. Certainly, the use of colors helps to identify user identification problems in a straightforward manner. For example, for VIS middle finger, eyes go straight to users U52 and U65. The system incorrectly assign U52 to U38, and U65 to U57 in two of the five samples used for testing. In the other shown table (NIR middle finger), the worst scenario gives 4 errors, but none of them with the same decision. That explains why the red intensity on the first row is lower than for example the second row. Anyway it is important to read the table from top to bottom and then try to figure out what is really happening with the wrong decisions.

The second way of representing PCM is with a size option. Instead of using bright red, it is used size. The bigger the error the bigger the size. The interpretation will be always the same. Figure 13.7 and Figure 13.8 offer this new view of the same performance matrix.

Listing 13.1: Pareto Confusion Matrix

```
% defBreak is the default error number to discard users. If it is 0,
% means users with 0 errors will be discarded
% getCongMat is the well known function that computes the standard confusion matrix
% this matrix generally is too big to be visualize

defBreak=0;
confmat=getConfMat(trueLab,decisions);
[dimx,dimy]=size(confmat);


%Compute the number of error for row (user)
totErrUs=sum(confmat,2);

%Sort the users according to its error from worst to best
[val,indx]=sort(totErrUs,descend);

%Take only users with errors greater than defBreak
[vl]=find(val<=defBreak);

%The last element to deal with is above that element
lastIx=vl(1)-1;

%The new pareto Confusion Matrix is build from worst to best
paretoCF1=zeros(lastIx,dimy);
for i=1:lastIx
    paretoCF1(i,:)=confmat(indx(i),:);
end

%Finally remove decision not taken
totDecUs=sum(paretoCF1);

%keep only those with non zero elements
[vl]=find(totDecUs~=0);

paretoCF=paretoCF1(:,vl);
```

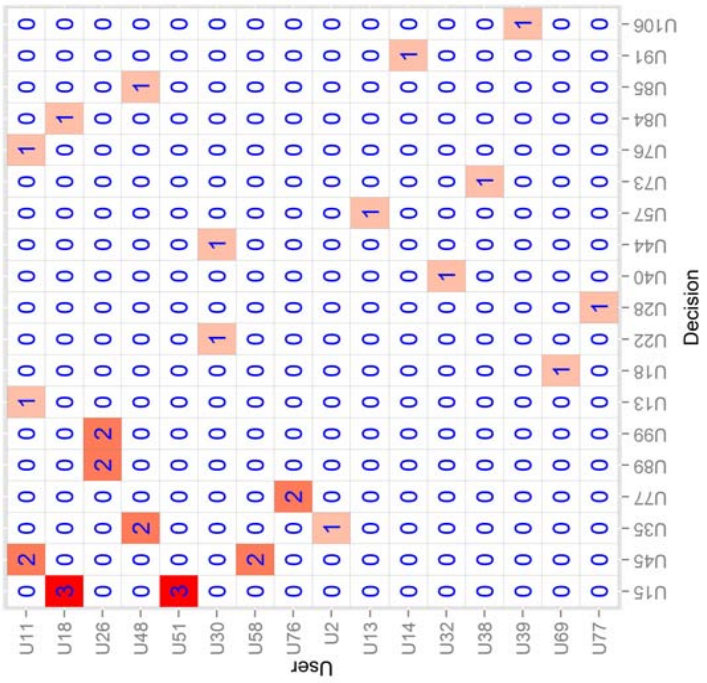

Figure 13.6.: *Pareto Confusion Matrix (heat-option) for NIR Middle Finger*

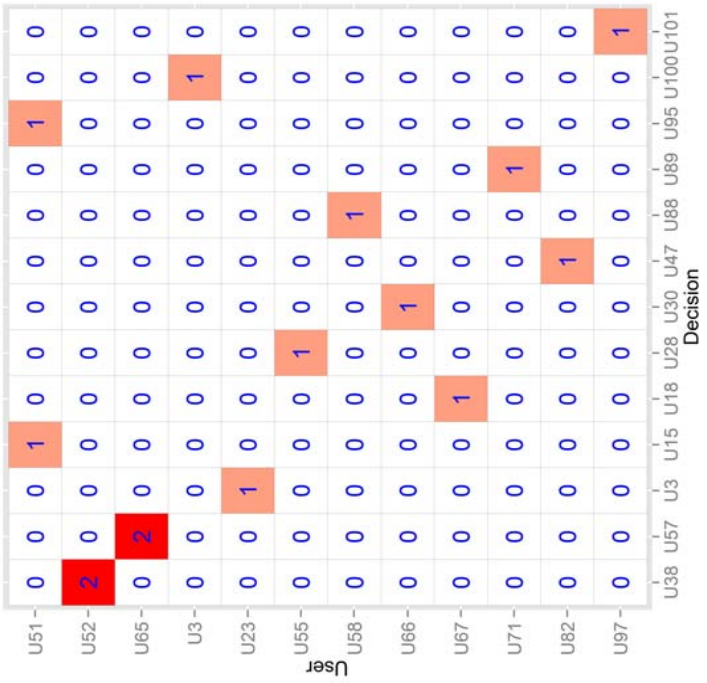

Figure 13.5.: *Pareto Confusion Matrix (heat-option) for VIS Middle Finger*

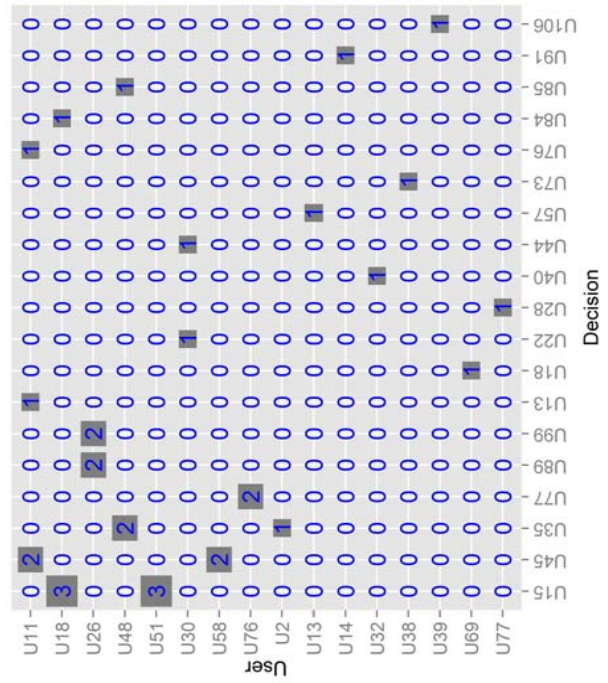

Figure 13.8.: *Pareto Confusion Matrix (size-option) for NIR Middle Finger*

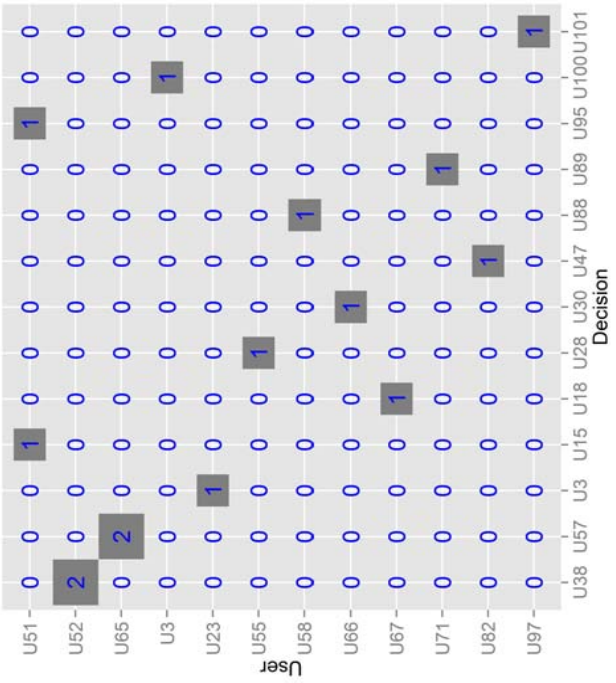

Figure 13.7.: *Pareto Confusion Matrix (size-option) for VIS Middle Finger*

When using a fusion strategy the resulting PCM it is supposed to be better. The key is to decrease the size of the PCM as can be seen in both figures (see Figure 13.9 and Figure 13.10). The number of users involved in the PCM has decreased from 12 to 7. Only the first user, depicted (U51) in the first row, delivers more than one error when testing is applied. Here, again the use of PCM can help significantly, because U51 does not work well in neither of the original cases studied. VIS middle finger fails two times with U51 assigning them to users U15 and U95 and NIR middle finger fails as well. With the NIR data set, U51 is assigned incorrectly to U15 in three of the 5 testing samples. Thus, the conclusion is loud and clear if both original data fail with U51 so do it the fusion approach.

If reader carefully inspect both, VIS and NIR tables, it will seen that there are only two users that are in both PCM. These are U51 and U58. Both of them fail with the improved fusion strategy. However, same attention should be made in order to avoid false claims.

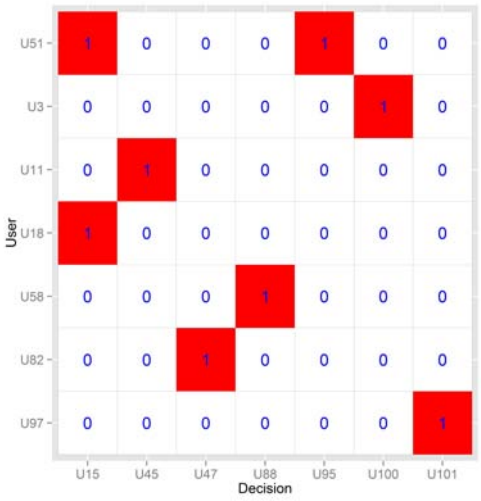

Figure 13.9.: *Pareto Confusion Matrix (heat-option) for VIS and NIR Middle Finger Fusion*

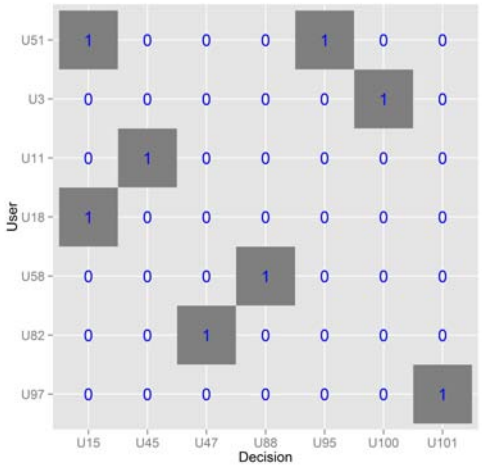

Figure 13.10.: *Pareto Confusion Matrix (size-option) for VIS and NIR Middle Finger Fusion*

Part V.

Thesis Conclusions and Future Extensions

Chapter 14.

Conclusions and Future Research Questions

Nelson Mandela

Education is the most powerful weapon which you can use to change the world..

Overview

This chapter highlight some of the originality assessments this thesis have developed and the implications that can be stated from it. From the beginning of this research work, no one could forecast the quality, neither the innovation presented, neither the improvements made. But as scientific research demands, the work, is in some sense, embrace doubt while walking along the winding path of clarity. Here, an accurate summary of the thesis contributions will be found.

Contents

14.1. Expanding Knowledge

It is clear that every thesis has an ambitious goal to make significant contribution to science. In other words, to make an impact. Quality is difficult to evaluate before publication, and even with that, work need time to find out the real advantage. Out there, is the fear of scientist, illustrated nicely by the well-known aphorism *publish or perish*. As a PhD student, we have follow a track that expose ourselves to critical evaluation and address a number of challenge problems this thesis help understanding.

As a general approach, that is what the research have gone through:

- $\Longrightarrow$ Quality of the objectives.
- $\Longrightarrow$ Quality of the experimental design.
- $\Longrightarrow$ Quality of the data and the pre-process deployed.
- $\Longrightarrow$ Quality of the arguments and the proofs that came into light.
- $\Longrightarrow$ Quality of the methods used.
- $\Longrightarrow$ Quality of the presentation.

The next following sections will cover the major thesis contribution as well as its conclusion.

14.2. Multispectral Hand-Based Database

Taking inspiration from multibiometrics, this thesis present the first hand-based database in three different multispectral bands, VIS, NIR and TIR. With the idea to understand the benefits of biometric system working only with hand information this database represent an essential starting point.

Key points of the Database:

- $\Longrightarrow$ VIS, NIR and TIR images from right hand.
- $\Longrightarrow$ Hand data from a 100 user. Obtained from five different sessions and two acquisition per session. A total of 10 samples per user.
- $\Longrightarrow$ Information related to user identification and gender.

A step further has been made to detail the segmentation process needed in order to

properly segment hand. The following subsections try to focus solely on the contributions made by the thesis:

VIS Segmentation

VIS segmentation take advantage of the exponential moving average to reduce noisy edges and overcome some bad lighting conditions.

NIR Segmentation

The proposed method is a mix of existing and well referenced image processing strategies.

TIR Segmentation

To avoid cold fingers and obtain reliable thermographic hands, information from VIS is used to avoid these problematic scenarios. The idea is take advantage of the device used, because it shoot the TIR and VIS image as well. Thus, there is a close relationship between them. Once computed the difference between both images, scale, translation and rotation can be used to apply VIS mask to the desired TIR region.

14.3. Holistic and Geometric Extraction Process

In order to look at the different information contained in the segmented hand image, we developed different data sets. Some of them are clear, such as the whole hand, the fingers, the finger widths but others are not so common (curvature, DCT from widths or polar coordinates).

What we have is a complete set of options that are shown below:

$\Longrightarrow$ Holistic Data.
- $\Rightarrow$ Hand
- $\Rightarrow$ Finger

$\Longrightarrow$ Geometric Data.
- $\Rightarrow$ Hand
- $\Rightarrow$ Finger

14.3.1. Holistic and Geometric Hand Conclusions

The idea to mix completely different data has a huge impact on performance. Just when two data sets are combined the performance increase drastically. Here it goes a summary table from both performed operations: identification (Table 14.1) and verification (Table 14.2)

Identification rates are extremely close to 1.000 and from Verification rates are also very low. The key point is the way data is combined. The best performance come from a particular way of mixing both data sets, from holistic and geometric. Despite of the general intuition that face give better performance, the results show a promising path to use hand biometric systems on real applications.

Holistic and Geometric Hand

Table 14.1.: *Identification Hand Summary*

		Two Data Sets				*Three Data Sets*				*Four Data Sets*			
	IdRate	1	2	3	4	1	2	3	4	1	2	3	4
VISh	0.988		■					■	■	■	■	■	■
NIRh	0.982	■	■	■		■	■	■	■		■	■	■
TIRh	0.79												
VIS15g	0.988			■	■	■		■			■		
VIS18g	0.984	■			■	■	■		■	■	■	■	■
Curv3g	0.944									■		■	
Curv4g	0.922						■			■			■
		1.000	**0.998**	**0.996**	**0.996**	**1.000**	**1.000**	**0.998**	**0.998**	**1.000**	**0.998**	**0.998**	**0.998**

HOLISTIC FINGER AND HAND GEOMETRIC

In these subsection another key result from the thesis, holistic finger data can improve hand performance when properly combined with hand geometric data sets. Again to carry out this process, the best solutions came from an intelligent way of combining data sets.

Table 14.2.: *Verification Hand Summary*

		Two Data Sets				*Three Data Sets*				*Four Data Sets*			
	EER	1	2	3	4	1	2	3	4	1	2	3	4
VISh	0.044		■				■			■		■	■
NIRh	0.060	■	■	■		■	■	■	■	■	■	■	
TIRh	0.146												
VIS15g	0.020			■	■	■				■	■		■
VIS18g	0.022	■			■	■	■	■	■	■	■	■	■
Curv3g	0.059							■			■	■	
Curv4g	0.069								■				■
		0.00017	**0.00115**	**0.00118**	**0.00210**	**0.00023**	**0.00026**	**0.00043**	**0.00056**	**0.00032**	**0.00049**	**0.00053**	**0.00062**

These tables shown how the best combination balance data from VIS, NIR and Hand Geometric. The easy interpretation is as diversity helps improving ecosystems, here diversity, or in other words different data sets make biometric system more robust.

In Table 14.3 there are results that are as good as those from hand or face as well. The table shows how the best solutions are choosen from the three different group of data sets (VIS fingers, NIR fingers and Hand geometric data sets). The other results, coming from verification, are displayed in Table 14.3. Again the way best data sets are selected is revealed.

14.4. Biometric Dispersion Matcher

Many of the original thesis objectives come from the study of this new method. Basically covering the effect of it on multibiometric environment. Results give no doubt about that, method goes always in a second face. At least when multi spectral data is used, and different extraction process are used. Performance is more data dependent than method dependent.

The results obtained through BDM can be repeated with LDA with exactly the same performance. Different methods like KNN works well but not better than BDM or LDA. The reason was found in chapter 12, section 4. The intention is not discredit any method,

but to understand who improve the performance the most, and results say, spectrum band.

From the perspective of normalization, there is not a clear rule to figure out how to proceed in general. Many results suggest the MinMax or the Z-Score normalization. But others suggest avoiding normalization. The common sense suggests the study of the set of modalities in order to select the appropriate normalization. As was stated in chapter 4, many normalization techniques can be improved and optimized. However, this approach increases computing time excessively.

From the perspective of fusion strategy or combination rule we found something similar. There is not a key rule to be applied always. In many cases the selected rule is the median, others the mean and in other situations the rule used is the product rule. Again some care and research has to be made in order to decide which fusion strategy follow.

14.5. Additional Contributions

14.5.1. Pareto Confusion Matrix

Pareto Confusion Matrix is a new performance measure we believe can help in many ways in complex situations. It is clear, and goes straight to the principal problem.

14.5.2. Gender Recognition

Gender Recognition can be used to solve this problem or reformulated to be used as a way to improve the main biometric system. The first issue account for a real contribution, and the second one stand for a future line of research.

14.5.3. Diversity Rule

What is clear in other fields, such as biology, here it turns out to be absolutely true. The best way to improve performance is through sources that come from different perspectives. In our case combining properly sensor (VIS and NIR) and/or combining properly extraction methods (holistic and geometric)

14.6. Open Questions

There are some interesting points that should be properly addressed. Some of them may be considered promising for future research.

BDM and LDA

As was already commented in the first chapter, BDM has stated as an interesting new classification method. Obviously the results from our experiments, from all data sets tested the performance of BDM has not exceed LDA performance in any way. What is more interesting, they offer quite equivalent response. From the results coming from chapter 12, the behaviour and the performance of both methods are the same, or to be more precise practically the same. Actually, from our data and with the ANOVA test results were clear. (see chapter 13)

Thermographic Data

There is some sense of disappointment in this particularly issue. Although well known for thermoregulation properties, it was a tiny hope to make thermographic data more relevant. There are good results, thought, but from our perspective not outstanding. From Hand Geometric Data and Hand Holistic Data section, where reader can check how TIRh has been selected as one of the best combining data sets. TIRh was selected together with VIS18g to give an EER of 0.513% and with NIRh and VIS18g to give an EER of 0.112%.

Our perspective is the following, it would be particularly interesting to obtain thermographic data with the same VIS and NIR resolution. What would have happened with a better camera and with 640×480 pixels resolution? What would have happened with a better environmental conditions?

NIR Data

The data coming from NIR gives good performance results. However, the device used is far to be a professional NIR camera, so improving the quality of this camera can be translated to better performance. Actually the cost of the NIR camera was extremely low ($20 euros$).

It is not enough to get high quality images from a good camera, there is at least another important issue that must be correctly addressed. This is the focus process.

Hand Scaling

A real key problem which we have ignored up until now has been what happens when the number of user increase. Here has been shown how good our hand biometric system were. The results are quite good,but for a hundred users, that is the point. However, there is no possible inference to a larger group. Actually, it is very difficult to obtain a huge database to test the system in a massive verification environment, like those you can find in an airport. What happens with computation time and performance when the

number of users ready to check the system increase to a thousand? and if this number gets larger to a hundred thousand? and if there are millions of users?

We think these are tough questions that require great effort and the collaboration with same government agency.

Gender Recognition

Using hand for gender recognition has been proved to work well enough. However, this thesis came up with some further interesting questions. Can finger alone reveal gender identity? Chapter 11 give a brief insight through a single geometric hand data set.

The open questions is clear, what happen when using different combinations of data sets or modalities? The thesis has saved some huge data from gender recognition that can be processed later on. The idea is to study a full set of combinations from different data sets and evaluate the performance. What happen if the modalities selected for person recognition are the same than from gender recognition?

14.7. Future Research

There are some long term objectives I am interested in. The first one is what happens with left hand? Our database have only right hand, but other public databases have both hands. The research has been involved with the dorsal hand side. This is important, at least for some real time applications. The dorsal hand side is the usual visible hand from persons walking or talking. A camera can track the hand (through skin detection) and perform a finger segmentation to obtain information of the user (say identification). This can be engineered in a mobile robot as a different way to identify granted persons.

Other interesting research tracks come from thermographic data. Improving resolution and sensitivity helps in the quality of the acquisition process. What happens with hand performance using this kind of camera? From other perspective, where our research group has been involved with, is health research. Can thermographic images, from lungs identify pneumonic problems?. The main idea is to avoid the use of the scanner, if the information can came from thermographic data and is equivalent.

Another interesting open questions is what happens with hand recognition when users can come from many different segments. For instance, does the age represent a problem for hand recognition? and for gender recognition? Imagine a hand database from user with ages from 1 to 100 years old. There is a clear limitation of how to proceed to acquire such Database. But again, can we infer age from hand and finger (holistic and geometric) reliably? What happens with race or with users with injured fingers?

Table 14.3.: *Holistic Finger and Hand Geometric Fusion. Identification*

		Two Data Sets				*Three Data Sets*			
	IdRate	1	2	3	4	1	2	3	4
Thumb_{VIS}	0.932								
Index_{VIS}	0.980		■			■	■		
Middle_{VIS}	0.970							■	
Ring_{VIS}	0.980								
Pinky_{VIS}	0.974								■
Thumb_{NIR}	0.914	■					■	■	
Index_{NIR}	0.940								■
Middle_{NIR}	0.936			■					
Ring_{NIR}	0.928				■				
Pinky_{NIR}	0.910					■			
VIS15g	0.988		■	■	■		■		
VIS18g	0.984	■				■		■	■
Curv3g	0.944								
Curv4g	0.922								
		0.998	**0.998**	**0.999**	**0.996**	**1.000**	**0.998**	**0.998**	**0.998**

Table 14.4.: *Holistic Finger and Hand Geometric Fusion. Verification*

		Two Data Sets				*Three Data Sets*			
	EER	1	2	3	4	1	2	3	4
Thumb_{VIS}	0.0899								
Index_{VIS}	0.0415					■		■	
Middle_{VIS}	0.0402								
Ring_{VIS}	0.0420						■		
Pinky_{VIS}	0.0538								
Thumb_{NIR}	0.0960								
Index_{NIR}	0.0740	■				■	■	■	
Middle_{NIR}	0.0760		■						
Ring_{NIR}	0.0920			■					
Pinky_{NIR}	0.0980				■				
VIS15g	0.0200	■	■	■	■	■	■		
VIS18g	0.0220							■	
Curv3g	0.0590								
Curv4g	0.0690								
		0.00036	**0.00038**	**0.00142**	**0.00152**	**0.00046**	**0.00046**	**0.00046**	

Bibliography

[1] Biometrics. http://www.biometrics.gov/. Online. One citation in page 32.

[2] Biometrics: Technologies and global markets. http://www.bccresearch.com/report/biometrics-technologies-markets-ift042c.html, 2010. Online. One citation in page 34.

[3] V.David Sanchez A. Advanced support vector machines and kernel methods. *Neurocomputing*, 55(1–2):5 – 20, 2003. <ce:title>Support Vector Machines</ce:title>. No citations.

[4] S. Pankanti A. K. Jain, R. Bolle. *Biometrics. Personal identification in a networked society*. Kluwer Academic Publishers, 1999. One citation in page 24.

[5] H. C. Shen A. K. Jain A. Kumar, D. C. Wong. *Audio-and Video-Based Biometric Person Authentication*, volume 2688 of *Lecture Notes in Computer Science*, chapter Personal Verification Using Palmprint and Hand Geometry Biometric, pages 668–678. Springer, 2003. One citation in page 109.

[6] A.K. Jain A. Ross, K. Nandakumar. *Handbook of multibiometrics*. Springer, 2006. 3 citations in pages 60, 63, and 68.

[7] et all. Abhijit Sinha. Estimation and decision fusion: A survey. *Neurocomputing*, 71:2650–2656, 2008. One citation in page 72.

[8] Mohamed Kamel Adams Kong, David Zhang. Palmprint identification using feature-level fusion. *Pattern Recognition*, 39:478–487, 2006. 2 citations in pages 93 and 94.

[9] Miguel Adan, Antonio Adan, Andres S. Vazquez, and Roberto Torres. Biometric verification/identification based on hands natural layout. *Image Vision Comput.*, 26(4):451–465, April 2008. One citation in page 104.

[10] Miguel Adán, Antonio Adán, Andrés S. Vázquez, and Roberto Torres. Biometric verification/identification based on hands natural layout. *Image and Vision Computing*, 26(4):451 – 465, 2008. 5 citations in pages , 95, 97, 98, and 99.

[11] A.M. Ahmad, A. Bade, and L.A.-H.Z. Abidin. Using principal component analysis and hidden markov model for hand recognition systems. In *Information and Multimedia Technology, 2009. ICIMT '09. International Conference on*, pages 323 –326, dec. 2009. One citation in page 64.

[12] Helen C.Shen Anil K. Jain Ajay Kumar, David C.M Wong. Personal authentication using hand images. *Pattern Recognition Letters*, 27:1478–1486, 2006. 2 citations in pages 93 and 95.

[13] Fawaz Alsaade, Aladdin Ariyaeeinia, Amit Malegaonkar, and Surosh Pillay. Qualitative fusion of normalised scores in multimodal biometrics. *Pattern Recognition Letters*, 30(5):564 – 569, 2009. One citation in page 70.

[14] G. Amayeh, G. Bebis, and M. Hussain. A comparative study of hand recognition systems. In *Emerging Techniques and Challenges for Hand-Based Biometrics (ETCHB), 2010 International Workshop on*, pages 1 –6, aug. 2010. One citation in page 101.

[15] Gholamreza Amayeh, George Bebis, Ali Erol, and Mircea Nicolescu. Peg-free hand shape verification using high order zernike moments. In *Proceedings of the 2006 Conference on Computer Vision and Pattern Recognition Workshop*, page 40, 2006. One citation in page 104.

[16] Gholamreza Amayeh, George Bebis, Ali Erol, and Mircea Nicolescu. Hand-based verification and identification using palmar-finger segmentation and fusion. *Computer Vision and Image Understanding*, 113(4):477 – 501, 2009. 3 citations in pages 97, 104, and 141.

[17] M. Arif, T. Brouard, and N. Vincent. Personal identification and verification by hand recognition. In *Engineering of Intelligent Systems, 2006 IEEE International Conference on*, pages 1 –6, 0-0 2006. No citations.

[18] Anil K. Jain Arun Ross. Human recognition using biometrics: An overview. *Annals of Telecomunications*, 62(1/2):11–35, 2007. One citation in page 42.

[19] T Astarita, G Cardone, G.M Carlomagno, and C Meola. A survey on infrared thermography for convective heat transfer measurements. *Optics & Laser Technology*, 32(7–8):593 – 610, 2000. <ce:title>Optical methods in heat and fluid flow</ce:title>. No citations.

[20] C. Bergamini, L.S. Oliveira, A.L. Koerich, and R. Sabourin. Combining different biometric traits with one-class classification. *Signal Processing*, 89(11):2117 – 2127, 2009. No citations.

[21] Christopher M. Bishop. *Pattern Recognition and Machine Learning*. Springer, 2006. One citation in page 21.

[22] Cuixiang Liu Boazhu Wang, Xiuying Chang. Skin detection and segmentation of human face in color images. *International Journal of Intelligent Engineering and Systems*, 4:10–17, 2011. 2 citations in pages 94 and 123.

[23] T. Bollerslev. Generalized autorregressive conditional heterokedasticity. *Journal of Econometrics*, 31:307–327, 1986. No citations.

[24] Djamel Bouchaffra and Abbes Amira. Structural hidden markov models for biometrics: Fusion of face and fingerprint. *Pattern Recognition*, 41(3):852 – 867, 2008. <ce:title>Part Special issue: Feature Generation and Machine Learning for Robust Multimodal Biometrics</ce:title>. No citations.

[25] Kevin W. Bowyer, Karen Hollingsworth, and Patrick J. Flynn. Image understanding for iris biometrics: A survey. *Computer Vision and Image Understanding*, 110(2):281 – 307, 2008. No citations.

[26] Yaroslav Bulatov, Sachin Jambawalikar, Piyush Kumar, and Saurabh Sethia. Hand recognition using geometric classifiers. In David Zhang and Anil K. Jain, editors, *Biometric Authentication, First International Conference, ICBA 2004, Hong Kong, China, July 15-17, 2004, Proceedings*, volume 3072 of *Lecture Notes in Computer Science*, pages 753–759. Springer, 2004. One citation in page 104.

[27] J.P. Campbell. Speaker recognition: a tutorial. In *Proceedings of the IEEE*, volume 85(9), pages 1437–1462, 1997. One citation in page 31.

[28] Bo Chen, Li Yuan, Hongwei Liu, and Zheng Bao. Kernel subclass discriminant analysis. *Neurocomputing*, 71(1–3):455 – 458, 2007. <ce:title>Dedicated Hardware Architectures for Intelligent Systems</ce:title> <ce:title>Advances on Neural Networks for Speech and Audio Processing</ce:title>. No citations.

[29] Yu Chengbo, Qing Huafeng, and Zhang Lian. A research on extracting low quality human finger vein pattern characteristics. In *Bioinformatics and Biomedical Engineering, 2008. ICBBE 2008. The 2nd International Conference on*, pages 1876 –1879, may 2008. No citations.

[30] Lin Chunyi, Li Mingzhong, and Sun Xiao. A finger vein recognition algorithm based on gradient correlation. *AASRI Procedia*, 1(0):40 – 45, 2012. <ce:title>AASRI Conference on Computational Intelligence and Bioinformatics</ce:title>. No citations.

[31] R. Clarke. Human identification for information systems: Management challenges and public policy issues. *Info. Technol. People*, 7(4):6–37, 1994. One citation in page 24.

[32] A. K. Jain S. Prabhakar D. Maltoni, D. Maio, editor. *Handbook of Fingerprint Recognition*. Springer-Verlag, 2003. No citations.

[33] Yanggang Dai, Beining Huang, Wenxin Li, and Zhuoqun Xu. A method for capturing the finger-vein image using nonuniform intensity infrared light. In *Image and Signal Processing, 2008. CISP '08. Congress on*, volume 4, pages 501 –505, may 2008. No citations.

[34] S.C. Dass, Yongfang Zhu, and A.K. Jain. Validating a biometric authentication system: Sample size requirements. *Pattern Analysis and Machine Intelligence, IEEE Transactions on*, 28(12):1902 –1319, dec. 2006. No citations.

[35] J. Daugman. How iris recognition works? *IEEE Trans. on Circuits and Systems for Video Technology*, 14(1):21–30, 2004. No citations.

[36] A. de Santos Sierra, J.G. Casanova, C.S. Avila, and V.J. Vera. Silhouette-based hand recognition on mobile devices. In *Security Technology, 2009. 43rd Annual 2009 International Carnahan Conference on*, pages 160 –166, oct. 2009. No citations.

[37] Damien Dessimoz, Jonas Richiardi, Christophe Champod, and Andrzej Drygajlo. Multimodal biometrics for identity documents (). *Forensic Science International*, 167(2-3):154 – 159, 2007. <ce:title>Selected Articles of the 4th European Academy of Forensic Science Conference (EAFS2006) June 13-16, 2006 Helsinki, Finland</ce:title>. One citation in page 60.

[38] O. Déniz, M. Castrillón, and M. Hernández. Face recognition using independent component analysis and support vector machines. *Pattern Recognition Letters*, 24(13):2153 – 2157, 2003. <ce:title>Audio- and Video-based Biometric Person Authentication (AVBPA 2001)</ce:title>. No citations.

[39] J. Doublet, O. Lepetit, and M. Revenu. Contact less hand recognition using shape and texture features. In *Signal Processing, 2006 8th International Conference on*, volume 3, 16-20 2006. No citations.

[40] J. Doublet, O. Lepetit, and M.J. Revenu. Contactless hand recognition based on distribution estimation. In *Biometrics Symposium, 2007*, pages 1 –6, sept. 2007. No citations.

[41] S. Manjunath D.S. Guru, M.G Suraj. Fusion of covariance matrices of pca and fld. *Pattern Recognition Le*, 32:432–440, 2011. One citation in page 68.

[42] Nicolae Duta. A survey of biometric technology based on hand shape. *Pattern Recognition*, 42(11):2797 – 2806, 2009. One citation in page 104.

[43] J. Egan. *Signal Detection Theory and ROC Analysis*. Academic Press, 1975. One citation in page 46.

[44] A. El-Sallam, F. Sohel, and M. Bennamoun. Robust pose invariant shape-based hand recognition. In *Industrial Electronics and Applications (ICIEA), 2011 6th IEEE Conference on*, pages 281 –286, june 2011. No citations.

[45] Matthew Emery, Jeffrey Jones, and Michael Brown. Clinical application of infrared thermography in the diagnosis of appendicitis. *The American Journal of Emergency Medicine*, 12(1):48 – 50, 1994. No citations.

[46] R. Engle. Autorregressive conditional heterokedasticity with estimates of unitedkingdom inflation. *Econometrika*, 50:987–1008, 1982. No citations.

[47] Bulent Sankur Erdem Yoruk, Helin Dutagaci. Hand biometrics. *Image and Vision Computing*, 24:483–497, 2006. 5 citations in pages 95, 96, 129, 130, and 177.

[48] Mekyska J. Espinosa-Duro V, Faundez-Zanuy M. Beyond cognitive signals. *Cognitive Computation*, 3:374–381, 2011. 2 citations in pages 117 and 118.

[49] Joan Fabregas. *Clasificador Biométrico por Dispersión*. PhD thesis, Universidad de Valladolid, 2008. One citation in page 3.

[50] Marcos Faundez-Zanuy. On-line signature recognition based on vq-dtw. *Pattern Recognition*, 40(3):981 – 992, 2007. One citation in page 31.

[51] Joan Fàbregas and Marcos Faundez-Zanuy. Biometric dispersion matcher. *Pattern Recognition*, 41(11):3412 – 3426, 2008. One citation in page 4.

[52] Joan Fàbregas and Marcos Faundez-Zanuy. Biometric dispersion matcher versus lda. *Pattern Recognition*, 42(9):1816 – 1823, 2009. 2 citations in pages 4 and 66.

[53] Joan Fàbregas and Marcos Faundez-Zanuy. On-line signature verification system with failure to enrol management. *Pattern Recognition*, 42(9):2117 – 2126, 2009. 2 citations in pages 4 and 31.

[54] Travieso C Alonso J. Ferrer M, Morales A. Low cost multi-modal biometric identification system based on hand geometry, palm and finger print texture. In *Security Technology, 2007 41st Annual IEEE International Carnahan Conference*, page 52–58, 2007. One citation in page 109.

[55] Julian Fierrez-Aguilar, Daniel Garcia-Romero, Javier Ortega-Garcia, and Joaquin Gonzalez-Rodriguez. Adapted user-dependent multimodal biometric authentication exploiting general information. *Pattern Recognition Letters*, 26(16):2628 – 2639, 2005. No citations.

[56] R.A. Fisher. The statistical utilization of multiple measurements. *Annals of Eugenics*, 8(4):376–386, 1938. One citation in page 66.

[57] Leong Lai Fong and Woo Chaw Seng. A comparison study on hand recognition approaches. In *Soft Computing and Pattern Recognition, 2009. SOCPAR '09. International Conference of*, pages 364 –368, dec. 2009. No citations.

[58] A. Martin M. Przybocki D. Reynolds G. Doddington, W. Liggett. Sheep, goats, lambs and wolves: A statistical analysis of speaker performance in the nist 1998 speaker recognition evaluation. In *Proceedings of the Fifth International Conference on Spoken Language Processing (ICSLP)*, 1998. No citations.

[59] Hui Gao and James W. Davis. Why direct lda is not equivalent to lda. *Pattern Recognition*, 39(5):1002 – 1006, 2006. No citations.

[60] Sonia Garcia-Salicetti, Charles Beumier, Gerard Chollet, Bernadette Dorizzi, JeanLerouxles Jardins, Jan Lunter, Yang Ni, and Dijana Petrovska-Delacretaz. Biomet: A multimodal person authentication database including face, voice, fingerprint, hand and signature modalities. In Josef Kittler and MarkS. Nixon, editors, *Audio- and Video-Based Biometric Person Authentication*, volume 2688 of *Lecture Notes in Computer Science*, pages 845–853. Springer Berlin Heidelberg, 2003. One citation in page 102.

[61] Gwilym M. Jenkins George E.P. Box. *Time Series Analysis: Forecasting and Control*. Holden Day, San Francisco., rev. ed. edition, 1976. No citations.

[62] Daniele Giansanti. Improving spatial resolution in skin-contact thermography: Comparison between a spline based and linear interpolation. *Medical Engineering & Physics*, 30(6):733 – 738, 2008. No citations.

[63] et al. Ginneken B. Active shape model segmentation with optimal features. *IEEE Transactions on Medical Imaging*, 2002. One citation in page 161.

[64] Javier Guerra-Casanova Alberto Santos-Sierra Gonzalo Bailador, Carmen Sanchez-Avila. Analysis of pattern recognition techniques for in-air signature biometrics. *Pattern Recognition*, 44(10-11):2468 – 2478, 2011. <ce:title>Semi-Supervised Learning for Visual Content Analysis and Understanding</ce:title>. No citations.

[65] Guodong Guo, Stan Z. Li, and Kap Luk Chan. Support vector machines for face recognition. *Image and Vision Computing*, 19(9–10):631 – 638, 2001. No citations.

[66] Jing-Ming Guo, Chih-Hsien Hsia, Yun-Fu Liu, Jie-Cyun Yu, Mei-Hui Chu, and Thanh-Nam Le. Contact-free hand geometry-based identification system. *Expert Systems with Applications*, 39(14):11728 – 11736, 2012. 2 citations in pages 98 and 129.

[67] James D. Hamilton. *Time Series Analysis*. Princeton University Press, 1994. No citations.

[68] Chin-Chuan Han. A hand-based personal authentication using a coarse-to-fine strategy. *Image and Vision Computing*, 22(11):909 – 918, 2004. No citations.

[69] Wei-Yu Han and Jen-Chun Lee. Palm vein recognition using adaptive gabor filter. *Expert Systems with Applications*, 39(18):13225 – 13234, 2012. No citations.

[70] Andrew Harvey. *The Econometric Analysis of Time Series*. Philip Allan, 1990. No citations.

[71] Andrew C. Harvey. *Time Series Models*. Harvester Wheatsheaf, 1993. No citations.

[72] J. Hashimoto. Finger vein authentication technology and its future. In *VLSI Circuits, 2006. Digest of Technical Papers. 2006 Symposium on*, pages 5 –8, 0-0 2006. No citations.

[73] Mingxing He, Shi-Jinn Horng, Pingzhi Fan, Ray-Shine Run, Rong-Jian Chen, Jui-Lin Lai, Muhammad Khurram Khan, and Kevin Octavius Sentosa. Performance evaluation of score level fusion in multimodal biometric systems. *Pattern Recognition*, 43(5):1789 – 1800, 2010. One citation in page 71.

[74] Xiaofu He and Pengfei Shi. A new segmentation approach for iris recognition based on hand-held capture device. *Pattern Recognition*, 40(4):1326 – 1333, 2007. One citation in page 29.

[75] Maleika Heenaye and Mamode Khan. A multimodal hand vein biometric based on score level fusion. *Procedia Engineering*, 41(0):897 – 903, 2012. <ce:title>International Symposium on Robotics and Intelligent Sensors 2012 (IRIS 2012)</ce:title>. 4 citations in pages , 70, 100, and 101.

[76] Jean Hennebert, Andreas Humm, Bruno Dumas, Rolf Ingold, Dijana Petrovska, Catherine Pugin, and Didier von Rotz. Myidea - sensors specifications and acquisition protocol. Technical Report 256-05-12, University of Fribourg, Department of Informatics, 2006. One citation in page 101.

[77] Gerald C. Holst. *Common Sense Approach to Thermal Imaging*. JCD Publishing and SPIE, 2000. One citation in page 80.

[78] Jiang Hong, Guo Shuxu, Li Xueyan, and Qian Xiaohua. Vein pattern extraction based on the position-gray-profile curve. In *Image and Signal Processing, 2009. CISP '09. 2nd International Congress on*, pages 1 –4, oct. 2009. One citation in page 100.

[79] N. Houmani, A. Mayoue, S. Garcia-Salicetti, B. Dorizzi, M.I. Khalil, M.N. Moustafa, H. Abbas, D. Muramatsu, B. Yanikoglu, A. Kholmatov, M. Martinez-Diaz, J. Fierrez, J. Ortega-Garcia, J. Roure Alcobé, J. Fabregas, M. Faundez-Zanuy, J.M. Pascual-Gaspar, V. Cardeñoso-Payo, and C. Vivaracho-Pascual. Biosecure signature evaluation campaign (bsec'2009): Evaluating online signature algorithms depending on the quality of signatures. *Pattern Recognition*, 45(3):993 – 1003, 2012. No citations.

[80] Rong-Xiang Hu, Wei Jia, David Zhang, Jie Gui, and Liang-Tu Song. Hand shape recognition based on coherent distance shape contexts. *Pattern Recognition*, 45(9):3348 – 3359, 2012. <ce:title>Best Papers of Iberian Conference on Pattern Recognition and Image Analysis (IbPRIA'2011)</ce:title>. No citations.

[81] Beining Huang, Yanggang Dai, Rongfeng Li, Darun Tang, and Wenxin Li. Finger-vein authentication based on wide line detector and pattern normalization. In *Pattern Recognition (ICPR), 2010 20th International Conference on*, pages 1269 –1272, aug. 2010. No citations.

[82] Katsuo Ikeda, Takashi Yamamura, Yasumasa Mitamura, Shiokazu Fujiwara, Yoshiharu Tominaga, and Takeshi Kiyono. On-line recognition of hand-written characters utilizing positional and stroke vector sequences. *Pattern Recognition*, 13(3):191 – 206, 1981. One citation in page 31.

[83] J.Ortega-Garcia et al. J. Fierrez, J. Galbally. Biosecureid: a multimodal biometric database. *Pattern Analysis and Applications*, 13:235–246, 2010. 3 citations in pages 27, 101, and 102.

[84] Mohd Shawal Jadin and Soib Taib. Recent progress in diagnosing the reliability of electrical equipment by using infrared thermography. *Infrared Physics & Technology*, 55(4):236 – 245, 2012. No citations.

[85] M. Jafarzadegan and H. Mirzaei. A new ensemble based classifier using feature transformation for hand recognition. In *Human System Interactions, 2008 Conference on*, pages 749 –754, may 2008. No citations.

[86] A.K. Jain. Biometric recognition: how do i know who you are? In *Signal Processing and Communications Applications Conference, 2004. Proceedings of the IEEE 12th*, pages 3 – 5, april 2004. No citations.

[87] A.K. Jain. Biometrics: Proving ground for image and pattern recognition. In *Image and Graphics, 2007. ICIG 2007. Fourth International Conference on*, page 3, aug. 2007. No citations.

[88] A.K. Jain, R. Chellappa, S.C. Draper, N. Memon, P.J. Phillips, and A. Vetro. Signal processing for biometric systems [dsp forum]. *Signal Processing Magazine, IEEE*, 24(6):146 –152, nov. 2007. No citations.

[89] A.K. Jain and S. Pankanti. A touch of money [biometric authentication systems]. *Spectrum, IEEE*, 43(7):22 – 27, july 2006. No citations.

[90] A.K. Jain, S. Pankanti, S. Prabhakar, Lin Hong, and A. Ross. Biometrics: a grand challenge. In *Pattern Recognition, 2004. ICPR 2004. Proceedings of the 17th International Conference on*, volume 2, pages 935 – 942 Vol.2, aug. 2004. No citations.

[91] A.K. Jain, A. Ross, and K. Nandakumar. An introduction to biometrics. In *Pattern Recognition, 2008. ICPR 2008. 19th International Conference on*, page 1, dec. 2008. One citation in page 21.

[92] A.K. Jain, A. Ross, and S. Pankanti. Biometrics: a tool for information security. *Information Forensics and Security, IEEE Transactions on*, 1(2):125 – 143, june 2006. No citations.

[93] A.K. Jain, A. Ross, and S. Prabhakar. An introduction to biometric recognition. *Circuits and Systems for Video Technology, IEEE Transactions on*, 14(1):4 – 20, jan. 2004. 2 citations in pages 21 and 32.

[94] A.K. Jain and U. Uludag. Hiding biometric data. *Pattern Analysis and Machine Intelligence, IEEE Transactions on*, 25(11):1494 – 1498, nov. 2003. No citations.

[95] Ani K. Jain and Nicolae Duta. Deformable matching of hand shapes for user verification. In *In: Proceedings of ICIP '99. Kobe*, 1999. One citation in page 104.

[96] Anil Jain, Karthik Nandakumar, and Arun Ross. Score normalization in multimodal biometric systems. *Pattern Recognition*, 38(12):2270 – 2285, 2005. One citation in page 74.

[97] et all Jian Yang. Feature fusion: Parallel strategy vs. seria strategy. *Pattern Recognition*, 36:1369–1381, 2003. One citation in page 70.

[98] et all Josef Kittler. On combining classifiers. *IEEE Transactions on Pattern Analysis and Machine Intelligence*, 20(3):226–239, 1998. One citation in page 60.

[99] Wenxiong Kang. Vein pattern extraction based on vectorgrams of maximal intra-neighbor difference. *Pattern Recognition Letters*, 33(14):1916 – 1923, 2012. <ce:title>Novel Pattern Recognition-Based Methods for Re-identification in Biometric Context</ce:title>. One citation in page 100.

[100] Muhammad Khurram Khan and Jiashu Zhang. Multimodal face and fingerprint biometrics authentication on space-limited tokens. *Neurocomputing*, 71(13-15):3026 – 3031, 2008. <ce:title>Artificial Neural Networks (ICANN 2006) / Engineering of Intelligent Systems (ICEIS 2006)</ce:title>. No citations.

[101] Hyunsoo Kim, Barry L. Drake, and Haesun Park. Multiclass classifiers based on dimension reduction with generalized lda. *Pattern Recognition*, 40(11):2939 – 2945, 2007. No citations.

[102] Kevin H. Knuth. Optimal data-based binning for histograms. Technical report, Department of Physics. University of Alabama, State University of NY, 2006. One citation in page 40.

[103] M.Özgün Korukçu and Muhsin Kilic. The usage of ir thermography for the temperature measurements inside an automobile cabin. *International Communications in Heat and Mass Transfer*, 36(8):872 – 877, 2009. No citations.

[104] Kathleen Kraninger. Testimony of deputy assistant secretary for policy. http://www.dhs.gov/news/2009/03/19/testimony-biometric-identification, 3 2009. One citation in page 20.

[105] Ajay Kumar, David C. M. Wong, Helen C. Shen, and Anil K. Jain. Personal verification using palmprint and hand geometry biometric. pages 668–678, 2003. No citations.

[106] Ajay Kumar, David C.M. Wong, Helen C. Shen, and Anil K. Jain. Personal authentication using hand images. *Pattern Recognition Letters*, 27(13):1478 – 1486, 2006. No citations.

[107] Zhang D. Kumar A. Incorporating user quality for performance improvement in hand identification. in: Control, automation, robotics and vision. icarcv 2008. 10th international conference. pages 1133 – 1136, 2008. One citation in page 109.

[108] Ludmila I. Kuncheva. *Combining Pattern Classifiers. Methods and Algorithms*. John Wiley and Sons, Ltd Publications, 2004. 2 citations in pages 60 and 73.

[109] E. Aviczer L. Lee, T. Berger. Reliable on-line human signature verification systems. *IEEE Trans. on Pattern Analysis and Machine Intelligence*, 18(6):643–647, 1996. No citations.

[110] J. A. Reeds M. H. Wright Lagarias, J.C. and P. E. Wright. Convergence properties of the nelder-mead simplex method in low dimensions. *SIAM Journal of Optimization*, 9(1):112–147, 1999. One citation in page 162.

[111] B.B. Lahiri, S. Bagavathiappan, T. Jayakumar, and John Philip. Medical applications of infrared thermography: A review. *Infrared Physics & Technology*, 55(4):221 – 235, 2012. 2 citations in pages 86 and 88.

[112] Jen-Chun Lee. A novel biometric system based on palm vein image. *Pattern Recognition Letters*, 33(12):1520 – 1528, 2012. No citations.

[113] Jain Anil K. Li, Stan Z., editor. *Handbook of face recognition*. Springer. One citation in page 26.

[114] Peihua Li and Hongwei Ma. Iris recognition in non-ideal imaging conditions. *Pattern Recognition Letters*, 33(8):1012 – 1018, 2012. <ce:title>Noisy Iris Challenge Evaluation II - Recognition of Visible Wavelength Iris Images Captured At-a-distance and On-the-move</ce:title>. One citation in page 29.

[115] Yixiong Liang, Weiguo Gong, Yingjun Pan, and Weihong Li. Generalizing relevance weighted lda. *Pattern Recognition*, 38(11):2217 – 2219, 2005. No citations.

[116] Zhizheng Liang and Pengfei Shi. Kernel direct discriminant analysis and its theoretical foundation. *Pattern Recognition*, 38(3):445 – 447, 2005. No citations.

[117] Zhizheng Liang, David Zhang, and Pengfei Shi. Robust kernel discriminant analysis and its application to feature extraction and recognition. *Neurocomputing*, 69(7–9):928 – 933, 2006. <ce:title>New Issues in Neurocomputing: 13th European Symposium on Artificial Neural Networks</ce:title> <xocs:full-name>13th European Symposium on Artificial Neural Networks 2005</xocs:full-name>. No citations.

[118] Zhi Liu, Yilong Yin, Hongjun Wang, Shangling Song, and Qingli Li. Finger vein recognition with manifold learning. *Journal of Network and Computer Applications*, 33(3):275 – 282, 2010. <ce:title>Recent Advances and Future Directions in Biometrics Personal Identification</ce:title>. No citations.

[119] Lumidigm. Whole hand multimodal biometric. http://www.lumidigm.com/whole-hand-multimodal-biometric/. 2 citations in pages 92 and 100.

[120] Honza Mikulka M. F.-Z. Marco Grassi, Ondrej Smirg. Face gender recognition using neural networks and dct image's coefficient selection. In *Neural Nets WIRN11 - Proceedings of the 21st Italian Workshop on Neural Nets*, 2011. One citation in page 171.

[121] D. Maltoni M. Golfarelli, D. Maio. On the error-reject tradeoff in biometric verification systems. *IEEE Transactions on Pattern Analysis Machine Intelligence*, 19(7):786–796, 1997. One citation in page 104.

[122] M C Jones M P Wand. *Kernel Smoothing*. Chapman & Hall/CRC, 1995. One citation in page 40.

[123] YingLiang Ma, F. Pollick, and W.T. Hewitt. Using b-spline curves for hand recognition. In *Pattern Recognition, 2004. ICPR 2004. Proceedings of the 17th International Conference on*, volume 3, pages 274 – 277 Vol.3, aug. 2004. No citations.

[124] Y.P Mack and M Rosenblatt. Multivariate k-nearest neighbor density estimates. *Journal of Multivariate Analysis*, 9(1):1 – 15, 1979. No citations.

[125] Matos H Campilho A. Magalhaes F, Oliveira HP. Hgc2011 - hand geometric points detection competition database. http://www.fe.up.pt/hgc2011, 2012. One citation in page 109.

[126] N. Mahri, S.A.S. Suandi, and B.A. Rosdi. Finger vein recognition algorithm using phase only correlation. In *Emerging Techniques and Challenges for Hand-Based Biometrics (ETCHB), 2010 International Workshop on*, pages 1 –6, aug. 2010. No citations.

[127] Dario; Jain Anil K.; Prabhakar Salil Maltoni, Davide; Maio. *Handbook of Fingerprint Recognition*. Springer, 2005. One citation in page 28.

[128] S. Manocha and M.A. Girolami. An empirical analysis of the probabilistic k-nearest neighbour classifier. *Pattern Recognition Letters*, 28(13):1818 – 1824, 2007. No citations.

[129] A. Martin, G. Doddington, T. Kamm, M. Ordowski, and M. Przybocki. The det curve in assessment of detection task performance. pages 1895–1898, 1997. One citation in page 48.

[130] A.M. Martinez. Recognizing imprecisely localized, partially occluded, and expression variant faces from a single sample per class. *Pattern Analysis and Machine Intelligence, IEEE Transactions on*, 24(6):748 – 763, 2002. One citation in page 26.

[131] Bryan J. O'Young et al. Mathew H.M. Lee, Jeffrey M. Cohen. *Rehabilitation Medicine and Thermography*. Impress Publications, 2008. One citation in page 87.

[132] Abel Sussman Matt Billeri. Biometrics in travel and transportation. http://identity.utexas.edu/media/id360/ID360-2012-MatthewBilleri-Presentation.pdf. One citation in page 35.

[133] Donald E. Maurer and John P. Baker. Fusing multimodal biometrics with quality estimates via a bayesian belief network. *Pattern Recognition*, 41(3):821 – 832, 2008. <ce:title>Part Special issue: Feature Generation and Machine Learning for Robust Multimodal Biometrics</ce:title>. One citation in page 70.

[134] G.K.O. Michael, T. Connie, Lau Siong Hoe, and A.T.B. Jin. Locating geometrical descriptors for hand biometrics in a contactless environment. In *Information Technology (ITSim), 2010 International Symposium in*, volume 1, pages 1 –6, june 2010. No citations.

[135] Goh Kah Ong Michael, Tee Connie, and Andrew Beng Jin Teoh. Touch-less palm print biometrics: Novel design and implementation. *Image and Vision Computing*, 26(12):1551 – 1560, 2008. No citations.

[136] Goh Kah Ong Michael, Tee Connie, and Andrew Beng Jin Teoh. A contactless biometric system using multiple hand features. *Journal of Visual Communication and Image Representation*, 23(7):1068 – 1084, 2012. No citations.

[137] M. Minsky. Logical versus analogical or symbolic versus connectionist or neat versus scruffy. *AI Magazine*, 12:34–51, 1991. One citation in page 60.

[138] M. Mohamed Syed Ibrahim, Faris Salman Al-Namiy, Marsaline Beno, and L. Rajaji. Biometric authentication for secured transaction using finger vein technology. In *Sustainable Energy and Intelligent Systems (SEISCON 2011), International Conference on*, pages 760 –763, july 2011. No citations.

[139] A. Morales, M.A. Ferrer, F. Díaz, J. Alonso, and C. Travieso. Contact-free hand biometric system for real environments. *Proceedings of the 16th European Signal Processing Conference (EUSIPCO)*, 2008. One citation in page 104.

[140] P. Ruchikachorn P. Taksaphan N. Covavisaruch, P. Prateepamornkul. Personal verification and identification using hand geometry. *ECTI Transaction CIT*, 2:134–139, 2005. One citation in page 104.

[141] V.V. Nabiyev. Intuitive approach in biometric recognition according to hand geometry and palmprint. In *Signal Processing and Communications Applications, 2006 IEEE 14th*, pages 1 –4, april 2006. No citations.

[142] Makram Nabti and Ahmed Bouridane. An effective and fast iris recognition system based on a combined multiscale feature extraction technique. *Pattern Recognition*, 41(3):868 – 879, 2008. <ce:title>Part Special issue: Feature Generation and Machine Learning for Robust Multimodal Biometrics</ce:title>. No citations.

[143] K. Nandakumar, Yi Chen, S.C. Dass, and A.K. Jain. Likelihood ratio-based biometric score fusion. *Pattern Analysis and Machine Intelligence, IEEE Transactions on*, 30(2):342 –347, feb. 2008. No citations.

[144] K. Nandakumar, A. Ross, and A.K. Jain. Biometric fusion: Does modeling correlation really matter? In *Biometrics: Theory, Applications, and Systems, 2009. BTAS '09. IEEE 3rd International Conference on*, pages 1 –6, sept. 2009. No citations.

[145] Loris Nanni and Alessandra Lumini. An experimental comparison of ensemble of classifiers for biometric data. *Neurocomputing*, 69(13–15):1670 – 1673, 2006. <ce:title>Blind Source Separation and Independent Component Analysis</ce:title> <ce:subtitle>Selected papers from the ICA 2004 meeting, Granada, Spain</ce:subtitle> <xocs:full-name>Blind Source Separation and Independent Component Analysis</xocs:full-name>. No citations.

[146] Loris Nanni and Alessandra Lumini. A novel local on-line signature verification system. *Pattern Recognition Letters*, 29(5):559 – 568, 2008. One citation in page 63.

[147] Jen-Philippe Thiran Nawal Houhou and Xavier Bresson. Fast texture segmentation based on semi-local region descriptor and active contour. *Numer. Math. Theor. Meth. Appl.*, 2(4):445–468, 2009. 2 citations in pages 94 and 161.

[148] Choon Boon Ng, Yong Haur Tay, and Bok-Min Goi. Vision-based human gender recognition: A survey. *CoRR*, abs/1204.1611, 2012. One citation in page 171.

[149] E.Y.-K. Ng. A review of thermography as promising non-invasive detection modality for breast tumor. *International Journal of Thermal Sciences*, 48(5):849 – 859, 2009. No citations.

[150] K. Niinuma, Unsang Park, and A.K. Jain. Soft biometric traits for continuous user authentication. *Information Forensics and Security, IEEE Transactions on*, 5(4):771 –780, dec. 2010. No citations.

[151] D.Ribaric N.Pavesic, S.Ribaric. Personal authentication using hand-geometry and palmprint features: the state of the art. In *BiometricsatICPR04*, 2004. One citation in page 104.

[152] Cenker Oden, Aytul Ercil, and Burak Buke. Combining implicit polynomials and geometric features for hand recognition. *Pattern Recognition Letters*, 24(13):2145 – 2152, 2003. <ce:title>Audio- and Video-based Biometric Person Authentication (AVBPA 2001)</ce:title>. One citation in page 109.

[153] Yildiz VT Kirmizitas H Buke Oden C, Ercil A. Hand recognition using implicit polynomials and geometric features. In *Proceedings of the Third International Conference on Audio- and Video-Based Biometric Person Authentication*, AVBPA '01, pages 336–341, London, UK, UK, 2001. Springer-Verlag. One citation in page 109.

[154] L. O'Gorman. Comparing passwords, tokens and biometrics for user authentication. In *Proceedings of the IEEE*, volume 91 of *12*, pages 2021–2040, 2003. One citation in page 21.

[155] Javier Ortega-Garcia, Julian Fierrez, Fernando Alonso-Fernandez, Javier Galbally, Manuel R. Freire, Joaquin Gonzalez-Rodriguez, Carmen Garcia-Mateo, Jose-Luis Alba-Castro, Elisardo Gonzalez-Agulla, Enrique Otero-Muras, Sonia Garcia-Salicetti, Lorene Allano, Bao Ly-Van, Bernadette Dorizzi, Josef Kittler, Thirimachos Bourlai, Norman Poh, Farzin Deravi, Ming N. R. Ng, Michael Fairhurst, Jean Hennebert, Andreas Humm, Massimo Tistarelli, Linda Brodo, Jonas Richiardi, Andrezj Drygajlo, Harald Ganster, Federico M. Sukno, Sri-Kaushik Pavani, Alejandro Frangi, Lale Akarun, and Arman Savran. The multiscenario multienvironment biosecure multimodal database (bmdb). *IEEE Trans. Pattern Anal. Mach. Intell.*, 32(6):1097–1111, June 2010. One citation in page 101.

[156] N. Otsu. A threshold selection method from gray-level histograms. *IEEE Transactions on Systems, Man, and Cybernetics*, 9(1):62–67, 1979. No citations.

[157] Unsang Park and A.K. Jain. Face matching and retrieval using soft biometrics. *Information Forensics and Security, IEEE Transactions on*, 5(3):406 –415, sept. 2010. One citation in page 26.

[158] Unsang Park, R.R. Jillela, A. Ross, and A.K. Jain. Periocular biometrics in the visible spectrum. *Information Forensics and Security, IEEE Transactions on*, 6(1):96 –106, march 2011. No citations.

[159] Peter Peer, Jure Kovac, and Franc Solina. Human skin colour clustering for face detection. International Conference on Computer (EUROCON), 2003. One citation in page 123.

[160] Jialiang Peng, Ning Wang, Ahmed A. Abd El-Latif, Qiong Li, and Xiamu Niu. Finger-vein verification using gabor filter and sift feature matching. In *Intelligent*

Information Hiding and Multimedia Signal Processing (IIH-MSP), 2012 Eighth International Conference on, pages 45 –48, july 2012. No citations.

[161] Claudio A. Perez, Leonardo A. Cament, and Luis E. Castillo. Methodological improvement on local gabor face recognition based on feature selection and enhanced borda count. *Pattern Recognition*, 44(4):951 – 963, 2011. One citation in page 26.

[162] Richard A. Davis Peter J. Brockwell. *Introduction to Time Series and Forecasting*. Springer Texts in Statistics, 1996. No citations.

[163] Maria Petrou and Costas Petrou. *Image Processing.The Fundamentals*. John Wiley and Sons, Ltd Publications, 2010. 2 citations in pages 123 and 148.

[164] Anika Pflug, Daniel Hartung, and Christoph Busch. Feature extraction from vein images using spatial information and chain codes. *Information Security Technical Report*, 17(1-2):26 – 35, 2012. <ce:title>Human Factors and Bio-metrics</ce:title>. No citations.

[165] Norman Poh, Thirimachos Bourlai, and Josef Kittler. A multimodal biometric test bed for quality-dependent, cost-sensitive and client-specific score-level fusion algorithms. *Pattern Recognition*, 43(3):1094 – 1105, 2010. No citations.

[166] Ovunc Polat and Tulay Yildirim. Hand geometry identification without feature extraction by general regression neural network. *Expert Systems with Applications*, 34(2):845 – 849, 2008. No citations.

[167] S. Prabhakar, A. Ivanisov, and A.K. Jain. Biometric recognition: Sensor characteristics and image quality. *Instrumentation Measurement Magazine, IEEE*, 14(3):10 –16, june 2011. No citations.

[168] S. Prabhakar, S. Pankanti, and A.K. Jain. Biometric recognition: security and privacy concerns. *Security Privacy, IEEE*, 1(2):33 – 42, mar-apr 2003. No citations.

[169] R. Deepak Prasanna, P. Neelamegam, S. Sriram, and Nagarajan Raju. Enhancement of vein patterns in hand image for biometric and biomedical application using various image enhancement techniques. *Procedia Engineering*, 38(0):1174 – 1185, 2012. <ce:title>INTERNATIONAL CONFERENCE ON MODELLING OPTIMIZATION AND COMPUTING</ce:title>. No citations.

[170] William K. Pratt. *DIGITAL IMAGE PROCESSING*. Fourth Edition. Wiley, 2007. 2 citations in pages 123 and 148.

[171] Xiaohua Qian, Shuxu Guo, Xueyan Li, Fei Zhong, and Xiangxin Shao. Finger-vein recognition based on the score level moment invariants fusion. In *Computational Intelligence and Software Engineering, 2009. CiSE 2009. International Conference on*, pages 1 –4, dec. 2009. No citations.

[172] Le qing Zhu and San yuan Zhang. Multimodal biometric identification system based on finger geometry, knuckle print and palm print. *Pattern Recognition Letters*, 31(12):1641 – 1649, 2010. <ce:title>Pattern Recognition of Non-Speech Audio</ce:title>. 3 citations in pages , 99, and 100.

[173] S. Pankanti N. Ratha A. Senior R. Bolle, J. Connell. The relationship between the roc curve and the cmc. In *Proceedings of Fourth IEEE Workshop on Automatic Identification Advanced Technologies (AutoID)*, 2005. One citation in page 53.

[174] R. Raghavendra, Bernadette Dorizzi, Ashok Rao, and G. Hemantha Kumar. Designing efficient fusion schemes for multimodal biometric systems using face and palmprint. *Pattern Recognition*, 44(5):1076 – 1088, 2011. One citation in page 71.

[175] Ravi P. Ramachandran, Kevin R. Farrell, Roopashri Ramachandran, and Richard J. Mammone. Speaker recognition—general classifier approaches and data fusion methods. *Pattern Recognition*, 35(12):2801 – 2821, 2002. <ce:title>Pattern Recognition in Information Systems</ce:title>. No citations.

[176] Daniel Ramos-Castro, Julian Fierrez-Aguilar, Joaquin Gonzalez-Rodriguez, and Javier Ortega-Garcia. Speaker verification using speaker- and test-dependent fast score normalization. *Pattern Recognition Letters*, 28(1):90 – 98, 2007. One citation in page 31.

[177] Afzel Noore Richa Singh, Mayank Vatsa. Integrated multilevel image fusion and match score fusion of visible and infrared face images for robust face recognition. *Pattern Recognition*, 41:880–893, 2008. One citation in page 70.

[178] G Erich Heberlein Richard A Epperly and Lowry G. Eads. Thermography, a tool for reliability and safety. *IEEE Industry Applications Magazine*, 99:28–36, 1999. One citation in page 88.

[179] Leandro Rodrıguez-Linares, Carmen Garcıa-Mateo, and Jose-Luis Alba-Castro. On combining classifiers for speaker authentication. *Pattern Recognition*, 36(2):347 – 359, 2003. No citations.

[180] Ricardo N. Rodrigues, Lee Luan Ling, and Venu Govindaraju. Robustness of multimodal biometric fusion methods against spoof attacks. *Journal of Visual Languages & Computing*, 20(3):169 – 179, 2009. <ce:title>ADVANCES IN

MULTIMODAL BIOMETRIC SYSTEMS</ce:title> <ce:subtitle>Multimodal Biometrics</ce:subtitle>. No citations.

[181] Arun Ross. A prototype hand geometry-based verification system. pages 166–171, 1999. One citation in page 104.

[182] Arun Ross and Anil Jain. Information fusion in biometrics. *Pattern Recognition Letters*, 24(13):2115 – 2125, 2003. <ce:title>Audio- and Video-based Biometric Person Authentication (AVBPA 2001)</ce:title>. 2 citations in pages 60 and 68.

[183] R.K. Rowe, U. Uludag, M. Demirkus, S. Parthasaradhi, and A.K. Jain. A multispectral whole-hand biometric authentication system. In *Biometrics Symposium, 2007*, pages 1 –6, sept. 2007. No citations.

[184] A.Gonzalez-Marcos R.Sanchez-Reillo, C.Sanchez-Avila. biometric identification through hand geometry measurements. *IEEE Transactions on Pattern Analysis Machine Intelligence*, 22, 2000. One citation in page 104.

[185] Robert Wayne Ruddock. *Basic Infrared Thermography Principles*. Terrence O'Hanlon, 2010. One citation in page 80.

[186] Andrew L. Rukhin and Igor Malioutov. Fusion of biometric algorithms in the recognition problem. *Pattern Recognition Letters*, 26(5):679 – 684, 2005. No citations.

[187] Dymitr Ruta and Bogdan Gabrys. An overview of classifier fusion methods. *Computing and Information Systems*, 7:1–10, 2000. One citation in page 60.

[188] J.B. Alonso M.A. Ferrer S. Gonzalez, C.M. Travieso. Automatic biometric identification system by hand geometry. In *Proceedings of the 37th Annual International Carnahan Conference on Security Technology*, 2003. One citation in page 10.

[189] Sanchez-Avila. Hand databases. group of biometrics, biosignals and security (gb2s). http://gb2s.es, 2012. One citation in page 109.

[190] Tadej Savič and Nikola Pavešić. Personal recognition based on an image of the palmar surface of the hand. *Pattern Recognition*, 40(11):3152 – 3163, 2007. No citations.

[191] S. Selvarajan, V. Palanisamy, and B. Mathivanan. Human identification and recognition system using more significant hand attributes. In *Computer and Communication Engineering, 2008. ICCCE 2008. International Conference on*, pages 1211 –1216, may 2008. No citations.

[192] Sharma SC. Shobha G, Krishna M. Development of palmprint verification system using biometrics. *Journal of Software*, 17:1824–1836, 2006. One citation in page 109.

[193] D. Sims. Biometric recognition: our hands, eyes, and faces give us away. *Computer Graphics and Applications, IEEE*, 14(5):14 –15, sept. 1994. No citations.

[194] Wonseok Song, Taejeong Kim, Hee Chan Kim, Joon Hwan Choi, Hyoun-Joong Kong, and Seung-Rae Lee. A finger-vein verification system using mean curvature. *Pattern Recognition Letters*, 32(11):1541 – 1547, 2011. No citations.

[195] S. Steininger, F. Schiel, O. Dioubina, and S. Raubold. Development of user-state conventions for the multimodal corpus in smartkom, 2002. One citation in page 102.

[196] Hand geometry to set the standard. *Biometric Technology Today*, 11(6):3 – 4, 2003. One citation in page 97.

[197] Multimodal module joins finger and vein. *Biometric Technology Today*, 17(4):4 –, 2009. No citations.

[198] Xiaoyang Tan, Songcan Chen, Zhi-Hua Zhou, and Fuyan Zhang. No citations.

[199] Darun Tang, Beining Huang, Rongfeng Li, and Wenxin Li. A person retrieval solution using finger vein patterns. In *Pattern Recognition (ICPR), 2010 20th International Conference on*, pages 1306 –1309, aug. 2010. No citations.

[200] Kar-Ann Toh, Jaihie Kim, and Sangyoun Lee. Biometric scores fusion based on total error rate minimization. *Pattern Recognition*, 41(3):1066 – 1082, 2008. <ce:title>Part Special issue: Feature Generation and Machine Learning for Robust Multimodal Biometrics</ce:title>. One citation in page 71.

[201] Kar-Ann Toh, Jaihie Kim, and Sangyoun Lee. Maximizing area under roc curve for biometric scores fusion. *Pattern Recognition*, 41(11):3373 – 3392, 2008. No citations.

[202] Robert Tibshirani Trevor Hastie and Jerome Friedman. *The Elements of Statistical Learning*. Springer Series in Statistics. Second edition, 2009. One citation in page 21.

[203] Filareti Tsalakanidou, Sotiris Malassiotis, and Michael G. Strintzis. A 3d face and hand biometric system for robust user-friendly authentication. *Pattern Recognition Letters*, 28(16):2238 – 2249, 2007. One citation in page 26.

[204] U. Uludag and A.K. Jain. Multimedia content protection via biometrics-based encryption. In *Multimedia and Expo, 2003. ICME '03. Proceedings. 2003 International Conference on*, volume 3, pages III – 237–40 vol.3, july 2003. No citations.

[205] U. Uludag, S. Pankanti, S. Prabhakar, and A.K. Jain. Biometric cryptosystems: issues and challenges. *Proceedings of the IEEE*, 92(6):948 – 960, june 2004. No citations.

[206] A. M.; Booij W. D. & Hendrikse A. J. Veldhuis, R. N.; Bazen. Hand-geometry recognition based on contour parameters. In *SPIE Biometric Technology for Human Identification*, 2005. One citation in page 104.

[207] Luc Vincent and Pierre Soille. Watersheds in digital spaces: An efficient algorithm based on immersion simulations. *IEEE Transactions Pattern Analysis and Machine Intelligence*, 13(6):583–598, 1991. One citation in page 123.

[208] Carlos Vivaracho-Pascual, Marcos Faundez-Zanuy, and Juan M. Pascual. An efficient low cost approach for on-line signature recognition based on length normalization and fractional distances. *Pattern Recognition*, 42(1):183 – 193, 2009. One citation in page 30.

[209] Jian-Gang Wang, Wei-Yun Yau, Andy Suwandy, and Eric Sung. Person recognition by fusing palmprint and palm vein images based on a laplacian palm representation. *Pattern Recognition*, 41(5):1514 – 1527, 2008. One citation in page 100.

[210] Kejun Wang, Hui Ma, O.P. Popoola, and Xuefeng Li. A novel finger vein pattern extraction method using oriented filtering technology. In *Intelligent Control and Automation (WCICA), 2010 8th World Congress on*, pages 6240 –6244, july 2010. No citations.

[211] Lingyu Wang, Graham Leedham, and David Siu-Yeung Cho. Minutiae feature analysis for infrared hand vein pattern biometrics. *Pattern Recognition*, 41(3):920 – 929, 2008. <ce:title>Part Special issue: Feature Generation and Machine Learning for Robust Multimodal Biometrics</ce:title>. No citations.

[212] Graham Leedham Wang Lingyu. Near- and far- infrared imaging for vein pattern biometrics. In *Proceedings of the IEEE International Conference on Video and Signal Based Surveillance (AVSS'06)*, 2006. 2 citations in pages and 100.

[213] Andrew R. Webb. *Statistical Pattern Recognition*. Second edition, 2002. One citation in page 21.

[214] Xue-Bing Wen and Xue-Zhang Liang. Research on enhancing human finger vein pattern characteristics based on adjacent node threshold image method. In *Frontier of Computer Science and Technology (FCST), 2010 Fifth International Conference on*, pages 552 –556, aug. 2010. No citations.

[215] Ra L. N. Wong and Pengcheng Shi. Peg-free hand geometry recognition using hierarchical geometry and shape matching. In *IAPR Workshop on Machine Vision Applications*, pages 281–284, 2002. One citation in page 104.

[216] Damon L. Woodard and Patrick J. Flynn. Finger surface as a biometric identifier. *Computer Vision and Image Understanding*, 100(3):357 – 384, 2005. One citation in page 104.

[217] Jian-Da Wu and Chiung-Tsiung Liu. Finger-vein pattern identification using principal component analysis and the neural network technique. *Expert Systems with Applications*, 38(5):5423 – 5427, 2011. One citation in page 64.

[218] Jian-Da Wu and Chiung-Tsiung Liu. Finger-vein pattern identification using svm and neural network technique. *Expert Systems with Applications*, 38(11):14284 – 14289, 2011. One citation in page 67.

[219] Jie Wu, Zhengding Qiu, and Dongmei Sun. A hierarchical identification method based on improved hand geometry and regional content feature for low-resolution hand images. *Signal Processing*, 88(6):1447 – 1460, 2008. No citations.

[220] Ying Wu and T.S. Huang. Hand modeling, analysis and recognition. *Signal Processing Magazine, IEEE*, 18(3):51 –60, may 2001. No citations.

[221] Yingquan Wu, Krassimir Ianakiev, and Venu Govindaraju. Improved k-nearest neighbor classification. *Pattern Recognition*, 35(10):2311 – 2318, 2002. No citations.

[222] Yong Xu, David Zhang, Zhong Jin, Miao Li, and Jing-Yu Yang. A fast kernel-based nonlinear discriminant analysis for multi-class problems. *Pattern Recognition*, 39(6):1026 – 1033, 2006. No citations.

[223] Li Xueyan, Guo Shuxu, Gao Fengli, and Li Ye. Vein pattern recognitions by moment invariants. In *Bioinformatics and Biomedical Engineering, 2007. ICBBE 2007. The 1st International Conference on*, pages 612 –615, july 2007. One citation in page 100.

[224] Jian Yang, Alejandro F. Frangi, and Jing yu Yang. A new kernel fisher discriminant algorithm with application to face recognition. *Neurocomputing*, 56(0):415 – 421, 2004. No citations.

[225] Jian Yang, Zhong Jin, Jing yu Yang, David Zhang, and Alejandro F Frangi. Essence of kernel fisher discriminant: Kpca plus lda. *Pattern Recognition*, 37(10):2097 – 2100, 2004. No citations.

[226] Jian Yang and Jing yu Yang. Why can lda be performed in pca transformed space? *Pattern Recognition*, 36(2):563 – 566, 2003. <ce:title>Biometrics</ce:title>. No citations.

[227] Jinfeng Yang, Yihua Shi, and Jinli Yang. Personal identification based on finger-vein features. *Computers in Human Behavior*, 27(5):1565 – 1570, 2011. <ce:title>2009 Fifth International Conference on Intelligent Computing</ce:title> <ce:subtitle>ICIC 2009</ce:subtitle> <xocs:full-name>2009 Fifth International Conference on Intelligent Computing</xocs:full-name>. 2 citations in pages 72 and 100.

[228] Jinfeng Yang and Xu Zhang. Feature-level fusion of fingerprint and finger-vein for personal identification. *Pattern Recognition Letters*, 33(5):623 – 628, 2012. One citation in page 70.

[229] Wenming Yang, Qing Rao, and Qingmin Liao. Personal identification for single sample using finger vein location and direction coding. In *Hand-Based Biometrics (ICHB), 2011 International Conference on*, pages 1 –6, nov. 2011. No citations.

[230] Yong-Fang Yao, Xiao-Yuan Jing, and Hau-San Wong. Face and palmprint feature level fusion for single sample biometrics recognition. *Neurocomputing*, 70(7-9):1582 – 1586, 2007. <ce:title>Advances in Computational Intelligence and Learning</ce:title> <ce:subtitle>14th European Symposium on Artificial Neural Networks 2006</ce:subtitle> <xocs:full-name>14th European Symposium on Artificial Neural Networks 2006</xocs:full-name>. One citation in page 70.

[231] E. Yoruk, E. Konukoglu, B. Sankur, and J. Darbon. Shape-based hand recognition. *Image Processing, IEEE Transactions on*, 15(7):1803 –1815, july 2006. 5 citations in pages 104, 109, 124, 129, and 130.

[232] Chengbo Yu and Huafeng Qin. Research on extracting human finger vein pattern characteristics. In *Intelligent Control and Automation, 2008. WCICA 2008. 7th World Congress on*, pages 3789 –3793, june 2008. No citations.

[233] Xiang Yu, Wenming Yang, Qingmin Liao, and Fei Zhou. A novel finger vein pattern extraction approach for near-infrared image. In *Image and Signal Processing, 2009. CISP '09. 2nd International Congress on*, pages 1 –5, oct. 2009. No citations.

[234] David Zhang. *Automated biometrics : technologies and systems*. Kluwer Academic Publishers, the kluwer international series on asian studies in computer and information science 4 edition, 2000. One citation in page 21.

[235] David D. Zhang. *Palmprint Authentication*. Kluwer Academic Pub, 2004. One citation in page 26.

[236] Tianhao Zhang, Xuelong Li, Dacheng Tao, and Jie Yang. Multimodal biometrics using geometry preserving projections. *Pattern Recognition*, 41(3):805 – 813, 2008. <ce:title>Part Special issue: Feature Generation and Machine Learning for Robust Multimodal Biometrics</ce:title>. No citations.

[237] Zhong Bo Zhang, Dan Yang Wu, Si Liang Ma, and Jie Ma. Multiscale feature extraction of finger-vein patterns based on wavelet and local interconnection structure neural network. In *Neural Networks and Brain, 2005. ICNN B '05. International Conference on*, volume 2, pages 1081 –1084, oct. 2005. No citations.

[238] Dongming Zhao and Jie Chen. Affine curve moment invariants for shape recognition. *Pattern Recognition*, 30(6):895 – 901, 1997. No citations.

[239] Wen-Yi Zhao, Rama Chellappa, P. Jonathon Phillips, and Azriel Rosenfeld. Face recognition: A literature survey. *ACM Comput. Surv.*, 35(4):399–458, 2003. One citation in page 25.

[240] Li Zhichao, Sun Dongmei, Liu Di, and Liu Hao. Two modality-based bi-finger vein verification system. In *Signal Processing (ICSP), 2010 IEEE 10th International Conference on*, pages 1690 –1693, oct. 2010. One citation in page 63.

[241] L. R. Zunkel. *Biometrics: Personal identification in a networked society*, pages 87–101. Kluwer Academic Publishers, 1999. No citations.